Combined Faculty of Natural Sciences and Mathematics
Heidelberg Universität, Germany

Theme:

The Greater Antilles Arc of Cuba, a natural laboratory to understand the evolution of intra-oceanic convergent margin magmatism

Presented by
MSc. Haoyu Hu

Supervisor:
Prof. Dr. Yamirka Rojas-Agramonte

Dissertation

Submitted to the
Combined Faculty of Natural Sciences and Mathematics
Heidelberg Universität, Germany
for the Degree of
Doctor of Natural Sciences (Dr. rer. nat.)

Presented by
MSc. Haoyu Hu
From Wuhan, China
Date of examination: 17.12.2025

Theme:

The Greater Antilles Arc of Cuba, a natural laboratory to understand the evolution of intra-oceanic convergent margin magmatism

MSc. Haoyu Hu

Examination committee:

Prof. Dr. Yamirka Rojas-Agramonte, PhD supervisor

Prof. Dr. Antonio García-Casco

Prof. Dr. Frank Kepler

Prof. Dr. Lucy Tacjmanova

Theme:

The Greater Antilles Arc of Cuba, a natural laboratory to understand the evolution of intra-oceanic convergent margin magmatism

MSc. Haoyu Hu

Supervisor:

Prof. Dr. Yamirka Rojas-Agramonte

Declaration

This thesis is submitted to the Combined Faculty of Natural Sciences and Mathematics of the Heidelberg University for the degree of Doctorate of Natural Sciences.

I, the undersigned, declare that this thesis is my own work and has not been submitted in any form from another degree, diploma or study at any university or other institution of tertiary education. Information derived from the published or unpublished work of others has been acknowledged in the text and a list of references is given.

_____

M.Sc. Haoyu Hu

Heidelberg October 8, 2025

Contents

Abstract

Intra-oceanic convergent margins represent one of the primary sites for the generation of juvenile continental crust through subduction-related processes. Magmas in these systems are derived from mantle sources with minimal continental input and preserve direct evidence of source components, magma differentiation, and crustal maturation. Most modern intra-oceanic arcs remain submerged, limiting direct observation of their crustal architecture and petrogenetic evolution. Fossil arcs that have been accreted and uplifted above sea level therefore provide invaluable archives for reconstructing the complete life cycle of intra-oceanic arc systems. Among these, the Greater Antilles Arc, a major segment of the Great Arc of the Caribbean, preserves one of the most extensive and accessible records of long-lived intra-oceanic subduction system spanning the Early Cretaceous to the Eocene. The central Cuban segment, where forearc ophiolites and mélanges, volcanic-plutonic sequences, and arc-related metamorphic complexes are well exposed, offers an exceptional window into the temporal and structural evolution of an intra-oceanic arc from its initiation to collisional termination.

This study examines the temporal, geochemical, and structural evolution of the Greater Antilles Arc system through three complementary investigations. First, a regional synthesis integrating over 650 radiometric ages and more than 1500 geochemical analyses from subduction-related rocks across Cuba, Hispaniola, Puerto Rico, and the Virgin Islands identified three major stages of arc evolution: subduction initiation, magmatic and metamorphic climax, and the waning of subduction magmatism and collisional termination. The temporal overlap between peak magmatism and emplacement of the Caribbean Large Igneous Province suggests a transient plume-arc interaction, most pronounced in the retro-arc region.

Building on the regional framework, the second part of the study focuses on the Mabujina Amphibolite Complex in central Cuba, a tectonically important arc-related metamorphic assemblage formed during active arc development, and long debated in regional tectonic reconstuctions. Petrochemical and isotopic data provide new constraints indicating that the protolith represents a proximal segment of the Caribbean arc, rather than a far-traveled exotic terrane derived from the Pacific realm. The accretionary event occurred during the mid-Cretaceous, when oblique convergence cross Caribbean arc system promoted a transspressional regime.

At a finer scale, the third component of this study investigates the Central Cuban Arc segment, which preserves an exceptional ~60 Myr record of magmatism from subduction initiation to collisional

termination. Field, geochemical, and geochronological data reveal a transition from early submarine tholeiitic to Late Cretaceous calc-alkaline magmatism. Pressure-senstive geochemical proxies and thermobarometric estimates indicate increasingly complex magma storage, progressive crustal thickening, and enhanced magmatic differentiation through time. Amphibole-bearing magmas tapped lower crustal levels approaching present-day Moho depths during major plutonism shortly after athe accretionary event. The mantle source remained largly homogeneous, with limited slab input, demonstrating that intra-oceanic arc systems can generate juvenile continental crust prior to collision.

Collectively, these results provide a comprehensive reconstruction of the Greater Antilles Arc as a natural laboratory for studying intra-oceanic arc construction, accretion, and crustal differentiation. Integration of regional and local datasets defines the Greater Antilles Arc as a long-lived oceanic arc that evolved from tholeiitic to calc-alkaline magmatism and progressively developed a hydrous, transcrustal plumbing system capable of generating proto-continental crust. This study offers new insights into the mechanisms of crustal growth and differentiation at intra-oceanic convergent margins.

Zusammenfassung

Intraozeanische Konvergenzränder stellen eine der primären Zonen für die Bildung juveniler kontinentaler Kruste durch subduktionsbezogene Prozesse dar. Magmen in diesen Systemen stammen aus Mantelquellen mit nur geringem kontinentalem Einfluss und bewahren direkte Hinweise auf Quellkomponenten, magmatische Differentiation und Krustenreifung. Da die meisten heutigen intraozeanischen Inselbögen submarin sind, ist die direkte Beobachtung ihrer Krustenarchitektur und petrogenetischen Entwicklung stark eingeschränkt. Fossile Inselbögen, die akkretierte und über den Meeresspiegel gehobene Abschnitte dieser Systeme repräsentieren, stellen daher unschätzbare Archive für die Rekonstruktion des vollständigen Lebenszyklus intraozeanischer Inselbogensysteme dar. Unter diesen bewahrt der Große Antillenbogen, ein Hauptsegment des „Great Arc of the Caribbean“, eine der umfangreichsten und am besten zugänglichen Aufzeichnungen eines lang andauernden intraozeanischen Subduktionssystems, das sich von der Unterkreide bis ins Eozän erstreckt. Das zentrale Segment Kubas, in dem Forearc-Ophiolithe und Mélanges, vulkanisch-plutonische Sequenzen sowie bogenbezogene metamorphe Komplexe gut aufgeschlossen sind, bietet ein außergewöhnliches Fenster in die zeitliche und strukturelle Entwicklung eines intraozeanischen Inselbogens – von seiner Initiierung bis zur terminierenden Kollision.

Diese Studie untersucht die zeitliche, geochemische und strukturelle Entwicklung des Großen-Antillenbogen-Systems anhand von drei ergänzenden Untersuchungen. Zunächst identifiziert eine regionale Synthese, die über 650 radiometrische Alter und mehr als 1500 geochemische Analysen subduktionsbezogener Gesteine aus Kuba, Hispaniola, Puerto Rico und den Jungferninseln integriert, drei Hauptphasen der Inselbogenentwicklung: die Subduktionsinitiierung, das magmatisch-metamorphe Maximum sowie das Abklingen des subduktionsbezogenen Magmatismus und die Kollisionsterminierung. Die zeitliche Überlappung zwischen maximalem Magmatismus und der Intrusion der Karibischen Large Igneous Province weist auf eine vorübergehende Interaktion zwischen Mantelplume und Inselbogen hin, die im Retro-Bogen-Bereich am deutlichsten ausgeprägt ist.

Aufbauend auf diesem regionalen Rahmen konzentriert sich der zweite Teil der Studie auf den Mabujina-Amphibolitkomplex in Zentralkuba – ein tektonisch bedeutendes, bogenbezogenes metamorphes Gesteinsensemble, das während der aktiven Inselbogenentwicklung entstand und seit Langem im Mittelpunkt regionaltektonischer Diskussionen steht. Petrochemische und isotopische Daten liefern neue Randbedingungen und deuten darauf hin, dass der Protolith dieses Komplexes ein

proximales Segment des Karibischen Bogens darstellt und nicht – wie zuvor angenommen – ein weit gereister exotischer Terran aus der pazifischen Region ist. Das Akkretionsereignis ereignete sich in der Mittleren Kreide, als eine Schrägkonvergenz entlang des Karibischen Bogens ein transpressionales Regime begünstigte.

In einem detaillierteren Maßstab untersucht der dritte Teil dieser Arbeit das zentrale Segment des Kubanischen Bogens, das eine außergewöhnliche, etwa 60 Millionen Jahre umfassende magmatische Aufzeichnung von der Subduktionsinitiierung bis zur Kollisionserstarrung dokumentiert. Geländebeobachtungen, geochemische Daten und Zirkon-Apatit-Geochronologie zeigen einen systematischen Übergang von frühem submarinem tholeiitischen zu spätkretazischem kalkalkalinen Magmatismus. Druckempfindliche geochemische Indikatoren und thermobarometrische Schätzungen belegen zunehmend komplexe Magmenreservoirbedingungen, fortschreitende Krustenverdickung und eine verstärkte magmatische Differentiation im Laufe der Zeit. Amphibolführende Magmen erreichten während der bedeutendsten Plutonismusphasen kurz nach dem Akkretionsereignis tiefere Krustenniveaus bis in die Nähe der heutigen Moho-Tiefe. Die Mantelquelle blieb weitgehend homogen, mit nur begrenztem episodischem Einfluss von Subduktionssedimenten, was zeigt, dass intraozeanische Inselbogensysteme in der Lage sind, juvenile kontinentale Kruste bereits vor der Kollision zu erzeugen.

In ihrer Gesamtheit liefern diese Ergebnisse eine umfassende Rekonstruktion des Großen Antillenbogens als natürliches Labor zur Untersuchung intraozeanischer Bogenbildung, Akkretion und Krustendifferenzierung. Die Integration regionaler und lokaler Datensätze definiert den Großen Antillenbogen als langlebigen ozeanischen Bogen, der sich von tholeiitischem zu kalkalkalinem Magmatismus entwickelte und schrittweise ein hydriertes, transkrustales Magmenfördersystem aufbaute, das in der Lage war, proto-kontinentale Kruste zu erzeugen. Diese Studie bietet neue Einblicke in die Mechanismen des Krustenwachstums und der Differentiation an intraozeanischen Konvergenzrändern.

1. Introduction

Intra-oceanic convergent margins (IOCMs) represent the oceanic end-member of subduction systems and are among the most important settings for generating juvenile continental crust (Stern, 2010). These systems form where one oceanic lithosphere subducts beneath another, producing magmas generated by partial melting of a mantle wedge metasomatized by fluids and melts released from the subducting slab, and largely free from contamination by pre-existing continental crust. Their geochemical signatures provide a direct record of mantle sources, slab inputs, and magmatic differentiation, revealing how IOCM magmas evolve through time. Magmatic sequences in these systems typically begin with mid-ocean ridge basalt (MORB)-like forearc basalts and boninites, followed by island arc tholeiites, calc-alkaline, and eventually shoshonitic (alkaline) magmas (Whattam & Stern, 2011; Straub et al., 2015). Modern IOCMs include well-known examples such as the Izu-Bonin-Mariana, Tonga-Kermadec, Vanuatu, South Sandwich, and Lesser Antilles arcs (Leat & Larter, 2003). Despite their importance for understanding subduction and crustal growth processes, most active IOCMs are submarine, and continuous temporal and structural records of their evolution are rarely accessible. Fossil IOCMs uplifted above sea level therefore provide exceptional natural laboratories for reconstructing the complete life cycle of an arc, from subduction initiation through tectono-magmatic growth to collisional accretion (Greene et al., 2006; Jagoutz & Schmidt, 2012; Ducea et al., 2015).

Among these fossil intra-oceanic systems, the Greater Antilles Arc (GAA), the western segment of the Great Arc of the Caribbean (Burke, 1988), is one of the most extensive and best-preserved examples on Earth (Fig. 1A). Spanning over 2000 km from Cuba to the Virgin Islands, the GAA records a long and continuous history of subduction-related magmatism and metamorphism from the Cretaceous to the Paleogene (Mann et al., 2007; Pindell & Kennan, 2009; Iturralde-Vinent et al., 2016). Most reconstructions attribute its origin to southwest-dipping subduction of Proto-Caribbean oceanic lithosphere beneath the eastward moving Caribbean plate, a fragment derived from the Pacific Farallon plate (Pindell & Kennan, 2009; Blanco-Quintero et al., 2010; Boschman et al., 2014). Throughout its evolution, a diverse assemblage of subduction-related magmatic and metamorphic rocks formed across distinct tectonic domains, ranging from forearc mélanges and ophiolites to volcanic-plutonic magmatic complexes and retro-arc, reflecting the diverse structural and petrogenetic environments characteristic of an intra-oceanic subduction system (Fig. 1B; Lidiak & Jolly, 1996; Lewis et al., 2006; García-Casco et al., 2008).

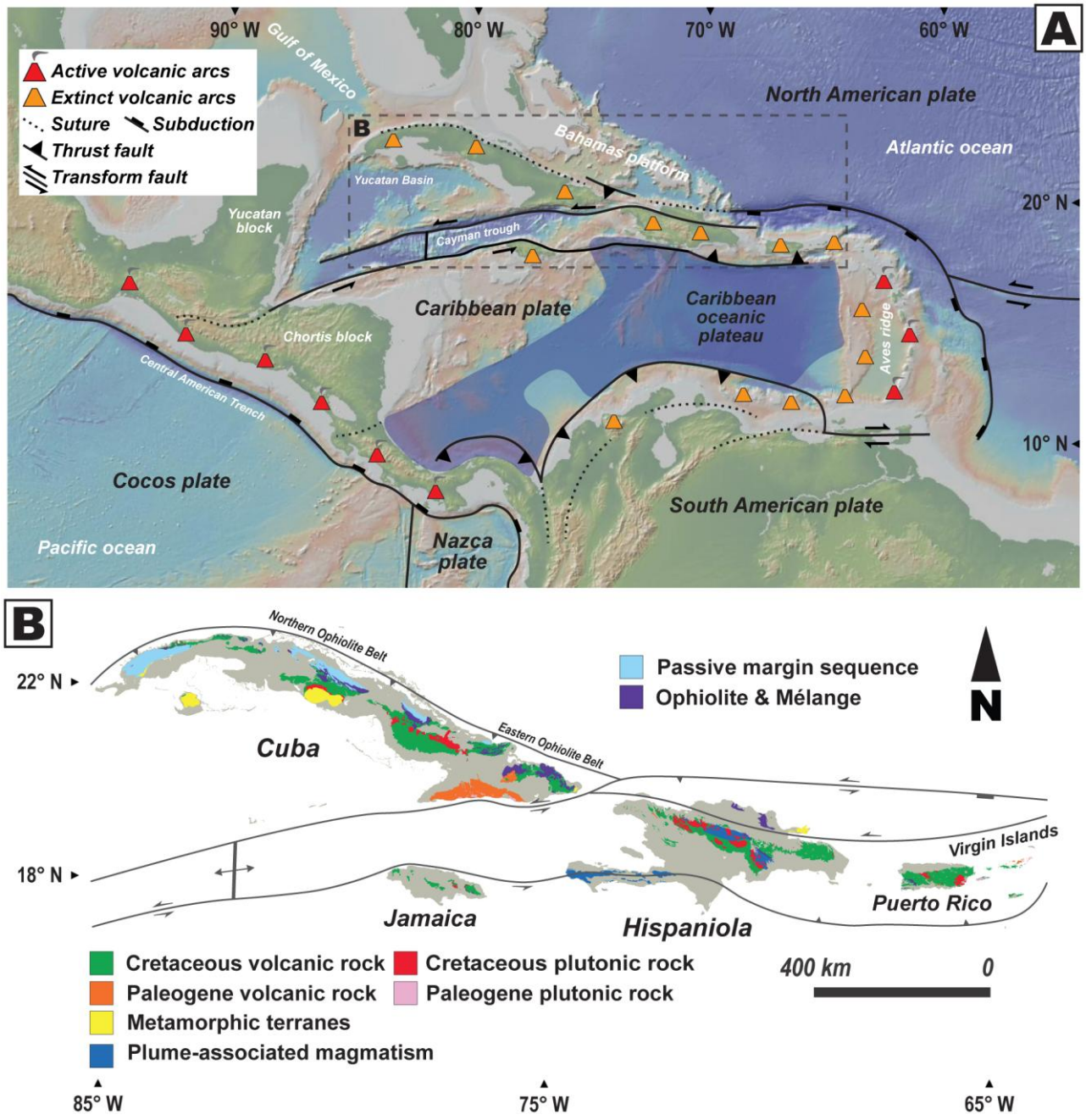

Figure 1. *(A) Geodynamic map of the Caribbean plate showing its main features. The locations of the active and extinct volcanic arcs indicated after Garcia-Casco et al. (2006). (B) Map of the Greater Antilles showing the location of passive margin sequences, ophiolites and mélange blocks, magmatic arcs, metamorphic terranes and plume-associated igneous rocks, modified from Torró et al. (2016) and Wilson et al. (2019).*

The geodynamic evolution of the Caribbean region can be traced back to the mid-late Jurassic breakup of Pangea and the formation of the Proto-Caribbean Ocean between the diverging American continents. This breakup produced the Proto-Caribbean ridge, the western continuation of the Central Atlantic spreading center, and an inter-American transform system along the northern margin of the Farallon plate (Burke, 1988; Pindell et al., 2012). By ca. 135 Ma, subduction of Proto-Caribbean oceanic lithosphere began beneath the northern and eastern edge of the Farallon plate, giving rise to the early intra-oceanic arc system. Subduction initiated with forearc seafloor spreading that generated ophiolitic sequences now preserved in northern Cuba and other parts of the GAA. As subduction progressed, magmatism migrated arc ward, establishing a mature volcanic-plutonic system (Rojas-Agramonte et al., 2011; Escuder-Viruete et al., 2014; Lázaro et al., 2016). Convergence between the Caribbean plate and the North American margin during the Late Cretaceous-Eocene led to a "soft collision," characterized by moderate deformation and limited crustal disruption. This event resulted in accretion of the western GAA to the North American plate and established a new left-lateral transform boundary marked by the Oriente Transform Fault and Cayman Trough (Fig. 1; Rosencrantz et al., 1988; van Hinsbergen et al., 2009; Iturralde-Vinent et al., 2016). Thus, the GAA provides an unparalleled geological record of intra-oceanic arc evolution from subduction initiation to eventual arc-continent collision, much of which remains remarkably well preserved above sea level.

Within this regional framework, Cuba preserves some of the most complete and accessible segments of the fossil GAA (Fig. 2A). Over 1000 km of well-exposed volcanic, plutonic, and metamorphic rocks document the arc's full evolutionary history, from subduction initiation to collisional shutdown (Iturralde-Vinent, 1996; Iturralde-Vinent et al., 2016). In central Cuba, the Cretaceous arc is exceptionally well preserved, providing a nearly complete crustal section. These exposures include both volcanic and plutonic components, allowing detailed reconstruction of an intra-oceanic arc across multiple crustal levels. In the Santa Clara region (Fig. 2B and C), Cretaceous volcanic arc rocks are exposed along a north-south transect, with the oldest and deepest units in the south in tectonic contact with the Mabujina Amphibolite Complex and progressively younger sequences to the north (García-Delgado, 1998; Iturralde-Vinent, 2021). Island-arc tholeiites (IAT) associated with subduction initiation are primarily recorded in the Los Pasos Formation (Kerr et al., 1999; Díaz de Villalvilla et al., 2003; Rojas-Agramonte et al., 2011; Torró et al., 2016). This unit is overlain by Aptian-Albian transitional sequences, such as the Mataguá Formation, and by late Albian-Campanian volcanic and volcano-sedimentary successions with calc-alkaline signatures (Díaz de Villalvilla, 1997; Kerr et al., 1999). The calc-alkaline Manicaragua Batholith intruded both the volcanic arc

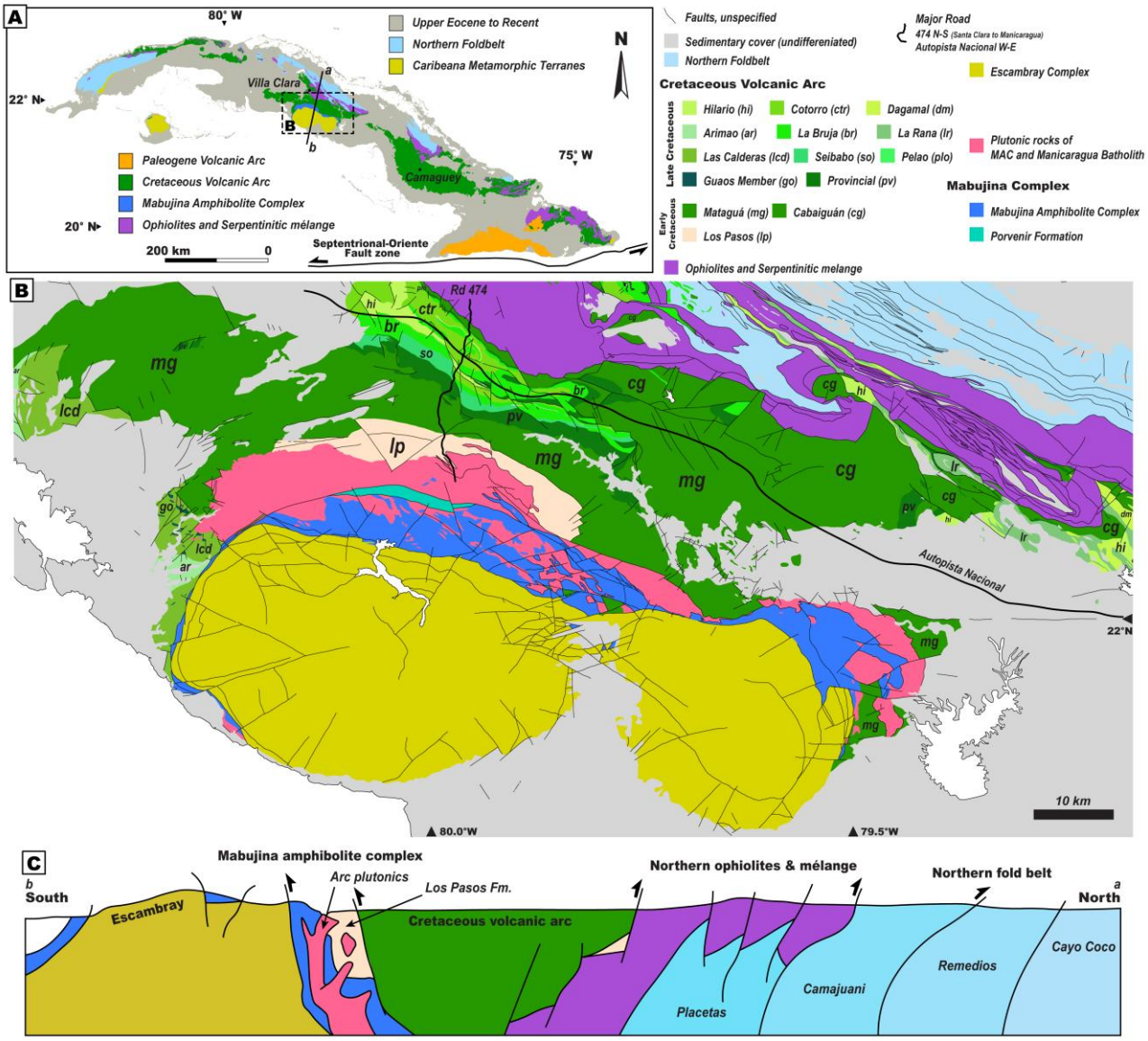

Figure 2. *(A) Simplified geological map of Cuba, modified after Wilson et al. (2019) and Hu et al. (2022). (B) Geological map of central Cuba showing sample locations, after García-Delgado (1998). (C) Cross-section of central Cuba (a-b in panel A), modified after Iturralde-Vinent (1998).*

sequence and the Mabujina Amphibolite Complex between ca. 89 and 81 Ma (Rojas-Agramonte et al., 2011). It consists mainly of granodiorites and tonalites, with subordinate quartz diorites containing mafic microgranular enclaves of dioritic composition (Somin & Millán, 1981; Sukar & Pérez, 1997; Bibikova et al., 1988; Blein et al., 2003).

Beneath the oldest volcanic formation in central Cuba lies the Mabujina Amphibolite Complex (MAC), a key metamorphic component of the Cuban arc system. The MAC comprises amphibolite- to epidote-amphibolite facies rocks derived from basaltic to basaltic-andesitic protoliths, along with

tonalitic-trondhjemitic orthogneisses and syn- to post-metamorphic granitoids (Somin & Millán, 1981; Dublan & Álvarez, 1986; Blein et al., 2003; Garcia-Casco et al., 2006, 2008; Stanek et al., 2019). Structurally, it is positioned between the overlying volcanic arc and the underlying high-pressure Escambray Complex (Somin & Millan 1981; Schneider et al. 2004; Garcia-Casco et al. 2008; Stanek et al. 2006, 2019; Despaigne-Díaz et al. 2016, 2017). The origin of the MAC remains debated, either as a metamorphosed section of the Caribbean arc or as an exotic arc fragment accreted from the Pacific realm (Blein et al., 2003; Rojas-Agramonte et al., 2011; Iturralde-Vinent et al., 2016). Resolving its tectonic affinity is essential for understanding intra-oceanic crustal growth, metamorphism, and accretion during Cretaceous oblique convergence.

This cumulative dissertation synthesizes the temporal, compositional, and structural evolution of the Caribbean intra-oceanic arc system through three complementary studies that integrate regional synthesis with detailed case analyses from central Cuba. Together, they aim to elucidate how intra-oceanic arcs form, evolve, and mature into proto-continental crust. The first paper provides a regional synthesis of geochronologic and geochemical data from the Greater Antilles Arc, reconstructing its full evolutionary history from subduction initiation to collisional shutdown and establishing a temporal-compositional framework for Caribbean arc evolution. The second paper investigates the Mabujina Amphibolite Complex, integrating petrographic, geochemical, and isotopic data to assess its provenance and tectonic relationship to the Cretaceous Caribbean arc, clarifying its role as a metamorphic and accretionary component within the intra-oceanic system. The third paper focuses on the Central Cuban Arc segment, combining field observations, whole-rock and mineral chemistry, and U-Pb zircon and apatite geochronology to document its Cretaceous magmatic history and to characterize crustal differentiation and thickening within a single well-preserved upper crustal volcanic transect.

Full versions of these three papers are included in the Appendix of this thesis, and all associated supplementary materials are provided in an accompanying electronic appendix.

2. Objectives

This research examines the temporal, geochemical, and petrological evolution of the Caribbean intra-oceanic arc system to assess the processes that govern crustal growth and differentiation in oceanic subduction environments. The study integrates regional synthesis with detailed investigations from central Cuba to link large-scale tectonic evolution with local magmatic processes. The specific objectives are:

1. To establish a temporal-geochemical framework for the GAA from subduction initiation to collisional termination.
2. To determine the provenance and tectonic significance of the MAC and its relationship to the Cretaceous Caribbean arc.
3. To reconstruct the magmatic evolution and crustal thickening history of the Central Cuban Arc segment through integrated geochemical, isotopic, and geochronologic analyses.
4. To develop a comprehensive petrogenetic and tectonic model of subduction processes, magma differentiation, and crustal growth, with implications for the generation and maturation of continental crust in intra-oceanic arcs.

These objectives aim to provide an integrated understanding of how long-lived intra-oceanic arcs evolve chemically and structurally into mature crustal systems prior to collision and accretion.

3. Methodology

3.1. Sampling and Sample Preparation

Samples of the Mabujina Amphibolite Complex previously collected were selected for thin-section preparation and whole-rock geochemical analysis. All processing was conducted at the University of Granada, where samples were crushed and powdered using a tungsten carbide mill. Whole-rock geochemical analyses of the powdered samples were performed at the Centro de Instrumentación Científica of the University of Granada (CIC-UGR).

Samples from the Central Cuban Arc, ranging from 1 to 3 kg, were systematically collected during the 2023 field campaign. These samples encompass almost all major lithological units within the Central Cuban Arc section, including volcanic, volcano-sedimentary, and sedimentary rocks. Given the effects of intense tropical weathering in Cuba, special care was taken to select the freshest possible material. Selection of representative specimens was guided by field observations of texture and mineralogy at each outcrop. In the laboratory at the University of Kiel (CAU), all samples were first washed to remove surface dust and soil, then sliced to eliminate weathered outer portions. Fresh interior portions were cut to examine representative textures, and selected areas, including micro-enclaves within granitoids were prepared for thin-section. Initial unpolished thin sections were examined to verify sample freshness before preparing polished thin sections for mineral chemical analysis.

For geochemical analysis, cleaned rock fragments were crushed into small chips, from which approximately 100 g of the freshest material was selected. These pieces were powdered in an agate mill after carefully removing secondary veins and visible weathering products.

The remaining material, including the weathered outer parts and residual pieces from thin-section and geochemical preparation, was used for heavy mineral separation (e.g., zircon and apatite). Each sample (typically 750 g to 2 kg) was crushed to a grain size of ~250 µm using a jaw crusher and agate mill, followed by sieving through a 250 µm mesh. Heavy mineral concentrates, primarily zircon and apatite, were obtained through panning with water and ethanol at the University of Kiel, followed by magnetic separation.

Zircons selected for isotopic analysis were handpicked under a binocular microscope and mounted in epoxy resin at the Beijing SHRIMP Center, China. The mounts were ground and polished to expose zircon interiors and subsequently imaged using cathodoluminescence (CL) to aid in spot selection during analysis. CL imaging was performed at the Beijing SHRIMP Center using a Hitachi S-3000N

scanning electron microscope (accelerating voltage 9 kV, beam current 109 μA), acquiring high-resolution images with a pixel dwell time of 400 μs.

3.2. X-ray Fluorescence (XRF)

Major elements and Zr concentrations of the Mabujina Amphibolite Complex samples were analysed at the Centro de Instrumentación Científica of the University of Granada (CIC-UGR). Major element and Zr compositions were determined from glass beads prepared by fusing 0.6 g of powdered sample with 6 g of $Li_2B_4O_7$ using a PHILIPS Magix Pro (PW-2440) XRF spectrometer. Analytical precision was better than ± 1.5% for elements with concentrations around 10 wt%, and better than ± 4% for Zr at a concentration of 100 ppm.

For the Central Cuban Arc samples, major element and Zr concentrations were determined on fused glass beads prepared by mixing approximately 0.6 g of finely ground sample powder with 3.6 g of $Li_2B_4O_7$ and melting at ~1100 °C in a platinum crucible. Analyses were performed using a Panalytical Zetium WD-XRF spectrometer equipped with a 1 kW rhodium anode X-ray tube at the University of Kiel (CAU).

Loss on ignition (LOI) was determined by heating powdered samples at 1000 °C for 2 hours, after which the weight loss was measured to calculate volatile contents.

3.3. Inductively Coupled Plasma Mass Spectrometry (ICP-MS)

Trace element analyses of the Mabujina Amphibolite Complex and Central Cuban Arc samples were performed at the Centro de Instrumentación Científica of the University of Granada (CIC-UGR) during different analytical sessions.

For the MAC samples, trace elements were determined by inductively coupled plasma mass spectrometry (ICP-MS) after acid digestion of 0.1 g of powdered sample in a Teflon-lined vessel using a mixture of HNO_3 and HF at 180 °C and 200 psi for 30 minutes. The resulting solutions were evaporated to dryness and redissolved in 100 ml of 4 vol.% HNO_3. International reference standards PM-S and WS-E (Govindaraju et al., 1994) were analysed as unknowns during each analytical session. Measured concentrations for these standards were within analytical uncertainty of the certified values. Analytical precision was better than ± 2 % for element concentrations of ~50 ppm and ± 5 % for concentrations around 5 ppm.

Trace element analyses of the Central Cuban Arc samples were also performed by ICP-MS after dissolution in high-pressure microwave-assisted digestion vessels using a 3:2 mixture of HF and

HNO_3. The solutions were evaporated to dryness twice, first after the addition of 2 ml of $HClO_4$ and again after adding 2 ml of HNO_3 to ensure complete removal of silica and fluorine. Rhodium was used as an internal standard, and the same external standards employed for major element calibration were used for quantitative analysis. Analytical precision was better than 3 % for analyte concentrations around 100 ppm.

3.4. Thermal Ionization Mass Spectrometry (TIMS)

MAC samples for Sr-Nd isotope analysis were digested following the same procedure used for ICP-MS trace element analysis, employing ultra-clean reagents. Sr-Nd isotopic compositions were measured by TIMS using a Finnigan MAT 262 spectrometer after chromatographic separation with ion exchange resins at the Centro de Instrumentación Científica of the University of Granada (CIC-UGR). Normalization ratios were $^{87}Sr/^{86}Sr = 0.1194$ and $^{146}Nd/^{144}Nd = 0.7219$. Total procedural blanks were 0.6 ng for Sr and 0.09 ng for Nd. External precision (2σ), based on ten replicate analyses of the international standard WS-E (Govindaraju et al., 1994), was better than 0.003% and 0.0015% for $^{87}Sr/^{86}Sr$ and $^{143}Nd/^{144}Nd$, respectively. The laboratory value for the NBS 987 Sr standard was $^{87}Sr/^{86}Sr = 0.710250 \pm 0.0000044$ (n = 89), and measurements of the La Jolla Nd standard yielded $^{143}Nd/^{144}Nd = 0.511844 \pm 0.0000065$ (n = 49), consistent with published reference values.

Sr-Nd isotopic analyses of Central Cuban Arc samples were performed at the Geochronology and Isotopic Geochemistry Facility of the Complutense University of Madrid. Samples were dissolved using ultrapure HF-HNO_3-HCl acids, followed by chromatographic separation of Sr and Nd using Dowex Resin AG®50x8 and Ln-Resin®, by steps respectively. Analyses were carried out on an IsotopX Phoenix® TIMS in dynamic multi-collection mode. $^{87}Sr/^{86}Sr$ ratios were normalized to $^{86}Sr/^{88}Sr = 0.1194$ (Nier, 1938) and corrected to the laboratory average for NBS 987 ($^{87}Sr/^{86}Sr = 0.710246 \pm 0.000017$, 2σ, n = 10). $^{143}Nd/^{144}Nd$ ratios were corrected for potential interferences from ^{142}Ce and ^{144}Sm and normalized to $^{146}Nd/^{144}Nd = 0.7219$ (O'Nions et al., 1979). Potential drifts of the isotope ratios of the samples were corrected using the Nd standard JNdi-1 with an average value of $^{143}Nd/^{144}Nd = 0.512112$ (n = 7), consistent with published values (Lugmair et al., 1983). Analytical uncertainties in $^{87}Sr/^{86}Sr$ and $^{143}Nd/^{144}Nd$ ratios were below 0.01% and below 0.006%, respectively. The procedural blanks of Sr and Nd are always less than 0.5 and 0.1 ng, respectively.

Pb isotopic analyses of Central Cuban Arc samples were conducted at GEOMAR Helmholtz Centre for Ocean Research Kiel using a Thermo Scientific TRITON Plus TIMS. About 100 to 200 mg of sample powder were leached in 2N HCl at 70°C for 180 minutes and then triple rinsed in 18.2 MΩ

water prior to digestion. Sample dissolution and Pb chromatography followed established standard procedures (Hoernle et al., 2008). Pb isotope ratios were measured using the Pb double-spike (DS) technique described in Hoernle et al. (2011) for mass-bias correction. Long term DS-corrected values for NBS981 are $^{206}Pb/^{204}Pb$ = 16.9408 ± 0.0018, $^{207}Pb/^{204}Pb$ = 15.4974 ± 0.0018 and $^{208}Pb/^{204}Pb$ = 36.7205 ± 0.0047 (2SD; n = 271) since installation of the instrument in 2014. USGS reference material BCR-2 processed along with the samples agrees well with the values of Fourny et al. (2016) and Todd et al. (2015). This comparison can be found in tabular form on the web site of the lab (https://www.geomar.de/en/research/fb4/fb4-muhs/infrastructure/tims). The total chemistry blank was 80 pg Pb and is considered negligible in relation to the amount of sample Pb processed.

3.5. Electron Micro Probe Analysis (EMPA)

Mineral analyses of Central Cuban Arc samples were conducted using a JEOL JXA-8900R EPMA at the University of Kiel (CAU). The instrument was operated at an accelerating voltage of 15 kV and a beam current of 15 or 20 nA. The analytical standards and lines used for analyses and the standard deviation (S.D.) were as follows: crn657s (Al_2O_3) with 0.09% S.D., rt_st8 (TiO_2) with 0.34% S.D., mic143966 (K_2O) with 0.26% S.D., Tug_Asti (Na_2O) with 0.27% S.D., chr117075 (Cr_2O_3) with 0.17% S.D., wolMAC (SiO_2; CaO) with 0.16 and 0.15%S.D. respectively, fay85276 (FeO) with 0.27% S.D., foMAC (MgO) with 0.14% S.D., and teph (MnO) with 0.15% S.D. The phi-rho-z matrix correction of Armstrong was used.

3.6. Sensitive high-resolution ion microprobe (SHRIMP)

U-Pb analyses of igneous zircons from Central Cuban Arc samples were performed using the SHRIMP II at the Beijing SHRIMP Center, Chinese Academy of Geological Sciences (CAGS), Beijing. Procedures and conditions were similar to those described by Williams (1998). The intensity of the primary O^{2-} ion beam was ~ 3.7nA, and the spot size was ~ 20 μm, with each site rastered for 2.5 min prior to analysis. Five scans through the mass stations were made for each age determination. Reference zircons M257 (U = 840 ppm, Nasdala et al., 2008) and TEMORA 1 ($^{206}Pb/^{238}U$ age = 417 Ma, Black et al., 2003) were used for elemental abundance and calibration of $^{206}Pb/^{238}U$, respectively. Common lead corrections were applied using the measured ^{204}Pb abundances and Cumming and Richards (1975) common Pb composition for the likely age of the rocks. Data processing was carried out using the SQUID and ISOPLOT programs (Ludwig, 2001, 2003a). Uncertainties in the isotopic ratios of individual analyses are given at 1σ, whereas uncertainties for weighted mean ages are quoted at 2σ.

3.7. Laser Ablation Inductively Coupled Plasma Mass Spectrometry (LA-ICP-MS)

Zircon U-Pb ages and trace element compositions of detrital zircon from Central Cuban Arc samples were measured in situ using an Agilent 7500a Quadrupole-ICP-MS coupled with a GeoLasHD 193 nm ArF excimer laser ablation system at Institute of Geology and Geophysics, Chinese Academy of Sciences (IGGCAS). Detailed analytical procedure followed those outlined in Xie et al. (2008). For most data reported here the density of energy at the ablation spots was 4.0 J cm^{-2} at 80 mJ output of energy and laser beam diameters were 32 μm at a repetition rate of 5 Hz. The dwell time for each isotope was set at 6 ms for ^{29}Si, ^{49}Ti, ^{93}Nb, ^{181}Ta, ^{91}Zr and REE, 15, 15, 30, 15 ms for ^{204}Pb, ^{206}Pb, ^{207}Pb and ^{208}Pb and 10 ms for ^{232}Th and ^{238}U. Each spot analysis comprised 20 s of gas background followed by 50 s of sample ablation. ARM-1 (Wu et al., 2019) were applied to calibrate the trace element concentration for all spot analyses. For most trace elements, the accuracy is better than 10%. The zircon standard 91500 (TIMS $^{207}Pb/^{206}Pb$ age = 1065.4 ± 0.3 Ma, 1s, n = 11; Wiedenbeck et al. 1995) was treated as an external reference zircon to calibrate mass bias and instrument drift, which measured twice every ten analyses. Another reference zircon SA01 (TIMS $^{206}Pb/^{238}U$ age = 535.08 ± 0.32 Ma; Huang et al., 2020) was analysed as an unknown to monitor the quality of age data. The $^{207}Pb/^{206}Pb$, $^{206}Pb/^{238}U$, $^{207}Pb/^{235}U$ and $^{208}Pb/^{232}Th$ ratios were calculated using the GLITTER program, whereas the ^{235}U signal was calculated from ^{238}U on the basis of the ratio $^{238}U/^{235}U$ = 137.818 (Hiess et al. 2012). The age calculations and plotting of Concordia diagrams were made using ISOPLOT (v3.23) (Ludwig 2003b).

U-Pb dating of igneous apatite from Central Cuban Arc samples was performed using an Element XR SF-ICP-MS instrument (Thermo Fisher Scientific, Bremen, Germany) coupled to a GeoLas HD 193 nm ArF excimer laser ablation system (Coherent, Gottingen, Germany) at the Institute of Geology and Geophysics, Chinese Academy of Sciences (CAS), Beijing, China. Procedures and instrument conditions were similar to those described by Wu et al. (2020). Low mass resolution (m/Δm = 300) was used to maximize sensitivity. Helium was used as the ablation gas to improve the transport efficiency of the ablated aerosols with 750 ml/min. A laser energy density of 3 J/cm^2 and a repetition rate of 5 Hz were used. The spot size was 32 μm. Prior to analysis, possible surface contamination was removed by pre-ablation with two laser pulses. The NW-1 apatite (Li et al., 2012) was used as a primary the reference standard for the age calculations. Calibration of the $^{207}Pb/^{206}Pb$ ratio was done using analyses of the NISTSRM 612 reference glass analysed under the same conditions as the unknowns. EML apatite (Chew et al., 2011) employed as secondary geochronology reference materials and were treated as unknowns to evaluate the precision and accuracy of the

method. Data processing package used VizualAgeUcomPbine data reduction scheme written for Iolite (version 3.71; Chew et al., 2014). Measured isotopic ratios for these apatites were corrected using the Stacey & Kramers (1975) model and their ages projected to concordia. Data is quoted at 2σ. Uncertainty propagation is by quadratic addition including long term reproducibility of secondary reference materials and the uncertainty of the primary reference material.

Hf isotopic compositions of igneous and detrital zircons from the Central Cuban Arc samples were measured using a Neptune Plus MC-ICP-MS (Thermo Fisher Scientific, Bremen, Germany) coupled with a 193 nm Analyte G2 laser ablation system (Photon Machines, USA, equipped with an ANU HelEx 2-volume cell) housed at the Institute of Geology and Geophysics, Chinese Academy of Sciences (IGGCAS). Procedures and instrument conditions were similar to those described by Huang et al. (2022). A standard sample cone in combination with a X-type skimmer cone was used. The laser fluence was set to 3 J/cm^2 with laser repetition rate set to 6 Hz, and the spot size to 40 μm for analysis. Helium was used as the carrier gas within the ablation cell. N_2 was added into the carrier gas at 4.4 ml/min though a three-way tube. ^{172}Yb, ^{173}Yb, ^{175}Lu, ^{176}Hf, ^{177}Hf, ^{178}Hf, ^{179}Hf and ^{177}Hf^{16}O ion beams were measured simultaneously by eight Faraday cups all connected with 1011 Ω amplifiers. Isotope and oxide signals were collected in one block comprising two hundred cycles with a 0.131 s integration time. SA01 zircon (^{176}Hf/^{177} = 0.282293 ± 0.000007, 2σ, n = 30; Huang et al., 2020) was used as primary standard for all spot analyses. SA02 zircon (^{176}Hf/^{177} = 0.282287 ± 0.000016, n = 31; Huang et al., 2021) was treated as an external reference to monitor the quality of data. All data of in situ Hf isotope analysis were reduced using an in-house Microsoft Excel macro written in VBA (Visual Basic for Applications). The detailed procedures were described by Wu et al. (2006). For isobaric interference corrections, the fractionation coefficient (βYb) was firstly calculated using the mean ^{173}Yb/^{172}Yb ratio of the individual spot. The contribution of ^{176}Yb to ^{176}Hf was determined by applying ratios of ^{176}Yb/^{172}Yb = 0.588673 and ^{173}Yb/^{172}Yb = 0.73925. The intensity of interference-free ^{175}Lu isotope was used for the correction of ^{176}Lu on ^{176}Hf with a recommended ^{176}Lu/^{175}Lu ratio of 0.02655 and assuming βLu = βYb. The ^{176}Yb/^{177}Hf, ^{176}Lu/^{177}Hf and ^{176}Hf/^{177}Hf ratios were normalized to ^{179}Hf/^{177}Hf = 0.7325 using the exponential law. The oxide ratio of Hf isotope is presented by ^{177}Hf^{16}O/^{177}Hf. All data obtained were reported with an uncertainty of two standard deviations unless noted otherwise.

3.8. Database Compilation

A fourfold tectonic subdivision of the GAA (Fig. 3) is adopted, based on a southwest-dipping subduction system widely accepted by most researchers working in the Caribbean region (e.g., Pindell et al., 2005; Escuder-Viruete et al., 2006a; Escuder-Viruete et al., 2007; García-Casco et al., 2006; García-Casco et al., 2008; Pindell & Kennan, 2009; Boschman et al., 2014; Rojas-Agramonte et al., 2021). This subdivision is based on modern geographic relationships of rock units relative to the present position of the magmatic arc and groups published data on GAA rocks into four tectonic domains:

(a) forearc mélange; (b) forearc ophiolite; (c) magmatic arc (Cretaceous and Paleogene); and (d) retro-arc region, including metamorphic terranes and igneous rocks.

Although this framework does not necessarily correspond to the precise geotectonic configuration of these complexes during the Cretaceous, it provides a useful approximation for comparing datasets across the arc. Geochronological and geochemical data compiled from the peer-reviewed literature for Cuba, Hispaniola, Puerto Rico, Jamaica, and the Virgin Islands were assigned to one of the four tectonic subdivisions.

The geochronological compilation, following the approach of Wilson et al. (2019). Whole-rock geochemical analyses were screened to exclude highly altered compositions, using loss on ignition (LOI) as a criterion; only samples with LOI < 4 wt.% were retained. Further filtering removed samples lacking trace element data, and only screened samples were used for plotting trace element diagrams. Immobile trace element ratios were employed to classify lithologies and distinguish the tectonic affinities of felsic and mafic GAA components. For tectonic discrimination diagrams, lithologies classified as basalt, basaltic andesite, and alkali basalt were grouped as “mafic” whereas dacite/rhyolite, trachy-andesite, and trachyte were grouped as “felsic”.

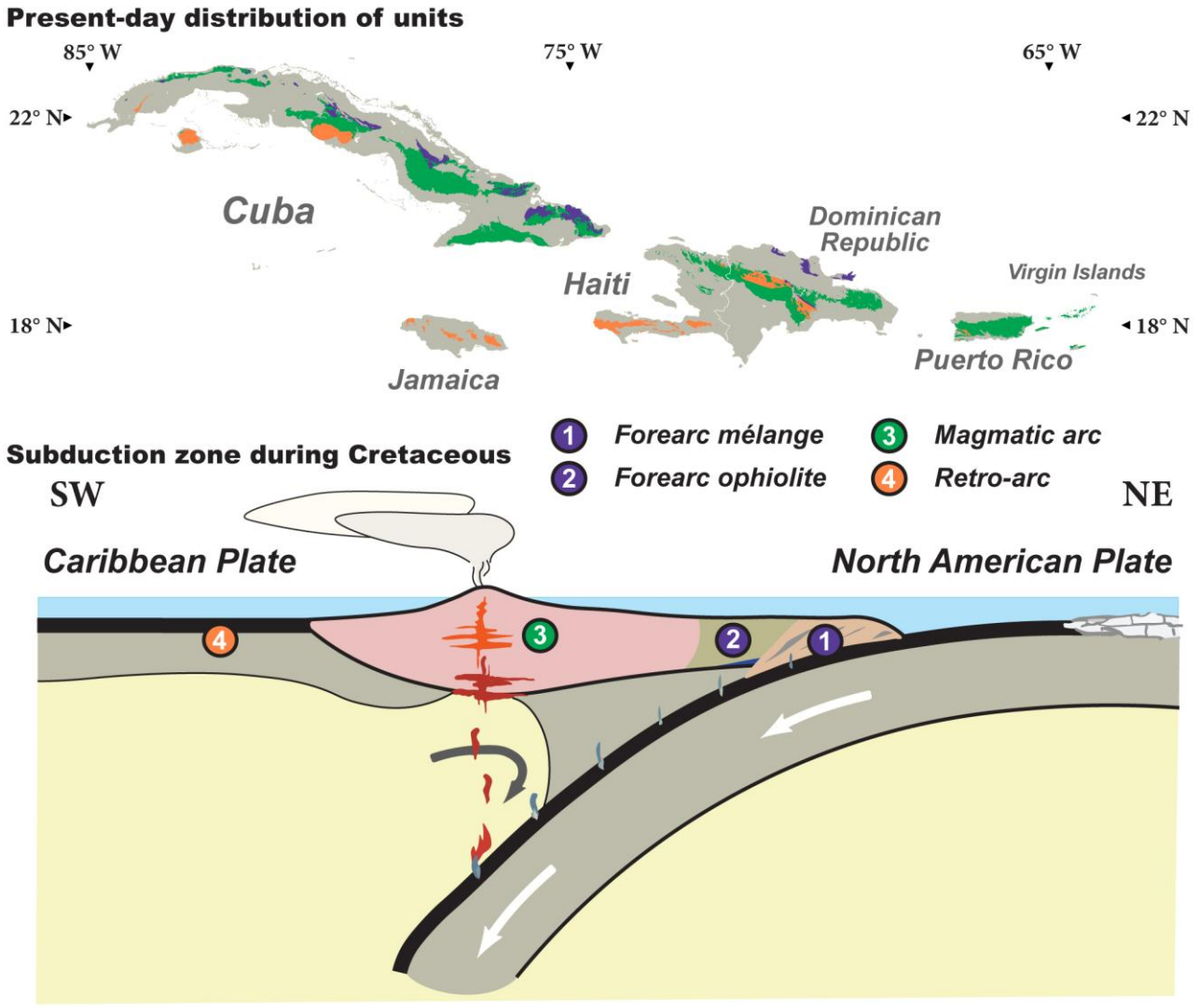

Figure 3. *Simplified tectonic map of the Greater Antilles Arc showing the present-day location of geologic units in the fourfold subdivision. Below shows simplified cross-section of the Greater Antilles Arc during Cretaceous times in the fourfold subdivision discussed here with respect to the location of the magmatic arc.*

3.9. Isotopic Modelling

The isotopic ratio and element concentrations of endmembers are summarized in the table below. Depleted mantle (DM) concentrations of Sr, Nd, Pb and isotopic ratios of $^{87}Sr/^{86}Sr$, $^{143}Nd/^{144}Nd$, $^{206}Pb/^{204}Pb$, $^{207}Pb/^{204}Pb$, and $^{208}Pb/^{204}Pb$ were adopted from Rehkämper and Hofmann (1997). Atlantic Cretaceous pelagic sediment (AKPS) and Site 144 sediment isotopic ratios of $^{87}Sr/^{86}Sr$, $^{143}Nd/^{144}Nd$, $^{206}Pb/^{204}Pb$, $^{207}Pb/^{204}Pb$, and $^{208}Pb/^{204}Pb$ from Jolly et al. (2006) and Carpentier et al. (2008), whereas element concentrations (Sr, Nd, Pb) were calculated using solid-fluid partition coefficients ($D_{sol/fluid}$) reported by Johnson and Plank (2000). Mixing lines were constructed using the isotopic mixture equation of Faure and Mensing (2005) (Eq. 5).

$$R_m = \frac{f_A C_A R_A + (1 - f_A) C_B R_B}{f_A C_A + f_B C_B}$$

Where, R_m is the isotopic ratio of the mixture, R_A and R_B are the isotopic ratios of the components A and B; C_A and C_B are the concentrations of the relevant element in components A and B; f_A and f_B are the weight fraction of components A and B in the mixture.

Summary of endmember and partition coefficients used for isotope mixing calculations.

	Dm[a]	Fluid AKPS 105/15/6[b]	Fluid AKPS 105/18/6[b]	Fluid AKPS 105/37/5[b]	Fluid AKPS 105/37/6[b]	Fluid AKPS 417D/18/2[b]
Sr (ppm)	11.300	243.956	868.132	191.209	197.802	89.011
Pb (ppm)	1.120	22.340	12.766	21.277	23.404	15.957
Nd (ppm)	0.049	23.153	16.563	22.715	27.097	16.840
$^{87}Sr/^{86}Sr$	0.7025	0.7144	0.7082	0.7143	0.7166	0.7284
$^{144}Nd/^{143}Nd$	0.51320	0.51273	0.51220	0.51215	0.51214	0.51196
$^{206}Pb/^{204}Pb$	18.00	18.88	18.93	18.75	18.73	18.99
$^{207}Pb/^{204}Pb$	15.43	15.69	15.68	15.70	15.69	15.68
$^{208}Pb/^{204}Pb$	37.70	38.93	38.86	38.97	38.92	39.06

	Fluid AKPS 417D/19/1[b]	Fluid AKPS 417d/21/3[b]	Fluid Site144 unit2[c]	Fluid Site144 unit3[c]	Fluid Site144 unit4&5[c]
Sr (ppm)	115.385	260.440	-	-	-
Pb (ppm)	18.085	25.532	6.574	5.585	9.979
Nd (ppm)	41.458	48.257	10.972	4.597	14.375
87Sr/86Sr	0.7149	0.7130	-	-	-
$^{144}Nd/^{143}Nd$	0.51219	0.51220	0.51191	0.51185	0.51211
$^{206}Pb/^{204}Pb$	18.90	19.35	19.80	21.84	18.90
$^{207}Pb/^{204}Pb$	15.72	15.71	15.83	15.92	15.69
$^{208}Pb/^{204}Pb$	39.08	38.63	39.61	39.42	38.98

	Partition coefficients
	$D_{sol/fluid}$[d]
Sr (ppm)	0.91
Nd (ppm)	1.44
Pb (ppm)	0.94

[a]DM: Depleted mantle; Salters and Stracke (2004)

[b]Fluid AKPS: Atlantic Cretaceous pelagic sediment fluid; Jolly et al. (2006)

[c]Site144: DSDP Site144 sediment fluid; Carpentier et al. (2008)

[d]Partition Coefficients of $D_{sol/fluid}$ from Johnson and Plank (1999)

3.10. Thermobarometry

Single-mineral thermobarometric models were applied to estimate crystallization pressures and temperatures from clinopyroxene, amphibole, and biotite in volcanic and volcaniclastic rocks (Ridolfi et al., 2010; Ridolfi, 2021; Petrelli et al., 2020; Wang et al., 2021; Jorgensen et al., 2022; Li & Zhang, 2022; Higgins et al., 2022; Ágreda-López et al., 2024). Both empirical and machine learning based calibrations were used, based on major-element mineral data obtained by EMPA. The analysed crystals include magmatic phenocrysts and crystal fragments, representing a range of magmatic and post-eruptive conditions.

Machine learning based thermobarometry approaches and traditional regression models can both be applied to sector-zoned mantles. For resorbed cores, traditional regression-based models calibrated using isothermal-isobaric experimental datasets or machine learning based models can still yield geologically realistic estimates of magmatic storage conditions (MacDonald et al., 2023). Analyses were selected from compositionally homogeneous domains identified in backscattered electron (BSE) images to minimize the effects of alteration and re-equilibration. Zoned and texturally complex crystals were also analysed to evaluate compositional and thermobarometric variations associated with disequilibrium growth. Calculations were performed on distinct crystal zones (core, mantle, rim) to ensure systematic assessment of equilibrium and disequilibrium domains. Results from strongly heterogeneous or resorbed areas were treated cautiously and used primarily to evaluate relative P-T trends rather than representative equilibrium conditions.

Model performance was evaluated using both calibration and validation statistics. Calibration parameters, including the coefficient of determination (R^2) and the standard error of estimate (SEE), quantify the fit between predicted and experimental values within the calibration dataset. Validation metrics, such as R^2 and the root mean square error (RMSE), assess predictive accuracy on independent data. Together, these statistics provide a comprehensive evaluation of model reliability and applicability to natural mineral compositions. Regression slopes and intercepts between predicted and experimental values were also examined to assess systematic bias relative to the ideal 1:1 relationship.

Summary of single-mineral thermobarometric calibrations used in this study. Abbreviations: Cpx: clinopyroxene; Amp: amphibole; Bt: biotite.

Calibration	Mineral	Approach	SEE (°C/kbar)	RMSE (°C/kbar)	R2 (T/P)	Slope(T/P)	Intercept(T/P)	Reported uncertainty (T/P)
Petrelli et al. 2020	Cpx	Machine learning (Extra trees)	-	66/3.2	0.83/0.88	-	-	-
Jorgenson et al. 2022	Cpx	Machine learning (Extra trees)	72.5/3.2	-	0.85/0.86	-	-	-
Higgins et al. 2022	Cpx	Machine learning (Extra trees)	53/2.3	-	-	-	-	-
Ágreda-López et al. 2024	Cpx	Machine learning (Extra trees)	-	57/2.5	0.86/0.90	0.85/0.92	173.1/0.4	-
Wang et al. 2021	Cpx	Empirical	36.6/1.66	-	0.86/0.86	-	157/0.73	-
Higgins et al. 2023	Amp	Machine learning (Extra trees)	41/1.6	-	-	-	-	-
Ridolfi et al. 2010	Amp	Empirical	-	-	-	-	-	-
Ridolfi 2021	Amp	Empirical	-	-	-	-	-	22°C/12%
Li and Zhang 2022	Bt	Machine learning (Extra trees)	-	65/4.7	0.85/0.80	-	-	-

4. Main results and discussions

Article 1 (Appendix 1): Review of Geochronologic and Geochemical Data of the Greater Antilles Volcanic Arc and Implications for the Evolution of Oceanic Arcs

The Greater Antilles Arc (GAA) preserves a fossil intra-oceanic convergent margin, and synthesis of its geochronologic and geochemical records provides a comprehensive framework for understanding the temporal and compositional evolution of Caribbean subduction systems. The integrated dataset, incorporating 662 radiometric age determinations and more than 1537 geochemical analyses from Cuba, Hispaniola, Puerto Rico, Jamaica, and the Virgin Islands, allows a detailed reconstruction of the magmatic, metamorphic, and tectonic history of this arc. When examined within the context of its four major structural domains: the fore-arc mélange, fore-arc ophiolite, magmatic arc, and retro-arc terranes, the data reveal a complete record of oceanic arc evolution, from subduction initiation in the Early Cretaceous to arc termination and continental collision in the Paleogene.

The integrated temporal and spatial distribution of radiometric ages defines a coherent history of the principal stages of arc development and metamorphic overprinting, offering critical insights into the tectonic architecture of the system and its progressive evolution. Ages range from about 155 to 30 Ma, with most clustering between 120 and 40 Ma, marking the main interval of arc activity. Three distinct peaks are recognized: an early stage between 120 and 110 Ma, a dominant magmatic-metamorphic pulse between 95 and 60 Ma, and a late event near 40 Ma (Fig. 4). The earliest ages correspond to subduction initiation and the formation of oceanic lithosphere within fore-arc ophiolitic sequences, recording the onset of Early Cretaceous supra-subduction magmatism and subduction-zone metamorphism. The 95-60 Ma interval represents the thermal and magmatic climax of the arc system, when magmatism, metamorphism, and crustal differentiation reached maximum intensity, producing the majority of plutonic and volcanic crystallization ages and extensive metamorphic resetting. The youngest peak, around 40 Ma, is associated with the waning of magmatic activity and the onset of collisional deformation along the western margin during convergence with North America. Collectively, the temporal and spatial patterns reveal a progressive migration of magmatic loci from trenchward to arcward through time, reflecting dynamic subduction geometry, progressive crustal growth, and the maturing thermal structure of the evolving GAA.

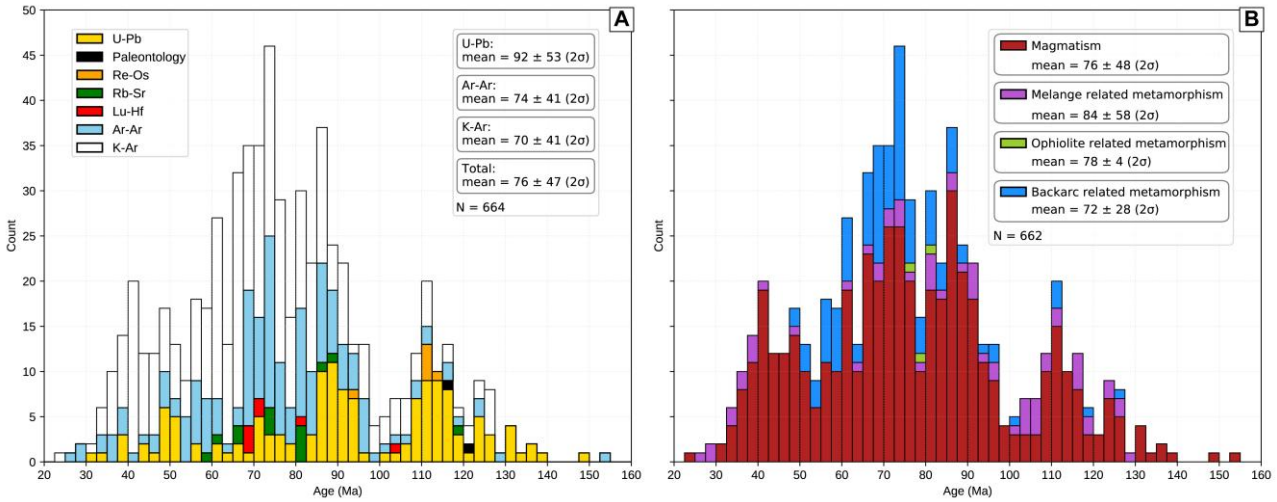

Figure 4. *Histogram of compiled age data for the GAA, including Cuba, Hispaniola, Jamaica, Puerto Rico, and Virgin Islands sorted by (a) geochronologic method and (b) magmatism and metamorphism (based on association to mélange, ophiolite or retro-arc). Results of radiometric dating and paleontology age constraints show the temporal spectrum of the GAA magmatic and metamorphic events. Ages range from 155 Ma (Jurassic) to 30 Ma (Oligocene), but the vast majority are Cretaceous and Paleogene.*

The geochemical dataset of the Greater Antilles Arc further illuminates its magmatic evolution and mantle dynamics. Arc rocks are predominantly mafic to intermediate in composition and display typical subduction-related trace element patterns (Fig. 5), with enrichments in large ion lithophile elements (LILE) and depletions in high field strength elements (HFSE), reflecting a mantle wedge metasomatized by slab-derived fluids and melts in an intra-oceanic setting. Major-element systematics indicate an early tholeiitic stage followed by later calc-alkaline differentiation trends. Across the arc, subtle but systematic geochemical variations are observed. Fore-arc and early-arc rocks display island-arc tholeiitic affinities, whereas retro-arc rocks exhibit transitional compositions trending toward mid ocean ridge basalt (MORB) and ocean island basalt (OIB) signatures (Fig. 5). This compositional gradient, reflecting increasing contributions from enriched mantle components away from the trench, suggests that the sub-arc mantle progressively interacted with upwelling material from the Caribbean Large Igneous Province (CLIP). The temporal coincidence between the 95-60 Ma magmatic peak and the emplacement of the CLIP indicates that the influx of hot, buoyant plume material affected the plate boundary of the GAA, particularly in retro-arc domains, as recorded in both magmatic and metamorphic assemblages. The extent and intensity of this plume arc interaction, however, require subjects for further investigation.

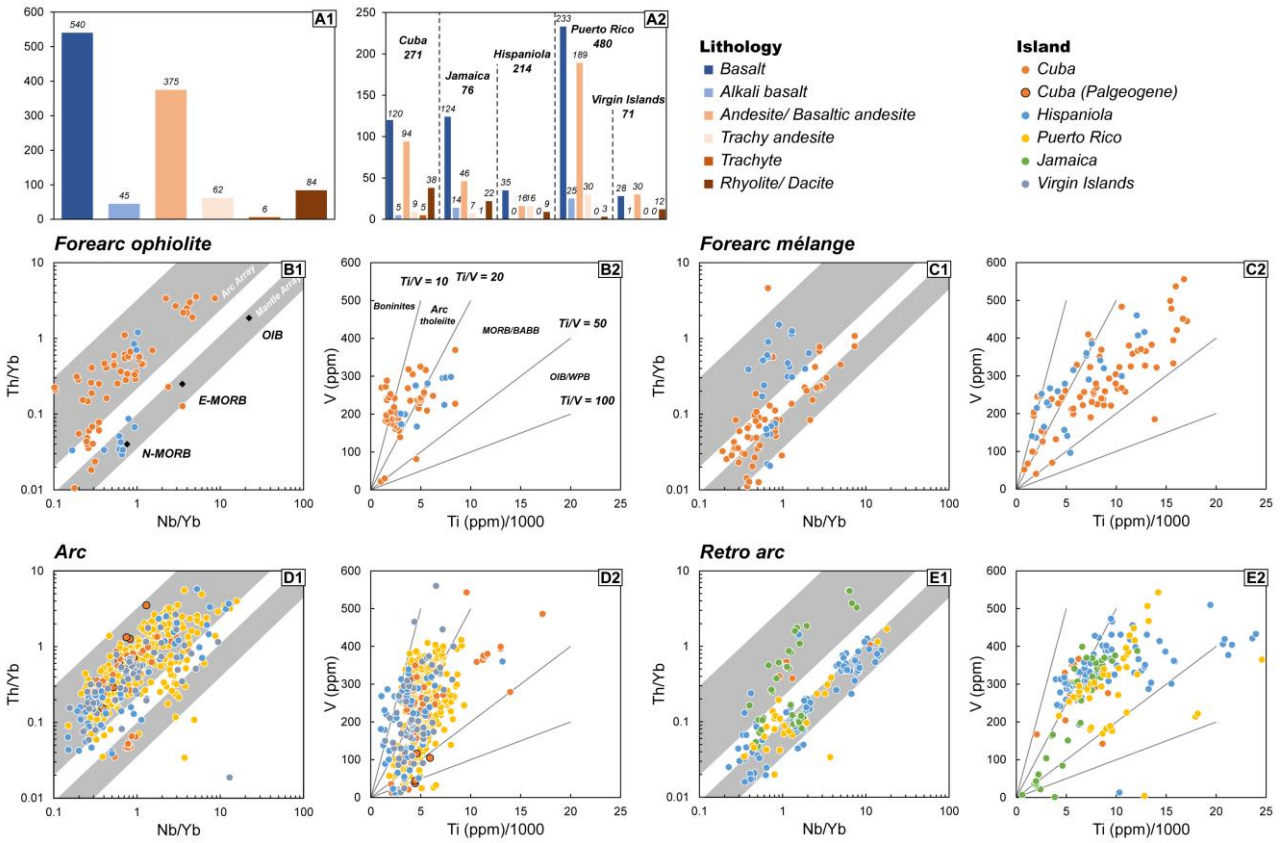

Figure 5. *(A1-2) Histogram with lithologies from 1112 Greater Antilles Arc samples based on the Zr/Ti versus Nb/Y classification (after Pearce, 1996). GAA mafic samples (of basalt, alkali basalt and andesite/basaltic andesite composition) plotted on the Th/Yb versus Nb/Yb of Pearce (2008). Volcanic arc array and mantle array are indicated. And Ti/1,000 (ppm) versus V (ppm) diagram from Shervais (1982). (B1-2) forearc ophiolite; (C1-2) forearc mélange; (D1-2) arc; (E1-2) retro-arc.*

The compilation of unfiltered sampling data also highlights potential biases that may influence the apparent patterns, including differences in analytical techniques, isotopic systems preferentially sensitive to particular geological processes, and uneven spatial coverage among islands. In particular, data gaps persist in submerged or poorly exposed segments of the subduction system. Recognizing these limitations, the integrated dataset not only refines the current model of Caribbean arc evolution but also identifies key regions for future targeted studies. Overall, the combined geochronologic and geochemical data establish the Greater Antilles Arc as a model example of an intra-oceanic arc that records a full evolutionary cycle, from subduction initiation to collisional extinction. The results further demonstrate that, in addition to subduction-driven processes, the system was influenced by interactions between the subducting slab and the upwelling Caribbean plume across distinct tectonic domains.

Article 2 (Appendix 2): Exotic vs local Caribbean origin for the arc-related Mabujina Amphibolite Complex (Cuba): implications for segmentation of the Caribbean arc during the Cretaceous

The Mabujina Amphibolite Complex (MAC) of central Cuba represents an arc-related metamorphic complex that provides crucial insight into accretionary and tectonic processes in intra-oceanic arc settings of the Caribbean region (Fig. 6A). While most authors have interpreted the Mabujina Complex (Porvenir Fm. and MAC; Fig. 6B and C) as the metamorphosed root of the Cretaceous volcanic arc (Somin & Millán, 1981; Dublan & Álvarez, 1986; Bibikova et al., 1988; Iturralde-Vinent, 1994; Grafe et al., 2001; Stanek et al., 2006), other studies have proposed that it represents an exotic volcanic arc section derived from the Pacific-related Guerrero volcanic arc terrane of central western Mexico, later accreted to the base of the Cuban arc during Cretaceous (e.g., Blein et al., 2003; Rojas-Agramonte et al., 2011). This study addresses this long-standing conundrum using extensive whole-rock geochemical and Sr-Nd isotopic data to constrain the provenance of the protolith and assess its tectonic significance within the regional Cretaceous arc framework.

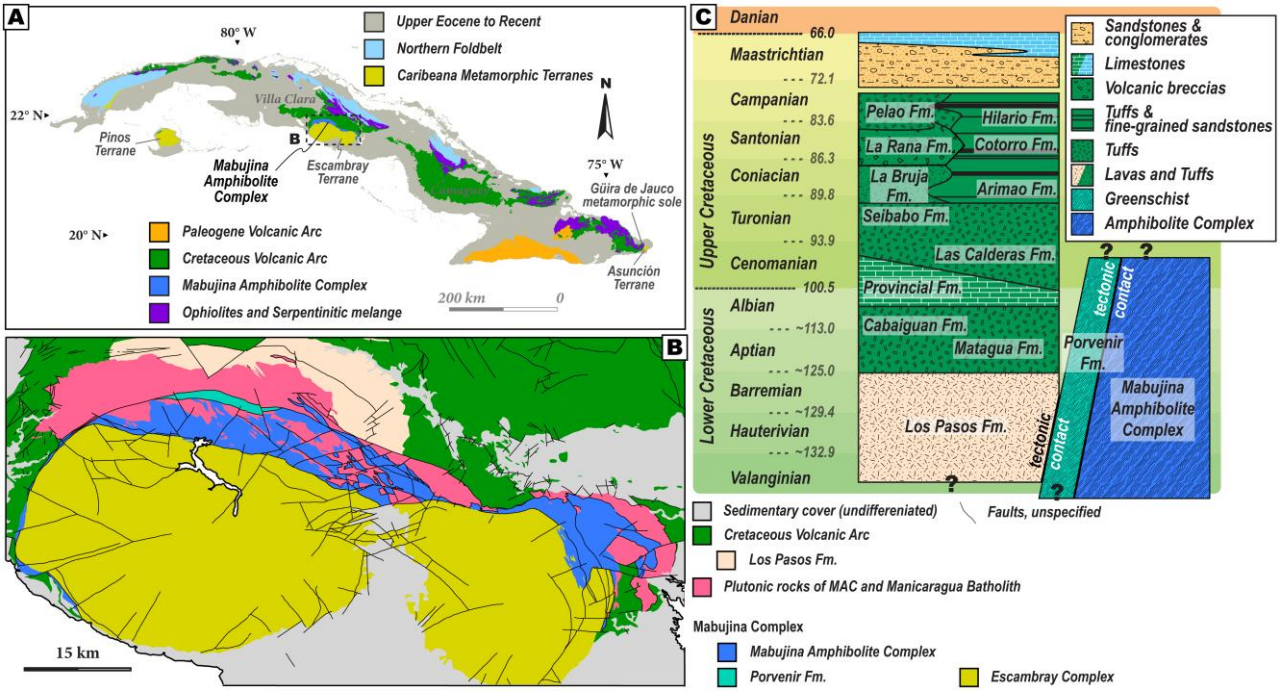

Figure 6. *(A) Simplified geological map of Cuba. (B) Geological map of south-central Cuba after García-Delgado (1998). (C) Stratigraphic sequences of volcanic and sedimentary units of the central Cuban arc and the Mabujina Complex which include the Mabujina Amphibolite Complex and the Porvenir Formation (slightly modified after Iturralde-Vinent 2019). The plutonic rocks represent ages, not intrusive contacts.*

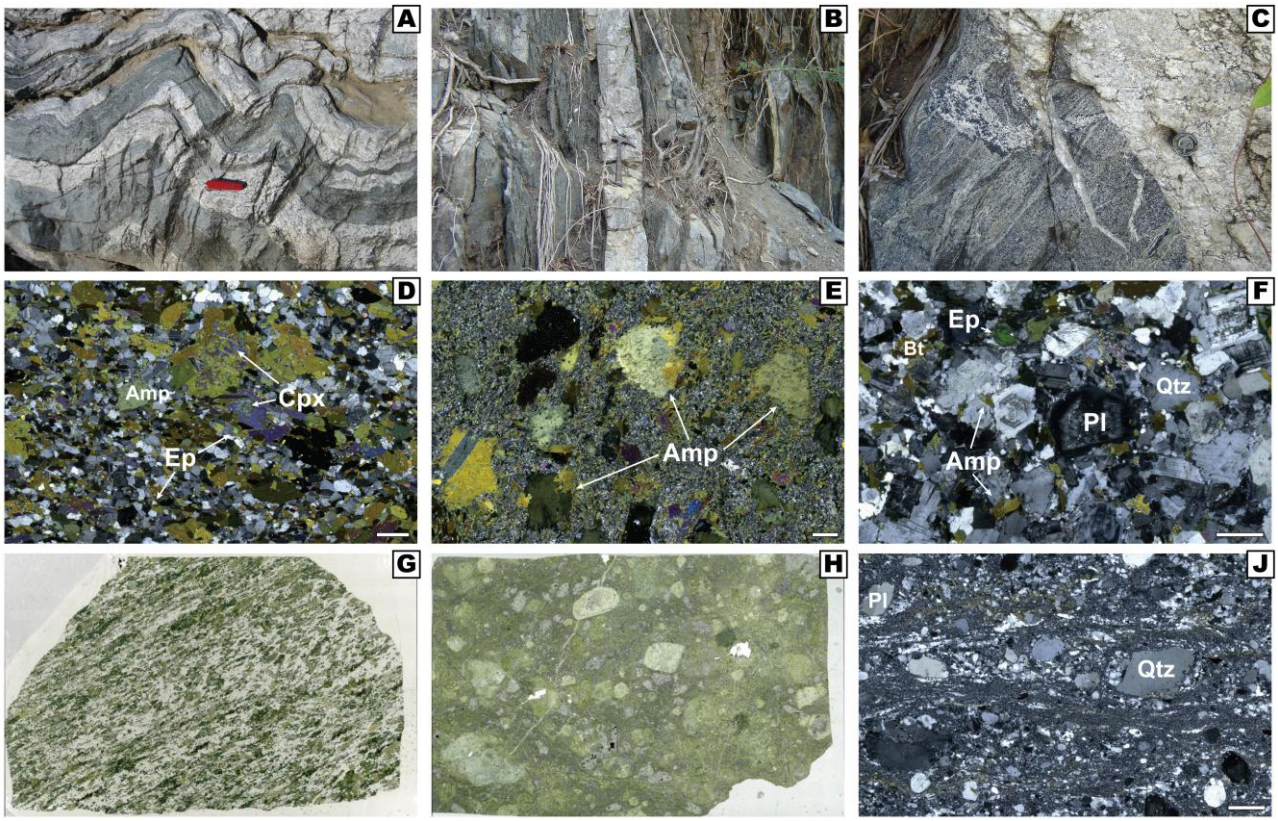

Figure 7. *Field photographs showing rock relationships within the Mabujina Amphibolite Complex (A-C) and photomicrographs of igneous and metamorphic rocks from the Mabujina Amphibolite Complex (D-F, J) showing under cross-polarized light and (G, H) showing whole thin section under plan-polarized light (3 x 5 cm in size). (A) Foliated and subsequently folded amphibolite and early tonalite-trondhjemite. Ductile deformation resulted in parallel tectonic contacts between these units, (B) Orthogneiss layers parallel to the main foliation of the amphibolites, (C) Leucocratic segregates crosscutting the metamorphic foliation of the amphibolite possibly generated by hydrated partial melting, (D) Foliated epidote-amphibolite shows relics of magmatic clinopyroxene, (E) Non-foliated amphibolite with remaining porphyritic subvolcanic texture from basaltic protolith, (F) Medium-grained undeformed tonalite from the MAC with oscillatory-zoned plagioclase crystals, (G) Foliated amphibolite, (H) Unfoliated amphibolite preserves magmatic texture, (J) concordant felsic vein from the MAC shows mylonitic texture, ribbons of quartz and plagioclase with pressure shadows. Abbreviations: Amp: amphibole; Cpx: clinopyroxene; Ep: epidote; Pl: plagioclase; Qtz: quartz. White bar indicates 500 µm.*

Petrographic observations show that the amphibolites of the MAC display predominantly nematoblastic textures with well-developed peak metamorphic foliation, though some less deformed samples retain subvolcanic features (Fig. 7). They consist mainly of amphibole and plagioclase in variable proportions, with epidote and locally clinopyroxene as stable peak phases, and minor biotite, titanite, apatite, magnetite, and ilmenite as accessory minerals. Relicts of magmatic pyroxene are locally preserved and partly replaced by amphibole ± metamorphic pyroxene, whereas recrystallized clinopyroxene forms polygonal grains in equilibrium with amphibole and plagioclase. Retrograde assemblages composed of actinolite-hornblende, epidote, albite, and chlorite indicate retrogression under epidote amphibolite to greenschist facies conditions. Associated orthogneisses are medium grained, inequigranular granitoids composed of plagioclase, quartz, K-feldspar, amphibole, biotite, and locally garnet, with apatite and zircon as accessories. Quartz shows variable undulose extinction to complete recrystallization, reflecting deformation followed by recovery, while chlorite and epidote are common retrograde phases.

Whole-rock immobile trace element data demonstrate that the MAC protoliths formed in a subduction-related environment and share strong compositional similarities with other sections of the Cretaceous Cuban arc (Fig. 8). The amphibolites are basaltic to basaltic-andesitic, and the orthogneisses are tonalitic in composition. Two geochemical subgroups of the amphibolite are recognized: a dominant calc-alkaline group and a subordinate tholeiitic group. Both exhibit enrichment in LILE and depletion in HFSE, producing marked negative Nb-Ta anomalies and Th enrichment typical of island arc basalts. The REE patterns of the calc-alkaline subgroup and tonalitic orthogneisses show highly enriched light over heavy rare earth elements and total REE concentrations similar to Late Cretaceous calc-alkaline igneous rocks of the Caribbean arc. In contrast, the tholeiitic subgroup displays flatter REE patterns and lower Th contents. These trace-element and Sr-Nd isotopic systematics are indistinguishable from those of the Cretaceous volcanic sequences in central Cuba, such as the early tholeiitic Los Pasos Formation and the transitional to calc-alkaline Mataguá and Cabaiguán Formations, but differ markedly from the more enriched, radiogenic signatures of the Guerrero Terrane (Fig. 8B; Blein et al., 2003).

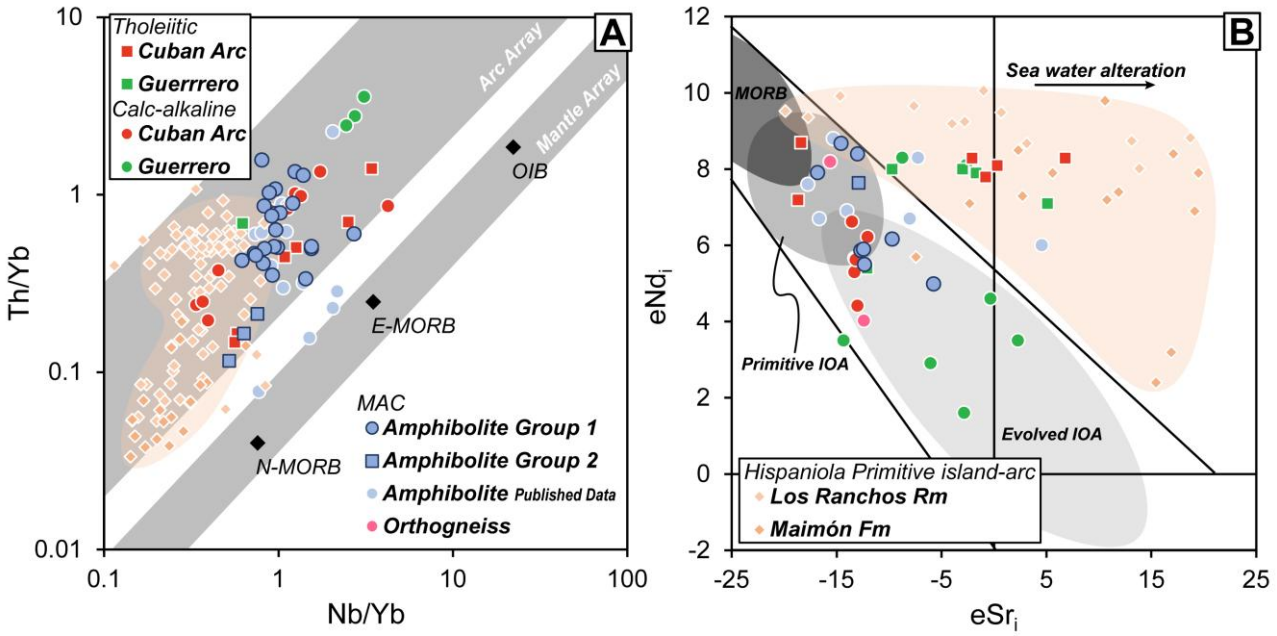

Figure 1: *(A) Basaltic and basaltic andesitic samples plotted on the Th/Yb versus Nb/Yb of Pearce (2008). (B) Age-corrected Sr-Nd radiogenic isotope ratios of whole-rocks from amphibolite and orthogneisses of the MAC. Comparing to tholeiitic and calc-alkaline rocks of Cuban Arc and Guerrero Arc, other tholeiitic sequences (Los Ranchos and Maimom formation) also indicated.*

The geochemical affinity between the MAC protolith and the Cretaceous volcanic sequences of the Caribbean arc in Cuba suggests that the >135 to ca. 93 Ma protolith formed within or near the Caribbean arc realm. Zircon U-Pb ages indicate that the oldest MAC protolith predates 133 Ma, slightly older or roughly coeval with the earliest arc magmatism in central Cuba (Los Pasos Formation, ~135-125 Ma), consistent with subduction initiation around 135 Ma. These constraints support the interpretation that the MAC represents an integral fragment of the Caribbean intra-oceanic arc rather than an exotic terrane (Fig. 9). Prior to its tectonic emplacement beneath central Cuba, the proto-MAC consisted of mafic magmatic rocks evolving from tholeiitic to calc-alkaline affinity between the Early and Late Cretaceous (~93 Ma). Its proximity to the central Cuban segment during the mid-Cretaceous, within a regional sinistral transpressional regime associated with oblique subduction, fragmented the arc and facilitated crustal juxtaposition along strike-slip shear zones comparable to those in Hispaniola between 95 and 74 Ma (Escuder-Viruete et al., 2006b). This tectonic regime likely enabled the accretion of the proto-MAC beneath the Central Cuban Arc by the late Turonian (~90 Ma), in a process analogous to intra-oceanic collisions observed in modern arcs such as the Philippine system.

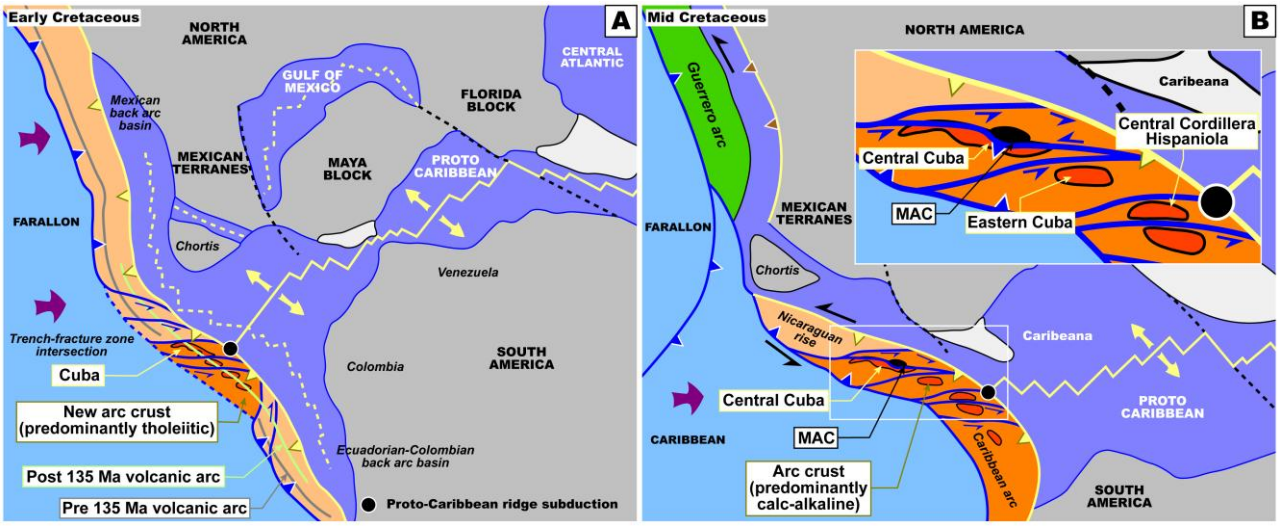

Figure 9. *A) and B) Early to Mid-Cretaceous geodynamic scenario for the development of the MAC following Pindell and Kennan (2009), Pindell et al. (2012), and Torró et al. (2016). The corresponding tholeiitic/calc-alkaline section of the Caribbean volcanic arc would have undergone metamorphism and deformation due to intra-arc collision triggered by strike-slip faulting and volcanic arc segmentation in a context of strong oblique subduction during the Cretaceous. b) Location of the Guerrero terrane in western Mexico related to Pacific (Farallon) subduction is indicated. Note that an exotic Guerrero origin of the MAC is not favored in this geodynamic scenario. Inset in b) Inferred position of Central Cuba, Eastern Cuba and Hispaniola. Evidence for the subduction of the ridge during the Mid-Cretaceous have been documented in Hispaniola by Rojas-Agramonte et al. (2021) and Escuder-Viruete et al. (2007).*

Collectively, the geochemical coherence and temporal alignment of the MAC with other Cuban arc units support its interpretation as part of a laterally continuous intra-oceanic arc system, rather than an exotic arc fragment emplaced from a distant Pacific source. The MAC therefore preserves a deep, metamorphosed section of the Cretaceous Caribbean arc crust, providing a rare window into sub-arc processes and crustal evolution during intra-oceanic subduction and subsequent arc-arc collisional deformation. However, further constraints on the P-T-t evolution of the MAC are needed to fully resolve the sequence and dynamics of this accretion and collision event.

Article 3 (Appendix 3): Prolonged evolution of an intra-oceanic island arc: The ~60 Myr record of Central Cuba

The continuous and well-exposed section in central Cuba offers one of the clearest examples of temporal and structural evolution of an intra-oceanic arc, recording its development from subduction initiation through magmatic differentiation and crustal thickening to eventual collisional shutdown. Within the framework of the regional geochemical and geochronological synthesis of the Caribbean system (Article 1), the central Cuban segment was selected for systematic study to better constrain the magmatic evolution of the arc. This stratigraphic and geochemical record allows direct comparison with the arc-related metamorphic complex (MAC, see Article 2) and provides a well-preserved reference for understanding the lithochemical evolution of intra-oceanic arc, from upper crustal volcanic sequences and associated plutonism.

The Central Cuban Arc records a prolonged, ~60 Myr evolution, documented through a series of temporally constrained volcanic and plutonic units dated by U-Pb zircon and apatite analyses. Although apatite ages are challenging to determine precisely due to low uranium contents and young crystallization ages, the stratigraphic and radiometric data are in good agreement. The earliest magmatic stage, prior to 125 Ma, corresponds to rapidly emplaced, lava flow dominated tholeiitic volcanism represented by the Los Pasos Formation. Whole-rock geochemical data exhibit flat to slightly LREE-depleted REE patterns consistent with high-degree partial melting of a dry, depleted mantle source. The rocks show elevated $^{87}Sr/^{86}Sr$ ratios attributed to seawater-rock interaction, consistent with submarine eruption. During the mid-Cretaceous (~120 to >95 Ma), transitional sequences show stronger LREE and Th enrichment and moderate MREE-HREE fractionation, recording the progressive addition of slab-derived components, including minor inputs of heterogeneous sediment and fluids derived from altered oceanic crust into the mantle wedge. By the late Cretaceous (~95-75 Ma), volcanic and volcaniclastic assemblages became compositionally more diverse, dominated by andesitic to dacitic rocks commonly containing amphibole phenocrysts. These calc-alkaline sequences are associated with more explosive volcanism and major plutonism, mark the development of a matured, hydrous, and thickened arc crust.

Sr-Nd-Pb isotopic compositions remain remarkably homogeneous throughout the arc evolution, consistent with a depleted mantle source and the absence of significant continental contamination. Initial εNd values consistently range from +7 to +8, and Pb isotopes plot close along the Northern Hemisphere Reference Line and DMM reservoir. Transitional units, such as the Cabaiguán Formation

trending toward higher $^{206}Pb/^{204}Pb$ ratios, which may reflect the incorporation of subducted Oceanic Anoxic Event (OAE1a-b) sediments characterized by elevated U/Pb ratios. Isotopic mixing models indicate that incorporation of only ~1% sediment-derived fluid is sufficient to account for the observed isotopic variations, with slab contributions increasing slightly from tholeiitic to calc-alkaline stages. The overall isotopic coherence indicates that magmatic source was governed primarily by slab-fluid metasomatism within an oceanic subduction environment, without significant involvement of continental crust or a major change in mantle source composition. Age distributions and Hf isotopes compositions of detrital zircon from interbedded volcaniclastic and sedimentary rocks confirm that grains are derivation from the active arc itself.

Mineralogical and textural features record the transition from a rapidly ascending, dry magmatic regime to a hydrous, storage dominated arc crust. Early to mid-Cretaceous assemblages are commonly composed of clinopyroxene ± orthopyroxene with weak or normal zoning, consistent with low-water, high-temperature tholeiitic differentiation at shallow crustal levels. In contrast, Late Cretaceous calc-alkaline rocks contain abundant amphibole and occasional biotite, reflecting crystallization under hydrous conditions. Phenocrysts in the Calc-alkaline stage commonly display disequilibrium textures such as oscillatory and sector zoning, resorbed cores, and complex overgrowths, indicating repeated magma recharge, mixing, and crystal recycling within compositionally zoned reservoirs. A prolonged magmatic storage regime with efficient isotopic homogenization during the Late Cretaceous is also inferred from the narrow Hf isotopic spectrum of magmatic zircons, in contrast to the broader and more variable signatures of earlier arc rocks. Thermobarometric estimates from phenocrysts reveal a vertically extensive magmatic system: clinopyroxene crystallized at ~1.5-4 kbar (upper to middle crust), with a tendency toward higher pressures in younger units, whereas zoned amphibole cores formed at ~6-8 kbar, corresponding to cooler lower crustal storage prior to ascend during the Late Cretaceous. Increased crustal thickness through time is recorded by increasing whole-rock Ce/Y ratios in mafic rocks and La/Yb and Sr/Y ratios in intermediate compositions (Fig. 10). The decrease in volcanic flux and onset of major plutonism following MAC accretion likely reflect a change in crustal thermal structure and enhanced fractionation. These geochemical proxies, combined with amphibole crystallization depths of 21-28 km (ρ = 2900 kg/m^3), indicate that by late Cretaceous time the arc crust had thickened to values comparable to present-day crust (approximately 24-30 km; González et al., 2012; Moreno Toirán, 2003; Possee et al., 2021) prior to arc-continent collision.

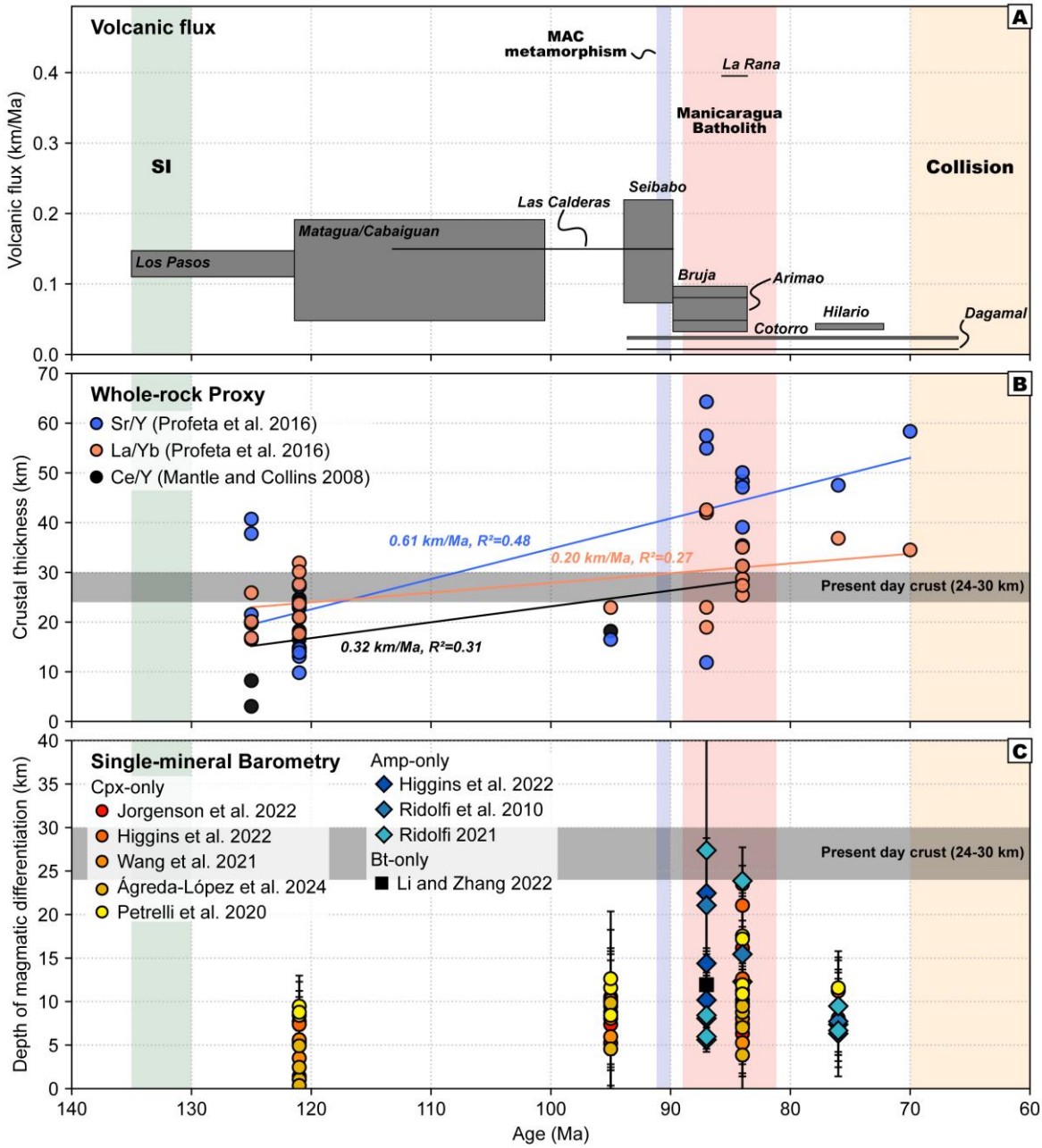

Figure 10. *Evolution of the Central Cuban arc illustrated by (A) volcanic flux calculated from the thickness and duration of each formation, with shaded bands showing low and high estimates, (B) whole-rock-derived crustal thickness with least-squares regression lines indicating linear rates of crustal growth (km/Ma) and corresponding R² values, using La/Yb and Sr/Y from intermediate rock after Profeta et al. (2016) and Ce/Y from basic rocks after Mantle and Collins (2008), and (C) single-mineral barometry-based crystallization depths converted to kilometers assuming a crustal density of 2900 kg/m³. Thermobarometry used: Clinopyroxene-only: Ágreda-López et al. (2024); Higgins et al. (2022); Jorgenson et al. (2022); Petrelli et al. (2020); Wang et al. (2021). Amphibole-only: Ridolfi et al. (2010); Ridolfi (2021); Higgins et al. (2022). Biotite-only: Li & Zhang (2022).*

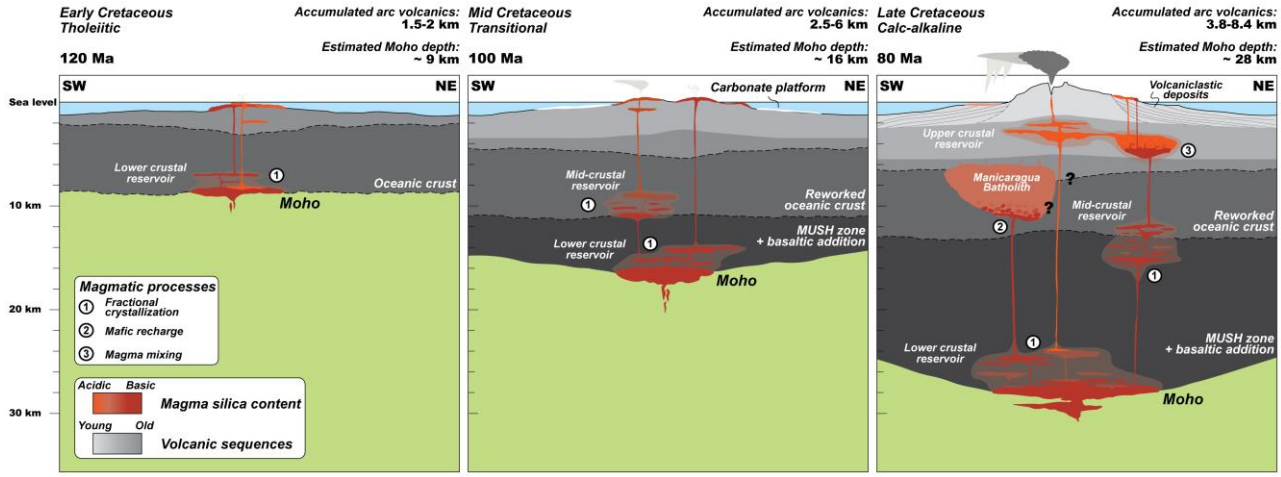

Figure 11. *Schematic cross-section of the arc crustal section illustrating three stages of progressive crustal thickning. In the early stage, a thin crust with limited magmatic differentiation produced tholeiitic to transitional magmas and led to formation of lower crustal cumulates. With continued thickening, a more hydrous and potentially cooler crustal structure favored differentiation toward calc-alkaline compositions, the development of multiple magma storage levels, magma mixing processes, and major plutonism. The thickness of volcanic sequences (upper crust) is based on Geología de Cuba: Compendio (Iturralde-Vinent, 2021) and interpreted Moho depth is constrined by single-mineral barometry from volcanic rocks of the Central Cuban Arc.*

Taken together, the petrological, geochemical, and geochronological data illustrate the evolution of the Central Cuban Arc from dry tholeiitic to hydrous calc-alkaline magmatism, driven by increasing slab-fluid flux and tectono-magmatic crustal thickening within a long-lived intra-oceanic subduction setting (Fig. 11). Throughout this evolution, the arc maintained a dominantly juvenile isotopic character, demonstrating that intra-oceanic arcs are capable generating substantial volumes of proto-continental type crust prior to final accretion.

5. Conclusions

This cumulative dissertation reconstructs the evolution of the Caribbean intra-oceanic arc system through an integrated synthesis of geochronologic, geochemical, isotopic, and petrological data from the Greater Antilles Arc, the Mabujina Amphibolite Complex, and the Central Cuban Arc segment. Together, these studies establish a unified temporal and compositional framework for understanding how intra-oceanic arcs generate juvenile continental crust. By combining regional-scale synthesis with detailed petrochemical investigations of key localities in central Cuba, this work elucidates the processes of subduction, crustal thickening, and magmatic differentiation that governed the Cretaceous evolution of the Caribbean Plate.

The integrated dataset from the Greater Antilles Arc focus on regional scale synthesis and provides a complete evolutionary framework for the intra-oceanic arc system, from subduction initiation in the Early Cretaceous to collisional termination in the Paleogene. It delineates three major stages: onset of subduction (120-110 Ma), magmatic and metamorphic climax (95-60 Ma), and collisional cessation (~40 Ma). Geochemically, the GAA records increasing contributions from enriched mantle components toward the retro-arc. The temporal overlap between the magmatic peak (95-60 Ma) and the emplacement of the CLIP suggests plume-arc interaction, which may have enhanced magmatic flux and introduced isotopic and chemical heterogeneity into the mantle wedge. These data establish the Greater Antilles Arc as a reference example of long-lived intra-oceanic arc evolution preserved from subduction initiation to arc-continent collision.

Zooming into smaller scale, petrographic, geochemical, and isotopic studies of Mabujina Amphibolite Complex demonstrate this arc-related metamorphic complex formed within Caribbean arc rather than representing an exotic terrane derived from the Pacific. The metamorphosed equivalents of arc crust comprise amphibolite- and epidote-amphibolite facies rocks of basaltic to tonalitic composition. Trace element and Sr-Nd isotopic compositions are indistinguishable from those of coeval volcanic sequences in central Cuba and contrast sharply with the more radiogenic signatures of the Guerrero Terrane. Petrochemical and isotopic data, combined with published zircon U-Pb ages, suggests that the protolith of MAC developed contemporaneously with other segments of the Caribbean arc. Its accretion beneath the Central Cuban Arc likely resulted from transpressional deformation during mid-Cretaceous oblique convergence, which fragmented and juxtaposed arc segments along strike-slip shear zones.

Finally, reconstruction of the Central Cuban Arc complements the regional synthesis by documenting a continuous ~60 Myr magmatic evolution and providing a crustal section that can be compared to the MAC. The volcanic sequences record a transition from early submarine tholeiitic magmatism, produced by the rapid ascent of dry mantle melts through thin crust, to hydrous calc-alkaline volcanism and plutonism associated with crustal thickening and transcrustal magma storage. Throughout this evolution, Sr-Nd-Pb-Hf isotopic data indicate a dominantly juvenile character, underscoring the arc's intra-oceanic nature and the absence of continental input. Minor temporal variations reflect episodic incorporation of heterogeneous sediment and increasing slab-derived components rather than changes in mantle source. Thermobarometric and whole-rock geochemical proxies record crustal thickening to ~24-30 km, comparable to present-day values during major Late Cretaceous plutonism following the accretion of the MAC. This record illustrates the tectono-magmatic processes in an intra-oceanic arc that led to the development of a hydrous, transcrustal magmatic system capable of generating proto-continental crust.

Taken together, the results from these three studies provide a coherent narrative of Caribbean arc evolution. From regional scale magmatic and tectonic framework, to detail records of intra-arc accretionary processes, to the petrogenetic and structural mechanisms of crustal differentiation and thickening within an active intra-oceanic setting. The integration of these datasets demonstrate that the Caribbean arc evolved through the interplay of subduction-driven mantle melting, slab-fluid metasomatism, and tectono-magmatic crustal thickening, illustrating how intra-oceanic arcs can generate substantial volumes of proto-continental crust prior to collisional accretion. The regional and local perspectives developed in this dissertation not only refine the understanding of Caribbean tectono-magmatic evolution but also provide broader insights into the mechanisms of crustal genesis, and continental growth in oceanic convergent settings worldwide.

6. Reference

Ágreda-López, M., Parodi, V., Musu, A., Jorgenson, C., Carfì, A., Mastrogiovanni, F., Caricchi, L., Perugini, D., & Petrelli, M. (2024). Enhancing machine learning thermobarometry for clinopyroxene-bearing magmas. Computers & Geosciences, 193, 105707. https://doi.org/10.1016/j.cageo.2024.105707

Bibikova, E. V., Somin, M. L., Graceva, T. V., Makarov, V. A., Millan, G., & Chukoljukov, J. A. (1988). Pervye rezultaty U-Pb-datirovanija metamorficeskich porod Bolschoi Antillskoi dugi: Vozrast kompleksa Mabuchina Kuby. Doklady AN SSSR, Ser. Geol., 302, 924–928. Doklady AN SSSR, Ser. Geol., 302, Article 302.

Black, L. P., Kamo, S. L., Allen, C. M., Aleinikoff, J. N., Davis, D. W., Korsch, R. J., & Foudoulis, C. (2003). TEMORA 1: A new zircon standard for Phanerozoic U–Pb geochronology. Chemical Geology, 200(1–2), 155–170. https://doi.org/10.1016/S0009-2541(03)00165-7

Blanco-Quintero, I. F., Garcia-Casco, A., Rojas-Agramonte, Y., Rodriguez-Vega, A., Lazaro, C., & Iturralde-Vinent, M. A. (2010). Metamorphic evolution of subducted hot oceanic crust (La Corea Melange, Cuba). American Journal of Science, 310(9), 889–915. https://doi.org/10.2475/11.2010.01

Blein, O., Guillot, S., Lapierre, H., de Lépinay, B. M., Lardeaux, J. -M., Trujillo, G. M., Campos, M., & Garcia, A. (2003). Geochemistry of the Mabujina Complex, Central Cuba: Implications on the Cuban Cretaceous Arc Rocks. The Journal of Geology, 111(1), Article 1. https://doi.org/10.1086/344666

Boschman, L. M., van Hinsbergen, D. J. J., Torsvik, T. H., Spakman, W., & Pindell, J. L. (2014). Kinematic reconstruction of the Caribbean region since the Early Jurassic. Earth-Science Reviews, 138, 102–136. https://doi.org/10.1016/j.earscirev.2014.08.007

Burke, K. (1988). Tectonic Evolution of the Caribbean. Annual Review of Earth and Planetary Sciences, 16(1), 201–230. https://doi.org/10.1146/annurev.ea.16.050188.001221

Chew, D. M., Petrus, J. A., & Kamber, B. S. (2014). VizualAge_UcomPbine data reduction scheme for Iolite (version 3.71) (Version VizualAge_UcomPbine for Iolite v3.71) [Computer software]. Trinity College Dublin.

Chew, D. M., Sylvester, P. J., & Tubrett, M. N. (2011). U–Pb and Th–Pb dating of apatite by LA-ICPMS. Chemical Geology, 280(1–2), 200–216. https://doi.org/10.1016/j.chemgeo.2010.11.010

Cumming, G. L., & Richards, J. R. (1975). Ore lead isotope ratios in a continuously changing earth. Earth and Planetary Science Letters, 28(2), 155–171. https://doi.org/10.1016/0012-821X(75)90223-X

Despaigne-Díaz, A.I., García-Casco, A., Govea, D.C., Jourdan, F., Wilde, S.A., & Trujillo, G.M. (2016), Twenty-five million years of subduction-accretion-exhumation during the Late Cretaceous–Tertiary in the northwestern Caribbean: The Trinidad Dome, Escambray complex, central Cuba: American Journal of Science, v. 316, no. 3, p. 203–240, https://doi.org/10.2475/03.2016.01.

Despaigne-Díaz, A.I., García Casco, A., Cáceres Govea, D., Wilde, S.A., & Millán Trujillo, G. (2017), Structure and tectonic evolution of the southwestern Trinidad dome, Escambray complex, Central Cuba: insights into deformation in an accretionary wedge. Tectonophysics 717, 139–161. https://doi.org/10.1016/j.tecto.2017.07.024.

Díaz de Villalvila, L. (1997). Caracterización geológica de las formaciones volcánicas y volcano-sedimentarias en Cuba central, provincias Cienfuegos, Villa Clara, Sancti Spiritus. In: Estudios sobre Geología de Cuba (Eds. Furrazola Bermudez, G.F., Núñez Cambra, K.E.). Centro Nacional de Información Geológica, La Habana, Cuba, 259–270.

Díaz de Villalvilla, L., Milia-González, I., Santa Cruz Pacheco, M., & Aguirre, G. (2003). Formación Los Pasos: Geología, Geoquímica y su Comparación con el Caribe. Estudios Sobre Los Arcos Volcánicos de Cuba, Centro Nacional de Información Geológica, Instituto de Geología y Paleontología de Cuba, Havana.

Dublan, L., & Alvarez, Sanchez., eds. (1986). Informe final del levantamiento geologico y evaluacion de minerales utiles, en escala 1:50000, del polıgono CAME I, zona Centro. Centro Nacional Fondo Geolo´gico, MINBAS, La Habana (unpubl. Report).

Ducea, M. N., Saleeby, J. B., & Bergantz, G. (2015). The Architecture, Chemistry, and Evolution of Continental Magmatic Arcs. Annual Review of Earth and Planetary Sciences, 43(1), 299–331. https://doi.org/10.1146/annurev-earth-060614-105049

Escuder-Viruete, J., Castillo-Carrión, M., & Pérez-Estaún, A. (2014). Magmatic relationships between depleted mantle harzburgites, boninitic cumulate gabbros and subduction-related tholeiitic basalts in the Puerto Plata ophiolitic complex, Dominican Republic: Implications for the birth of the Caribbean island-arc. Lithos, 196–197, 261–280. https://doi.org/10.1016/j.lithos.2014.03.013

Escuder-Viruete, J., Contreras, F., Stein, G., Urien, P., Joubert, M., Pérez-Estaún, A., Friedman, R., & Ullrich, T. (2007). Magmatic relationships and ages between adakites, magnesian andesites and Nb-enriched basalt-andesites from Hispaniola: Record of a major change in the Caribbean island arc magma sources. Lithos, 99(3–4), Article 3–4. https://doi.org/10.1016/j.lithos.2007.01.008

Escuder-Viruete, J., Díaz de Neira, A., Hernáiz Huerta, P. P., Monthel, J., Senz, J. G., Joubert, M., Lopera, E., Ullrich, T., Friedman, R., & Mortensen, J. (2006a). Magmatic relationships and ages of Caribbean Island arc tholeiites, boninites and related felsic rocks, Dominican Republic. Lithos, 90(3–4), Article 3–4. https://doi.org/10.1016/j.lithos.2006.02.001

Escuder-Viruete, J., Contreras, F., Stein, G., Urien, P., Joubert, M., Ullrich, T., ... & Pérez-Estaún, A. (2006b). Transpression and strain partitioning in the Caribbean Island-arc: Fabric development, kinematics and Ar–Ar ages of syntectonic emplacement of the Loma de Cabrera batholith, Dominican Republic. Journal of structural geology, 28(8), 1496-1519.

Faure, G., & Mensing, T. M. (2005). Isotopes: Principles and Applications (3rd ed.). Wiley.

Fourny, A., Weis, D., & Scoates, J. S. (2016). Comprehensive P b- S r- N d- H f isotopic, trace element, and mineralogical characterization of mafic to ultramafic rock reference materials. Geochemistry, Geophysics, Geosystems, 17(3), 739–773. https://doi.org/10.1002/2015GC006181

García-Delgado, D. E., (1998). Mapa geológico de Cuba central (provincias Cienfuegos, Villa Clara y Sancti Spiritus) Escala 1:100000: Instituto de Geología y Paleontología, La Habana.

Garcia-Casco, A., Iturralde-Vinent, M. A., & Pindell, J. (2008). Latest Cretaceous Collision/Accretion between the Caribbean Plate and Caribeana: Origin of Metamorphic Terranes in the Greater Antilles. International Geology Review, 50(9), Article 9. https://doi.org/10.2747/0020-6814.50.9.781

Garcia-Casco, A., Torres-Roldán, R. L., Iturralde-Vinent, M. A., Millán, G., Cambra, K. N., Lázaro, C., & Vega, A. R. (2006). High pressure metamorphism of ophiolites in Cuba. Geologica Acta, 26.

González, O., Moreno, B., Romanelli, F., & Panza, G. F. (2012). Lithospheric structure below seismic stations in Cuba from the joint inversion of Rayleigh surface waves dispersion and receiver functions: Lithosphere below seismic stations in Cuba. Geophysical Journal International, 189(2), 1047–1059. https://doi.org/10.1111/j.1365-246X.2012.05410.x

Govindaraju, K., Potts, P. J., Webb, P. C., & Watson, J. S. (1994). Report on Whin sill dolerite WS-S from England and Pitscurrie microgabbro PM-S from Scotland: Assessment by one hundred and four international laboratories. Geostandards and Geoanalytical Research, 18(2), Article 2. https://doi.org/10.1111/j.1751-908X.1994.tb00520.x

Grafe, F., Stanek, K. P., Baumann, A., Maresch, W. V., Hames, W. E., Grevel, C., & Millan, G. (2001). Rb-Sr and 40Ar/39Ar Mineral Ages of Granitoid Intrusives in the Mabujina Unit, Central Cuba: Thermal Exhumation History of the Escambray Massif. The Journal of Geology, 109(5), Article 5. https://doi.org/10.1086/321966

Greene, A. R., DeBARI, S. M., Kelemen, P. B., Blusztajn, J., & Clift, P. D. (2006). A Detailed Geochemical Study of Island Arc Crust: The Talkeetna Arc Section, South–Central Alaska. Journal of Petrology, 47(6), Article 6. https://doi.org/10.1093/petrology/egl002

Hiess, J., Condon, D. J., McLean, N., & Noble, S. R. (2012). 238 U/235 U Systematics in Terrestrial Uranium-Bearing Minerals. Science, 335(6076), 1610–1614. https://doi.org/10.1126/science.1215507

Higgins, O., Sheldrake, T., & Caricchi, L. (2022). Machine learning thermobarometry and chemometry using amphibole and clinopyroxene: A window into the roots of an arc volcano (Mount Liamuiga, Saint Kitts). Contributions to Mineralogy and Petrology, 177(1), Article 1. https://doi.org/10.1007/s00410-021-01874-6

Hoernle, K., Abt, D. L., Fischer, K. M., Nichols, H., Hauff, F., Abers, G. A., Van Den Bogaard, P., Heydolph, K., Alvarado, G., Protti, M., & Strauch, W. (2008). Arc-parallel flow in the mantle wedge beneath Costa Rica and Nicaragua. Nature, 451(7182), 1094–1097. https://doi.org/10.1038/nature06550

Hoernle, K., Hauff, F., Kokfelt, T. F., Haase, K., Garbe-Schönberg, D., & Werner, R. (2011). On- and off-axis chemical heterogeneities along the South Atlantic Mid-Ocean-Ridge (5–11°S): Shallow or deep recycling of ocean crust and/or intraplate volcanism? Earth and Planetary Science Letters, 306(1–2), 86–97. https://doi.org/10.1016/j.epsl.2011.03.032

Hu, H. Y., Stern, R. J., Rojas-Agramonte, Y., & Garcia-Casco, A. (2022). Review of Geochronologic and Geochemical Data of the Greater Antilles Volcanic Arc and Implications for the Evolution of Oceanic Arcs. Geochemistry, Geophysics, Geosystems, 23(4), Article 4. https://doi.org/10.1029/2021GC010148

Huang, C., Wang, H., Yang, J., Ramezani, J., Yang, C., Zhang, S., Yang, Y., Xia, X., Feng, L., Lin, J., Wang, T., Ma, Q., He, H., Xie, L., & Wu, S. (2020). SA01 – A Proposed Zircon

Reference Material for Microbeam U-Pb Age and Hf-O Isotopic Determination. Geostandards and Geoanalytical Research, 44(1), 103–123. https://doi.org/10.1111/ggr.12307

Huang, C., Wang, H., Yang, J., Yang, C., Li, Z., Yang, Y., Feng, L., Xie, L., & Wu, S. (2021). Characterization of the potential reference material SA02 for micro-beam U–Pb geochronology and Hf–O isotopic composition analysis of zircon. Journal of Analytical Atomic Spectrometry, 36(2), 368–374. https://doi.org/10.1039/d0ja00409j

Huang, C., Yang, Y., Wang, H., Xie, L., Wu, S., Xu, L., Yang, J., & Wu, F. (2022). In-run measuring 177Hf16O/177Hf as a routine technique for in-situ Hf isotopic compositions analysis in zirconium-bearing minerals by laser ablation MC-ICP-MS. Spectrochimica Acta Part B: Atomic Spectroscopy, 194, 106486. https://doi.org/10.1016/j.sab.2022.106486

Iturralde-Vinent, M. (1994). CUBAN GEOLOGY: A NEW PLATE-TECTONIC SYNTHESIS. Journal of Petroleum Geology, 17(1), Article 1. https://doi.org/10.1111/j.1747-5457.1994.tb00113.x

Iturralde-Vinent, M. ed., (1996). Ofiolitas y arcos volcánicos de Cuba. First Contribution IGCP Project 364, University of Miami Press, 265 pp.

Iturralde-Vinent, M. (1998). Sinopsis de la Constitución Geológica de Cuba. Acta Geológica Hispánica, 33, Article 33.

Iturralde-Vinent, M. (2021). Compendio de geología de Cuba y del Caribe. DVD. Havana, CITMATEL.

Iturralde-Vinent, M., Garcia-Casco, A., Rojas-Agramonte, Y., Proenza, J. A., Murphy, J. B., & Stern, R. J. (2016). The geology of Cuba: A brief overview and synthesis. GSA Today, 4–10. https://doi.org/10.1130/GSATG296A.1

Jagoutz, O., & Schmidt, M. W. (2012). The formation and bulk composition of modern juvenile continental crust: The Kohistan arc. Chemical Geology, 298–299, 79–96. https://doi.org/10.1016/j.chemgeo.2011.10.022

Johnson, M. C., & Plank, T. (2000). Dehydration and melting experiments constrain the fate of subducted sediments. Geochemistry, Geophysics, Geosystems, 1(12), 1999GC000014. https://doi.org/10.1029/1999GC000014

Jorgenson, C., Higgins, O., Petrelli, M., Bégué, F., & Caricchi, L. (2022). A Machine Learning-Based Approach to Clinopyroxene Thermobarometry: Model Optimization and Distribution

for Use in Earth Sciences. Journal of Geophysical Research: Solid Earth, 127(4), Article 4. https://doi.org/10.1029/2021JB022904

Kerr, A. C., Iturralde-Vinent, M. A., D. Saunders, A., & Tarney, J. (1999). New plate tectonic model of the Caribbean: Implications from a geochemical reconnaissance of Cuban Mesozoic volcanic rocks. Geological Society of America Bulletin, 19.

Lázaro, C., Blanco-Quintero, I. F., Proenza, J. A., Rojas-Agramonte, Y., Neubauer, F., Núñez-Cambra, K., & Garcia-Casco, A. (2016). Petrogenesis and 40Ar/39Ar dating of proto-forearc crust in the Early Cretaceous Caribbean arc: The La Tinta mélange (eastern Cuba) and its easterly correlation in Hispaniola. International Geology Review, 58(8), 1020–1040. https://doi.org/10.1080/00206814.2015.1118647

Leat, P. T., & Larter, R. D. (2003). Intra-oceanic subduction systems: Introduction. Geological Society, London, Special Publications, 219(1), Article 1. https://doi.org/10.1144/GSL.SP.2003.219.01.01

Lewis, J. F., Draper, G., Proenza Fernández, J. A., Espaillat, J., & Jiménez, J. (2006). Ophiolite-Related Ultramafic Rocks (Serpentinites) in the Caribbean Region: A Review of their Occurrence, Composition, Origin, Emplacement and Ni-Laterite Soil Formation. Geologica Acta, 237–264. https://doi.org/10.1344/105.000000368

Li, Q.-L., Li, X.-H., Wu, F.-Y., Yin, Q.-Z., Ye, H.-M., Liu, Y., Tang, G.-Q., & Zhang, C.-L. (2012). In-situ SIMS U–Pb dating of phanerozoic apatite with low U and high common Pb. Gondwana Research, 21(4), 745–756. https://doi.org/10.1016/j.gr.2011.07.008

Li, X., & Zhang, C. (2022). Machine Learning Thermobarometry for Biotite-Bearing Magmas. Journal of Geophysical Research: Solid Earth, 127(9), e2022JB024137. https://doi.org/10.1029/2022JB024137

Lidiak, E. G., & Jolly, W. T. (1996). Circum-Caribbean Granitoids: Characteristics and Origin. International Geology Review, 38(12), 1098–1133. https://doi.org/10.1080/00206819709465385

Ludwig, K. R. (2001). Isoplot/Ex Version 2.49: A Geochronological Toolkit for Microsoft Excel [Computer Program / Software Manual]. Berkeley Geochronology Center.

Ludwig, K. R. (2003a). SQUID 1.12: A User's Manual [Computer software]. Berkeley Geochronology Center.

Ludwig, K. R. (2003b). ISOPLOT 3.00: A Geochronological Toolkit for Microsoft Excel. Berkeley Geochronology Center, California, Berkeley.

Lugmair, G. W., Shimamura, T., Lewis, R. S., & Anders, E. (1983). Samarium-146 in the Early Solar System: Evidence from Neodymium in the Allende Meteorite. Science, 222(4627), 1015–1018. https://doi.org/10.1126/science.222.4627.1015

Mann, P., Rogers, R., & Gahagan, L. (2007). Overview of plate tectonic history and its unresolved tectonic problems. In J. Bundschuh & G. E. Alvarado (Eds.), Central America: Geology, resources and hazards (pp. 201–237). Taylor and Francis/Balkema.

Mantle, G. W., & Collins, W. J. (2008). Quantifying crustal thickness variations in evolving orogens: Correlation between arc basalt composition and Moho depth. Geology, 36(1), 87. https://doi.org/10.1130/G24095A.1

Moreno Toiran, B. (2003). The crustal structure of Cuba derived from Receiver Function Analysis. Journal of Seismology, 7(3), 359–375. https://doi.org/10.1023/A:1024566803893

Nasdala, L., Hofmeister, W., Norberg, N., Martinson, J. M., Corfu, F., Dörr, W., Kamo, S. L., Kennedy, A. K., Kronz, A., Reiners, P. W., Frei, D., Kosler, J., Wan, Y., Götze, J., Häger, T., Kröner, A., & Valley, J. W. (2008). Zircon M257 - a Homogeneous Natural Reference Material for the Ion Microprobe U-Pb Analysis of Zircon. Geostandards and Geoanalytical Research, 32(3), 247–265. https://doi.org/10.1111/j.1751-908X.2008.00914.x

Nier, A. O. (1938). The Isotopic Constitution of Strontium, Barium, Bismuth, Thallium and Mercury. Physical Review, 54(4), 275–278. https://doi.org/10.1103/PhysRev.54.275

O'Nions, R. K., Carter, S. R., Evensen, N. M., & Hamilton, P. J. (1979). Geochemical and Cosmochemical Applications of Nd Isotope Analysis. Annual Review of Earth and Planetary Sciences, 7(1), 11–38. https://doi.org/10.1146/annurev.ea.07.050179.000303

Pearce, J. A. (1996). A user's guide to basalt discrimination diagrams. Trace Element Geochemistry of Volcanic Rocks: Applications for Massive Sulphide Exploration. Geological Association of Canada, Short Course Notes, 12(79), Article 79.

Pearce, J. A. (2008). Geochemical fingerprinting of oceanic basalts with applications to ophiolite classification and the search for Archean oceanic crust. Lithos, 100(1–4), Article 1–4. https://doi.org/10.1016/j.lithos.2007.06.016

Petrelli, M., Caricchi, L., & Perugini, D. (2020). Machine Learning Thermo-Barometry: Application to Clinopyroxene-Bearing Magmas. Journal of Geophysical Research: Solid Earth, 125(9), e2020JB020130. https://doi.org/10.1029/2020JB020130

Pindell, J., Kennan, L., Maresch, W. V., Stanek, K.-P., Draper, G., & Higgs, R. (2005). Plate-kinematics and crustal dynamics of circum-Caribbean arc-continent interactions: Tectonic

controls on basin development in Proto-Caribbean margins. In H. G. A. Lallemant & V. B. Sisson, Caribbean-South American plate interactions, Venezuela. Geological Society of America. https://doi.org/10.1130/0-8137-2394-9.7

Pindell, J. L., & Kennan, L. (2009). Tectonic evolution of the Gulf of Mexico, Caribbean and northern South America in the mantle reference frame: An update. Geological Society, London, Special Publications, 328(1), Article 1. https://doi.org/10.1144/SP328.1

Pindell, J., Maresch, W. V., Martens, U., & Stanek, K. (2012). The Greater Antillean Arc: Early Cretaceous origin and proposed relationship to Central American subduction mélanges: implications for models of Caribbean evolution. International Geology Review, 54(2), Article 2. https://doi.org/10.1080/00206814.2010.510008

Possee, D., Rychert, C., Harmon, N., & Keir, D. (2021). Seismic Discontinuities Across the North American Caribbean Plate Boundary From S-to-P Receiver Functions. Geochemistry, Geophysics, Geosystems, 22(7), e2021GC009723. https://doi.org/10.1029/2021GC009723

Profeta, L., Ducea, M. N., Chapman, J. B., Paterson, S. R., Gonzales, S. M. H., Kirsch, M., Petrescu, L., & DeCelles, P. G. (2016). Quantifying crustal thickness over time in magmatic arcs. Scientific Reports, 5(1), Article 1. https://doi.org/10.1038/srep17786

Rehkämper, M., & Hofmann, A. W. (1997). Recycled ocean crust and sediment in Indian Ocean MORB. Earth and Planetary Science Letters, 147(1–4), 93–106. https://doi.org/10.1016/S0012-821X(97)00009-5

Ridolfi, F. (2021). Amp-TB2: An Updated Model for Calcic Amphibole Thermobarometry. Minerals, 11(3), 324. https://doi.org/10.3390/min11030324

Ridolfi, F., Renzulli, A., & Puerini, M. (2010). Stability and chemical equilibrium of amphibole in calc-alkaline magmas: An overview, new thermobarometric formulations and application to subduction-related volcanoes. Contributions to Mineralogy and Petrology, 160(1), Article 1. https://doi.org/10.1007/s00410-009-0465-7

Rojas-Agramonte, Y., Hu, H. Y., Iturralde-Vinent, M., Lewis, J., De Lepinay, B, M., & García-Casco, A. (2021). A Late Cretaceous Adakitic intrusion from Northern Haiti: Additional evidence for slab melting and implications for migration of ridge-trench-trench triple junction during the Cretaceous in the Greater Antilles. International Geology Review, 1–10. https://doi.org/10.1080/00206814.2021.1998800

Rojas-Agramonte, Y., Kröner, A., Garcia-Casco, A., Somin, M., Iturralde-Vinent, M., Mattinson, J. M., Millán Trujillo, G., Sukar, K., Pérez Rodríguez, M., Carrasquilla, S., Wingate, M. T. D.,

& Liu, D. Y. (2011). Timing and Evolution of Cretaceous Island Arc Magmatism in Central Cuba: Implications for the History of Arc Systems in the Northwestern Caribbean. The Journal of Geology, 119(6), Article 6. https://doi.org/10.1086/662033

Rosencrantz, E., Ross, M. I., & Sclater, J. G. (1988). Age and spreading history of the Cayman Trough as determined from depth, heat flow, and magnetic anomalies. Journal of Geophysical Research: Solid Earth, 93(B3), 2141–2157. https://doi.org/10.1029/JB093iB03p02141

Shervais, J. W. (1982). Ti-V plots and the petrogenesis of modern and ophiolitic lavas. Earth and Planetary Science Letters, 59(1), 101–118. https://doi.org/10.1016/0012-821x(82)90120-0

Somin, M. L., & Millan, G. (1981). Geologija metamorficheskich kompleksov Kuby. Isdat. Nauka, Moskva, 219 p.

Schneider, J. Bosch, D., Monié, P., Guillot, S., García-casco, A., Lardeaux, J.M., Torres Roldan, R.L., & Millán Trujillo, G. (2004), Origin and evolution of the Escambray Massif (Central Cuba): an example of HP/LT rocks exhumed during intraoceanic subduction. Journal of Metamorphic Geology 22, 227–247. DOI 10.1111/j.1525-1314.2004.00510.x.

Stacey, J. S., & Kramers, J. D. (1975). Approximation of terrestrial lead isotope evolution by a two-stage model. Earth and Planetary Science Letters, 26(2), 207–221. https://doi.org/10.1016/0012-821X(75)90088-6

Stanek, K. P., Maresch, W. V., Grafe, F., Grevel, C., & Baumann, A. (2006). Structure, tectonics and metamorphic development of the Sancti Spiritus Dome (eastern Escambray massif, Central Cuba). Geologica Acta, 20.

Stanek, K. P., Maresch, W. V., Scherer, E., Krebs, M., Berndt, J., Sergeev, S. S., Rodionov, N., Pfänder, J., & Hames, W. E. (2019). Born in the Pacific and raised in the Caribbean: Construction of the Escambray nappe stack, central Cuba. A review. European Journal of Mineralogy, 31(1), Article 1. https://doi.org/10.1127/ejm/2019/0031-2795

Stern, R. J. (2010). The anatomy and ontogeny of modern intra-oceanic arc systems. Geological Society, London, Special Publications, 338(1), Article 1. https://doi.org/10.1144/SP338.2

Straub, S. M., Woodhead, J. D., & Arculus, R. J. (2015). Temporal Evolution of the Mariana Arc: Mantle Wedge and Subducted Slab Controls Revealed with a Tephra Perspective. Journal of Petrology, 56(2), 409–439. https://doi.org/10.1093/petrology/egv005

Sukar, K., & Perez, M. (1997). Granitoides del arco volcánico de la región central de Cuba antigua provincia de Las Villas. In Furrazola Bermúdez, G. F., and Núñez Cambra, K. E., eds.

Estudios sobre geología de Cuba. Havana, Instituto de Geología y Paleontología, Centro Nacional de Información Geológica, pp. 371–386.

Todd, E., Stracke, A., & Scherer, E. E. (2015). Effects of simple acid leaching of crushed and powdered geological materials on high-precision Pb isotope analyses. Geochemistry, Geophysics, Geosystems, 16(7), 2276–2302. https://doi.org/10.1002/2015GC005804

Torró, L., Proenza, J. A., Melgarejo, J. C., Alfonso, P., Farré de Pablo, J., Colomer, J. M., Garcia-Casco, A., Gubern, A., Gallardo, E., Cazañas, X., Chávez, C., Del Carpio, R., León, P., Nelson, C. E., & Lewis, J. F. (2016). Mineralogy, geochemistry and sulfur isotope characterization of Cerro de Maimón (Dominican Republic), San Fernando and Antonio (Cuba) lower Cretaceous VMS deposits: Formation during subduction initiation of the proto-Caribbean lithosphere within a fore-arc. Ore Geology Reviews, 72, 794–817. https://doi.org/10.1016/j.oregeorev.2015.09.017

van Hinsbergen, D. J. J., Iturralde-Vinent, M. A., van Geffen, P. W. G., Garcia-Casco, A., & van Benthem, S. (2009). Structure of the accretionary prism, and the evolution of the Paleogene northern Caribbean subduction zone in the region of Camagüey, Cuba. Journal of Structural Geology, 31(10), Article 10. https://doi.org/10.1016/j.jsg.2009.06.007

Wang, X., Hou, T., Wang, M., Zhang, C., Zhang, Z., Pan, R., Marxer, F., & Zhang, H. (2021). A new clinopyroxene thermobarometer for mafic to intermediate magmatic systems. European Journal of Mineralogy, 33(5), Article 5. https://doi.org/10.5194/ejm-33-621-2021

Whattam, S. A., & Stern, R. J. (2011). The ‘subduction initiation rule’: A key for linking ophiolites, intra-oceanic forearcs, and subduction initiation. Contributions to Mineralogy and Petrology, 162(5), 1031–1045. https://doi.org/10.1007/s00410-011-0638-z

Wiedenbeck, M., Allé, P., Corfu, F., Griffin, W. L., Meier, M., Oberli, F., Quadt, A. V., Roddick, J. C., & Spiegel, W. (1995). Three natural zircon standards for U-Th-Pb, Lu-Hf, trace element and REE analyses. Geostandards Newsletter, 19(1), 1–23. https://doi.org/10.1111/j.1751-908X.1995.tb00147.x

Williams, I. S. (1998). U–Th–Pb Geochronology by Ion Microprobe. In Applications of Microanalytical Techniques to Understanding Mineralizing Processes (pp. 1–35). Society of Economic Geologists.

Wilson, F. H., Orris, G., & Gray, F. (2019). Preliminary geologic map of the Greater Antilles and the Virgin Islands: U.S. Geological Survey Open-File Report 2019–1036, pamphlet 50 p., 2 sheets, scales 1:2,500,000 and 1:300,000, https://doi.org/10.3133/ofr20191036.

Wu, F.-Y., Yang, Y.-H., Xie, L.-W., Yang, J.-H., & Xu, P. (2006). Hf isotopic compositions of the standard zircons and baddeleyites used in U–Pb geochronology. Chemical Geology, 234(1–2), 105–126. https://doi.org/10.1016/j.chemgeo.2006.05.003

Wu, S., Wörner, G., Jochum, K. P., Stoll, B., Simon, K., & Kronz, A. (2019). The Preparation and Preliminary Characterisation of Three Synthetic Andesite Reference Glass Materials (ARM-1, ARM-2, ARM-3) for In Situ Microanalysis. Geostandards and Geoanalytical Research, 43(4), 567–584. https://doi.org/10.1111/ggr.12301

Wu, S., Yang, M., Yang, Y., Xie, L., Huang, C., Wang, H., & Yang, J. (2020). Improved in situ zircon U–Pb dating at high spatial resolution (5–16 μm) by laser ablation–single collector–sector field–ICP–MS using Jet sample and X skimmer cones. International Journal of Mass Spectrometry, 456, 116394. https://doi.org/10.1016/j.ijms.2020.116394

Xie, L., Zhang, Y., Zhang, H., Sun, J., & Wu, F. (2008). In situ simultaneous determination of trace elements, U-Pb and Lu-Hf isotopes in zircon and baddeleyite. Science Bulletin, 53(10), 1565–1573. https://doi.org/10.1007/s11434-008-0086-y

Financial supports

This thesis was supported by the Federal State Funding of Christian-Albrechts-Universität zu Kiel during the stay at Kiel University, as well as by Heidelberg University through an academic staff position funded by the State of Baden-Württemberg.

Declaration of generative AI in the writing process and author responsibility

During the preparation of this work, ChatGPT (developed by OpenAI) was used to improve the clarity, readability, and grammatical accuracy of the text. Author take full responsibility for the integrity, originality, and accuracy of the work, and have reviewed and approved the final version of the work.

Appendix

1. Publikation/*Publication*:

Vollständige bibliographische Referenz/*Complete bibliographic reference:*

Hu, H. Y., Stern, R. J., Rojas‐Agramonte, Y., & Garcia‐Casco, A. (2022). Review of geochronologic and geochemical data of the Greater Antilles volcanic arc and implications for the evolution of oceanic arcs. Geochemistry, Geophysics, Geosystems, 23(4), e2021GC010148.

2. Erst- oder gleichberechtigte Autorenschaft/*First or equal authorship:* **Ja/*Yes*** ☑ **Nein/*No*** ☐

3. Veröffentlicht/*Published* ☑ **Zur Veröffentlichung akzeptiert/*Accepted*** ☐

Q1/Q2:* **Ja/*Yes*** ☑ **Nein/*No*** ☐

**SCImago Journal Rank (SJR) indicator*

Im Erscheinungsjahr oder im letzten verfügbaren Vorjahr/*In the year of publication or the last prior year available:* 2022

Eingereicht/*Submitted* ☐ **Noch nicht eingereicht/*Not yet submitted*** ☐

4. Beteiligungen/*Contributions***

Contributor Role	**Doktorand/in/ *Doctoral student***	**Co-Autor/in 1/ *Co-author 1***	**Co-Autor/in 2/ *Co-author 2***
Name, first name	Haoyu Hu	Yamirka Rojas-agramonte	Robert J. Stern
Methodology	☑	☐	☐
Software	☐	☐	☐
Validation	☐	☐	☐
Formal analysis	☑	☑	☐
Investigation	☑	☑	☐
Resources	☐	☐	☐
Data Curation	☑	☐	☑
Writing-Original Draft	☑	☐	☐
Writing-Review&Editing	☑	☑	☑
Visualization	☑	☐	☑
Supervision	☐	☑	☐
Project administration	☐	☑	☐
Funding acquisition	☐	☑	☐

***Kategorien des CRediT (Contributor Roles Taxonomy, https://credit.niso.org/)*

Hiermit bestätige ich, dass alle obigen Angaben korrekt sind/*I confirm that all declarations made above are correct.*

Unterschrift/*Signature* _____ Doktorand/in/*Doctoral student*

_____ Co-Autor/in 1/*Co-author 1*

Robert Stern Digitally signed by Robert Stern Date: 2025.10.29 10:58:35 -07'00'

_____ Co-Autor/in 2/*Co-author 2*

Betreuungsperson/*Supervisor:*

Hiermit bestätige ich, dass alle obigen Angaben korrekt sind und dass die selbstständigen Arbeitsanteile des/der Doktoranden/in an der aufgeführten Publikation hinreichend und signifikant sind/*I confirm that all declarations made above are correct and that the doctoral student's independent contribution to this publication is significant and sufficient to be considered for the cumulative dissertation.*

Pro. Dr. Yamirka Rojas-agramonte
Name/*Name*

Unterschrift/*Signature*

30.10.2025
Datum/*Date*

Appendix 1

Review of Geochronologic and Geochemical Data of the Greater Antilles Volcanic Arc and Implications for the Evolution of Oceanic Arcs

Authors

Haoyu Hu, Robert J. Stern, Yamirka Rojas-Agramonte, & Antonio Garcia-Casco

Abstract

The Greater Antilles islands of Cuba, Hispaniola, Puerto Rico and Jamaica plus the Virgin Islands host fragments of the fossil convergent margin that records Cretaceous subduction (operated for about 90 m.y.) of the American plates beneath the Caribbean plate and ensuing arc-continent collision in Late Cretaceous-Eocene time. The “soft” collision between the Greater Antilles Arc (GAA) and the Bahamas platform (and the margin of the Maya Block in western Cuba) preserved much of the convergent margin. This fossil geosystem represents an excellent natural laboratory for studying the formation and evolution of an intra oceanic convergent margin. We compiled geochronologic (664 ages) and geochemical data (more than 1,500 analyses) for GAA igneous and metamorphic rocks. The data was classified with a simple fourfold subdivision: fore-arc mélange, fore-arc ophiolite, magmatic arc, and retro-arc to inspect the evolution of GAA through its entire lifespan. The onset of subduction recorded by fore-arc units, together with the oldest magmatic arc sequence shows that the GAA started in Early Cretaceous time and ceased in Paleogene time. The arc was locally affected (retro-arc region in Hispaniola) by the Caribbean Large Igneous Province (CLIP) in Early Cretaceous and strongly in Late Cretaceous time. Despite multiple biases in the database presented here, this work is intended to help overcome some of the obstacles and motivate systematic study of the GAA. Our results encourage exploration of offshore regions, especially in the east where the forearc is submerged. Offshore explorations are also encouraged in the south, to investigate relations with the CLIP.

1. Introduction

The fossil Greater Antilles Arc (GAA), part of the Great Arc of the Caribbean (Burke, 1988), provides an unusual opportunity to examine the complete evolution of an intra-oceanic convergent margin from birth to demise, especially because much of it is exposed above sea-level. Igneous and metamorphic rocks of the GAA (Figure 1) record subduction beneath the Caribbean plate during the Cretaceous and Paleogene spanning about 90 m.y. all through the present ca. 2,000 km length of the convergent margin (e.g., Iturralde-Vinent et al., 2016; Mann et al., 2007; Pindell & Kennan, 2009 and references therein). In most interpretations, the subducting lithosphere corresponds to the North and South American plates separated by the Proto-Caribbean ridge during the GAA lifetime (e.g., Blanco-Quintero et al., 2010; Pindell & Kennan, 2009). Convergence was terminated with the subduction of passive margin sequences (Despaigne-Díaz et al., 2016, 2017; García-Casco, Iturralde-Vinent, & Pindell, 2008); the ensuing soft collision with the margins of the Maya Block and the Bahamas Platform began in Cuba in the Latest Cretaceous (Iturralde-Vinent et al., 2008; van Hinsbergen et al., 2009) and propagated to Hispaniola and further east (e.g., Escuder-Viruete, Pérez-Estaún, Booth-Rea, & Valverde-Vaquero, 2011; Escuder-Viruete, Perez-Estaún, Gabites, & Suarez-Rodriguez, 2011; Mann, 1999; Pindell & Barrett, 1990). After frontal to oblique collision ended in Eocene time, convergence between the Caribbean and North American plates stopped and the western part of the convergent margin (Cuba) accreted to the North American plate. A new transform boundary—the left-lateral Oriente Transform Fault (Rojas-Agramonte et al., 2005, 2008)—and associated formation of the Cayman Trough during the collision (Middle Eocene) - separated Cuba from the Caribbean plate and eastern GAA fragments (Rosencrantz et al., 1988). This was a “soft” collision, so deformation was mostly modest and most of the arc was not disrupted, making the GAA one of Earth's best-preserved fossil oceanic convergent margins. In fact, the GAA is still an active convergent margin east of the Dominican Republic, where slow, highly oblique convergence with Atlantic oceanic lithosphere continues today (e.g., Mann et al., 2002).

The GAA evolved as an intra-oceanic convergent margin; a contemporary analog is the Izu-Bonin-Mariana (IBM) arc system (Figure 1c; Stern et al., 2012) which is mostly submerged. GAA sedimentary, metamorphic and magmatic units developed in subduction-related (fore-arc, arc and retro-arc) environments. These are recognized as follows: (a) extended passive margins of the Bahamas and the Maya Block accreted to the overriding plate in Cuba, (b) ophiolites and ophiolitic mélanges, and (c) magmatic arcs (Cretaceous and Paleogene). Plume-associated igneous rocks were

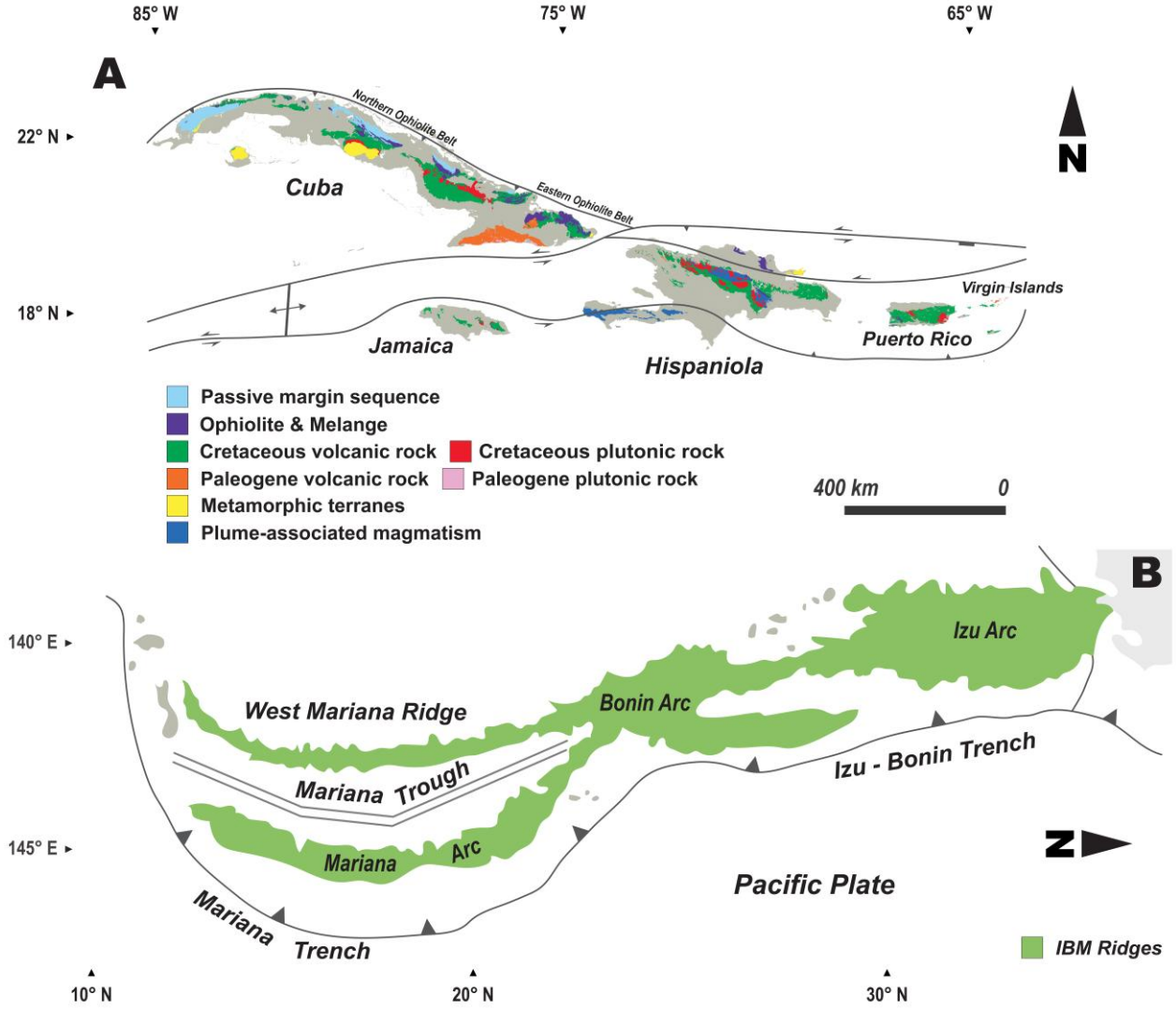

Figure 1. *Comparison of fossil and active arcs, at the same scale. (a) Map of the Greater Antilles showing the location of passive margin sequences, ophiolites and mélange blocks, magmatic arcs, metamorphic terranes and plume-associated igneous rocks, modified from Torró, Proenza-Fernández, et al. (2016) and Wilson et al. (2019). (b) Tectonic map of the Izu-Bonin-Mariana arc system, modified after Stern and Bloomer (1992).*

also developed in the GAA retro-arc region. These four tectonic units are not developed on every island, but volcanic rocks are exposed on each.

Previous reviews focused on a range of related issues including the larger geodynamic evolution of the Caribbean plate (e.g., Boschman et al., 2014; Pindell et al., 2005, 2012); terrane accretion history (e.g., García-Casco, Iturralde-Vinent, & Pindell, 2008), the geology of Cuba (e.g., Iturralde-Vinent

et al., 2016), high-pressure metamorphism in Cuba (e.g., García-Casco et al., 2006), ophiolitic units (Lewis et al., 2006) and GAA arc igneous rocks (e.g., Lidiak & Anderson, 2015; Lidiak & Jolly, 1996). This paper is the first systematic overview of the magmatism and metamorphism of the entire GAA convergent margin system.

Here, we summarize published petrologic, geochronological, and geochemical data for GAA ophiolites, mélange blocks, the magmatic arc, and retro-arc extensional features and use this information to provide new insights into GAA evolution. We also suggest some potentially fruitful directions for future study. Our approach is to use geochronologic and geochemical data to constrain the entire magmatic and metamorphic history of the convergent margin, from subduction initiation (SI) through maturity and death. The reconstruction does not include other important geological issues, such as deformation, sedimentation, etc. We have two goals in this paper: First, we want to explore if SI models (Stern & Gerya, 2018) are useful for understanding GAA evolution, using the general approach of Hu and Stern (2020). Second, we hope to motivate further systematic study of the GAA convergent margin system.

2. Methods

We imposed a simple fourfold tectonic subdivision on the GAA based on a SW dipping subduction system agreed to by most scholars working in the Caribbean (e.g., Boschman et al., 2014; Escuder-Viruete, Diaz de Neira, et al., 2006; Escuder-Viruete, Contreras, Stein, et al., 2007; García-Casco et al., 2006; García-Casco, Iturralde-Vinent, & Pindell, 2008; Pindell & Kennan, 2009; Pindell et al., 2005; Rojas-Agramonte et al., 2021). In addition we used modern geographic relationships of rock units relative to the present position of the magmatic arc to put published data about GAA rocks into 4 tectonic domains: (a) forearc mélange; (b) forearc ophiolite; (c) magmatic arc (Cretaceous and Paleogene); and (d) retro-arc region, including metamorphic terranes and igneous rocks. This subdivision does not strictly correlate with the geotectonic position of the different geologic complexes in the Cretaceous to their present geographic positions, but it is a useful approximation. Geochronological and geochemical data published in the peer-reviewed literature for Cuba, Hispaniola, Puerto Rico, Jamaica, and the Virgin Islands were assigned into one of the four present tectonic subdivisions (Figure 2).

The compiled units are listed in Table S1. The geochronological compilation was done after Wilson et al. (2019) and includes a total of 664 samples including 2 paleontologically constrained lava flow

ages and 662 radiometric ages determined by six dating techniques: K-Ar (329 samples, 49.5% of data), U-Pb zircon (138 samples, 20.8% of data), 40Ar-39Ar (168 samples, 25.3% of data), Rb-Sr (14 samples, 2.1% of data), Re-Os (6 samples, 0.9% of data), and Lu-Hf (7 samples, 1.1% of data). These age data are compiled from 92 studies. A total of 1,537geochemical analyses were compiled from 51 studies. Samples were screened to avoid highly altered samples using loss on ignition (LOI); only samples with less than 4 wt.% LOI (1,185 samples, Figure 3) were selected, then further filtered to remove samples with no trace element data, leaving 1,112 samples for plotting on trace element diagrams. Immobile trace element plots were used to classify lithologies and to distinguish the tectonic affinities of GAA felsic and mafic components. For the purposes of plotting on tectonic discrimination diagrams, lithologies classified as basalt, basalt-andesite, and alkali basalt are plotted as "mafic"; all other lithologies including dacite/rhyolite, trachy-andesite, and trachyte are classified as "felsic." Details of geochronological data and sources are provided in the supplementary documents (Tables S1 and S2) and listed in the references.

3. Results

Below we first explain the fourfold subdivision of the GAA (Section 3.1), then what age data was compiled and filtered (Section 3.2), and finally how immobile trace element data was compiled and filtered (Section 3.3).

3.1. Fourfold Subdivision of the Greater Antilles Arc

In northern Cuba extensive relics of oceanic lithosphere are recognized as the "northern ophiolites" and "eastern ophiolites" (Iturralde-Vinent, 1998; Iturralde-Vinent et al., 2006). This forms a discontinuous belt of out cropping ophiolites that can be traced more than 1,000 km from Cajálbana in the west to Baracoa in the east (Figures 1aand 4). Three main segments with seven major exposures can be distinguished along strike, from west to east: Cajálbana represents the western segment; the central segment is represented by Havana-Matanzas, Villa Clara, Camagüey, and Holguín; while Mayarí-Cristal and Moa-Baracoa make up the eastern segment. The ophiolite belt lies north of the magmatic arc and overthrusts sedimentary rocks of the North American continental margin in western and central Cuba, revealing that they formed in what became the forearc. Ophiolites in the eastern segment are tectonically emplaced from the SW on top of the Cretaceous volcanic arc, in contrast to other massifs of the western and the central segments. Hence, there is doubt as to whether this segment represents a forearc or formed in a back-arc environment (Marchesi et al., 2006, 2007). A

few ophiolitic slices are also present in the geographic rear-arc setting in the Escambray massif to the south of the magmatic arc which likely represent fragments of the subducted Proto caribbean ocean or Caribbean forearc (García-Casco et al., 2006, and references therein). García-Casco et al.

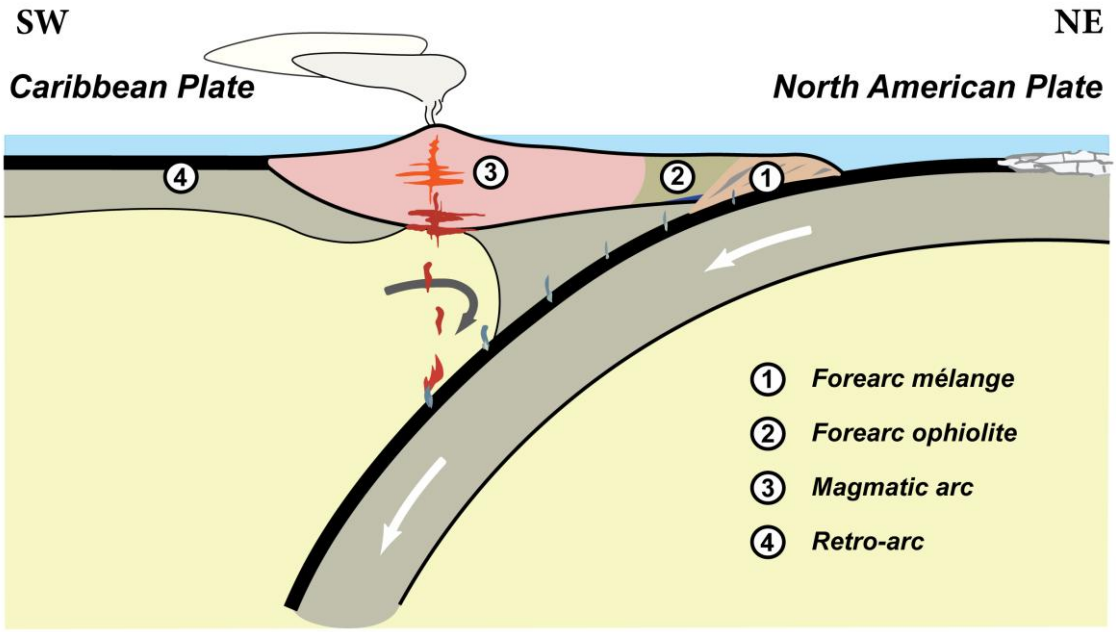

Figure 2. *Simplified cross-section of the Greater Antilles Arc during Cretaceous times showing present-day location of geologic bodies in the fourfold subdivision discussed here with respect to the location of the magmatic arc.*

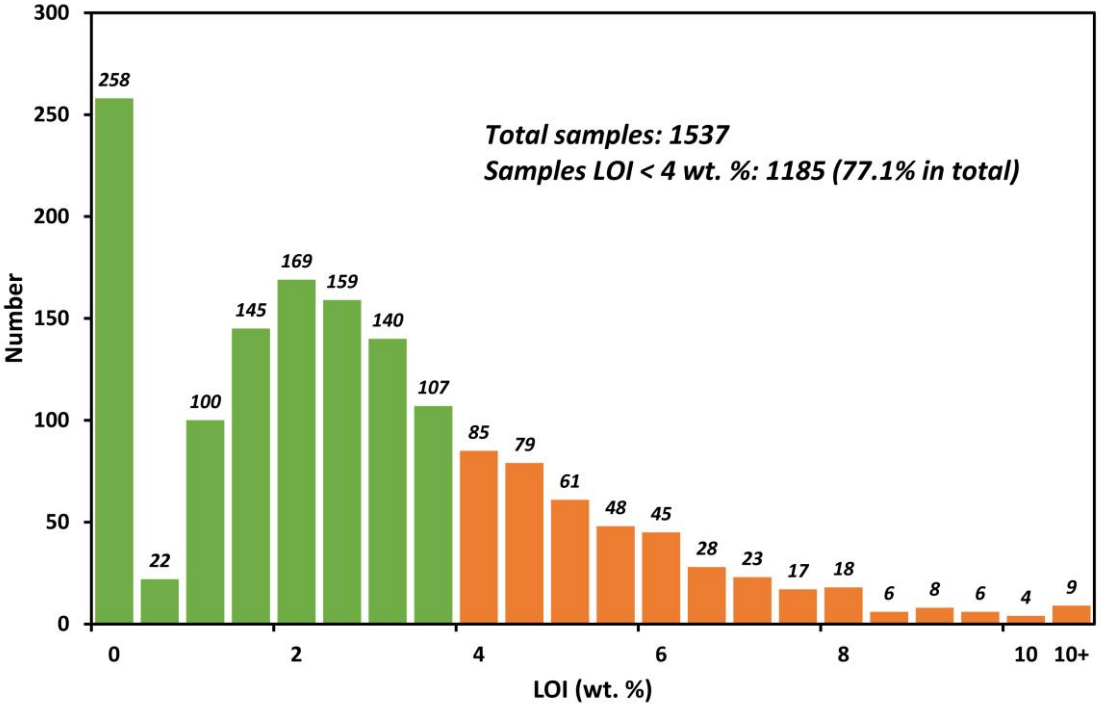

Figure 3. *Histogram of loss on ignition from compiled Greater Antilles Arc geochemical data.*

(2006) noted the contrasting petrologic evolution of high-pressure metamorphic complexes within mélange between the eastern segment and western-central segments (clockwise vs. counterclockwise P-T path), as a likely consequence of timing of subduction-accretion and tectonic setting of formation (onset of subduction vs. mature subduction) (Blanco-Quintero et al., 2010; Blanco-Quintero, Gerya et al., 2011; García-Casco, Lázaro, et al., 2008; Lázaro et al., 2009).

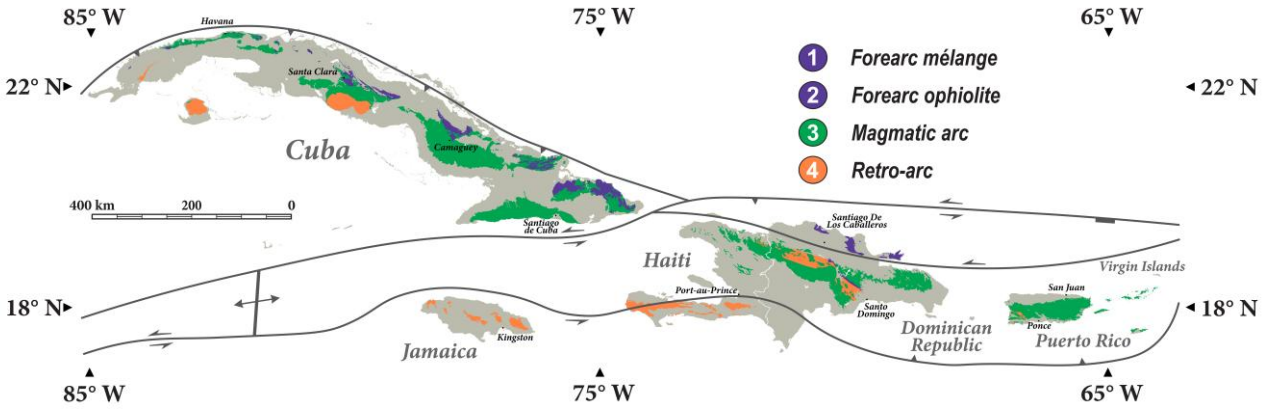

Figure 4. *Simplified tectonic map of the Greater Antilles Arc showing the location of geologic units in the fourfold subdivision. See text for further discussion.*

Forearc ophiolites refer to the massifs of Cajálbana, Havana-Matanzas, Santa Clara, Camagüey, and Holguín within the northern ophiolite belt. For simplicity, the eastern ophiolite belt (Mayarí-Baracoa) and its volcanic and plutonic sequences are also included here as an apparent forearc ophiolite. High-pressure metamorphic rocks within serpentinite mélange intermingled with ophiolitic massifs, such as mélange in Cajálbana (in olistostromes) and Habana-Matanzas-Villa Clara and mélange associated with the eastern ophiolite belt, are assigned to the forearc mélange belt. Magmatic arc units include island arc tholeiites and calc-alkaline suites, and alkaline magma hybridized calc-alkaline rocks (Torró et al., 2020 and references therein). These plutonic and volcanic arc rocks include the Cretaceous arc south of the northern ophiolite belt and Paleogene igneous rocks of the Sierra Maestra of southeastern Cuba. The Mabujina arc-related complex (Rojas-Agramonte et al., 2011), and the subducted passive margin-related Pinos, Cangre and Escambray metamorphic terranes (Despaigne-Díaz et al., 2016, 2017; García-Casco et al., 2001; García-Casco, Iturralde-Vinent, & Pindell, 2008) exposed south of the magmatic arc are assigned to the retro-arc based on their present geographic position.

In northern Hispaniola, ophiolites associated with the accretionary complex are present in the Cordillera Septentrional-Samaná Peninsula in the Dominican Republic. These fragments of oceanic lithosphere are part of the Puerto Plata ophiolitic complex (Escuder-Viruete et al., 2014; Hernaiz Huerta et al., 2012) and the Río San Juan metamorphic complex (Escuder-Viruete & Pérez-Estaún, 2006, 2013; Escuder-Viruete, Friedman, et al., 2011;Escuder-Viruete, Pérez-Estaún, Booth-Rea, & Valverde-Vaquero, 2011; Escuder-Viruete, Perez-Estaún, Gabites,& Suarez-Rodriguez, 2011; Escuder-Viruete, Valverde-Vaquero, Rojas-Agramonte, Gabites, Carrion Castillo, &Perez-Estaun, 2013; Escuder-Viruete, Valverde-Vaquero, Rojas-Agramonte, Gabites, Pérez-Estaún, 2013; Krebset al., 2008, 2011) which include the Río San Juan high-pressure serpentinite mélange and Gaspar Hernández serpentinized peridotite. Escuder-Viruete and Castillo-Carrión (2016) suggested that the high-pressure Cuaba mafic gneisses and amphibolites of the southern Río San Juan metamorphic complex represent exhumed subducted GAA fore-arc, while (ultra-) high-pressure ultramafic rocks from the Cuaba subcomplex are considered to be arc cumulates (Hattori et al., 2010) or mantle plume fragments in an ultra-high pressure oceanic complex (Abbott & Draper, 2007, 2013; Gazel et al., 2011). High-pressure accretionary wedge materials within the Cordillera Septentrional are assigned to the fore-arc mélange. The Punta Balandra unit of the Samaná complex consists of eclogite- and blueschist-interleaved sepentinitic mélange thrust over non-eclogitic units that represent the subducted passive margin (Escuder-Viruete & Pérez-Estaún, 2006); this is assigned to the fore-arc mélange subdivision. Island arc tholeiites and calc-alkaline series igneous rocks are exposed in the Central and Eastern Cordilleras, including volcanic rocks from the Early Cretaceous Los Ranchos and Maimón formations and Tireo group and granitoids which are included in the volcanic arc unit (Escuder-Viruete, Contreras, Stein, et al., 2007; Escuder-Viruete, Diaz de Neira, et al., 2006; Torró, Garcia-Casco, et al., 2016; Torró, Proenza, Marchesi, et al., 2017). Igneous rocks associated with arc-rifting and back-arc spreading in central Hispaniola, and Caribbean Large Igneous Province (CLIP)-associated units such as the Duarte Complex (Dominican Republic) and Dumisseau formation (Haiti and southwestern Dominican Republic) are assigned to the retro-arc (Escuder Viruete et al., 2008; Escuder-Viruete, Joubert, et al., 2016; Escuder Viruete, Perez-Estaún, et al., 2007; Escuder-Viruete, Perez-Estaún, et al., 2011; Sen et al., 1988; Sinton et al., 1998).

Cretaceous and Paleogene volcanic and plutonic rocks of Jamaica (Mitchell, 2020 and references therein), Puerto Rico (e.g., Jolly et al., 1998, 2002, 2008a), and the Virgin Islands (e.g., Jolly & Lidiak, 2006; Lidiak & Jolly, 1998) are included in this study. Jamaican rocks are assigned to the retro-arc. The southern wall of Puerto Rico Trench comprises schists and serpentinites of a submerged

accretionary prism (Perfit et al., 1980b). Ophiolitic mélange and peridotite belts of southwestern Puerto Rico (Lidiak et al., 2011; Schellekens, 1998a) belong to the retro-arc region in the fourfold subdivision according to its current geographic location.

3.2. Age and Technique Distribution in the Greater Antilles

A systematic difference in ages occurs between different techniques shown in Figure 5a. For example, U-Pb zircon ages display an older mean of 92 ± 53 (2σ) Ma compared to younger mean ages from Ar-Ar (74 ± 41 Ma) and K-Ar (70 ± 41 Ma) systems. These results indicate that a significant number of Ar-Ar and K-Ar ages represent cooling or reset ages, which is particularly evident in the case of Cenozoic K-Ar ages of Cretaceous volcanic arc igneous rocks in Cuba, for example. Figure 5b distinguishes ages determined for igneous versus metamorphic rocks. Metamorphic rocks are further divided into mélange-related metamorphism, ophiolite-related metamorphism, and metamorphism of present-day complexes located in the retroarc (see further discussion in Section 4.4). Mélange-related metamorphic ages show an older mean of 84 ± 58 Ma compared to ophiolite-related metamorphic ages (78 ± 4 Ma) and metamorphic ages of present-day retroarc (72 ± 28 Ma). Igneous ages (76 ± 48 Ma) are similar to these two younger metamorphic ages. As mentioned in the geographic sampling bias section, the Caribbean realm is under sampled in many regions and caution must be taken when interpreting age histograms.

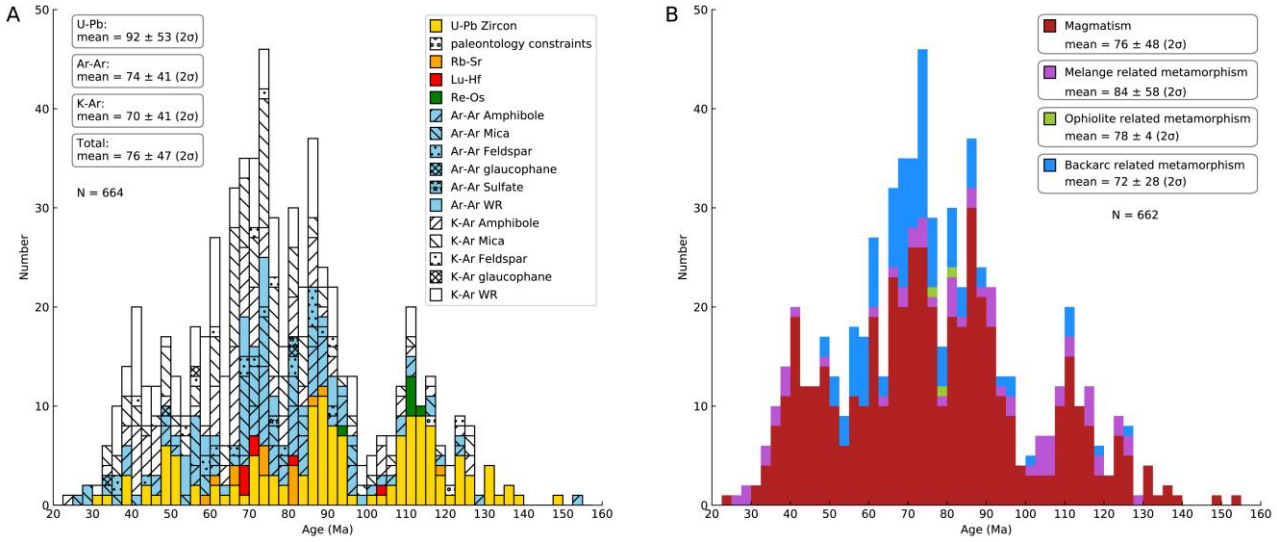

Figure 5. *Histogram of compiled age data for the Greater Antilles Arc (GAA), including Cuba, Hispaniola, Jamaica, Puerto Rico, and Virgin Islands sorted by (a) geochronologic method and (b) magmatism and metamorphism (based on association to mélange, ophiolite or retro-arc). Results of radiometric dating and paleontology age constraints show the temporal spectrum of the GAA magmatic and metamorphic events. Ages range from 155 Ma (Jurassic) to 30 Ma (Oligocene), but the vast majority (except for two dates) are Cretaceous and Paleogene. Data sources listed in Table S1.*

Some peaks stand out in the histograms, especially in the Late Cretaceous - early Paleocene from 95 to 60 Ma (Figure 5b). This interval is shown in both igneous and metamorphic rocks and is especially clear in $^{40}Ar/^{39}Ar$ ages and K-Ar ages. Two subordinate peaks are observed at 120-110 Ma and ~40 Ma. The older peak is especially clear in U-Pb zircon and Re-Os ages and reflects both magmatic and metamorphic activity, including partial melting of metamorphic rocks in a hot subduction zone (eastern Cuba). The younger peak is dominated by K-Ar and $^{40}Ar/^{39}Ar$ ages and mostly reflects igneous activity. These differences are good examples of technique bias (the difference between ages from different techniques) and potential resetting of the K-Ar isotopic system. There is also geologic bias, the difference between U-Pb zircon, which mostly is used for dating igneous crystallization, and $^{40}Ar/^{39}Ar$, which is often used for dating metamorphic and cooling events below ca. 400°C. These biases are discussed further in Section 4.1.

In the next sections, we examine the age distributions of the four tectonic units: forearc ophiolite, forearc mélange, magmatic arc, and retro-arc.

3.2.1. Forearc Mélange

Age data of the forearc mélange in Cuba and Hispaniola come from high-pressure metamorphic rocks within serpentinite mélange, presumably reflecting the GAA subduction zone metamorphic history (Figure 6). Ninety-three dates or 14.0% of the 664 ages in our compilation are for this tectonic subdivision. Some of these are ages of igneous protoliths (esp. U-Pb zircon ages), whereas many others are metamorphic. In Cuba, samples are from mélange intermingled with ophiolites within the northern ophiolite belt and mélanges of Sierra del Convento and La Corea in the Eastern Moa-Baracoa Ophiolite. In northern Hispaniola, ages of high-pressure metamorphic rocks and tectonic blocks of serpentinized peridotite within the Río San Juan serpentinite mélange and Samaná complex are included. In the Puerto Rico Trench, a mica-epidote schist and muscovite from a greenschist yield K-Ar ages of 63 ± 3 Ma and 66 ± 6 Ma (Perfit et al., 1980b). Age distributions of forearc mélange in Hispaniola display a younger mean (72 Ma), larger 2σ (±52 Ma), and a wider range (139–26 Ma) compared to an older mean (105 Ma), smaller 2σ (±24 Ma), and narrower range (130–83 Ma) of Cuba. The possible significance of the difference in ages is explored in the discussion.

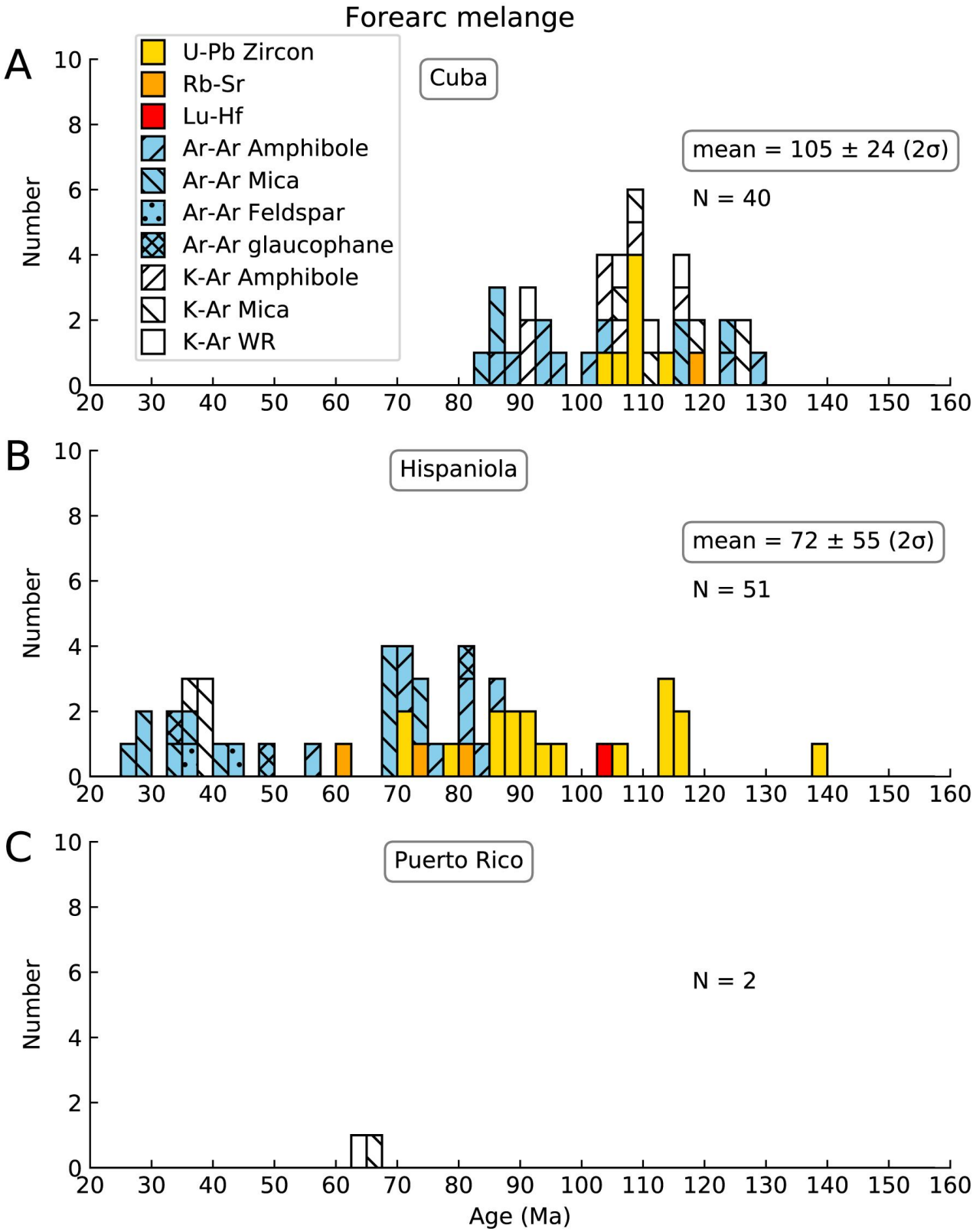

Figure 6. *Histogram of compiled age data for forearc mélange in the Greater Antilles Arc fourfold subdivision, (a) Cuba, (b) Hispaniola, and (c) Puerto Rico. See text for further discussion.*

3.2.2. Forearc Ophiolite

GAA forearc ophiolites are exposed between the trench (the suture zone in the west and Puerto Rico Trench in the east) and the magmatic arc, mainly exposed in tectonically uplifted regions in Cuba and Hispaniola (Figure 4). There are limited data for Cuba (N = 22) and Hispaniola (N = 8; Figure 7); only 4.6% of available ages are for this tectonic subdivision. Hispaniola shows older forearc ophiolite ages than Cuba. Within the Rio San Juan metamorphic complex, an evolved gabbro sill intruded into the Gaspar Hernandez serpentinized peridotite-tectonite yielded a concordant zircon U-Pb age of 136.4 ± 0.34 Ma and an even older hornblende 40Ar-39Ar age of 153.5 ± 8.9 Ma (Escuder-Viruete, Friedman, et al., 2011). One zircon $^{206}Pb/^{238}U$ age of 126.1 ± 0.3 Ma for an olivine gabbro from the Puerto Plata ophiolitic complex (Monthel, 2010) shows a similar age to the oldest forearc ophiolite ages in Cuba (Lázaro et al., 2016). Ophiolite ages show a wider range, from 127 to 60 Ma, in the northern ophiolite belt in central and western Cuba. In the Havana-Matanzas section, one whole rock $^{40}Ar-^{39}Ar$ age of 98.1 ± 0.5 Ma was reported for a plagiogranite (Llanes Castro et al., 2019). Ages of intrusive (arc-related) tonalitic and granitic rocks within the Villa Clara ophiolite range from 85 to 61 Ma (Iturralde-Vinent et al., 1996; Rojas-Agramonte et al., 2010), and ages of dolerite and basalt in the Holguín ophiolite range from 127 to 72 Ma (Iturralde-Vinent et al., 1996). In the eastern ophiolite belt, one gabbro sample in the Moa massif yielded a zircon $^{206}Pb/^{238}U$ age of 124.3 ± 0.9 Ma (Rojas-Agramonte et al., 2016) and the Río Grande intrusive in the Mayarí-Cristal ophiolitic massif provided a hornblende $^{40}Ar-^{39}Ar$ age of 89.70 ± 0.50 Ma (Proenza et al., 2006). Lázaro et al. (2015) reported hornblende $^{40}Ar-^{39}Ar$ age of 77–81 Ma obtained for amphibolites from the Güira de Jauco metamorphic sole. Thus, forearc ophiolites and metamorphic soles in Cuba and Hispaniola both yield a wide range of ages reflecting varied geodynamic processes affecting the oceanic lithosphere since its formation in the Early Cretaceous.

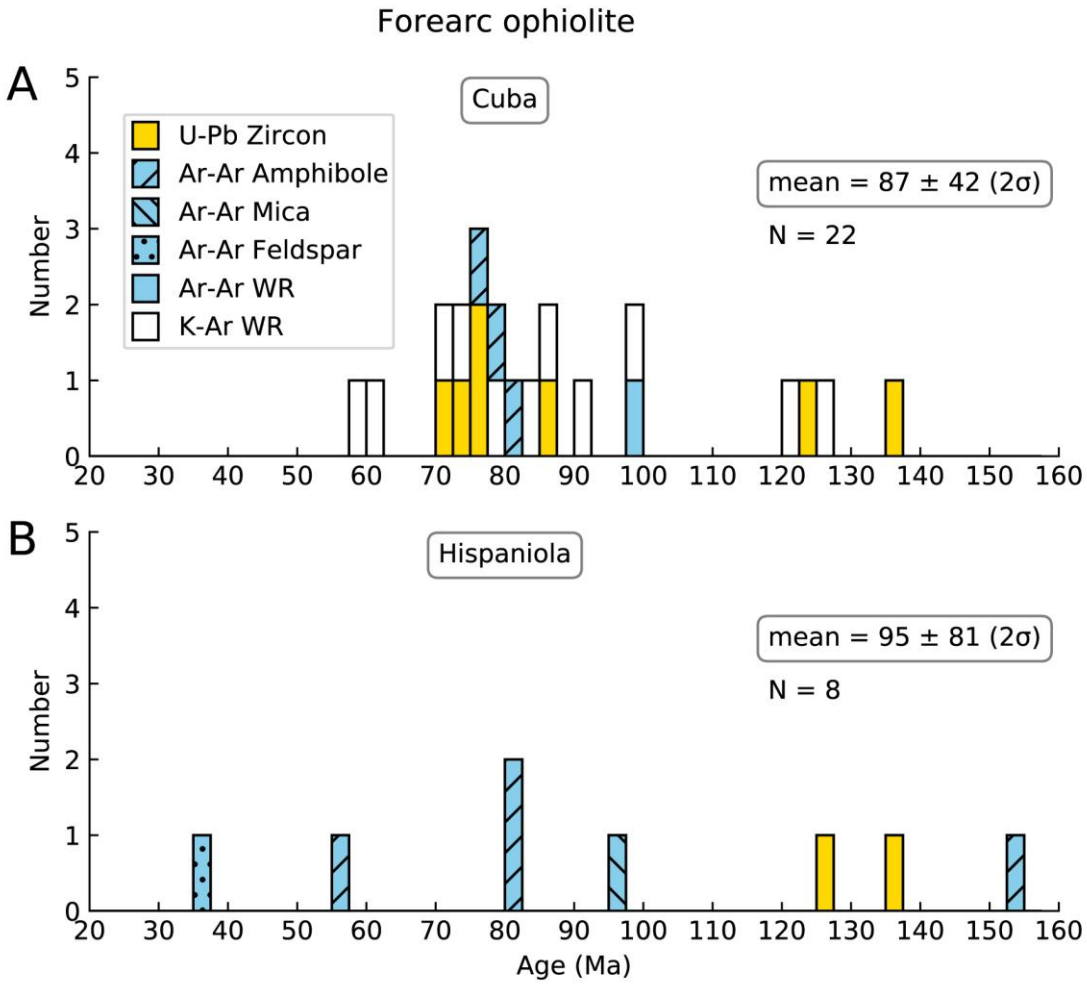

Figure 7. *Histograms of compiled age data for forearc ophiolite in (a) Cuba and (b) Hispaniola.*

3.2.3. Magmatic Arc

Age data for GAA Cretaceous and Paleogene magmatic arcs come from Cuba, Hispaniola, Puerto Rico, and the Virgin Islands (Figure 8). Volcanic and plutonic rocks from the Cretaceous and Paleogene arcs are included; 373 ages or 56.2% of the 664 ages in our compilation are for this unit. Magmatism in these four islands shows a broadly similar range but with very different distributions. A strong early peak in magmatism (120–110 Ma) is shown in Hispaniola; this peak is robust because it is dominated by U-Pb zircon ages. A few ages in this range are found in Cuba but the main peak is around 90 to 70 Ma. Puerto Rico and Virgin Islands show mostly much younger ages, mostly 75–40 Ma in Puerto Rico and 45-30 Ma in the Virgin Islands. This is a good example of geographic bias. The oldest mean age (85 ± 49 Ma) is found for Hispaniola, and lower mean ages of 77 ± 30 Ma are found for Cuba, 57 ± 32 Ma for Puerto Rico, and 52 ± 43 Ma for the Virgin Islands. The possible significance of the difference in ages is explored in the discussion.

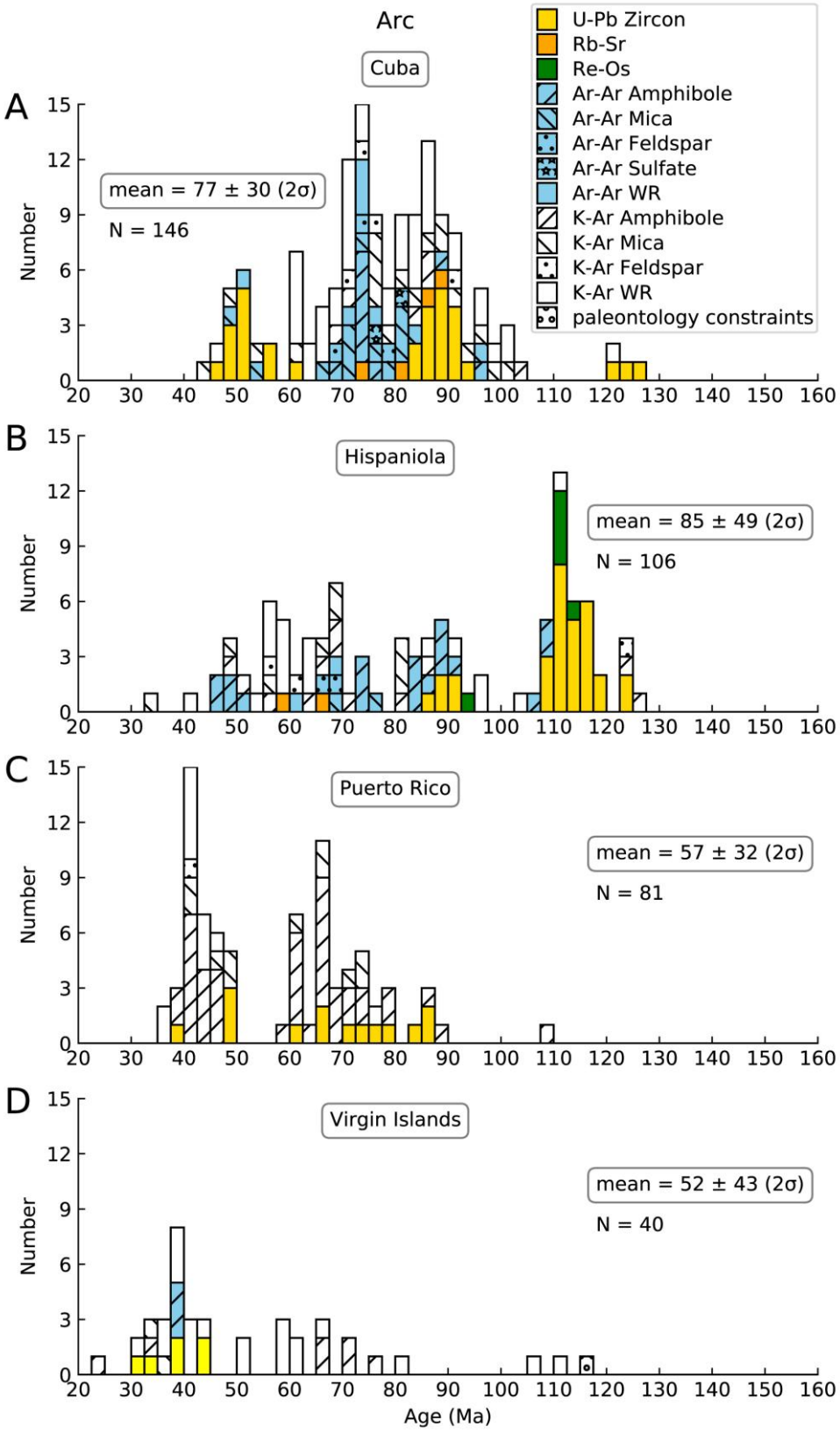

Figure 8. *Histogram of compiled age data for the Greater Antilles Arc magmatic arc in (a) Cuba, (b) Hispaniola, (c) Puerto Rico, and (d) Virgin Islands.*

3.2.4. Retro-Arc

The retro-arc subdivision encompasses igneous and metamorphic samples from the region south of the GAA magmatic arc. This subdivision includes magmatic and metamorphic events (Figure 9). Age data of the retro-arc region in Cuba include igneous and metamorphic rocks of the passive margin-related Pinos and Escambray metamorphic terranes and the volcanic arc-related Mabujina complex in western and central Cuba. One-hundred sixtyeight ages or 25.3% of the 664 ages in our compilation are for this unit. The metamorphic and magmatic age of the Cuban retro-arc region ranges from 132 to 50 Ma and peak at around 75 to 65 Ma, giving a mean of 74 ± 34 Ma (2σ). In Hispaniola, the retro-arc region consists of oceanic plateau (Escuder-Viruete, Joubert, et al., 2016; Sen et al., 1988) and transitional and oceanic crust, which formed during Late Cretaceous back-arc basin opening (Escuder-Viruete et al., 2008). The age of Hispaniola retro-arc samples ranges from 126 to 53 Ma, with a peak around 90 Ma and a mean of 90 ± 28 Ma (2σ).

In the southwestern corner of Puerto Rico, the Bermeja Complex lies behind (south of) the Cretaceous magmatic arc. Two samples from Las Palmas Amphibolite provide hornblende K-Ar ages of 126 ± 3 Ma and 112 ± 15 Ma (Cox et al., 1977). Zircons from amphibolite boulders in the Bermeja complex show older ages (ca. 130 Ma; Pérez, 2008).

Jamaica falls in the GAA retro-arc region due to its location well to the south and west of the magmatic arc in Cuba and Hispaniola, respectively. Metamorphic and magmatic rocks in Jamaica range in age from 120 to 53 Ma. Granitoids and high-pressure metamorphic rocks range from 78 to 53 Ma. Paleontology constraint on the Devils Racecourse Formation provides the oldest age of 120 Ma. Jamaica retroarc rocks give a mean of 65 ± 29 Ma (2σ).

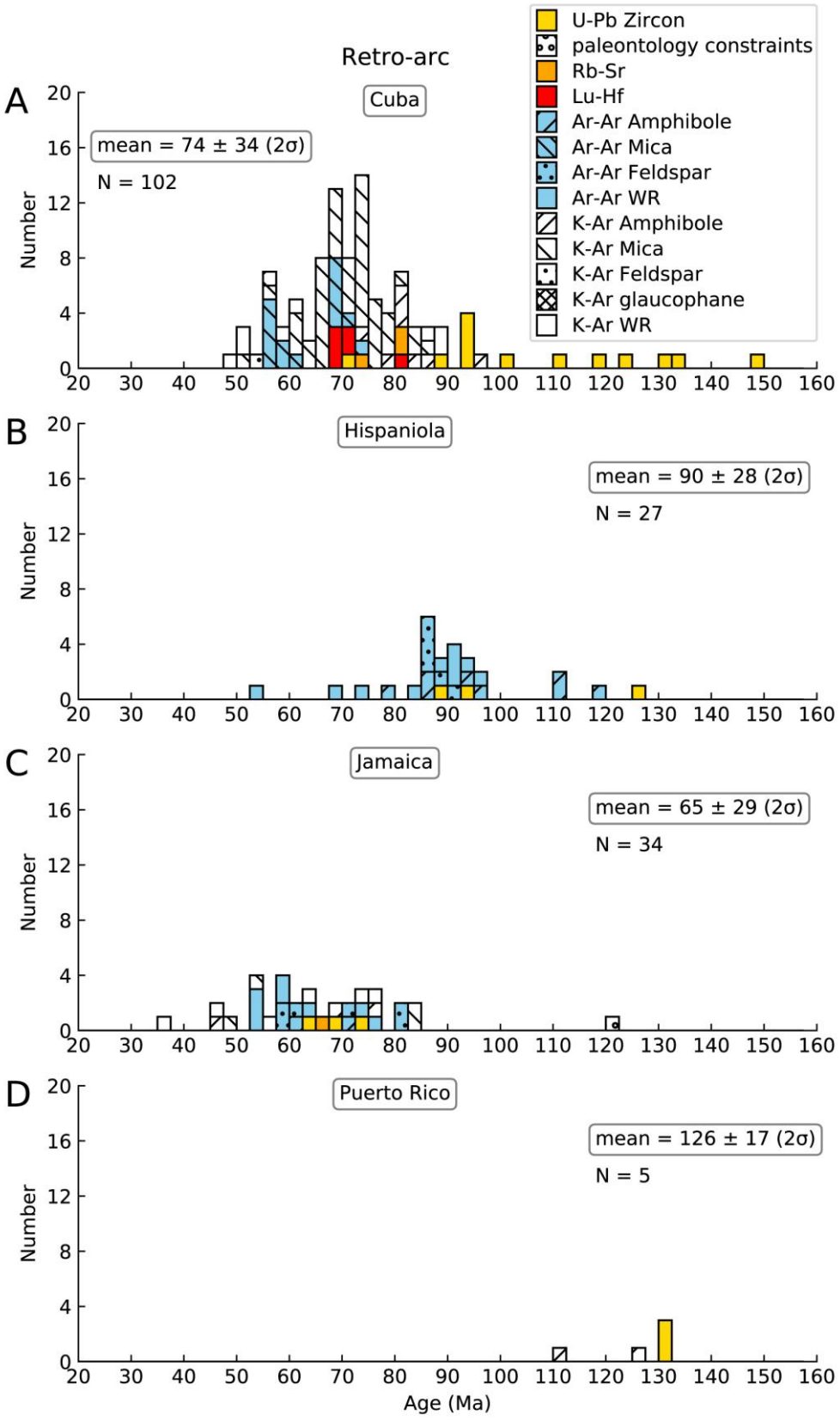

Figure 9. *Histograms of compiled age data for the Greater Antilles Arc magmatic arc in (a) Cuba, (b) Hispaniola, (c) Jamaica, and (d) Puerto Rico.*

3.3. Immobile Trace Element Geochemistry of the GAA

We used immobile trace element plots to determine original lithologies because these are less susceptible to alteration and better allow identification of petrogenetic and geodynamic attributes of GAA igneous rocks. First, the 1,112 screened igneous origin rocks are classified on the basis of incompatible element ratios Zr/Ti versus Nb/Y (Figure 10a). Most data (91%) plot in low Nb/Y sub-alkaline fields: basalt (49%), andesite/basaltic andesite (34%), and rhyolite/dacite (8%). Far fewer data plot in the high Nb/Y alkaline fields: alkali basalt (4%), trachy-andesite (5.6%), and trachyte (0.5%). Based on this classification, subalkaline basalts dominate the GAA, followed by andesite and basaltic andesite.

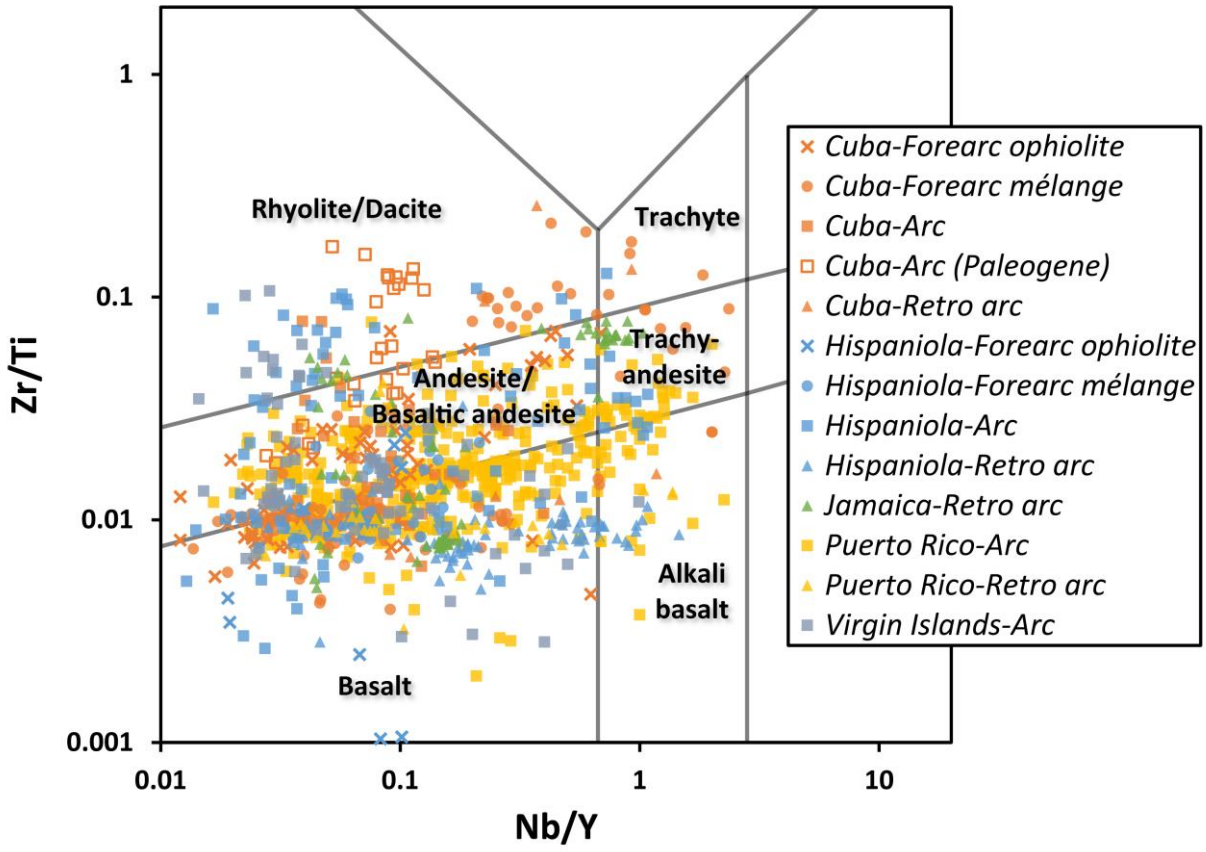

Figure 10. *Zr/Ti versus Nb/Y diagram (after Pearce, 1996) for Greater Antilles Arc igneous rocks.*

There is a noticeable geographic bias in the 1,112 samples, with 271 analyses from Cuba (52% of GAA area, 24% of data), 214 analyses from Hispaniola (38% of GAA area, 19% of data), 76 analyses from Jamaica (5.5% of GAA area, 6.9% of data), 480 analyses from Puerto Rico (4.5% of GAA area, 43% of data), and 71 analyses from Virgin Islands (0.1% of GAA area, 6.4% of data; Figure 11b).

For plotting on tectonic discrimination diagrams, the 6 lithologies indicated above are further grouped into mafic and felsic rocks. Mafic refers to basalt, alkali basalt, and andesite/basaltic andesite (86% of data); and felsic refers to trachy-andesite, trachyte, and rhyolite/dacite (14% of data). By this measure, the GAA is overwhelmingly a mafic construction, as expected for intra-oceanic arcs (Stern, 2010)

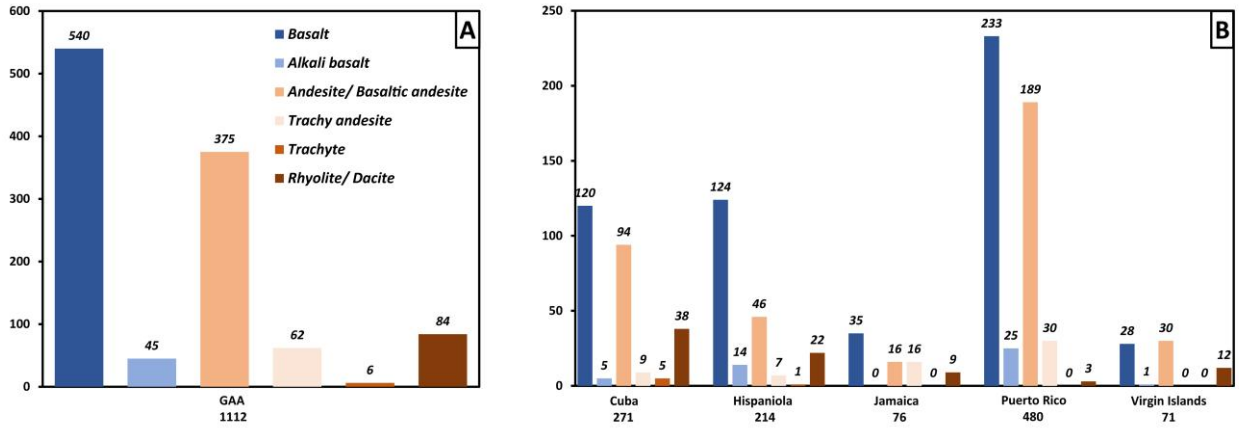

Figure 12. *Felsic rocks (of trachy-andesite, trachyte and rhyolite/dacite composition) of the Greater Antilles Arc in the tectonic discrimination diagram of Pearce, Harris, and Tindle (1984). See text for further discussion.*

3.3.1. Felsic Rocks: Ta-Yb Plot

GAA felsic rocks are found in all four tectonic settings: forearc ophiolite (Cuba), forearc mélange (Cuba), magmatic arc (Hispaniola, Puerto Rico, Virgin Islands; Cuba Paleogene arc), and retro-arc (Jamaica). Most data fall into the volcanic arc granite (VAG) field on the Ta-Yb tectonic discriminant diagram (Pearce, Harris, & Tindle, 1984; Figure 12). A few samples plot in adjoining fields near VAG.

3.3.2. Mafic Rocks: Th/Yb-Nb/Yb Plot

This diagram (Figure 13) allows assessing the extent of subduction-related metasomatism and contamination by continental crust on the one hand versus magmas derived from mantle that was not affected by subduction, like mid-ocean ridge basalts (MORB), enriched mid-ocean ridge basalts (E-MORB), and ocean island basalts (OIB; Pearce, 2008). Th and Nb are both more incompatible than Yb so Th/Yb and Nb/Yb covary for unmodified mantle, with low Nb/Yb and Th/Yb for basalts from depleted unmodified mantle like N-MORB and high Nb/Yb and Th/Yb for basalts from enriched mantle like OIB. The covariation defines the N-MORB to OIB "unmodified mantle array." Basalts generated from mantle that has been affected by melts/fluids evolved from subducted sediments or

that interacted with continental crust will plot above the unmodified mantle array. Because the GAA was built on oceanic crust and is not underlain by continental crust, the samples that plot above the mantle array crystallized from magmas that formed above a subduction zone, as expected.

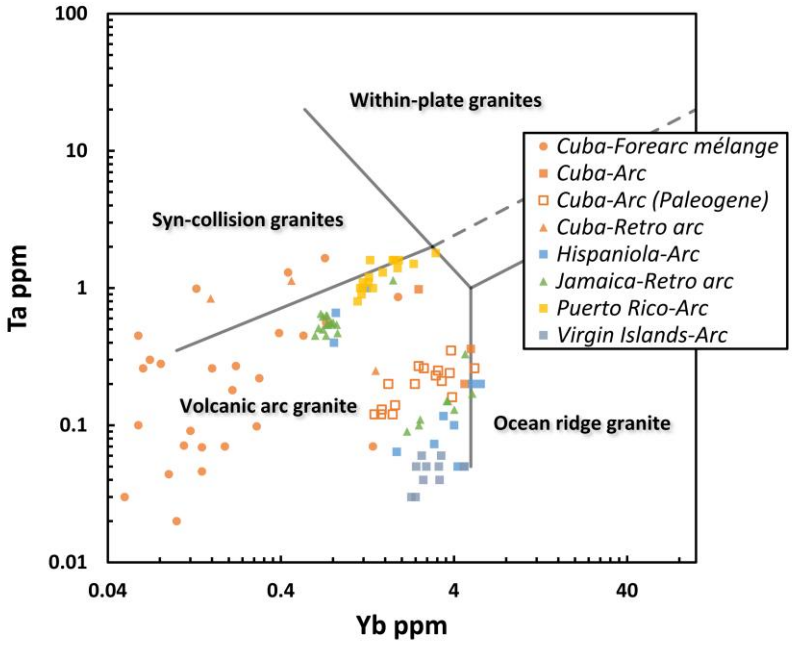

Figure 12. *Felsic rocks (of trachy-andesite, trachyte and rhyolite/dacite composition) of the Greater Antilles Arc in the tectonic discrimination diagram of Pearce, Harris, and Tindle (1984). See text for further discussion.*

GAA forearc ophiolites are plotted in Figure 13a. These mostly show elevated Th/Yb, consistent with formation at a convergent plate margin. The metasomatized mantle source involved N-MORB and E-MORB mantle for the few samples from Hispaniola, and the wider spectrum in Cuba indicate that these sources were metasomatized as well as (local) metasomatized OIB mantle source. Figure 13b shows that forearc mélange blocks in Cuba and Hispaniola exhibit a similar spectrum of mantle sources to those of forearc ophiolites, but Cuba data shows derivation from less metasomatized mantle sources compared to more metasomatized mantle sources suggested from Hispaniola data. Nearly all magmatic arc data show arc affinities, as expected. The magmatic arc of Hispaniola, Puerto Rico, and Virgin Islands present a wide spectrum of metasomatized mantle sources from N-MORB to OIB, in contrast to the Cretaceous and Paleogene magmatic arcs of Cuba, for which samples are more confined to metasomatized N-MORB to E-MORB (Figure 13c). Retro-arc samples show variable results, with Hispaniola-Cuba-Puerto Rico mostly plotting in the mantle array and Jamaica showing a clear arc affinity (Figure 13d).

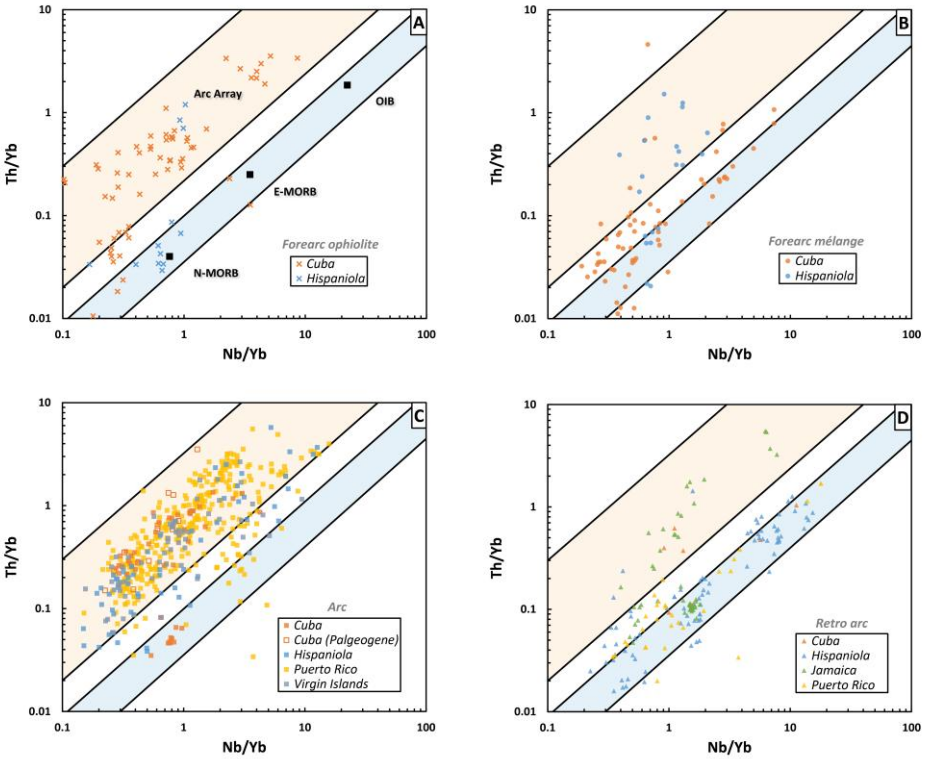

Figure 13. *GAA mafic samples (of basalt, alkali basalt and andesite/basaltic andesite composition) plotted on the Th/Yb versus Nb/Yb of Pearce (2008). Light orange field indicates volcanic arc array and light blue field indicates mantle array. See text for further discussion.*

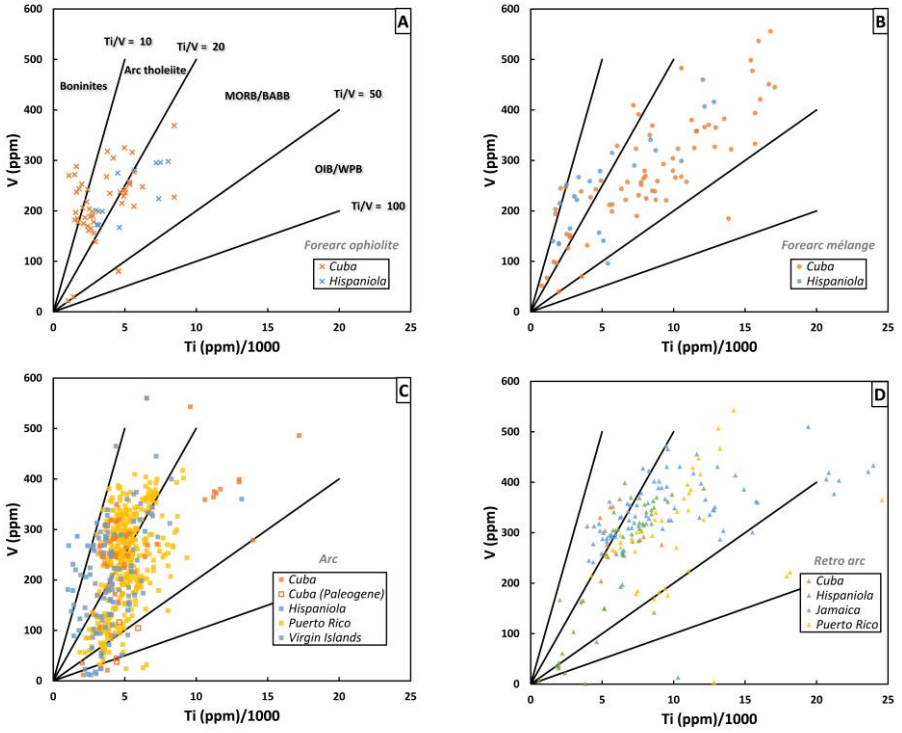

Figure 14. *Ti/1,000 (ppm) versus V (ppm) diagram from Shervais (1982) for Greater Antilles Arc mafic rocks (basalt, alkali basalt, and andesite/basaltic andesite). See text for further discussion.*

3.3.3. Ti-V Plot

The Ti-V plot reveals variations in the behavior of V during partial melting and fractionation, which is thought to reflect magmatic oxygen fugacity. The basis of this plot is that Ti is always +4 and behaves as an incompatible element but V can be +3 or +4 in magmas and V+3 is more compatible than V+4. Because convergent margin magmas are more oxidized than MORB or OIB, arc magmas have lower Ti/V. Arc magmas have Ti/V ratios equal to and less than 20, except for calc-alkaline magmas which show the effects of magnetite fractionation, therefore plotting magmatically evolved rocks should be done with caution. MORB and continental flood basalts have Ti/V ratios of about 20–50 and alkaline rocks have Ti/V generally >50. Back-arc basin basalts may have either arc-like or MORB-like Ti/V ratios.

Figure 14 shows that most mafic rocks of GAA fall into island arc tholeiite (IAT) and MORB/BABB fields. Most forearc ophiolite data show IAT and MORB/BABB affinity and some data from Cuba fall into the boninite field (Figure 14a). In Figure 14b, most forearc mélange data from Cuba fall into the MORB/BABB field, with fewer showing IAT affinity. The vast majority of magmatic arc data exhibit IAT and MORB/BABB affinity (Figure 14c), though there are also a few data showing boninite (Hispaniola) or OIB affinity. Most retro-arc data cluster in the IAT and MORB/BABB field and few rocks show OIB affinity (Figure 14d).

3.3.4. Sr/Y Versus Y and La/Yb Versus Yb Plots

The Sr/Y versus Y and La/Yb versus Yb plots are typically used to discriminate adakite from normal arc andesitic, dacitic and rhyolitic magmas. The term adakite was coined by Defant and Drummond (1990) to describe intermediate to felsic, high Sr/Y and La/Yb volcanic and plutonic rocks produced by melting of the basaltic portion of oceanic crust in subduction zones. This requires unusual “hot” subduction and high-pressure evolution of magma where garnet is stable. In addition to slab melting (young and hot oceanic lithosphere and ridge subduction), high Sr/Y and La/Yb ratios can be produced by melting of mafic lower arc crust, fractional crystallization of hydrous mafic magmas, and high-pressure fractional crystallization of arc mafic magmas (Castillo, 2012; Moyen, 2009).

Figure 15 shows that most GAA intermediate to felsic rocks have high Y and Yb content and low Sr/Y and La/ Yb ratios, falling into the normal island arc field. In Figure 15a, a few samples from forearc ophiolite, forearc mélange and retro-arc of Cuba and the volcanic arc of Hispaniola, Puerto Rico and Virgin Islands fall into the high Sr/Y adakite field. In Figure 15b, a few samples from forearc

mélange and retro-arc of Cuba, volcanic arc of Hispaniola, Puerto Rico and retro-arc of Jamaica fall into the high Sr/Y and La/Yb adakite field.

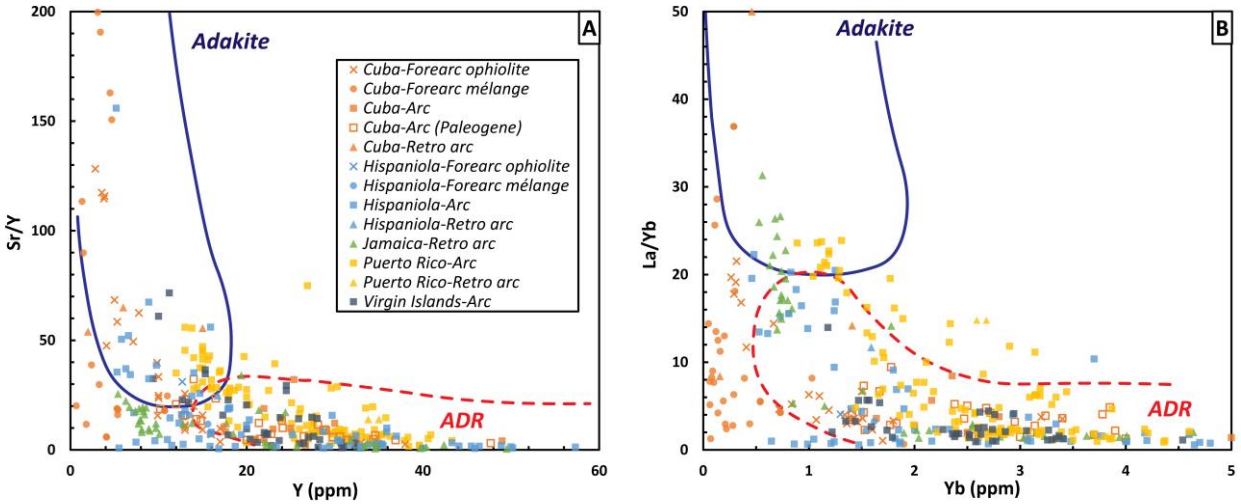

Figure 15. *Plots of (a) Sr/Y versus Y and (b) La/Yb versus Yb after Castillo (2012) discriminating between adakitic and island-arc andesite, dacite and rhyolite (ADR) lavas for Greater Antilles Arc rocks with silica content greater than 56 wt%. See text for further discussion.*

4. Discussion

Below we discuss five aspects of our compilation. First, we discuss the extent to which our compiled data are biased. Second, we discuss the extent to which a SI model can be usefully applied to the system. Third, we discuss the extent to which the CLIP affected the GAA. Fourth, we discuss some complications and considerations. Finally, we offer some suggestions for future research.

4.1. What Are the Biases in the Data and Assumptions in Our Approach?

We are aware of four significant biases in our compilation: technique, geologic, geographic, and land/sea. Technique bias reflects the fact that some radiometric methods (e.g., U-Pb zircon, ^{40}Ar-^{39}Ar) are more reliable than others (e.g., K-Ar). Geologic bias refers to the fact that ages pertain to either igneous or metamorphic episodes. Geographic bias refers to the fact that some islands have more geochronologic and geochemical data per unit area than others. Land/sea bias reflects the fact that nearly all the data in our compilation comes from subaerial exposures and we know little about the submerged GAA.

4.1.1. Technique Bias

Technique bias is a significant consideration for the geochronology compilation. A total of 662 radiometric ages and two paleontology constraints from the literature were compiled for Cuba, Hispaniola, Jamaica, Puerto Rico, and Virgin Islands, as shown in Figure 5. These studies used a wide range of radiometric techniques, with U-Pb zircon (21% of ages) and ^{40}Ar-^{39}Ar (25% of ages) being the preferred techniques and K-Ar (50% of ages) considered least reliable. Ages determined by four other techniques (Rb-Sr, Re-Os, Lu-Hf, and paleontology) make up 4% of the age compilation and contribute little to technique bias. Ages by the three major techniques are distributed differently among the islands. Cuba accounts for about half (46.7%) of the 310 ages we compiled, 55% of which (169) are K-Ar ages. Hispaniola has 192 ages (29%), only 24% (46) of which are K-Ar ages. Jamaica has 5% of the data (34), 38% of which are K-Ar ages. Puerto Rico has 13% of the age data in our compilation, 80% of which are K-Ar ages. The Virgin Islands have 6% of the age data (40), 75% of which are K-Ar ages. We conclude that there is significant technique bias in the geochronology compilation.

Future geochronologic research will surely emphasize U-Pb zircon and ^{40}Ar-^{39}Ar techniques and promise to reduce technique bias. It is noteworthy that some modern thermochronologic techniques (e.g., monazite, titanite, and xenotime U-Pb) have not yet been conducted on GAA rocks. Fission track work on Cretaceous and Paleogene volcanic arc rocks in southeastern Cuba (Rojas-Agramonte et al., 2006) and Jamaica (Comer et al., 1980) reveals GAA exhumation history, and recent zircon and apatite (U-Th)/He ages on volcanic rocks in Jamaica (Cochran et al., 2017) and Puerto Rico (Román et al., 2021) provide further constraints on the kinematics of GAA collision and uplift.

4.1.2. Geologic Bia

Ages determined by radiometric techniques can be subdivided into those that date when a magma crystallized (crystallization age) or when a metamorphic rock cooled below a closure temperature (metamorphic age). A systematic difference in age is seen for some techniques in Figure 5a. For example, U-Pb zircon ages display an older mean of 92 Ma compared to younger mean ages from ^{40}Ar-^{39}Ar (74 Ma) and K-Ar (70 Ma) systems. These results indicate that ^{40}Ar-^{39}Ar and K-Ar ages are strongly influenced by resetting and/or represent cooling below ca. 400°C rather than the igneous/metamorphic formation age of the rock bodies. Four-hundred seventy nine ages are igneous crystallization ages and 183 are metamorphic/cooling ages. Igneous activity is better approximated with U-Pb zircon ages whereas metamorphic evolution and cooling/decompression rates are better

approximated by ^{40}Ar-^{39}Ar dating of amphiboles and micas. This may account for the significant difference between mean U-Pb zircon age (92 Ma) and younger mean age from ^{40}Ar-^{39}Ar (74 Ma). Figure 5b distinguishes ages determined for igneous versus metamorphic rocks, but no significant difference in age is observed; igneous ages show a mean of 76 ± 48 Ma whereas metamorphic ages show a mean of 77 ± 43 Ma

4.1.3. Geographic Bias

Geographic bias refers to whether a region is sampled in proportion to its exposures or not. One way to do this is to compare data density on an island basis, using the area of basement exposed on each island. Cuba has ~58% of exposed GAA basement, Hispaniola has ~30%, Jamaica has 2.3%, Puerto Rico has ~9.3%, and the Virgin Islands have ~0.7% (estimated basement, non-sedimentary outcrop, exposure areas calculated from Iturralde-Vinent et al. [2016], Escuder Viruete, Perez-Estaún, et al. [2007], Mitchell [2020], Lidiak and Anderson [2015], and Wilson et al. [2019]). These are the proportions expected for geographically unbiased data. Relative to this expectation, for geochronology Cuba is slightly undersampled with 46.7% of ages, Hispaniola is proportionally sampled (29% of ages) whereas Jamaica (5% of ages), Puerto Rico (13% of ages), and Virgin Islands (6% of ages) are oversampled (Figure 11b). Within Hispaniola, Haiti is undersampled (31% of basement exposures, 14.1% of the ages) relative to the Dominican Republic (69% of basement, 85.9% of the ages). Geographic bias is more pronounced in 1,112 samples with geochemical data. Cuba is undersampled with 271 analyses (58% of GAA area, 24% of plotted data) as is Hispaniola with 214 analyses (30% of GAA area, 19% of plotted data). Within Hispaniola, nearly all data come from the Dominican Republic (99.4%). Jamaica is oversampled with 76 analyses (2.3% of GAA area, 6.9% of data), Puerto Rico is strongly oversampled with 480 analyses (9.3% of GAA area, 43% of data), as are the Virgin Islands with 71 analyses (0.7% of GAA area, 6.4% of data; Figure 11b).

It should be noted that there is also geographic bias within countries. For example, in Hispaniola, there are significantly more samples for geochronology in the Central Cordillera than in the rest of the island.

4.1.4. Land/Sea Bias

This bias deals with the fact that GAA samples in our compilation mostly come from the islands and few data come from offshore. This is a particular problem for the forearc ophiolite and mélange and retro-arc, for which samples mostly come from the western collided half of the GAA. In the east, where slow oblique convergence continues, forearc ophiolite and mélange that are the eastern

equivalents of their western counterparts are submerged, requiring marine geoscientific techniques to study. Some studies have been conducted in the submerged eastern forearc. Marbles and other metasediments dredged from ca. 400 km along the southern wall of the Puerto Rico Trench are reported derived primarily from island-arc and pelagic component, and some magnesian schists and serpentinites are found in the accretionary prism (Heezen et al., 1985; Perfit et al., 1980b). Forearc ophiolite and mélange also include possible submerged fragments of the North Slope terrane of northern Puerto Rico (Larue & Ryan, 1998). More studies also need to be conducted in the submerged Beata Ridge to the south of Hispaniola (Dürkefälden et al., 2019). The ridge has been classified as part of the Mesozoic CLIP (Hoernle et al., 2004)

4.1.5. Subduction Initiation in the Greater Antilles Arc

Investigating SI is the key to understanding the tectonic evolution of a convergent margin. It is increasingly recognized that suprasubduction zone ophiolites (Pearce, Lippard, & Roberts, 1984), metamorphic soles (Agard et al., 2007; van Hinsbergen et al., 2015), and sometimes boninites are generated during SI (Stern & Gerya, 2018), creating the fore-arc (Stern et al., 2012). Within the GAA, a long ophiolite belt parallels the western section of the magmatic arc in Cuba, offering an opportunity to study how this convergent plate margin and underlying subduction zone formed. Equivalent forearc units presumably exist offshore north of the eastern GAA, providing an attractive target for 21st century research.

Petrological and geochemical studies of ophiolitic crustal sequences mixed with volcanic arc units show both mid-ocean ridge basalt (MORB) and IAT signatures in the central (Andó et al., 1996) and the eastern parts (Marchesi et al., 2007; Proenza et al., 2006) of Cuba. Although the vertical relationships are unclear, such basalts are expected in a SI environment (Whattam & Stern, 2011). Boninite is also characteristic of some SI ophiolites and is found in the Havana ophiolite of Cuba (Fonseca et al., 1989; Kerr et al., 1999) and Puerto Plata ophiolitic complex, Cacheal complex (Escuder-Viruete et al., 2014), and Los Ranchos (Escuder-Viruete, Diaz de Neira, et al., 2006), Maimón (Torró, Garcia-Casco, et al., 2016; Torró, Proenza, Marchesi, et al., 2017; Torró, Proenza-Fernández, et al., 2016), and Amina (Escuder-Viruete, Contreras, Joubert, et al., 2007) Formations in Hispaniola. Also, Late Cretaceous volcanic rocks from Los Pasos Formation in Cuba (Torró, Proenza-Fernández, et al., 2016) and Cuaba subcomplex in Rio San Juan metamorphic complex (Escuder-Viruete & Castillo-Carrión, 2016) exhibit boninitic, low-Ti island arc tholeiitic, and normal tholeiitic signatures. However, Late Cretaceous Téneme Formation lavas in eastern Cuba show

similar low-Ti IAT signatures with boninitic affinity suggesting later additions to the convergent margin (Proenza et al., 2006).

Spinels in ophiolitic peridotites are used to infer tectonic settings, with the highest Cr# spinels (Cr# = (Cr/ Cr + Al)) associated with forearcs (Bonatti & Michael, 1989). SI-related forearc peridotite spinels vary widely (Morishita et al., 2011). Ophiolitic peridotite spinels from harzburgites in Havana-Matanzas ophiolites vary in Cr# from 0.21 to 0.73 (Llanes-Castro et al., 2018). A similar range of Cr# in ophiolitic peridotite spinels from eastern segment harzburgites varies from 0.36 to 0.72 (Gervilla et al., 2005; González-Jiménez et al., 2011; Marchesi et al., 2006; Proenza et al., 1999). Peridotites with coexisting high- and low Cr# spinels indicate variable melt compositions as expected for a magmatic system that produced both boninitic magmas (from ultra-depleted peridotites with high Cr# spinels) as well as tholeiitic melts (from less depleted peridotites with moderate Cr# spinels; Morishita et al., 2011). Alternatively, this may indicate a multi-episodic history of partial melting and/or refertilization processes.

Radiometric ages of ophiolites range from Early to Late Cretaceous (Figure 7a), with the oldest ophiolites in Cuba and Hispaniola giving similar ages (126 Ma; Escuder-Viruete et al., 2014; Escuder-Viruete, Friedman, et al., 2011; Lázaro et al., 2016; Rojas-Agramonte et al., 2016; Rui et al., 2020). Radiolarians in sediments that overly pillow basalt at Holguín provide biostratigraphic constraints that are between Hauterivian (132.9–129.4 Ma) and Barremian (129.4–125.0 Ma; Andó et al., 1996). Despite GAA fore-arc ophiolite ages showing a rather broad range, the oldest ages of forearc ophiolites together with active magmatic arc suggest SI in the Early Cretaceous beginning around 130 Ma (cf., Escuder-Viruete et al., 2014; Escuder-Viruete, Diaz de Neira, et al., 2006; Lázaro et al., 2016; Pindell et al., 2012; Rojas-Agramonte et al., 2011). To date, only one metamorphic sole has been identified in the Caribbean realm, and it has not been related to Early Cretaceous subduction inception. It is the Guira de Jauco amphibolite in eastern Cuba, with an 40Ar-39Ar cooling age of 77–81 Ma, that has been related to the emplacement of the Moa-Baracoa ophiolite during the Late Cretaceous (90–85 Ma) in a new subduction zone perhaps related to the effects of the Caribbean plume (Lázaro et al., 2013, 2015). Clearly, further work is needed to constrain the magmatic ages of GAA forearc ophiolites and formation ages of metamorphic soles.

4.1.6. Comparison to the S Tibet SI Example

The GAA SI sequence and evolution can be usefully compared to that of the convergent margin of southern Tibet, showing significant similarities and differences. The southern margin of Tibet is an

excellent place to study SI because the rocks are well-exposed, forearc ophiolite and metamorphic sole ages cluster tightly (as expected from the SI hypothesis) and younger elements of a mature convergent margin (such as magmatic arc and forearc basin) are also present. The significance of especially the differences between the ages of similar features in GAA and clear examples of SI like Tibet need to be understood in our efforts to test and further develop SI hypotheses. Figure 16 shows that they have similar spatial scales, both being about 2,000 km long. As Figure 16 shows, the two convergent systems both began in Early Cretaceous time, both experienced prolonged subduction (~70–80 million years), and both were sites of Eocene collision. However, S Tibet ophiolites are dominantly the same age whereas a wider range of ages is found for GAA ophiolites. S Tibet metamorphic soles are about the same age as most SI ophiolites (~120 Ma) whereas GAA ophiolitic soles are associated with younger events (Lázaro et al., 2013, 2015). S. Tibet experienced abundant igneous activity with collision whereas the GAA did not. These observations underscore the importance of further research into the age and nature of especially GAA SI sequences.

The wider range of ophiolite ages within the GAA might reflect continued fore-arc extension after SI began in the Early Cretaceous. The formation of Late Cretaceous metamorphic soles and low-Ti IAT volcanism in eastern Cuba is further evidence of a more complicated subduction history for GAA compared to S Tibet. This might be due to changing subduction regimes, the influence of the CLIP (94–83 Ma; Escuder-Viruete, Perez-Estaún, et al., 2011; Hauff, Hoernle, Tilton, et al., 2000; Sinton et al., 1998), along-strike extension, or a combination of these. Some of these tectonic complexities and the possible effect of the CLIP on the GAA are discussed in separate section below.

4.2. The Role of the Caribbean Large Igneous Province (CLIP)

In this section, we discuss the extent to which the CLIP might have affected the Cretaceous evolution of the GAA. The CLIP consists of thickened oceanic crust (up to 20 km) in the central (submarine) part of the Caribbean Plate (Mauffret & Leroy, 1997) and is also accreted/uplifted as subaerial flood basalt sequences exposed around the margins of the Caribbean Sea and northwestern South America. Most authors favor an origin in the Pacific Ocean for the CLIP, possibly above the Galápagos mantle plume, and subsequent emplacement in the inter-America gap during the Cretaceous-Tertiary (e.g., Boschman et al., 2014; Duncan & Hargraves, 1984; Hastie & Kerr, 2010; Hoernle et al., 2002; Mann et al., 2007; Pindell et al., 2012; Sinton et al., 1997, 1998). Remnants of these terranes can be found in Central America, Colombia, Ecuador and in the Caribbean on Curaçao, Aruba, Hispaniola and Jamaica (e.g., Hastie et al., 2016; Hauff, Hoernle, Tilton, et al., 2000; Hauff, Hoernle, van den

Bogaard, et al., 2000; Hoernle et al., 2004; Kerr et al., 1996; Loewen et al., 2013; Révillon et al., 2000; Sinton et al., 1998). New data from Dürkefälden et al. (2019) support long-term CLIP volcanism for at least 18 Ma, from ~92 to ~74 Ma with main magmatic activity from 89 to 90 Ma,

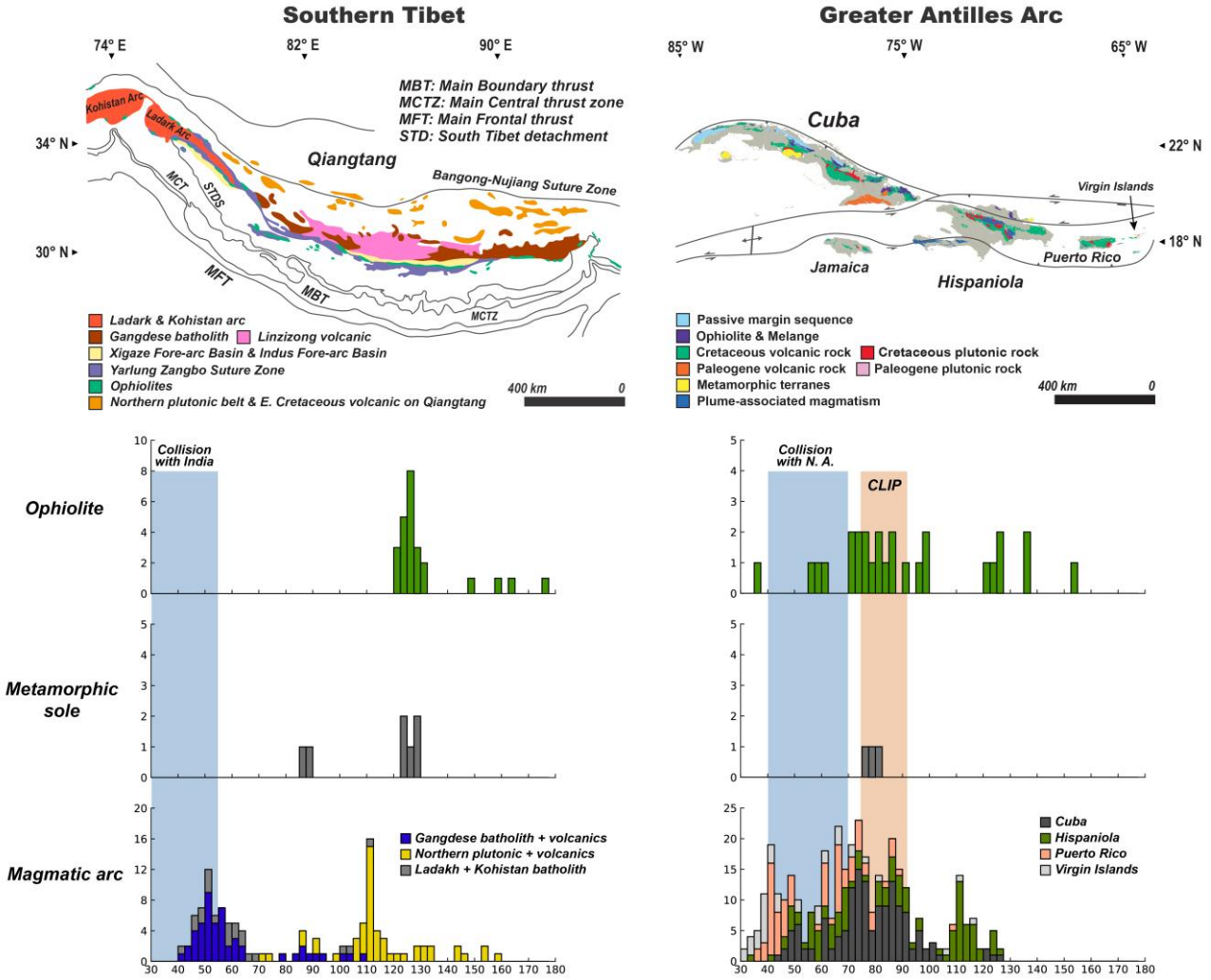

Figure 16. *Comparison of two fossil convergent plate margins, at the same scale. Geochronologic data from ophiolite, metamorphic soles and magmatic arc of the Greater Antilles Arc (GAA) compared to the convergent system of southern Tibet (Hu & Stern, 2020). On the top left, simplified tectonic map of southern Tibet showing major ophiolitic massifs of the Yarlung Zangbo Suture Zone, Xigaze and Indus forearc basin and volcanic belts of the Lhasa terrane, modified after Hébert et al. (2012). On the top right, tectonic map of GAA from Figure 1a. First panel: histogram of compiled age data for ophiolites along the Yarlung Zangbo Suture Zone versus ophiolite of GAA. Second panel: histogram of compiled age data for metamorphic soles within the mélange from Yarlung Zangbo Suture Zone versus GAA. Third panel: histogram of compiled age data of plutonic and associated volcanic rocks in the Lhasa terrane versus GAA. See text for further discussion.*

though CLIP-related Duarte Complex lavas in the Dominican Republic date back to the Early Cretaceous (Escuder Viruete, Perez-Estaún, et al., 2007). Remnants of rocks with CLIP affinity in the GAA (Hispaniola, Jamaica, Puerto Rico, and offshore Hispaniola in the Beata Ridge) occur in a retro-arc position in our four-fold subdivision.

Recent papers, for example, by Dürkefälden et al. (2019) and Hastie, Ramsook, et al. (2010) still favor the idea of Duncan and Hargraves (1984) and Burke (1988) that collision between the ~90 Ma CLIP and the Great Arc of the Caribbean along an east-dipping subduction zone was responsible for a polarity reversal event during the Santonian-Campanian (~80–85 Ma; Burke, 1988), when a new west-dipping subduction zone was established. Recently, geochemistry of Cretaceous lavas from the Virgin Islands without a mantle plume component led Hastie et al. (2021) to conclude that the Caribbean subduction polarity reversal occurred in the Turonian-Campanian. However, the OIB-E-MORB source identified in the forearc, arc and retroarc (Figure 13) suggests the opposite. Furthermore, the geology and geochronology of Cuba, Hispaniola and Puerto Rico do not support the idea of a polarity reversal event at any stage of the Cretaceous arc-building process (Boschman et al., 2014; Braszus et al., 2021; Mann et al., 2007; Pindell et al., 2005, 2012; Rojas-Agramonte et al., 2011). Rather, the CLIP influence observed in other GAA islands suggests that varied degree of tectonic or geochemical interaction with the convergent margin was responsible for a significant amount of melting as well as metamorphism. For example, the CLIP shows tectonic influence on the Cuban segment of GAA, metamorphism of the Mabujina Amphibolite Complex (MAC) in central Cuba occurred during the Turonian (ca. 90–93 Ma) when it became part of the Cuban volcanic arc and was shortly after intruded by plutonic rocks of the Manicaragua batholith (Figure 8a; Turonian-Campanian; ca. 89–83 Ma; Rojas-Agramonte et al., 2011). Lázaro et al. (2013, 2015) postulated that the Late Cretaceous formation of the Güira de Jauco metamorphic sole (Figure 7a) and onset of obduction of the Moa-Baracoa ophiolite was triggered by the emplacement and development of the CLIP plume head. In Hispaniola, CLIP component has been identified in the geochemistry of igneous rocks of the supra-subduction zone environment (Escuder-Viruete et al., 2008). Farré-de-Pablo et al. (2020) conclude that chromitite from Loma Caribe peridotite formed by plume-derived melts that interacted with supra-subduction zone mantle in a Late Cretaceous back-arc setting in Hispaniola. The extent of interaction between CLIP and different segments of the GAA is still unclear, however, multiple lines of tectonic and geochemical interaction with the convergent margin of GAA and geochronology data displayed in Figure 16 suggests the emplacement of the CLIP during the Late Cretaceous imposes influence on the subduction zone magmatic, metamorphic and tectonic processes.

4.3. Other Complications and Considerations

We must keep in mind that our fourfold subdivision of units into mélange, forearc ophiolite, magmatic arc, and retro-arc may be flawed. For example, there may have been more than one subduction zone, as Jamaica rocks that fall into the retro-arc subdivision show an arc affinity (Figure 14d). Another complication may be that during the Early Cretaceous, a subducting proto-Caribbean ridge separated the North and South American plates (Blanco-Quintero, Gerya, et al., 2011; Blanco-Quintero, Lázaro, et al., 2011; García-Casco, Lázaro, et al., 2008; Pindell et al., 2005). This ridge may have been subducted beneath the eastern Cuban segment of the arc (trench-trench-ridge triple junction) in Early Cretaceous time (ca. 120 Ma; Blanco-Quintero et al., 2010), with the North American plate subducted beneath the Cuban arc and the South American plate subducted beneath the Hispaniola-Puerto Rico branch of the arc. The eastern migration of the triple point during the mid-Cretaceous in Hispaniola (Escuder-Viruete, Contreras, Stein, et al., 2007) could have resulted from the segmentation of proto-Caribbean ridge by transform faults (Rojas-Agramonte et al., 2021), causing Late Cretaceous adakitic magmatism in Hispaniola. The location of the triple junction during the Late Cretaceous is not known, but a shift toward the east (present coordinates) can be inferred if it was connected to the Central Atlantic ridge. Hence, with time, more and more North American plate was subducted below the GAA.

Also, Cenozoic normal and strike-slip faulting may have displaced geologic bodies from their original position to their present geographic position. We do not think that there has been major shuffling of original GAA tectonic units because the N. Caribbean transform fault system, with the largest displacements, trends sub-parallel to the GAA trend. However, large-scale thrusting may have had an effect in re-locating some tectonic units. This is, for example, the case of latest Cretaceous-Eocene orogenic thrust tectonics in western Cuba, where the oceanic arc-ophiolitic Bahía Honda-Cajálbana units now lie north of the North America passive margin sequences and can be restored 220 km to the south of its present position (e.g., Saura et al., 2008). On the other hand, metamorphic complexes made of sediments and igneous rocks in Cuba (Escambray complex and Pinos terrane) now located in the retro-arc originated in the North American passive margin and were metamorphosed beneath the Cretaceous forearc during subduction of Mesozoic passive margin sequences (Cruz-Gámez et al., 2016; Despaigne-Díaz et al., 2016, 2017; García-Casco, Iturralde-Vinent, & Pindell, 2008). Furthermore, serpentinite mélange units of the Escambray complex contain subducted oceanic crust (eclogites and blueschists) similarly formed in the Cretaceous forearc (García-Casco et al., 2006; Schneider et al., 2004).

Concerning ophiolites, the Cuban eastern ophiolite belt (Mayarí-Cristal and Moa-Baracoa) overthrusts volcanic arc exposures now located to the south. Hence, its classification as forearc ophiolite is controversial. In fact, most publications consider these ophiolitic rocks as formed in the Cretaceous back-arc (Iturralde-Vinent, 1998; Lázaro et al., 2013, 2015; Marchesi et al., 2006, 2007, 2011, 2016). However, Lázaro et al. (2016) identified fore-arc basaltic blocks within La Tinta mélange, which is associated to the Moa-Baracoa ophiolitic complex, while Rui et al. (2020) suggests that the Moa-Baracoa harzburgites originated in a nascent forearc mantle.

In Hispaniola, the Loma Caribe peridotite, the largest ophiolitic complex of the Dominican Republic, formed in an intra-arc/back-arc basin, in line with its present position, but the peridotite belts of southwestern Puerto Rico, now present in the retro-arc, may have formed in different Cretaceous tectonic positions, including the Farallon plate (Pacific-derived) in the retro-arc and the incoming Proto-Caribbean lithosphere (Atlantic-derived; Escuder-Viruete et al., 2008, 2009; Farré-de-Pablo et al., 2020; Lewis et al., 2006; Lidiak et al., 2011; Montgomery et al., 1994; Proenza et al., 2007).

In the retro-arc region, there are Late Cretaceous-Paleocene volcanic arc rocks in the Cayman Ridge and Nicaraguan Rise. The Cayman Ridge has been interpreted variously including a remnant arc after the GAA split in two and formed the Yucatan Basin since the Maastrichtian (Perfit & Heezen, 1978; Rosencrantz, 1990). However, granitoids of intermediate composition recovered from the Cayman Ridge show distinct continental affinity (Kysar et al., 2009; Lewis et al., 2005), in contrast to island arc composition of the Sierra Maestra in southeastern Cuba (Rojas-Agramonte et al., 2004). Lewis et al. (2011) indicated that granitoids recovered from the Nicaraguan Rise fall in the high-K calc-alkaline field of GAA granitoids, similar to those intrusions in Jamaica and Haiti, which they suggest formed in response to another northward subduction system.

4.4.Suggestions for Future Research

Our compilation indicates that there is much more work to be done before we have a full understanding of how the GAA intraoceanic arc system formed and evolved. The geographic bias we document indicates that geochemical and geochronological research in Cuba and Haiti needs to increase significantly. Large geologic systems that cross political boundaries require special efforts compared to those within a single political entity. In this situation, co-ordination between geologists in the entities is called for, for example, reinforcing the Caribbean Geological Conference and the Caribbean Journal of Earth Science (http://www.caribjes.com/) and other local journals and, perhaps, the formation of a Greater Antilles Geological Society. Such efforts would also stimulate research

co-operation between geoscientists of GAA nations and territories and attract international researchers.

Another opportunity exists to apply modern thermochronologic techniques (e.g., U-Th-He, monazite, titanite, and xenotime U-Pb), that should be carried out to decipher uplift history across and along the GAA, especially its relationship to collision with Maya Block and the Bahamas Platform.

Another opportunity is to exploring how a trench with active convergence changes along strike into a suture zone. Oblique convergence continues in the east (Mann et al., 2002) and an active subduction zone can be traced by deep seismicity as far west as western Dominican Republic (Hayes, 2018). GAA along with the Izu collision zone of Japan and the Makran-Zagros transition in Iran are the only places in the world where a trench with active subduction can be traced along strike into a suture zone. Such transitions warrant further investigation so we can better understand what happens when a subduction zone becomes a collision zone.

Because so much of the GAA is above sea-level, we can build on what we know from studying exposed arc crust and mantle and extend this offshore, especially to the N into the forearc and S into the retroarc and the CLIP. There is much we can learn about SI from studying the GAA forearc. We are beginning to make progress understanding the on-land forearc, represented by the long ophiolite belt that parallels and lies north of the west-central magmatic arc in Cuba, but we know nothing about equivalent forearc crust that must exist offshore north of the eastern GAA, where subduction continues. Marine geoscientific research to study the eastern GAA forearc is needed. Studies of retroarc crust should begin with studying steep exposures south of SE Cuba and the Aves Ridge, the natural continuation of the island arc to the east and south of the GAA. In this regard, the effects of subduction of the Proto-Caribbean ridge, separating North and South American plates and now totally consumed, should be considered in understanding the evolution of the volcanic arc.

5. Conclusions

The Greater Antilles islands of Cuba, Hispaniola, Puerto Rico, Jamaica, and the Virgin Islands are fragments of the GAA, an unusually well-preserved fossil intra-oceanic convergent margin. The GAA is the result of subduction of the North and South American plate beneath the Caribbean plate that lasted for ~90 m.y. in the west and continues today in the east. The “soft” collision between GAA and Maya and Bahamas margins caused uplift and exposure of the western GAA, providing an

excellent natural laboratory for studying the formation and evolution of an intra-oceanic convergent margin. We compiled 664 (mostly) radiometric ages and more than 1,500 geochemical analyses for GAA igneous and metamorphic rocks and assigned these to a simple fourfold subdivision of the GAA based on relative geographic position to the magmatic arc: fore-arc mélange, fore-arc ophiolite, magmatic arc, and retro-arc and use these data to inspect the evolution of the GAA, from SI through maturity and demise. The oldest ages of forearc ophiolites together with those of the magmatic arc suggest subduction began in Early Cretaceous time at around 130 Ma. The geochronological data suggest that the GAA was, at least partially, strongly affected by the CLIP in Late Cretaceous time (e.g., MAC, Central Cuba; Güira de Jauco metamorphic sole, Eastern Cuba; Loma Caribe peridotite). Some peaks are seen in the histograms, especially in the Late Cretaceous from 95 to 60 Ma, that may relate to the CLIP event(s) and with events of collision with passive margins. Two subordinate peaks are observed at 120–110 Ma and ~40 Ma. Immobile trace element geochemical data show that the GAA is dominated by mafic igneous rocks, as expected for an intraoceanic convergent margin. The arc shows trace element concentrations expected for convergent margin magmas and these trace element concentrations for retroarc igneous rocks in central and southern Hispaniola are more like OIB and MORB. In spite of multiple biases, the database presented here is a useful step forward in the effort to help overcome some of the obstacles and motivate systematic study of the GAA. Our results encourage forming of regional partnerships, involvement of international partners, and exploration of offshore regions.

Data Availability Statement

Data sets for geochronologic compilation of this research are available through the following references (and its Supporting Information S1 files): Abbott et al. (2016), Alminas et al. (1994), Barabas (1982), Bellon, Mecier de Lepinay, and Vila (1985), Bellon, Vila, and Mercier de Lepinay (1985), Blanco-Quintero, Rojas-Agramonte, et al. (2011), Bowin (1975), Cárdenas-Párraga et al. (2012), Castro et al. (2019), Cheilletz et al. (1978), Chubb and Burke (1963), Cochran et al. (2017), Cox et al. (1977), Despaigne-Díaz et al. (2016), Donnelly (1966), Draper and Nagle (1991), Escuder-Viruete (2010), Escuder-Viruete, Diaz de Neira, et al. (2006), Escuder-Viruete, Contreras, et al. (2006), Escuder Viruete, Perez-Estaún, et al. (2007), Escuder-Viruete, Contreras, Stein, et al. (2007), Escuder-Viruete et al. (2008), Escuder-Viruete et al. (2010), Escuder-Viruete, Perez-Estaún, Gabites, and Suarez-Rodriguez (2011), Escuder-Viruete, Friedman, et al. (2011), Escuder-Viruete, Perez-Estaún, et al. (2011), Escuder-Viruete, Valverde-Vaquero,

Rojas-Agramonte, Gabites, Carrion Castillo, et al. (2013), Escuder-Viruete, Valverde-Vaquero, Rojas-Agramonte, Gabites, and Pérez-Estaún (2013), Escuder-Viruete, Joubert, et al. (2016), Escuder-Viruete, Suárez-Rodríguez, et al. (2016), García-Casco et al. (2001), García-Casco et al. (2002), GarcíaCasco et al. (2003), Grafe (2000), Grafe et al. (2001), Hall et al. (2004), Hastie (2007), Hastie et al. (2009), Hastie, Kerr, et al. (2010), Hastie, Ramsook, et al. (2010), Hastie et al. (2013), Hatten et al. (1988), Hertwig et al. (2016), Hernaiz Huerta et al. (2012), Iturralde-Vinent et al. (1996), Japan International Cooperation Agency (1985), Jolly and Lidiak (2006), Joyce and Aronson (1987), Kesler (1971), Kesler and Sutter (1979), Kesler et al. (1977), Kesler et al. (1991), Kesler et al. (2004), Kesler, Campbell, and Allen (2005), Kesler, Campbell, Smith, et al. (2005), Khudoley (1967), Kirk et al. (2014), Krebs et al. (2008), Kysar et al. (1998), Lapierre et al. (1999), Laverov et al. (1967), Lázaro et al. (2009), Lázaro et al. (2015), Lázaro et al. (2016), Lewis et al. (1973), Loewen et al. (2013), Monthel (2010), Mueller et al. (2008), Nelson et al. (2015), Odin et al. (2001), Pérez (2008), Perfit et al. (1980a), Proenza et al. (2006), Rankin (2002), Rojas-Agramonte et al. (2004), Rojas-Agramonte et al. (2006), Rojas-Agramonte et al. (2010), Rojas-Agramonte et al. (2011), Rojas-Agramonte et al. (2016), Rojas-Agramonte et al. (2021), Rui et al. (2020), Schneider et al. (2004), Schrecengost (2010), Sinton et al. (1998), Speed et al. (1979), Stanek et al. (2019), Torró, Camprubí, et al. (2017), Torró, Proenza, Camprubí, et al. (2017), Torró et al. (2018), Vila et al. (1986), Wadge et al. (1982), and West et al. (2014). Data sets for geochemical compilation of this research are available through the following references (and its Supporting Information S1 files): Abbott et al. (2016), Blanco-Quintero et al. (2010), Blanco-Quintero, Lázaro, et al. (2011), Castro et al. (2019), Cazañas et al. (1998), Cruz-Gámez et al. (2016), Escuder-Viruete, Diaz de Neira, et al. (2006), Escuder Viruete, Perez-Estaún, et al. (2007), Escuder-Viruete, Contreras, Stein, et al. (2007), Escuder-Viruete et al. (2008), Escuder-Viruete et al. (2009), Escuder-Viruete et al. (2010), Escuder-Viruete, Friedman, et al. (2011), Escuder-Viruete, Perez-Estaún, et al. (2011), Escuder-Viruete et al. (2014), Escuder-Viruete, Joubert, et al. (2016), Escuder-Viruete, SuárezRodríguez, et al. (2016), Cintron Franqui et al. (2017), Schellekens and Smith (1998), Hastie et al. (2007), Hastie et al. (2008), Hastie, Kerr, et al. (2010), Hastie et al. (2013), Jolly and Lidiak (2006), Jolly et al. (1998), Jolly et al. (2002), Jolly et al. (2008a), Jolly et al. (2008b), Kerr et al. (1999), Lázaro and García-Casco (2008), Lázaro et al. (2011), Lázaro et al. (2013), Lewis et al. (2011), Lidiak and Jolly (1998), Lidiak et al. (2011), Marchesi et al. (2006), Marchesi et al. (2007), Pérez (2008), Proenza et al. (2006), Rojas-Agramonte et al. (2004), Rojas-Agramonte et al. (2016), Rojas-Agramonte et al. (2021), Schellekens (1998a), Schellekens (1998b), Torró,

Proenza, Marchesi, et al. (2017), Torró, Camprubí, et al. (2017), Torró et al. (2020), and West et al. (2014).

Acknowledgments

The authors greatly appreciate Javier Escuder Viruete and two anonymous reviewers with many constructive suggestions that helped we improve the manuscript. Haoyu Hu acknowledges support by Federal State Funding at Kiel University while Yamirka Rojas-Agramonte acknowledges support by the Deutsche Forschungsgemeinschaft (DFG) grant RO4174/3-3 and Antonio Garcia-Casco acknowledges support by the Agencia Estatal de Investigación (AEI) grant MICINN PID2019-105625RB-C21. This is UTD Geosciences contribution #1682. Open access funding enabled and organized by Projekt DEAL.

References

Abbott Jr., R.N., & Draper, G. (2007), Petrogenesis of UHP eclogite from the Cuaba Gneiss, Rio San Juan Complex, Dominican Republic. International Geology Review 49,1069–1093.

Abbott Jr., R.N., & Draper, G. (2013), The case for UHP conditions in the Cuaba Terrane, Rio San Juan metamorphic complex, Dominican Republic. Geologica Acta 11 (3).http://dx.doi.org/10.1344/ 105.000001841.

Abbott Jr, R. N., West, D. P., Bandy, B. R., & McAleer, R. J. (2016). Petrology and tectonic history of the Green Bay Schist, Portmore, St. Catherine Parish, Jamaica. Caribbean Journal of Earth Science, 48, 1-18.

Alminas, H. V., Foord, E. E., & Tucker, R. E. (1994). Geochemistry, mineralogy, and geochronology of the U.S. Virgin Islands, U.S. Geol. Surv. Bull., 2057, 36 pp.

Agard, P., Jolivet, L., Vrielynck, B., Burov, E., & Monié, P. (2007), Plate acceleration: The obduction trigger?, Earth Planet. Sci. Lett., 258, 428–441, doi:10.1016/j.epsl.2007.04.002.

Andó, J., Harangi, S., Szakmany, B., & Dosztaly, L. (1996), Petrology of the ophiolitic association of Holguín. In: Iturralde-Vinent, M., (Editor) 1996. Ophiolites and volcanic arcs of Cuba, First Contribution IGCP Project 364, p. 154-176.

Barabas, A. H. (1982). Potassium-argon dating of magmatic events and hydrothermal activity associated with porphyry copper mineralization in west central Puerto Rico. Economic Geology, 77(1), 109-126.

Bellon, H., Mecier de Lepinay, B., & Vila, J.M. (1985a), Cronologie 40K/39Ar et affinités geochemiques des manifestacions magmatiques au Cretace et au Paleogene dans l'ile d'Hispaniola (Grandes Antilles): Centre National de la Recherche Scientifique, Institut Français de Recherche pour l'Explotation de la Mer, Géodynamiques des Caraïbes Symposium, Paris, France, February 5–8, 1985, Proceedings, p. 329–339.

Bellon, H., Vila, J. M., and Mercier de Lepinay, B. (1985b) Chronologie "°Ar-39Ar et affinités geochimiques des manifestations magmatiques au Crétacé et au Paleogene dans L'Ile d'Hispaniola: Paris, France, Geodynamique des Caraibes, Editions Technip, p. 12-24.

Blanco-Quintero, I. F., García-Casco, A., Rojas-Agramonte, Y., Rodríguez-Vega, A., Lázaro, C., & Iturralde-Vinent, M. A. (2010), Metamorphic evolution of subducted hot oceanic crust (La Corea Mélange, Cuba). American Journal of Science, 310(9), 889-915.

Blanco-Quintero, I.F., Gerya, T.V., García-Casco, A., & Castro, A. (2011a), Subduction of young oceanic plates: A numerical study with application to aborted thermal-chemical plumes: Geochemistry, Geophysics, Geosystems, v. 12, p. Q10012. doi:10.1029/2011GC003717.

Blanco-Quintero, I.F., Lázaro, C., García-Casco, A., Proenza, J., & Rojas-Agramonte, Y. (2011b), Barium-rich fluids and melts in the subduction environment (La Corea and Sierra del Convento mélanges, eastern Cuba): Contributions to Mineralogy and Petrology, v. 162, p. 395–413. doi:10.1007/ s00410-010-0603-2.

Blanco-Quintero, I. F., Rojas-Agramonte, Y., García-Casco, A., Kröner, A., Mertz, D. F., Lázaro, C., Blanco-Moreno, P.R., & Renne, P. R. (2011c). Timing of subduction and exhumation in a subduction channel: Evidence from slab melts from La Corea Mélange (eastern Cuba). Lithos, 127(1-2), 86-100.

Bonatti, E., & Michael, P.J. (1989), Mantle peridotites from continental rifts to ocean basins to subduction zones. Earth Planet. Sci. Lett. 91, 297-311.

Boschman, L. M., Van Hinsbergen, D. J. J., Torsvik, T.H., Spakman, W., & Pindell, J. L. (2014), Kinematic reconstruction of the Caribbean region since the Early Jurassic. Earth-Science Reviews 138, 102–36.

Bowin, C. (1975). The geology of Hispaniola. In The Gulf of Mexico and the Caribbean (pp. 501-552). Springer, Boston, MA.

Braszus, B., Goes, S., Allen, R., Rietbrock, A., Collier, J., Harmon, N., ... & Wilson, M. (2021). Subduction history of the Caribbean from upper-mantle seismic imaging and plate reconstruction. Nature communications, 12(1), 1-14.

Burke, K. (1988), Tectonic evolution of the Caribbean. Annu. Rev. Earth Planet. Sci. 16:201–230.

Cárdenas-Párraga, J., García-Casco, A., Harlow, G. E., Blanco-Quintero, I. F., Agramonte, Y. R., & Kröner, A. (2012). Hydrothermal origin and age of jadeitites from Sierra del Convento Mélange (Eastern Cuba). European Journal of Mineralogy, 24(2), 313-331.

Castillo, P. R. (2012), Adakite petrogenesis. Lithos, 134-135, 304–316. doi:10.1016/j.lithos.2011.09.013.

Castro, A. I. L., Furnes, H., Gámez, E. M. C., Rodriguez, M. P., & Cruz, O. L. (2019). Petrogenesis of plagiogranite and associated diorites and mafic rocks in the Habana–Matanzas ophiolites, northwestern half of central Cuba. Journal of the Geological Society, 176(5), 992-1006.

Cazañas, X., Proenza, J.A., Kysar, G.M., Lewis, J., & Melgarejo, J.C. (1998). Volcanic rocks of the Lower and Middle series of the El Cobre Group in the Sierra Maestra (Eastern Cuba): volcanism generated in a tholeiitic island arc. Acta Geologica Hispanica, 33 (1), 57-74.

Cheilletz, A., Kachrillo, J. J., Sonet, J., & Zimmermann, J. L. (1978). Petrographie et geochronologie de deux complexes intrusifs a porphyres cupriferes d'Haiti; contribution a la connaissance de la province cuprifere laramienne de l'arc insulaire des Grandes Antilles. Bulletin de la Societe geologique de France, 7(6), 907-914.

Chubb, L. J., & Burke, K. (1963). Age of the Jamaican granodiorite. Geological Magazine, 100(6), 524-532.

Cochran, W.J., Spotila, J.A., Prince, P.S. & McAleer, R.J. (2017), Rapid exhumation of Cretaceous arc-rocks along the Blue Mountains restraining bend of the Enriquillo– Plantain Garden fault, Jamaica, using thermochronometry from multiple closure systems. Tectonophysics, 721, 292–309, https://doi.org/10.1016/j.tecto.2017. 09.021.

Comer, J.B., Naeser, C.W., & McDowell, F.W. (1980), Fission-track ages of zircon from Jamaican bauxite and Terra Rossa. Econ. Geol. 75, 117–121.

Cox, D. P., Marvin, R. F., M'Gonigle, J. W., Mcintyre, D. H., & Rogers, C. L. (1977), Potassium–argon geochronology of some metamorphic, igneous, and hydrothermal events in Puerto Rico and the Virgin Islands. US Geological Survey Journal of Research 5, 689–703.

Cruz-Gámez, E., Velazco-Tapia, F., García-Casco, A., Despaigne-Díaz, A.I., Lastra Rivero, J.F., & Cáceres Govea, D. (2016), Geoquímica del magmatismo mesozoico asociado al margencontinental pasivo en el occidente y centro de Cuba. Revista mexicana de Ciencias deLa Tierra. Boletín de La Sociedad Geológica Mexicana 68, 443–475.

Defant, M.J., & Drummond, M.S. (1990), Derivation of some modern arc magmas by melting of young subducted lithosphere. Nature 347, 662–665A.

Despaigne-Díaz, A.I., García-Casco, A., Govea, D.C., Jourdan, F., Wilde, S.A., & Trujillo, G.M. (2016), Twenty-five million years of subduction-accretion-exhumation during the Late Cretaceous–Tertiary in the northwestern Caribbean: The Trinidad Dome, Escambray complex, central Cuba: American Journal of Science, v. 316, no. 3, p. 203–240, https://doi.org/10.2475/03.2016.01.

Despaigne-Díaz, A.I., García Casco, A., Cáceres Govea, D., Wilde, S.A., & Millán Trujillo, G. (2017), Structure and tectonic evolution of the southwestern Trinidad dome, Escambray complex, Central Cuba: insights into deformation in an accretionary wedge. Tectonophysics 717, 139–161. https://doi.org/10.1016/j.tecto.2017.07.024.

Donnelly, T.W. (1966). Geology of St. Thomas and St. John, U.S. Virgin Islands. In Hess, H. (ed.). Caribbean Geological Investigations. Geological Society of America Memoir, 98, 5-176

Draper, G., & Nagle, F. (1991). Geology, structure, and tectonic development of the Rio San Juan Complex, northern Dominican Republic. Geologic and tectonic development of the North America-Caribbean plate boundary in Hispaniola. Geological Society of America Special Paper, 262, 77-95.

Duncan, R.A., & Hargraves, R.B. (1984), Plate tectonic evolution of the Caribbean region in the mantle reference frame. Geological Society of America Memoirs 162, 81–94. https://doi.org/10.1130/MEM162-p81.

Dürkefälden, A., Hoernle, K., Hauff, F., Wartho, J. A., van den Bogaard, P., & Werner, R. (2019), Age and geochemistry of the Beata Ridge: Primary formation during the main phase (~ 89 Ma) of the Caribbean Large Igneous Province. Lithos, 328, 69-87.

Escuder-Viruete, J. (2010). Petrología de rocas ígneas y metamórficas de la Cordillera Septentrional. Proyecto Sysmin. Dirección General de Minería, Santo Domingo, 54.

Escuder-Viruete, J., & Pérez-Estaún, A. (2006), Subduction-related P–T path for eclogites and garnet glaucophanites from the Samana Peninsula basement complex, northern Hispaniola. Int J Earth Sci (Geol Rundsch) 95:995–1017.

Escuder-Viruete J, & Pérez-Estaún A. (2013), Contrasting exhumation P-T paths followed by high-P rocks in the northern Caribbean subduction-accretionary complex: insights from the structural geology, microtextures and equilibrium assemblage diagrams. Lithos 160–161:117–144. doi:10.1016/j.lithos.2012.11.028.

Escuder-Viruete, J., Diaz de Neira, A., Hernaiz Huerta, P.P., Monthel, J., Garcia Senz, J., Joubert, M., Lopera, E., Ullrich, T., Friedman, R., Mortensen, J., & Perez-Estaún, A. (2006a), Magmatic relationships and ages of Caribbean island arc tholeiites, boninites and related felsic rocks, Dominican Republic: Lithos, v. 90, p. 161–186, doi:10.1016/j.lithos.2006.02.001.

Escuder-Viruete, J., Contreras, F., Stein, G., Urien, P., Joubert, M., Ullrich, T., ... & Pérez-Estaún, A. (2006b). Transpression and strain partitioning in the Caribbean Island-arc: Fabric development, kinematics and Ar–Ar ages of syntectonic emplacement of the Loma de Cabrera batholith, Dominican Republic. Journal of structural geology, 28(8), 1496-1519.

Escuder Viruete, J., Perez-Estaún, A., Contreras, F., Joubert, M., Weis, D., Ullrich, T., & Spades, P. (2007a), Plume mantle source heterogeneity through time: Insights from the Duarte complex, Hispaniola, northeastern Caribbean: Journal of Geophysical Research, v. 112, p. B04203, doi:04210.01029/02006JB004323.

Escuder-Viruete, J., Contreras, F., Joubert, M., Urien, P., Stein, G., Weis, D., & Pérez-Estaún, A. (2007b), Tectónica y geoquímica de la formación Amina: registro del Arco Isla caribeñoprimitivo en la cordillera central, república dominicana. Bol. Geol. Min. 118, 221–242.

Escuder-Viruete, J. E., F., Stein, G., Urien, P., Joubert, M., Pérez-Estaún, A., Friedman, R., & Ullrich, T. (2007c). Magmatic relationships and ages between adakites, magnesian andesites and Nb-enriched basalt-andesites from Hispaniola: record of a major change in the Caribbean island arc magma sources. Lithos, 99(3-4), 151-177.

Escuder-Viruete, J., Joubert, M., Urien, P., Friedman, R., Weis, D., Ullrich, T., & Pérez-Estaún, A. (2008), Caribbean island-arc rifting and backarc basin development in the Late Cretaceous: geochemical, isotopic and geochronological evidence from Central Hispaniola, Lithos, 104, 378–404.

Escuder-Viruete, J., Pérez-Estaún, A., & Weis, D. (2009), Geochemical constraints on the origin of the late Jurassic proto-Caribbean oceanic crust in Hispaniola. International Journal of Earth Sciences 98, 407–425.

Escuder-Viruete, J., Pérez-Estaún, A., Weis, D., & Friedman, R. (2010). Geochemical characteristics of the Río Verde Complex, Central Hispaniola: Implications for the paleotectonic reconstruction of the Lower Cretaceous Caribbean island-arc. Lithos, 114(1-2), 168-185.

Escuder-Viruete J, Perez-Estaún A, Gabites J, Suarez-Rodriguez A. (2011a), Structural development of a high-pressure collisional accretionary wedge: the Samana complex, Northern Hispaniola. J Struct Geol 33(5):928–950. doi:10.1016/j.jsg.2011.02.006.

Escuder-Viruete, J., Pérez-Estaún, A., Booth-rea, G. & Valverde-Vaquero, P. (2011b), Tectonometamorphic evolution of the Samaná complex, northern Hispaniola: Implications for the burial and exhumation of high pressure rocks in a collisional accretionary wedge. Lithos, 125, 190–210.

Escuder-Viruete, J., Friedman, R., Castillo-Carrion, M., Jabites, J., & Perez-Estaún, A. (2011c), Origin and significance of the ophiolitic high-P melanges in the northern Caribbean convergent margin: Insights from the geochemistry and large-scale structure of the Rıo San Juan metamorphic complex. Lithos, 127(3), 483–504.

Escuder-Viruete, J., Perez-Estaún, A., Joubert, M., & Weis, D. (2011d), The Pelona-Pico Duarte basalts Formation, Central Hispaniola: an on-land section of Late Cretaceous volcanism related to the Caribbean large igneous province, Geol. Acta, 9(3), 307–328, doi:10.1344/105.000001716.

Escuder-Viruete, J., Valverde-Vaquero, P., Rojas-Agramonte, Y., Gabites, J., & Carrion Castillo, M. (2013a), Timing of deformational events in the Río San Juan complex: Implications for the tectonic controls on the exhumation of high-P rocks in the northern Caribbean subduction–accretionary prism: Lithos, v. 177, p. 416–435. doi:10.1016/j.lithos.2013.07.006.

Escuder-Viruete, J., Valverde-Vaquero, P., Rojas-Agramonte, Y., Gabites, J., & Pérez-Estaún, A. (2013b), From intra-oceanic subduction to arc accretion and arc–continent collision: Insights from the structural evolution of the Río San Juan metamorphic complex, northern Hispaniola: Journal of Structural Geology, v. 46, p. 34–56. doi:10.1016/j. jsg.2012.10.008.

Escuder-Viruete, J., Castillo-Carrión, M., & Pérez-Estaún, A. (2014), Magmatic relationships between depleted mantle harzburgites, boninitic cumulate gabbros and subduction-related tholeiitic basalts in the Puerto Plata ophiolitic complex, Dominican Republic: Implications for the birth of the Caribbean island-arc: Lithos 196-197, 261–280. doi:10.1016/j.lithos.2014.03.013.

Escuder-Viruete, J., & Castillo-Carrión, M. (2016), Subduction of fore-arc crust beneath an intra-oceanic arc: The high-P Cuaba mafic gneisess and amphibolites of the Rio San Juan Complex, Dominican Republic. Lithos, 262, 298–319. https://doi.org/10.1016/j. lithos.2016.07.024.

Escuder-Viruete, J., Joubert, M., Abad, M., Pérez-Valera, F., & Gabites, J. (2016a), The basaltic volcanism of the Dumisseau Formation in the Sierra de Bahoruco, SW Dominican Republic: A record of the mantle plume-related magmatism of the Caribbean Large Igneous Province. Lithos 254-255:67-83.

Escuder-Viruete, J., Suárez-Rodríguez, Á., Gabites, J., & Pérez-Estaún, A. (2016b). The Imbert Formation of northern Hispaniola: a tectono-sedimentary record of arc–continent collision and ophiolite emplacement in the northern Caribbean subduction–accretionary prism. Solid Earth, 7(1), 11-36.

Farré-de-Pablo, J., Proenza, J.A., González-Jiménez, J.M., Aiglsperger, T., Garcia-Casco, A., Escuder-Viruete, J., Colás, V., & Longo, F. (2020), Ophiolite hosted chromitite formed by supra-subduction zone peridotite - plume interaction. Geoscience Frontiers 11 (6), 2083-2102. DOI: 10.1016/j.gsf.2020.05.005.

Fonseca, E., González, R., & Savieleva, G. (1989), Presencia de efusivos ofiolíticos y de boninitas en las provincias de La Habana y Matanzas. Boletín Técnico, Geología, Ministerio de Industria Básica, 1, 1-9.

García-Casco, A., Torres-Roldán, R.L., Millán, G., Monié, P., & Haissen, F. (2001), High-grade metamorphism and hydrous melting of metapelites in the Pinos terrane (W Cuba): Evidence for crustal thickening and extension in the northern Caribbean collisional belt: Journal of Metamorphic Geology, v. 19, p. 699–715, https://doi .org/10.1046/j.0263-4929.2001.00343.x.

García-Casco, A., Torres-Roldán, R. L., Millán, G., Monié, P., & Schneider, J. (2002). Oscillatory zoning in eclogitic garnet and amphibole, Northern Serpentinite Melange, Cuba: a record of tectonic instability during subduction?. Journal of Metamorphic Geology, 20(6), 581-598.

García-Casco, A., de Arce, P., Millán, G., Iturralde-Vinent, M., Fonseca, E., Torres-Roldán, R., Núñez, K., Morata, D. (2003). Metabasites from the northern serpentinite belt (Cuba) and a metamorphic perspective of the plate tectonic models for the Caribbean region. In Field workshop of the IGCP Project 433 Scientific Meeting, V Geological and Mining Congress of the Cuban Geological Society.

García-Casco, A., Torres-Roldán, R.L., Iturralde-Vinent, M., Millán-Trujillo, G., Núñez-Cambra, K., Lázaro-Calisalvo, C., & Rodríguez Vega, A. (2006), High-pressure metamorphism of ophiolites in Cuba. Geologica Acta, 4 (1-2): 63-88, doi: 10.1344/105.000000358.

Garcia-Casco, A., Iturralde-Vinent, M. A., & Pindell, J. (2008a), Latest Cretaceous collision/accretion between the Caribbean Plate and Caribeana: origin of metamorphic terranes in the Greater Antilles. International Geology Review, 50(9), 781-809.

García-Casco, A., Lázaro, C., Rojas-Agramonte, Y., Kröner, A., Torres-Roldán, R.L., Núñez, K., Neubauer, F., Millán, G., & Blanco-Quintero, I. (2008b), Partial melting and counterclockwise P-T path of subducted oceanic crust (Sierra del Convento Mélange, Cuba): Journal of Petrology, v. 49, p. 129–161.

Gazel, E., Abbott Jr., R.N., & Draper, G. (2011), Garnet-bearing ultramafic rocks from theDominican Republic: fossil mantle plume fragments in an ultra-high pressure oceaniccomplex? Lithos 125, 393–404.

Gervilla, F., Proenza-Fernández, J.A., Frei, R., González-Jiménez, J.M., Garrido, C.J., Melgarejo, J.C., Meibom, A., Díaz-Martínez, R., & Lavaut-Copa, W. (2005), Distribution of Platinum-Group elements and Os isotopes in chromite ores from Mayarí-Baracoa Ophiolitic Belt (eastern Cuba). Contributions to Mineralogy and Petrology, 150: 589-607.

González-Jiménez, J.M., Proenza-Fernández, J.A., Gervilla, F., Melgarejo, J.C., Blanco-Moreno, J.A., Ruiz-Sánchez, R., & Griffin, W.L. (2011), High-Cr and high-Al chromitites from the Sagua de Tánamo district, Mayarí-Cristal ophiolitic massif (eastern Cuba): Constraints on their origin from mineralogy and geochemistry of chromian spinel and platinum-group elements. Lithos, doi:10.1016/j.lithos.2011.01.016.

Grafe, F. (2000). Geochronology of metamorphic complexes using the example of the Cretaceous island arc-continent collision zone central Cuba - analytical possibilities of isotopic age determination and fissure trace dating of subduction-bound high pressure metamorphic rocks. Univ. Bochum, 227 p., DOI 10.23689 / fidgeo-421.

Grafe, F., Stanek, K. P., Baumann, A., Maresch, W. V., Hames, W. E., Grevel, C., & Millán, G. (2001). Rb-Sr and 40Ar/39Ar mineral ages of granitoid intrusives in the Mabujina Unit, Central Cuba: thermal exhumation history of the Escambray massif. The Journal of Geology, 109(5), 615-631.

Hall, C. M., Kesler, S. E., Russell, N., Piñero, E., Sánchez C, R., Pérez R, M., ... & Borges, M. (2004). Age and tectonic setting of the Camagüey volcanic-intrusive arc, Cuba: Late Cretaceous extension and uplift in the western Greater Antilles. The Journal of Geology, 112(5), 521-542.

Hastie, A. R. (2007). Tectonomagmatic evolution of the Caribbean plate: Insights from igneous rocks on Jamaica. Cardiff University (United Kingdom).

Hastie, A.R., & Kerr, A.C. (2010), Mantle plume or slab window? Physical and geochemical constraints on the origin of the Caribbean oceanic plateau. Earth- Science Reviews 98, 283–293. http://www.sciencedirect.com/science/article/pii/S0012825209001767.

Hastie, A., Kerr, A., Mitchell, S., and Millar, I., 2009, Geochemisty and tectonomagmatic significance of Lower Cretaceous island arc lavas from the Devil's Racecourse Formation, eastern Jamaica, in James, K., Lorente, M.A., and Pindell, J.L., eds., Origin and evolution of the caribbean region: Geological Society of London, Special Publication, v. 328, p. 399–409, doi: 10.1144/SP328.

Hastie, A. R., Kerr, A. C., McDonald, I., Mitchell, S. F., Pearce, J. A., Millar, I. L., ... & Mark, D. F. (2010a). Geochronology, geochemistry and petrogenesis of rhyodacite lavas in eastern Jamaica: A new adakite subgroup analogous to early Archaean continental crust?. Chemical Geology, 276(3-4), 344-359.

Hastie, A. R., Ramsook, R., Mitchell, S. F., Kerr, A. C., Millar, I. L., & Mark, D. F. (2010b). Geochemistry of compositionally distinct late Cretaceous back-arc basin lavas: Implications for the tectonomagmatic evolution of the Caribbean plate. The Journal of Geology, 118(6), 655-676.

Hastie, A. R., Mitchell, S. F., Treloar, P. J., Kerr, A. C., Neill, I., & Barfod, D. N. (2013). Geochemical components in a Cretaceous island arc: the Th/La–(Ce/Ce*) Nd diagram and implications for subduction initiation in the inter-American region. Lithos, 162, 57-69.

Hastie, A.R., Fitton, J.G., Kerr, A.C., McDonald, I., Schwindrofska, A., & Hoernle, K. (2016), The composition of mantle plumes and the deep Earth. Earth and Planetary Science Letters 444, 13–25. https://doi.org/10.1016/j.epsl.2016.03.023.

Hatten, C. W., Somin, M. L., Millán, G., Renne, P., Kistler, R. W., & Mattinson, J. M. (1988). Tectonostratigraphic units of central Cuba. In Transactions of the 11th Caribbean Geological Conference, Barbados (Vol. 35, pp. 1-35).

Hattori, K. H., Guillot, S., Saumur, B.-M., Tubrett, M. N., Vidal, O., & Morfin, S. (2010), Corundum-bearing garnet peridotite from northern Dominican Republic: A metamorphic product of an arc cumulate in the Caribbean subduction zone. Lithos, 114(3-4), 437–450. doi:10.1016/j.lithos.2009.10.010

Hauff, F., Hoernle, K., Tilton, G., Graham, D.W., Kerr, A.C. (2000a), Large volume recycling of oceanic lithosphere over short time scales: geochemical constraints from the Caribbean large Igneous Province. Earth and Planetary Science Letters 174, 247–263. http://www.sciencedirect.com/science/article/pii/S0012821X99002721.

Hauff, F., Hoernle, K., van den Bogaard, P., Alvarado, G.E., & Garbe-Schönberg, D. (2000b), Age and geochemistry of basaltic complexes in western Costa Rica: contributions to the geotectonic evolution of Central America. Geochemistry, Geophysics, Geosystems 1, 1–41. https://doi.org/10.1029/1999gc000020., b.

Hayes, G. (2018), Slab2 - A Comprehensive Subduction Zone Geometry Model: U.S. Geological Survey data release, https://doi.org/10.5066/F7PV6JNV.

Hébert, R., Bezard, R., Guilmette, C., Dostal, J., Wang, C. S., & Liu, Z. F. (2012), The Indus–Yarlung Zangbo ophiolites from Nanga Parbat to Namche Barwa syntaxes, southern Tibet: First synthesis of petrology, geochemistry, and geochronology with incidences on geodynamic reconstructions of Neo-Tethys. Gondwana Research, 22(2), 377–397. doi:10.1016/j.gr.2011.10.013.

Heezen, B. C., Nesteroff, W. D., Rawson, M., & Freeman-Lynde, R. P. (1985), Visual evidence for subduction in the western Puerto Rico Trench, in Mascle, A., ed., Caribbean Geodynamics Symposium, Paris, March 5–8: Paris, France, Editions Technip, p. 287–304.

Hernaiz Huerta, P.P., Perez-Valera, F., Abad, M., Monthel, J., & Diaz de Neira, A. (2012), Melanges and olistostromes in the Puerto Plata area (northern Dominican Republic) as a record of subduction and collisional processes between the Caribbean and NorthAmerican plates. Tectonophysics 568–569:266–281. http://dx.doi.org/10.1016/j. tecto.2011.10.020.

Hertwig, A., McClelland, W. C., Kitajima, K., Schertl, H. P., Maresch, W. V., Stanek, K., ... & Sergeev, S. A. (2016). Inherited igneous zircons in jadeitite predate high-pressure metamorphism and jadeitite formation in the Jagua Clara serpentinite mélange of the Rio San Juan Complex (Dominican Republic). Contributions to Mineralogy and Petrology, 171(5), 48.

van Hinsbergen, D.J.J., Iturralde-Vinent, M.A., van Geffen, P.W., García-Casco, A., & van Benthem, S. (2009), Structure of the accretionary prism, and the evolution of the Paleogene northern Caribbean subduction zone in the region of Camagüey, Cuba. Journal of Structural Geology. 31, 1130-1144. doi 10.1016/j.jsg.2009.06.007.

van Hinsbergen, D. J., Peters, K., Maffione, M., Spakman, W., Guilmette, C., Thieulot, C., Plümper, O., Gürer, D., Brouwer, F. M., & Aldanmaz, E. (2015), Dynamics of intraoceanic subduction initiation: 2. Suprasubduction zone ophiolite formation and metamorphic sole exhumation in context of absolute plate motions, Geochem., Geophys., Geosyst., 16, 1771–1785, doi:10.1002/2015GC005745.

Hoernle, K., van den Bogaard, P., Werner, R., Lissinna, B., Hauff, F., Alvarado, G., & Garbe-Schönberg, D. (2002), Missing history (16-71 Ma) of the Galápagos hotspot: implications for the tectonic and biological evolution of the Americas. Geology 30, 795–798. http://geology.gsapubs.org/content/30/9/795.abstract.

Hoernle, K., Hauff, F., & van den Bogaard, P. (2004), 70 m.Y. History (139-69 Ma) for the Caribbean large igneous province. Geology 32, 697–700. http://geology.gsapubs.org/content/32/8/697.abstract.

Hu, H., & Stern, R. J. (2020), Early Cretaceous Subduction Initiation in Southern Tibet Caused the Northward Flight of India. Geoscience Frontiers 11, 1123-1131.

Iturralde-Vinent, M.A. (1998), Sinopsis de la Constitución Geológica de Cuba: Acta Geológica Hispánica, v. 33, p. 9–56.

Iturralde-Vinent, M., Millán-Trujillo, G., Korpas, L., Nagy, E., & Pajón-Morejón, J.M. (1996), Geological interpretation of the Cuban K-Ar database. En: Iturralde-Vinent, M., (Editor) 1996. Ofiolitas y arcos volcánicos de Cuba, First Contribution IGCP Project 364, pág. 48-69.

Iturralde-Vinent, M.A., Díaz-Otero, C., Díaz-Martínez, R. (2006), Tectonic implications of paleontologic dating of Cretaceous-Danian sections of Eastern Cuba, Geologica Acta 4, 89-102.

Iturralde-Vinent, M. A., Diaz otero, C., Garcia-casco, A., & van Hinsbergen, D. J. J. (2008), Paleogene foredeep basin deposits of North Central Cuba: a record of arc–continent collision between the Caribbean and North American Plates. International Geology Review, 50, 863–884.

Iturralde-Vinent, M.A., García-Casco, A., Rojas-Agramonte, Y., Proenza, J.A., Murphy, J.B., & Stern, R.J. (2016), The geology of Cuba: a brief overview and synthesis. GSA Today. 26(10):4 10. https://doi.org/10.1130/GSATG296A.1.

Japan International Cooperation Agency (1985) Report on Geological Survey of Las Canitas area, Dominican Republic, Phase II: Metal Mining Agency of Japan, 63 p.

Jolly, W. T. & Lidiak, E. G. (2006), Role of crustal melting in petrogenesis of the Cretaceous Water Island Formation (Virgin Islands, northeast Antilles Island arc). Geologica Acta 4, 7^33.

Jolly, W.T., Lidiak, E.G., Dickin, A.P., & Wu, T.-W. (1998), Geochemical diversity of Mesozoic island arc tectonic blocks in eastern Puerto Rico, in Lidiak, E.G., and Larue, D.K., eds., Tectonics and Geochemistry of the Northeastern Caribbean: Geological Society of America Special Paper 322, p. 67–98, doi:10.1130/0-8137-2322-1.67.

Jolly, W.T., Lidiak, E.G., Dickin, A.P., & Wu, T.S. (2002), Recycling in the Puerto Rican mantle wedge, Greater Antilles island arc. The Island Arc, 11, 10-24.

Jolly, W.T., Lidiak, E.G., & Dickin, A.P. (2008a), Bimodal volcanism in northeast Puerto Rico and the Virgin Islands (Greater Antilles Island Arc): Genetic links with Cretaceous subduction of the Mid-Atlantic Ridge Caribbean spur: Lithos, v. 103, p. 393–414, doi:10.1016/j.lithos.2007.10.008.

Jolly, W. T., Lidiak, E. G., & Dickin, A. P. (2008b), The case for persistent southwest-dipping Cretaceous convergence in the northeast Antilles: Geochemistry, melting models, and tectonic implications. Geological Society of America Bulletin, 120(7-8), 1036-1052.

Joyce, J., & Aronson, J. (1987), K-Ar ages for blueschist metamorphism on the Samaná Peninsula, Dominican Republic. In Transaction of 10th Caribbean Geological Conference, Cartagena (pp. 454-458).

Kesler, S. E. (1971). Petrology of the Terre-Neuve igneous province, northern Haiti. Caribbean geophysical, tectonic, and petrologic studies. Geological Society of America Memoir, 130, 119-137.

Kesler, S. E., & Sutter, J. F. (1979). Compositional evolution of intrusive rocks in the eastern Greater Antilles island arc. Geology, 7(4), 197-200.

Kesler, S. E., Sutter, J. F., Jones, L. M., & Walker, R. L. (1977). Early Cretaceous basement rocks in Hispaniola. Geology, 5(4), 245-247.

Kesler, S. E., Sutter, J. F., Barton, J. M., & Speck, R. C. (1991). Age of intrusive rocks in northern Hispaniola. Geologic and tectonic development of the North America–Caribbean plate boundary in Hispaniola. Boulder (Colorado), Geological Society of America, 262, 165-185.

Kesler, S. E., Hall, C. M., Russell, N., Piñero, E., Sánchez, R. C., Pérez, M. R., & Moreira, J. (2004). Age of the Camaguey gold-silver district, Cuba: Tectonic evolution and preservation of epithermal mineralization in volcanic arcs. Economic Geology, 99(5), 869-886.

Kesler, S. E., Campbell, I. H., & Allen, C. M. (2005a). Age of the Los Ranchos Formation, Dominican Republic: Timing and tectonic setting of primitive island arc volcanism in the Caribbean region. Geological Society of America Bulletin, 117(7-8), 987-995.

Kesler, S. E., Campbell, I. H., Smith, C. N., Hall, C. M., & Allen, C. M. (2005b). Age of the Pueblo Viejo gold-silver deposit and its significance to models for high-sulfidation epithermal mineralization. Economic Geology, 100(2), 253-272.

Kerr, A.C., Marriner, G.F., Arndt, N.T., Tarney, J., Nivia, A., Saunders, A.D., & Duncan, R.A. (1996a), The petrogenesis of Gorgona komatiites, picrites and basalts: new field, petrographic and geochemical constraints. Lithos 37, 245–260. https://doi.org/10.1016/0024-4937(95)00039-9.

Kerr, A. C., Iturralde-Vinent, M. A., Saunders, A. D., Babbs, T. L., & Tarney, J. (1999). A new plate tectonic model of the Caribbean: Implications from a geochemical reconnaissance of Cuban Mesozoic volcanic rocks. Geological Society of America Bulletin, 111(11), 1581-1599.

Khudoley, K. M., 1967, Reply: Am. Assc. Petroleum Geologists Bull., v. 51, No.7, p. 789-791.

Kirk, J. D., Ruiz, J., Kesler, S. E., Simon, A., & Muntean, J. L. (2014). Re-Os age of the pueblo Viejo epithermal deposit, Dominican Republic. Economic Geology, 109(2), 503-512.

Krebs, M., Maresch, W. V., Schertl, H.-P., Münker, C., Baumann, A., Draper, G., Idleman, B., & Trapp, E. (2008), The dynamics of intra-oceanic subduction zones: A direct comparison between fossil petrological evidence (Rio San Juan Complex, Dominican Republic) and numerical simulation. Lithos, 103(1-2), 106–137. doi:10.1016/j.lithos.2007.09.003.

Krebs, M., Schertl, H.-P., Maresch, W. V., & Draper, G. (2011), Mass flow in serpentinite-hosted subduction channels: P–T–t path patterns of metamorphic blocks in the Rio San Juan mélange (Dominican Republic). Journal of Asian Earth Sciences, 42(4), 569–595. doi:10.1016/j.jseaes.2011.01.011.

Kysar, G., Mortensen, J. K., & Lewis, J. F. (1998). U-Pb zircon age constraints for Paleogene igneous rocks of the Sierra Maestra, Southeastern Cuba; implications for short-lived arc magmatism along the northern Caribbean margin. In Geological Society of America, Abstracts with Programs (Vol. 30, No. 7, pp. A-185).

Kysar, G., Lewis, J.F., Perfit, M.R., et al., “Granitoids with a continental affinity from the NW wall of the Cayman Trench: implications for subduction zone magmatism in the Cayman. Sierra Maestra. N Chortis Block and Nicaraguan Rise,” in Third Cuban Convention of Earth

Science, Proceed. Geociencias 2009 “Subduction Zones of the Caribbean,” Havana, Cuba, 2009 (Havana, 2009).

Lapierre, H., Dupuis, V., Mercier de Lépinay, B., Bosch, D., Monié, P., Tardy, M., ... & Cotten, J. (1999). Late Jurassic oceanic crust and Upper Cretaceous Caribbean plateau picritic basalts exposed in the Duarte igneous complex, Hispaniola. The Journal of geology, 107(2), 193-207.

Larue, D. K., & Ryan, H. F. (1998), Seismic reflection profiles of the Puerto Rico trench: Shortening between the North American and Caribbean plates, in Lidiak, E., and Larue, D., eds., Tectonics and geochemistry of the northeastern Caribbean: Geological Society of America Special Paper, v. 322, p. 193–210.

Laverov, N. P., L. L. Shanin, and R. Cabrera-Ortega, 1967.Absolyutnyy vozrast nekotorykh gornykh porod Kuby, p.188-190, in Pushcharovsky, Yu. M., ed., Geology and mineral resources of Cuba: Moscow, Pub. Off. “Nauka”, 190 p. (in Russian).

Lázaro, C., García-Casco, A., Rojas Agramonte, Y., Kröner, A., Neubauer, F., & Iturralde-Vinent, M.A. (2009), Fifty-five-million-year history of oceanic subduction and exhumation at the northern edge of the Caribbean plate (Sierra del Convento melange, Cuba), J. Metamorph. Geol., 27, 19–40.

Lázaro, C., Blanco-Quintero, I.F., Marchesi, C., Bosch, D., Rojas-Agramonte, Y., & García-Casco, A. (2011), The imprint of subducion fluids on subducted MORB-derived melts (Sierra del Convento mélange, Cuba): Lithos, v. 126, p. 341–354. doi:10.1016/j.lithos.2011.07.011.

Lázaro, C., Blanco-Quintero, I.F., Rojas-Agramonte. Y., Proenza, J.A., NúñezCambra, K., & García-Casco, A. (2013), First description of a metamorphic sole related to ophiolite obduction in the northern Caribbean: geochemistry and petrology of the Güira de Jauco Amphibolite complex (eastern Cuba) and tectonic implications. Lithos 179: 193–210.

Lázaro, C., García-Casco, A., Blanco-Quintero, I.F., Rojas-Agramonte, Y., Corsini, M., & Proenza, J.A. (2015), Did the Turonian–Coniacian plume pulse trigger subduction initiation in the Northern Caribbean? Constraints from 40Ar/ 39Ar dating of the Moa-Baracoa metamorphic sole (eastern Cuba): International Geology Review 57, 919–942. doi:10.1080/00206814.2014.924037.

Lázaro, C., Blanco-Quintero, I.F., Proenza-Fernández, J.A., Rojas-Agramonte, Y., Neubauer, F., Núñez-Cambra, K., & García-Casco, A. (2016), Petrogenesis and 40Ar/39Ar dating of proto-forearc crust in the early Cretaceous Caribbean Arc: The La Tinta melange (eastern

Cuba) and its easterly correlation in Dominican Republic. International Geology Review, 58: 1020-1040, doi: 10.1080/00206814.2015.1118647.

Lewis, J. F., Harper, C. T., Kemp, A. W., & Stipp, J. J. (1973). Potassium-argon retention ages of some Cretaceous rocks from Jamaica. Geological Society of America Bulletin, 84(1), 335-340.

Lewis, J. F., Perfit, M. R., Kysar, M. G., Aravalo, R., Mortensen, J., Ullrich, T., Friedman, R., & Kamenov, G. (2005), Anomalous granitoid compositions from the northwestern Cayman Trench: Implications for the composition and evolution of the Cayman ridge: Transactions of the 17th Caribbean Conference, San Juan de Puerto Rico.

Lewis, J.F., Draper, G., Proenza, J.A., Espaillat, J., & Jiménez, J. (2006), Ophiolite-Related Ultramafic Rocks (Serpentinites) in the Caribbean Region: A Review of their Occurrence, Composition, Origin, Emplacement and Ni-Laterite Soil Formation. Geologica Acta, 4(1-2), 237-263.

Lewis, J.F., Mattietti, G.K., Perfit, M., & Kamenov, G. (2011), Geochemistry and petrology of three granitoid rock cores from the Nicaraguan Rise, Caribbean Sea: Implications for its composition, structure and tectonic evolution: Geologica Acta, v. 9, no. 3, p. 467–479.

Lidiak, E. G., & Jolly, W. T. (1996), Circum-Caribbean granitoids: characteristics and origin. International Geology Review 38, 1098–1133.

Lidiak, E.G., & Jolly, W.T. (1998), Geochemistry of intrusive igneous rocks, St. Croix, U.S. Virgin Islands, in Lidiak, E.G., and Larue, D.K., eds., Tectonics and Geochemistry of the Northeastern Caribbean: Geological Society of America Special Paper 322, p. 133–153, doi:10.1130/0-8137-2322-1.133.

Lidiak, E.G., Jolly, W.T., & Dickin, A.P. (2011), Pre-arc basement complex and overlying early island arc strata, Southwestern Puerto Rico: overview, geologic evolution, and revised data bases. Geologica Acta, vol. 9, núm. 3-4, 273-287.

Lidiak, E.G. & Anderson, T.H. (2015), Evolution of the Caribbean plate and origin of the Gulf of Mexico in light of plate motions accommodated by strike-slip faulting. In Late Jurassic Margin of Laurasia-A Record of Faulting Accommodating Plate Rotation; Anderson, T.H., Didenko, A.N., Johnson, C.L., Khanchuk, A.I., MacDonald, J.H., Jr., Eds.; Geological Society of America: Boulder, CO, USA, 2015.

Llanes-Castro, J.A., Proenza J.A., & Cruz-Gámez, E.M. (2018), Forearc ophiolite in Habana-Matanzas, Western Cuba: evidence from serpentinized mantle peridotite REE geochemistry and Cr-spinel composition. Acta Geologica Sinica (English Edition), 92(supp.2):19-21.

Llanes Castro, A.I., Furnes, H., Gámez, E.M.C., Rodriguez, M.P., & Cruz, O.L. (2019), Petrogenesis of plagiogranite and associated diorites and mafic rocks in the Habana–Matanzas ophiolites, northwestern half of central Cuba. Journal of the Geological Society, London, 176, 992–1006, https://doi.org/10.1144/ jgs2018-116.

Loewen, M.W., Duncan, R.A., Kent, A.J.R., & Krawl, K. (2013), Prolonged plume volcanism in the Caribbean large Igneous Province: New insights from Curaçao and Haiti. Geochemistry, Geophysics, Geosystems 14, 4241–4259. https://doi.org/10.1002/ggge.20273.

Mann, P. (1999), Caribbean Sedimentary Basins" Classification and Tectonic Setting from Jurassic to Present. Caribbean Basins. Sedimentary Basins of the World, 4 edited by E Mann (Series Editor: K.J. Hsti), pp. 3-31.

Mann, P., Calais, E., Ruegg, J.-C., DeMets, C., Jansma, P.E., & Mattioli, G.S. (2002), Oblique collision in the northeastern Caribbean from GPS measurements and geological observations. Tectonics 21(6) 1057, doi:10.1029/2001TC001304.

Mann, P., Rogers, R., & Gahagan, L. (2007), Overview of plate tectonic history and its unresolved tectonic problems. In: Bundschuh, J. and Alvarado, G.E. (eds) Central America: Geology, Resources and Hazards. Taylor and Francis/Balkema, Leiden, The Netherlands, 201–237.

Marchesi, C., Garrido, C.J., Godard, M., Proenza, J.A., Gervilla, F., & Blanco-Moreno, J. (2006), Petrogenesis of highly depleted peridotites and gabbroic rocks from the Mayarí-Baracoa Ophiolitic Belt (eastern Cuba). Contributions to Mineralogy and Petrology, v. 151, p. 717–736. doi:10.1007/s00410-006-0089-0.

Marchesi, C., Garrido, C.J., Bosch, D., Proenza, J.A., Gervilla, F., Monie, P., & Rodriguez-Vega, A. (2007), Geochemistry of Cretaceous magmatism in eastern Cuba: Recycling of North American continental sediments and implications for subduction polarity in the Greater Antilles Paleo-arc. Journal of Petrology, v. 48, p. 1813–1840. doi:10.1093/petrology/egm040.

Marchesi, C., Jolly, W.T., Lewis, J.F., Garrido, C.J., Proenza, J.A., & Lidiak, E.G. (2011), Petrogenesis of fertile mantle peridotites from the Monte del Estado massif (Southwest Puerto Rico): A preserved section of Proto-Caribbean lithospheric mantle?: Geologica Acta, v. 9, p. 289–306.

Marchesi, C., Garrido, C.J., Proenza, J.A., Hidas, K., Varas-Reus, M.I., Butjosa, L., & Lewis. J.F. (2016), Geochemical record of subduction initiation in the sub-arc mantle: insights from the Loma Caribe peridotite (Dominican Republic). Lithos, 252–253, pp. 1-15.

Mauffret, A., & Leroy, S. (1997), Seismic stratigraphy and structure of the Caribbean igneous province. Tectonophysics 283, 61–104. http://www.sciencedirect.com/science/article/pii/S0040195197001030.

Mitchell, S.F. (2020), Cretaceous geology and tectonic assembly of Jamaica. Geological Society, London, Special Publications, 504, 2 September 2020. https://doi.org/10.1144/SP504-2019-210.

Montgomery, H., Pessagno, E.A., Jr, Lewis, J.F., & Schellekens, J.H. (1994), Paleogeography of Jurassic fragments in the Caribbean. Tectonics, 13, 725-732.

Monthel, J. (2010), Mapa Geológico de la Hoja a E. 1:50.000 nº 6075-I (Puerto Plata). Proyecto SYSMIN de Cartografía Geotemática de la República Dominicana. Programa. Dirección General de Minería, Santo Domingo, p. 310.

Morishita, T., Tani, K., Shukuno, H., Harigane, Y., Tamura, A., Kumagai, H., & Hellebrand, E. (2011), Diversity of melt conduits in the Izu–Bonin–Mariana forearc mantle: Implications for the earliest stage of arc magmatism. Geology, 39, 411–414.

Moyen, J.-F (2009), High Sr/Y and La/Yb ratios: The meaning of the “adakitic signature.” Lithos, 112(3-4), 556–574. doi:10.1016/j.lithos.2009.04.001.

Mueller, A. G., Hall, G. C., Nemchin, A. A., & O’Brien, D. (2008). Chronology of the Pueblo Viejo epithermal gold–silver deposit, Dominican Republic: formation in an Early Cretaceous intra-oceanic island arc and burial under ophiolite. Mineralium Deposita, 43(8), 873.

Nelson, C. E., Stein, H., Dominguez, H., Carrasco, C., Barrie, T., Torró, L., & Proenza, J. (2015). Re-Os dating of molybdenite from the Pueblo Viejo Au-Ag-Cu and Douvray Cu-Au districts, Hispaniola. Economic Geology, 110(4), 1101-1110.

Odin, G.S., Desreumaux, C., Gillot, P.-Y., Gardin, S., Hernandez, J.H., Coccioni, R. (2001). K–Ar d’un neveau volcanoclastiquemaastricthien de Haiti. In: Odin, G.S. (Ed.), The Campa-nian–Maastrichtian Stage Boundary. Elsevier, Amsterdam,pp. 766–774.

Pearce, J.A. (1996), A users guide to basalt discrimination diagrams. In: Wyman DA, editor. Trace Element Geochemistry of Volcanic Rocks: Applications for Massive Sulphide Exploration. Short Course Notes 12. St. John’s, Canada: Geological Association of Canada, pp. 79-113.

Pearce J.A. (2008), Geochemical fingerprinting of oceanic basalts with applications to ophiolite classification and the search for Archean oceanic crust. Lithos 100:14–48. doi:10.1016/j. lithos. 2007.06.016.

Pearce, J.A., Harris, N.B.W., & Tindle, A.G. (1984a), Trace element discrimination diagrams for the tectonic interpretation of granitic rocks: Journal of Petrology, v. 25, p. 956–983.

Pearce, J.A., Lippard, S.J., & Roberts, S. (1984b), Characteristics and tectonic significance of supra-subduction zone ophiolites. Geol. Soc. Lond., Spec. Publ. 16, 77–94.

Pérez, R. (2008), Oxygen isotope geochemistry of plutonic rocks from Puerto Rico [M.A. thesis]: Mayagüez, Puerto Rico, University of Puerto Rico, 140 p.

Perfit, M. R., & Heezen, B. C. (1978), The geology and evolution of the Cayman Trench: Geological Society of America Bulletin, v. 89, p. 1155–1174.

Perfit, M. R., Heezen, B. C., Rawson, M., & Donnely, T. W. (1980a), Metamorphic rocks from the Puerto Rico trench: Their origin and tectonic significance: Marine Geology, v. 34, p. 125–156.

Perfit, M. R., Heezen, B. C., Rawson, M., & Donnelly, T. W. (1980b). Chemistry, origin and tectonic significance of metamorphic rocks from the Puerto Rico Trench. Marine Geology, 34(3-4), 125-156.

Pindell, J.L., & Barrett, S.F. (1990), Geological evolution of the Caribbean region: a plate-tectonic perspective. In G. Dengo, J.E. Case (Eds.), The Caribbean Region, The Geology of North America, H, Geological Society of America, Boulder, Colorado (1990), pp. 405-432.

Pindell, J.L., & Kennan, L. (2009), Tectonic evolution of the Gulf of Mexico, Caribbean and northern South America in the mantle reference frame: an update. K.H. James, M.A. Lorente, J.L. Pindell (Eds.), The Origin and Evolution of the Caribbean plate, Geological Society, London, Special Publications, 328 (2009), pp. 1-55.

Pindell, J., Kennan, L., Maresch, W. V., Stanek, K.-P., Draper, G., & Higgs, R. (2005), Plate-kinematics and crustal dynamics of circum-Caribbean arc-continent interactions: Tectonic controls on basin development in Proto-Caribbean margins. Special Paper 394: Caribbean-South American Plate Interactions, Venezuela, 7–52. doi:10.1130/0-8137-2394-9.7.

Pindell, J., Maresch, W. V., Martens, U., & Stanek, K. (2012), The Greater Antillean Arc: Early Cretaceous origin and proposed relationship to Central American subduction mélanges: implications for models of Caribbean evolution. International Geology Review 54, 131–43.

Proenza, J., Gervilla, F., Melgarejo, J.C., & Bodinier, J.L. (1999), Al- and Cr- rich chromitites from the Mayarí-Baracoa Ophiolitic Belt (eastern Cuba): consequence of interaction between volatile-rich melts and peridotite in suprasubduction mantle. Economic Geology, 94, 547-566.

Proenza, J.A., Díaz-Martínez, R., Iriondo, A., Marchesi, C., Melgarejo, J.C., Gervilla, F., Garrido, C.J., Rodríguez-Vega, A., Lazano-Santacruz, R., & Blanco-Moreno, J.A. (2006), Primitive Cretaceous island-arc volcanic rocks in eastern Cuba: the Téneme Formation. Geologica Acta, 4, 103-121.

Proenza, J.A., Zaccarini, F., Lewis, J.F., Longo, F., & Garuti, G. (2007), Chromite composition and platinum-group mineral assemblage of PGE-rich Loma Peguera chromitites, Loma Caribe peridotite, Dominican Republic. Canadian Mineralogist, 45, 211-228.

Rankin, D. (2002). Geology of St. John, U.S. Virgin Islands. United States Geologicl Survey Professional Paper, 1631, 1-36.

Révillon, S., Arndt, N.T., Chauvel, C., & Hallot, E. (2000), Geochemical study of ultramafic volcanic and plutonic rocks from Gorgona Island, Colombia: the plumbing system of an oceanic plateau. Journal of Petrology 41, 1127–1153. https://doi.org/10.1093/petrology/41.7.1127.

Rojas-Agramonte, Y., Neubauer, F., Kröner, A., Wan, Y. S., Liu, D. Y., Garcia-Delgado, D. E., & Handler, R. (2004). Geochemistry and early Palaeogene SHRIMP zircon ages for island arc granitoids of the Sierra Maestra, southeastern Cuba. Chemical Geology, 213(4), 307-324.

Rojas-Agramonte, Y., Neubauer, F., Handler, R., García-Delgado, D. E., Friedl, G., & Delgado-Damas, R. (2005), Variation of palaeostress patterns along the Oriente transform wrench corridor, Cuba: significance for Neogene–Quaternary tectonics of the Caribbean realm. Tectonophysics, 396(3-4), 161-180.

Rojas-Agramonte, Y., Neubauer, F., Bojar, A.V., Hejl, E., Handler, R., & GarcíaDelgado, D.E. (2006), Geology, age and tectonic evolution of the Sierra Maestra Mountains, southeastern Cuba: Geologica Acta, v. 4, p. 123–150.

Rojas-Agramonte, Y., Neubauer, F., Garcia-Delgado, D. E., Handler, R., Friedl, G., & Delgado-Damas, R. (2008), Tectonic evolution of the Sierra Maestra Mountains, SE Cuba, during Tertiary times: From arc-continent collision to transform motion. Journal of South American Earth Sciences, 26(2), 125-151.

Rojas-Agramonte, Y., Kröner, A., García -Casco, A., Kemp, T., Hegner, E., Pe´rez, M., Barth, M., Liu, D., & Fonseca-Montero, A. (2010), Zircon ages, Sr-Nd-Hf isotopic compositions and geochemistry for granitoids associated with the northern ophiolite me´lange of central Cuba: tectonic implication for late Cretaceous magmatism in the northwestern Caribbean. Am. J. Sci. 310:1453–1479.

Rojas-Agramonte, Y., Kröner, A., García-Casco, A., Somin, M., Iturralde-Vinent, M., Mattinson, J. M., Millán Trujillo, G., Sukar, K., Pérez Rodríguez, M., Carrasquilla, S., Wingate, M.T.D., & Liu, D. Y. (2011), Timing and Evolution of Cretaceous Island Arc Magmatism in Central Cuba: Implications for the History of Arc Systems in the Northwestern Caribbean. The Journal of Geology, 119(6), 619–640. doi:10.1086/662033.

Rojas-Agramonte, Y., Garcia-Casco, A., Kemp, A., Kröner, A., Proenza, J.A., Lázaro, C., & Liu, D. (2016), Recycling and transport of continental material through the mantle wedge above subduction zones: A Caribbean example: Earth and Planetary Science Letters, v. 436, p. 93–107. doi:10.1016/j.epsl.2015.11.040.

Rojas-Agramonte, Y., Hu, H. Y., Iturralde-Vinent, M., Lewis, J., de Lepinay, B, M., & García-Casco, A. (2021). A Late Cretaceous Adakitic intrusion from Northern Haiti: additional evidence for slab melting and implications for migration of ridge-trench-trench triple junction during the Cretaceous in the Greater Antilles. International Geology Review, 1-10.

Román, Y. A., Pujols, E. J., Cavosie, A. J., & Stockli, D. F. (2021). Timing and magnitude of progressive exhumation and deformation associated with Eocene arc-continent collision in the NE Caribbean plate. GSA Bulletin, 133(5-6), 1256-1266.

Rosencrantz, E. (1990), Structure and tectonics of the Yucatan Basin, Caribbean Sea, as determined from seismic reflection studies: Tectonics, v. 9, p. 1037–1059.

Saura, E., Vergés, J., Brown, D., Pujianto, L., Soriano, S., Torrescusa, S., García, R., Sánchez, J.R., Sosa, C., Tenreyro, R. (2008), Structural and tectonic evolution of western Cuba fold and thrust belt. Tectonics 27(4),TC4002. https://doi.org/10.1029/2007TC002237.

Rosencrantz, E., Ross, M. I., & Sclater, J. G. (1988). Age and spreading history of the Cayman Trough as determined from depth, heat flow, and magnetic anomalies. Journal of Geophysical Research: Solid Earth, 93(B3), 2141-2157.

Rui, H., Yang, J., Wu, W., Lian, D., & Qiu, T. (2020). Geochronology and Geochemistry of Gabbros from Moa-Baracoa Ophiolitic Massif, Eastern Cuba: Implication for Early Cretaceous SSZ Magmatism. Acta Geologica Sinica-English Edition, 94(S1), 47-48.

Schellekens, J. H. (1998a), Composition, metamorphic grade, and origin of metabasites in the Bermeja Complex, Puerto Rico. International Geology Review, 40, 722–747.

Schellekens, J. H. (1998b), Geochemical evolution and tectonic history of Puerto Rico. Special Paper 322: Tectonics and Geochemistry of the Northeastern Caribbean, 35–66. doi:10.1130/0-8137-2322-1.35

Schneider, J. Bosch, D., Monié, P., Guillot, S., García-casco, A., Lardeaux, J.M., Torres Roldan, R.L., & Millán Trujillo, G. (2004), Origin and evolution of the Escambray Massif (Central Cuba): an example of HP/LT rocks exhumed during intraoceanic subduction. Journal of Metamorphic Geology 22, 227–247. DOI 10.1111/j.1525-1314.2004.00510.x.

Schrecengost, K. L. (2010). Geochemistry and U/Pb zircon geochronology of the Virgin Islands Batholith, British Virgin Islands [M.Sc. thesis]: University of North Carolina, Chapel Hill

Sen, G., Hickey-Vargas, R., Waggoner, D. G., & Maurrasse, F. (1988). Geochemistry of basalts from the Dumisseau Formation, southern Haiti: implications for the origin of the Caribbean Sea crust. Earth and Planetary Science Letters, 87(4), 423-437.

Shervais, J. W. (1982), Ti-V plots and the petrogenesis of modern and ophiolitic lavas, Earth Planet. Sci. Lett., 59(1), 101 ± 118, 1982.

Sinton, C. W., Duncan, R. A., & Denyer, P. (1997), Nicoya Peninsula, Costa Rica: A single suite of Caribbean oceanic plateau magmas. Journal of Geophysical Research: Solid Earth, 102(B7), 15507-15520.

Sinton, C.W., Duncan, R.A., Storey, M., Lewis, J., & Estrada, J.J. (1998), An oceanic flood basalt province within the Caribbean plate. Earth and Planetary Science Letters 155, 221–235. http://www.sciencedirect.com/science/article/pii/S0012821X97002148.

Speed, R. C., Gerhard, L. C., & McKee, E. H. (1979). Ages of deposition, deformation, and intrusion of Cretaceous rocks, eastern St. Croix, Virgin Islands. Geological Society of America Bulletin, 90(7), 629-632.

Stanek, K. P., Maresch, W. V., Scherer, E., Krebs, M., Berndt, J., Sergeev, S. S., ... & Hames, W. E. (2019). Born in the Pacific and raised in the Caribbean: construction of the Escambray nappe stack, central Cuba. A review. European Journal of Mineralogy, 31(1), 5-34.

Stern, R.J. (2010), The Anatomy and Ontogeny of Modern Intra-Oceanic Arc Systems. Kusky, T. M., Zhai, M.-G. & Xiao, W. (eds) The Evolving Continents: Understanding Processes of Continental Growth. Geological Society, London, Special Publications, 338, 7–34.

Stern, R. J., & Bloomer, S. H. (1992), Subduction zone infancy: Examples from the Eocene Izu-Bonin-Mariana and Jurassic California arcs. Geological Society of America Bulletin, 104 (12), 1621–1636v.

Stern, R.J., & Gerya, T. (2018), Subduction Initiation in nature and models: A review. Tectonophysics 746, 173-198.

Stern, R.J., Reagan, M., Ishizuka, O., Ohara, Y. & Whattam, S. (2012), To understand subduction initiation, study forearc crust: to understand forearc crust, study ophiolites. – Lithosphere 4: 69–483.

Torró, L., Proenza-Fernández, J.A., Melgarejo, J.C., Alfonso, P., Farré de Pablo, J., Colomer, J.M., García-Casco, A., Gubern, A., Gallardod, E., Cazañas-Díaz, X., Chávez, C., Del Carpio, R., León, P., Nelson, C.E.,& Lewis, J.F. (2016a), Mineralogy, geochemistry and sulfur isotope characterization of Cerro de Maimón (Dominican Republic), San Fernando and Antonio (Cuba) lower Cretaceous VMS deposits: Formation during subduction initiation of the proto-Caribbean lithosphere within a fore-arc. Ore Geology Reviews, 72: 794-817.

Torró, L., Garcia-Casco, A., Proenza, J.A., Blanco-Quintero, I.F., Gutiérrez-Alonso, G., & Lewis, J.F. (2016b), High-pressure greenschist to blueschist facies transition in the Maimón Formation (Dominican Republic) suggests mid-cretaceous subduction of the Early Cretaceous Caribbean arc: Lithos, v. 266, p. 309–331. doi:10.1016/j. lithos.2016.10.026.

Torró, L., Proenza, J.A., Marchesi, C., Garcia-Casco, A., & Lewis, J. F. (2017a), Petrogenesis of meta-volcanic rocks from the Maimón Formation (the Dominican Republic): Geochemical record of the nascent Greater Antilles paleo-arc: Lithos, v. 278, p. 255– 273. doi:10.1016/j.lithos.2017.01.031.

Torró, L., Camprubí, A., Proenza, J. A., León, P., Stein, H. J., Lewis, J. F., ... & Melgarejo, J. C. (2017b). Re-Os and U-Pb geochronology of the Doña Amanda and Cerro Kiosko deposits, Bayaguana district, Dominican Republic: looking down for the porphyry Cu-Mo roots of the Pueblo Viejo-type mineralization in the island-arc tholeiitic series of the Caribbean. Economic Geology, 112(4), 829-853.

Torró, L., Proenza, J. A., Camprubí, A., Nelson, C. E., Domínguez, H., Carrasco, C., ... & Melgarejo, J. C. (2017c). Towards a unified genetic model for the Au-Ag-Cu Pueblo Viejo district, central Dominican Republic. Ore Geology Reviews, 89, 463-494.

Torró, L., Proenza, J. A., Rojas-Agramonte, Y., Garcia-Casco, A., Yang, J. H., & Yang, Y. H. (2018). Recycling in the subduction factory: Archaean to Permian zircons in the oceanic Cretaceous Caribbean island-arc (Hispaniola). Gondwana Research, 54, 23-37.

Torró, L., Cambeses, A., Rojas-Agramonte, Y., Butjosa, L., Iturralde-Vinent, M., Lázaro, C., Piñero, E., Proenza, J.A., & Garcia-Casco, A. (2020), Cryptic alkaline magmatism in the oceanic Caribbean arc (Camagüey area, Cuba). Lithos. 376-377. https://doi.org/10.1016/j.lithos.2020.105736.

Vila, J. M., Andreieff, P., Bellon, H., & Mascle, A. (1986). Tectonique de collage le long d'un accident décrochant, ante oligocène, est-ouest, dans les Iles Vierges septentrionales (Antilles). Comptes rendus de l'Académie des sciences. Série 2, Mécanique, Physique, Chimie, Sciences de l'univers, Sciences de la Terre, 302(3), 141-144.

Wadge, G., Jackson, T. A., Isaacs, M. C., & Smith, T. E. (1982). The ophiolitic Bath-Dunrobin Formation, Jamaica: significance for Cretaceous plate margin evolution in the north-western Caribbean. Journal of the Geological Society, 139(3), 321-333.

West Jr, D. P., Abbott Jr, R. N., Bandy, B. R., & Kunk, M. J. (2014). Protolith provenance and thermotectonic history of metamorphic rocks in eastern Jamaica: Evolution of a transform plate boundary. Bulletin, 126(3-4), 600-614.

Whattam, S.A., & Stern, R.J. (2011), The 'subduction initiation rule': A key for linking ophiolites, intra-oceanic forearcs and subduction initiation. Contrib. Mineral. Petrol. 162, 1031-1045

Wilson, F.H., Orris, G. & Gray, F. (2019), Preliminary geologic map of the Greater Antilles and the Virgin Islands. U.S. Geological Survey Open-File Report, 2019–1036, pamphlet 50 pp., 2 sheets, scales 1:2,500,000 and 1:300,000.

Formblatt Kumulative Dissertation Stand 14.02.2023

1. Publikation/*Publication*:

Vollständige bibliographische Referenz/*Complete bibliographic reference:*

Hu, H., Rojas-Agramonte, Y., Carrasquilla, S., Lázaro, C., Vinent, I., & Garcia-Casco, A. (2024). Exotic vs local Caribbean origin for the arc-related Mabujina Amphibolite Complex (Cuba): implications for segmentation of the Caribbean arc during the Cretaceous. International Geology Review, 66(1), 254-277.

2. Erst- oder gleichberechtigte Autorenschaft/*First or equal authorship:* **Ja/*Yes*** ☑ **Nein/*No*** ☐

3. Veröffentlicht/*Published* ☑ **Zur Veröffentlichung akzeptiert/*Accepted*** ☐

Q1/Q2:* **Ja/*Yes*** ☑ **Nein/*No*** ☐

**SCImago Journal Rank (SJR) indicator*

Im Erscheinungsjahr oder im letzten verfügbaren Vorjahr/*In the year of publication or the last prior year available:* 2024

Eingereicht/*Submitted* ☑ **Noch nicht eingereicht/*Not yet submitted*** ☐

4. Beteiligungen/*Contributions***

Contributor Role	**Doktorand/in/ *Doctoral student***	**Co-Autor/in 1/ *Co-author 1***	**Co-Autor/in 2/ *Co-author 2***
Name, first name	Haoyu Hu	Yamirka Rojas-agramonte	Antonio Garcia-Casco
Methodology	☑	☐	☐
Software	☐	☐	☐
Validation	☐	☐	☐
Formal analysis	☑	☐	☐
Investigation	☑	☑	☑
Resources	☐	☐	☐
Data Curation	☑	☐	☑
Writing-Original Draft	☑	☐	☐
Writing-Review&Editing	☑	☑	☑
Visualization	☑	☐	☐
Supervision	☐	☑	☑
Project administration	☐	☑	☐
Funding acquisition	☐	☑	☐

***Kategorien des CRediT (Contributor Roles Taxonomy, https://credit.niso.org/)*

Hiermit bestätige ich, dass alle obigen Angaben korrekt sind/*I confirm that all declarations made above are correct.*

Unterschrift/*Signature* _____ _____ GARCIA CASCO ANTONIO - 08804875S Firmado digitalmente por GARCIA CASCO ANTONIO - 08804875S Fecha: 2025.10.28 17:46:08 +01'00' _____

Doktorand/in/*Doctoral student* | Co-Autor/in 1/*Co-author 1* | Co-Autor/in 2/*Co-author 2*

Betreuungsperson/*Supervisor:*

Hiermit bestätige ich, dass alle obigen Angaben korrekt sind und dass die selbstständigen Arbeitsanteile des/der Doktoranden/in an der aufgeführten Publikation hinreichend und signifikant sind/*I confirm that all declarations made above are correct and that the doctoral student's independent contribution to this publication is significant and sufficient to be considered for the cumulative dissertation.*

Pro. Dr. Yamirka Rojas-agramonte		30.10.2025
Name/*Name*	Unterschrift/*Signature*	Datum/*Date*

Appendix 2

Exotic vs local Caribbean origin for the arc related Mabujina Amphibolite Complex (Cuba): implications for segmentation of the Caribbean arc during the Cretaceous

Authors

Haoyu Hu, Yamirka Rojas-Agramonte, Sandra Carrasquilla, Concepción Lázaro, Iturralde Vinent & Antonio Garcia-Casco

Abstract

The Mabujina Complex exposed in south-central Cuba consists of an elongated body of metamorphosed volcanic and subvolcanic mafic rocks and tonalitic gneisses. The complex is largely composed of greenschist facies rocks (Porvenir Formation) directly below the Cretaceous volcanic arc section and of a deeper sequence of deformed amphibolite facies rocks (Mabujina Amphibolite Complex). The origin of the protolith of the Mabujina Complex has been the subject of intense debate in the past. While some authors consider the Mabujina Complex to represent the deepest and oldest (Early Cretaceous) exposed section (root) of the Cretaceous Caribbean volcanic arc others suggested an exotic (non-Caribbean related) Early Cretaceous volcanic arc section. The later proposal implies the tectonic emplacement underneath the Caribbean arc of a segment of the Pacific-related Early Cretaceous Mexican Guerrero volcanic arc terrane. A new set of whole-rock geochemical analyses presented in this study shows that the protoliths of the Mabujina Amphibolite Complex constitute an island-arc sequence with a) less abundant island-arc tholeiitic mafic rocks similar to the Early Cretaceous tholeiitic island arc of the Caribbean and b) dominant transitional to calc-alkaline mafic and felsic igneous rocks that resemble the Early to Late Cretaceous magmatism of the Caribbean arc. The high initial Nd ratios of the rocks from the Mabujina Amphibolite Complex are indistinguishable from the tholeiitic to calc-alkaline sequences from the Caribbean arc, reflecting a depleted MORB mantle source with limited subduction-related component input. The present data, together with published geochemical and geochronological data of the protoliths, allow identifying a Caribbean origin for the Mabujina Complex instead of an exotic provenance in the Guerrero Arc of western Mexico. However, even if the interpretation of the geochemical data favours a Caribbean origin, the Mabujina Amphibolite Complex cannot represent the root of the volcanic arc. Here, we propose that the Mabujina Amphibolite Complex is a fragment of the Early to Mid-Cretaceous Caribbean arc that was tectonically emplaced below this same arc as a likely consequence of arc segmentation and strike-slip trans-compression triggered by oblique subduction during the mid-Cretaceous.

1. Introduction

After the Jurassic (~180 Ma) break-up of Pangea and the formation of the Proto-Caribbean sea in between the Americas, the Caribbean intra-oceanic arc system began to form during the Early Cretaceous along the northeastern edge of the Farallon (Pacific) plate due to SW-dipping subduction of the Proto-Caribbean lithosphere (Pindell et al. 2012; Boschman et al. 2014). During mid-late Cretaceous time, the Caribbean arc (also known as the Protoantillean arc) migrated to the northeast and east, probably with a strong axis-parallel stretching component due to the sinistral oblique subduction of the Proto-Caribbean lithosphere. The arc migrated first towards the southeastern flank of the Chortis block, then towards the southern flank of the Maya Block and the Caribeana terrane, and finally towards the Bahamas platform (Pindell et al. 2005, 2012; Garcia-Casco et al. 2008; Boschman et al. 2014). Volcanic arc activity in the Cuban segment of the Caribbean arc produced sedimentary, volcanic, and plutonic rocks during Cretaceous times (ca. 135–70 Ma) (Rojas-Agramonte et al. 2011 and references therein) that can broadly be separated into three sequences of tholeiitic and calc-alkaline to cryptic-alkaline suites (Iturralde-Vinent et al. 1996; Kerr et al. 1999; Torró et al. 2020 and references therein). This reflects a regional geochemical evolution of magmatic products from the inception of subduction to a mature stage (Lidiak and Anderson 2015 and references therein; Hu et al. 2022), as in other volcanic-arc systems worldwide (e.g., Whattam and Stern 2011).

Cuba, the largest island in the Caribbean, consists of Caribbean-plate-related volcanic arc and ophiolites sequences that have been part of the North American Plate since the late Eocene when the collision between the volcanic arc and the continental margins of North America terminated (Iturralde-Vinent et al. 2016 and references therein). Cuba is separated from other islands in the Caribbean by the North Caribbean Transform Fault System (including the Oriente Fault), which defines the present-day North American-Caribbean plate boundary south of Cuba (Figure 1a).

The Cuban segment of the Caribbean arc is well preserved and uplifted above sea level as a result of the soft collision of the leading edge of the Caribbean plate with the North American passive margin during the latest Cretaceous-Eocene times (Garcia-Casco et al. 2008; Iturralde-Vinent et al. 2008, 2016; van Hinsbergen et al. 2009). In central Cuba, the section of the Caribbean accretionary complex (Figures. 1a, b) is almost complete and contains from NE to SW: 1) the Bahamian borderland units related to the North American passive margin in the north, and 2) ophiolitic sequences containing

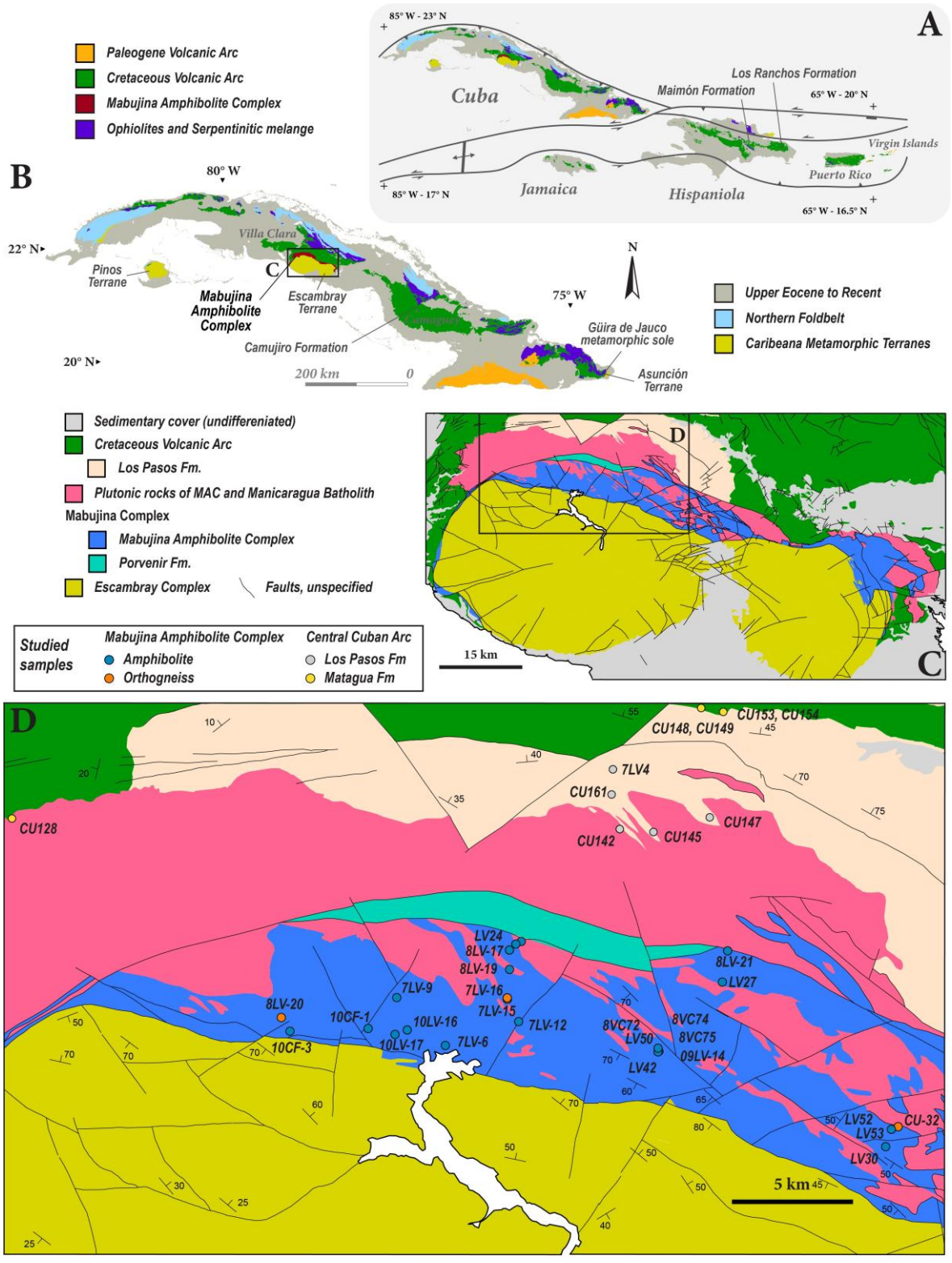

Figure 1. *(a) Simplified geological map of the Caribbean arc showing location of island arc tholeiitic units in Hispaniola (Los Ranchos and Maimón Formations). (b) Simplified geological map of Cuba. (c) Geological map of south-central Cuba after García-Delgado (1998). (d) Detailed map with sample locations. Geological maps a and B modified after Wilson et al. (2019) and Hu et al. (2022).*

high pressure mélanges (Ducloz and Vuagnat 1962; Kantchev et al. 1978; Somin and Millan 1981; Álvarez-Sánchez et al. 1991; Garcia-Casco et al. 2002, 2006; Álvarez-Sánchez and Bernal-Rodríguez 2015; Niu et al. 2022; Butjosa et al. 2023, 2023) emplaced above the passive margin units. Further to the SW, 3) a volcanic-sedimentary series records volcanic arc magmatism since pre-middle Hauterivian to Campanian times and, below the arc. These series contain layers of limestones and conglomerates that denote punctuated interruptions of volcanic arc activity, uplift, and erosion. Tectonically below the non-metamorphic volcanic are series, 4) the volcanic arc related Mabujina Complex, composed by the Porvenir Formation and the Mabujina Amphibolite Complex (MAC), appear deformed and metamorphosed to the greenschist and amphibolite facies, respectively (Somin and Millan Trujillo 1976; Kantchev et al. 1978; Somin and Millan 1981; Dublan and Alvarez 1986; Díaz de Villalvila 1997; García-Delgado 1998; Grafe et al. 2001; Díaz de Villalvilla et al. 2003; Blein et al. 2003; Stanek et al. 2006, 2019; Rojas-Agramonte et al. 2011, 2011; Torró et al. 2016, 2016, 2020). Finally, and tectonically emplaced below the Mabujina Amphibolite Complex, 5) the subduction-related Escambray Complex is made of a thrust pile of the intra-Proto-Caribbean Caribeana terrane metamorphosed to high-pressure conditions (Somin and Millan 1981; Dublan and Alvarez 1986; Millán 1997; Schneider et al. 2004; Garcia-Casco et al. 2006, 2008; Stanek et al. 2006, 2019; Cruz-Gámez et al. 2016; Despaigne-Díaz et al. 2016, 2017).

While most of the geological elements of this section of the Caribbean accretionary complex are well understood, the origin of the Mabujina Complex in the context of Caribbean geodynamics still remains elusive. While most authors have interpreted the Mabujina Complex as the metamorphosed root of the Cretaceous Volcanic Arc (Somin and Millan 1981; Dublan and Alvarez 1986; Bibikova et al. 1988; Somin 1993; Iturralde-Vinent 1994, 1998; Millan, 1996; Grafe et al. 2001; Stanek et al. 2006, 2019), other studies, however, have suggested that it represents an exotic volcanic arc section of the Pacific-derived Guerrero island arc terrane of central western Mexico accreted to the base of the Cuban Cretaceous arc (e.g. Blein et al. 2003; Rojas-Agramonte et al. 2011). On a global scale, Mabujina Complex constitutes an important example to understand accretionary tectonic processes and metamorphism in intra-oceanic volcanic arc settings. In the present study, the origin of the Mabujina Complex is discussed in light of an extensive dataset of whole-rock geochemical and Sr-Nd isotopic data of mafic and felsic rocks from the MAC. These data are compared to published data from the Guerrero terrain, the Early Cretaceous island arc rocks of central Cuba, and Cretaceous tholeiitic to calc-alkaline transitional arc sequences of central Cuba and the Dominican Republic.

2. Geological setting

2.1. The Mabujina Amphibolite Complex

The MAC forms a 5–10 km-wide strip in southern central Cuba (Figure 1a, b) that is in tectonic contact with the Porvenir Formation of the Mabujina Complex, which crops out as a narrow strip along the northern part of the MAC. The Porvenir Formation (Fm.) is dominated by basalts, pyroclastic rocks, quartzites, and gabbros metamorphosed in the greenschist facies (Dublan and Alvarez 1986; Díaz de Villalvilla 1994; Grafe et al. 2001). On the other hand, the MAC occurs tectonically above and surrounds the dome-shaped, high-pressure Escambray Complex, which comprises strongly deformed tectonic slices of extended passive continental margin meta-sediments, metavolcano-sedimentary rocks, and meta-ophiolite (Somin and Millan 1981; Millan and Somin 1985; Dublan and Alvarez 1986; Iturralde-Vinent 1994, 2021; Grafe et al. 2001; Schneider et al. 2004; Garcia-Casco et al. 2006; Stanek et al. 2006, 2019; Despaigne-Díaz et al. 2016, 2017).

The MAC is composed of volcanic to subvolcanic/ plutonic mafic protoliths that were deformed and metamorphosed to the amphibolite facies. As part of the complex, felsic granitic to gneissic rocks (metaplagiogranites and metagranitoids) emplaced during pre-, syn, and post-metamorphic conditions have also been described (Kantchev et al. 1978; Somin and Millan 1981; Millán 1997; Grafe et al. 2001; Blein et al. 2003; Rojas-Agramonte et al. 2011; Iturralde-Vinent et al. 2016). Late- to post-metamorphic granitoids (tonalite-granodiorite-granite) and pegmatites crosscut the main metamorphic fabric of the MAC (Millan and Somin 1985; Bibikova et al. 1988; Somin 1993; Sukar and Perez 1997). Field relationships are complex and locally obscured due to tropical weathering; however, several generations of granitoids variably foliated, boudinaged, and locally strongly folded with significant strain gradients can be observed. The intrusion of massive, unfoliated calc-alkaline plutonic rocks (granodiorites, tonalites that contain mafic microgranular enclaves with dioritic composition, and minor quartz-diorites) and pegmatites are mostly related to the emplacement of the mid-Cretaceous (81–89 Ma) Manicaragua Batholith (Figures. 1b, c (Somin and Millan 1981; Bibikova et al. 1988; Somin 1993; Sukar and Perez 1997; Blein et al. 2003); Rojas-Agramonte et al. (2011)). The southern and northern contacts of the batholith crosscut the MAC and the Cretaceous Volcanic Arc, respectively (Figure 1), and place an upper limit for the magmatic formation and metamorphism (hence accretion) of the MAC at 89 Ma. However, the age of the lower part of the Mabujina Complex is still under debate. Early studies considered a Precambrian age for the Mabujina protolith based on Pb-Pb method (Boyanov et al. 1975; Linares et al. 1985; Mossakovski et al. 1986). Somin and Millan (1981), Stanik (1981) and Dublan and Alvarez (1986) suggested a Cretaceous age

similar to the central Cuban arc based on limited K-Ar ages (see Iturralde-Vinent et al. 1996) and fossil pollen (see summary of Álvarez-Sánchez 2022. A recent study reported U-Pb zircon ages (Rojas-Agramonte et al. (2011) that yielded the oldest ages from granitoid rocks within the MAC dating back to ca. 133 Ma. This age suggests that the basaltic protoliths of the MAC formed since at least Valanginian time and that both the basaltic protoliths and granitoids shared a common geologic history up to the Turonian (ca. 90–93 Ma) when deformation and metamorphism took place.

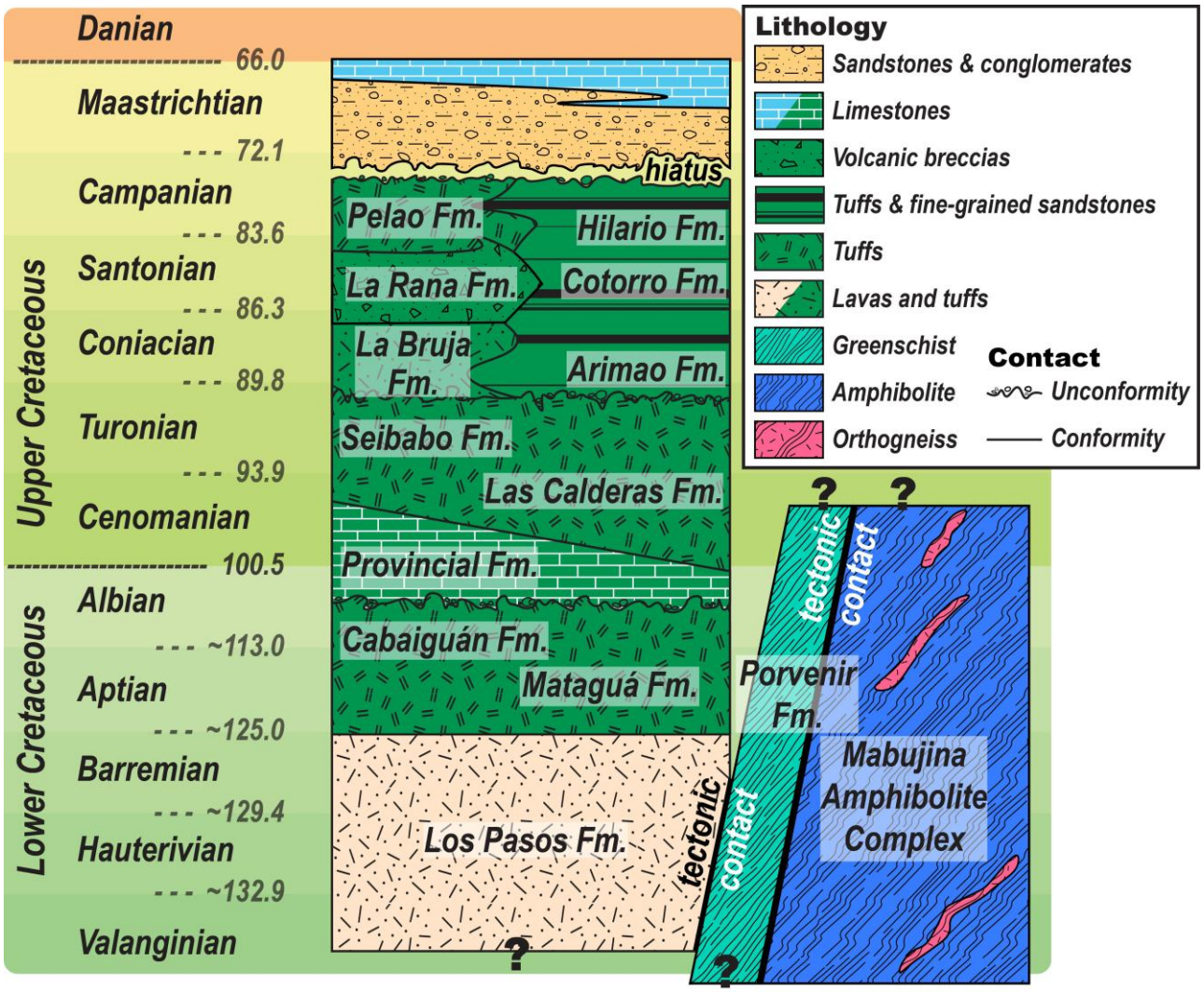

Figure 2. *Stratigraphic sequences of volcanic and sedimentary units of the central Cuban arc and the Mabujina Complex which include the Mabujina Amphibolite Complex and the Porvenir Formation (slightly modified after Iturralde-Vinent 2019). The plutonic rocks represent ages, not intrusive contacts.*

2.2. The cretaceous volcanic arc

Where not obliterated by the intrusion of the Manicaragua batholith, the contact between the Cretaceous Volcanic Arc and the Mabujina Complex is tectonic (Figures 1 and 2) (Kantchev et al. 1978; Somin and Millan 1981). Two stages of Cretaceous Volcanic Arc magmatism are identified in the southern part of central Cuba. The early stage is documented by an Early Cretaceous (Mid-Valanginian? to Barremian age) tholeiitic island arc suite (Los Pasos Fm.; Figure 2) while the second stage of volcanism started with the Aptian Lower Albian Mataguá and Cabaiguán Fms. that overlain the Los Pasos Fm. The Los Pasos Fm. (Figure 2) consists of predominantly felsic volcanics of plagiorhyolite and plagiodacite and basaltic sequences associated with volcanogenic massive sulphide deposits formed in a submarine environment. Díaz de Villalvilla et al. (2003) and Torró et al. (2016) suggested that the volcanic rocks of the Los Pasos Fm. correspond to a bimodal volcano-plutonic association including felsic intrusive and gabbroic bodies. It also contains intercalations of pyroclastic, epiclastic, and sedimentary rocks with manifestations of local subaerial magmatism. This formation correlates with the Early Cretaceous tholeiitic island arc Maimón and Los Ranchos Fms. in the Dominican Republic. The base of the Los Pasos Fm. is not exposed and its upper contact with the Mataguá and Cabaiguán Fms. is considered conformable (Díaz de Villalvilla et al. 2003). The Aptian-Albian Mataguá and Cabaiguán Fms. are distributed to the south of the city of Villa Clara (Figures 1 and 2) extending to the provinces of Cienfuegos to the west and Sancti Spiritus to the east (Hatten et al. 1958). The Mataguá Fm. formed in a shallow-water environment and consists of basalts, andesites, and tuff, with intercalations of sandstone (Díaz de Villalvilla et al. 2003). The Mataguá Fm. transitions laterally and upward to the Cabaiguán Fm., which most abundant lithology is tuff of predominant andesitic to dacitic compositions. Subvolcanic bodies of diabase are present as well as variably altered basalts. The Cabaiguán volcanics erupted in an underwater environment with the presence of radiolarians in the intercalated sedimentary rocks. According to their geochemical composition, the Mataguá and Cabaiguán Fms. are transitional between tholeiitic to calc-alkaline volcanism (Díaz de Villalvila 1997). A Late Albian angular unconformity separates the Mataguá and Cabaiguán Fms. from the overlying Provincial Fm. This unit is represented by basal conglomerates and limestones (Figure 2; Iturralde-Vinent 1994, 2021; Rojas-Consuegra et al. 1995; Iturralde-Vinent et al. 1996; Díaz de Villalvila 1997). The latest Albian to mid-Campanian section of the Cretaceous arc is represented by several calc-alkaline volcanosedimentary lithostratigraphic units described in Díaz de Villalvila (1997) and Iturralde-Vinent (1994, 1996, 2021) (see Figure 2).

To the east of central Cuba, in the Camagüey region (Figure 1b), the Pre-Camujiro sequence represents the oldest part of the arc. It consists of intercalations including deep marine volcanic and volcaniclastic rocks of tuffs, dacites, tuffites, sandstones with island arc tholeiitic (IAT) affinity, and conglomerate with carbonate beds containing Aptian-Albian fossils (Piñero Pérez et al. 1997). This early arc sequence is overlain by the late Albian-Turonian Camujiro Fm., which represents the mature stage of calc-alkaline magmatism and cryptic alkaline magmatism (Kerr et al. 1999; Torró et al. 2020). The Camujiro Formation consists of thick piles of pillow basalts and andesite flows, tuffs, and agglomerates (Iturralde-Vinent et al. 1996; Piñero Pérez et al. 1997; Iturralde-Vinent 2021).

3. Field relations

The amphibolites of the MAC show a variable degree of metamorphism and deformation (Figure 3a–c). Highly deformed amphibolites are well recrystallized and may display proto-mylonitic fabrics defined by amphibole and plagioclase (Grafe et al. 2001). Locally, metamorphic calcic clinopyroxene joins the main calcic amphibole plagioclase assemblage, indicating relatively high metamorphic peak conditions. Less deformed amphibolites with an apparent similar degree of metamorphism (calcic amphibole, plagioclase ± clinopyroxene) preserve, locally, the volcanic/subvolcanic texture and relict magmatic minerals of the protolith (clinopyroxene and plagioclase).

Metatonalitic-metatrondhjemitic rocks alternate with the amphibolites showing a dominant foliation parallel to the main foliation of the amphibolites (Figure 3b), thus indicating pre-metamorphic intrusion. Syn metamorphic felsic layers, dykes, and veins occur parallel and crosscutting the main metamorphic foliation of the amphibolites. They contain small amphibolitic enclaves rich in hornblende interpreted as melanosomic material (i.e., restitic) within trondhjemitic leucosome produced after local partial melting of amphibolite (Figure 3c). Locally, these leucocratic bodies are strongly deformed, showing a dynamic recrystallization process. According to their field occurrence related to the amphibolite, the granitoid rocks can be broadly visualized as a dominant group of concordant deformed granitoids and orthogneisses and a less abundant group of concordant to discordant felsic veins. In this study, the first group of deformed granitoids and orthogneisses are identified as the felsic protolith of MAC for geochemical comparisons.

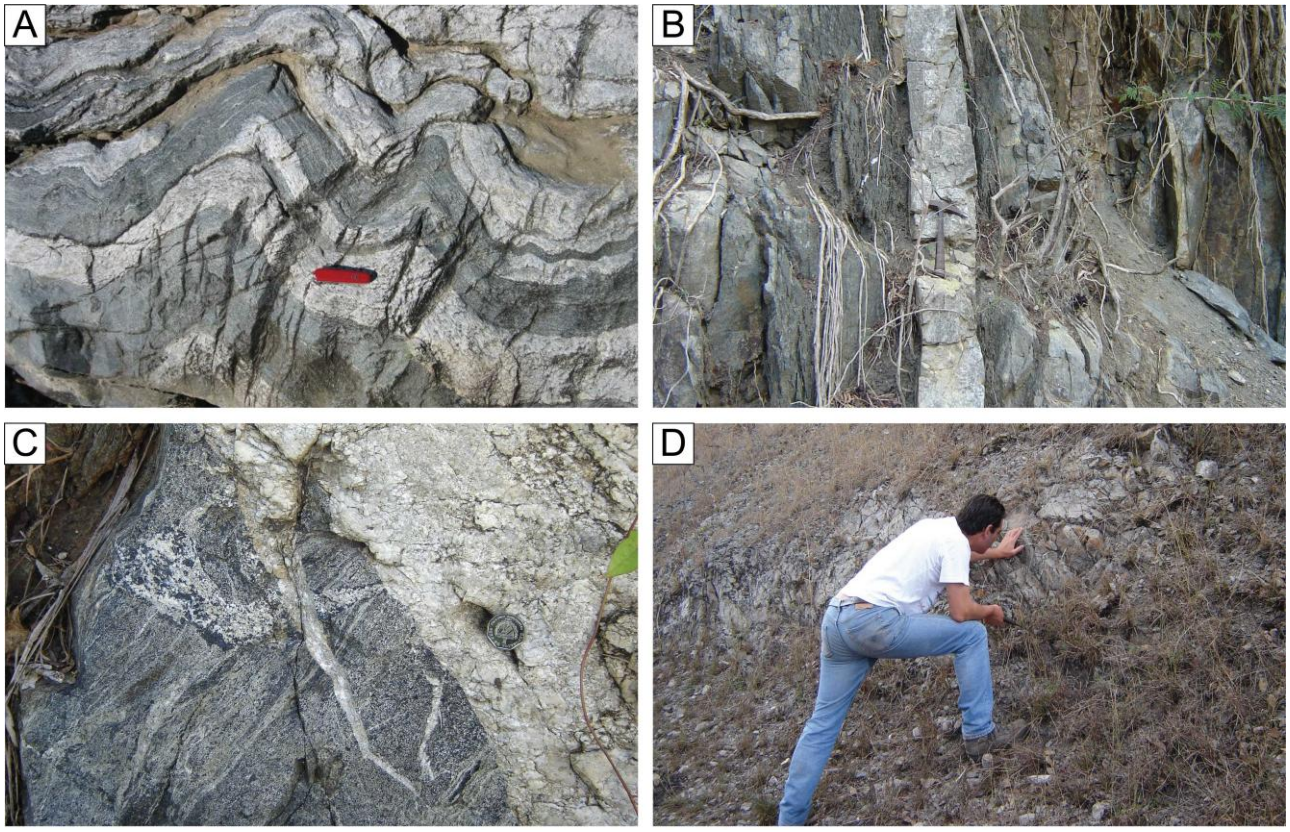

Figure 3. *Field photographs showing rock relationships within the Mabujina Amphibolite Complex (a-c) and Los Pasos formation (d). (a) Foliated and subsequently folded amphibolite and early tonalite-trondhjemite (Jicaya River, east of Guinia de Miranda). Ductile deformation resulted in parallel tectonic contacts between these units, (b) Orthogneiss layers parallel to the main foliation of the amphibolites, (c) Leucocratic segregates crosscuting the metamorphic foliation of the amphibolite possibly generated by hydrated partial melting. (d) Outcrops of massive plagiorhyolite from Los Pasos Formation.*

The volcanic arc sequences located structurally above the Mabujina Complex and south of the ophiolites are deformed in a broad syncline with an E-W axis. The southern flank (Los Pasos and Mataguá Fms.) forms a monocline dipping to the north, mostly slightly deformed, but locally with extensive folding and a low degree of alteration (Millán Trujillo 1973; Rojas-Agramonte et al. 2011, and references therein). The southern flank of the syncline is intruded by the Manicaragua batholith.

The Mataguá and Cabaiguán Fms. are distributed in the south of Villa Clara extending to the province of Cienfuegos and Sancti Spiritus (Hatten et al. 1958). Mataguá Fm. lateral and vertical upward transition to Cabaiguán Fm. Both formations are overlain by the Albian-Cenomanian limestone of the Provincial Fm., which most authors assign an Aptian-Albian age for their stratigraphic position

(Figure 2; Dublan and Alvarez 1986). The transition to limestones of the Provincial Fm. is mostly conformable, however, uniformities also appear between Mataguá Formation and Provincial Fms.

Cobble-sized samples were collected from different outcrops covering a great extension of the MAC and Cretaceous Volcanic Arc (Figure 1c). The geographical coordinate of the studied samples is included in Supp. Table S1.

4. Analytical methods

Samples selected for whole-rock geochemistry (Supp. Table S1) were powdered in a tungsten carbide mill. The analyses of powdered rock samples were carried out in the Centro de Instrumentación Científica of the University of Granada (CIC-UGR). Major elements and Zr compositions were determined on glass beads made of 0.6 g of powdered sample diluted in 6 g of $Li_2B_4O_7$ by a PHILIPS Magix Pro (PW-2440) X-ray fluorescence (XRF) equipment. Precision was better than ±1.5% for an analyte concentration of 10 wt.%. Precision for Zr was better than ±4% at 100 ppm concentration. Trace elements were analysed using the ICP-MS spectrometry after HNO3 + HF digestion of 0.1 g of sample powdered in a Teflon-lined vessel at 180°C and 200 p.s.i. for 30 minutes, evaporation to dryness, and dissolution in 100 ml of 4 vol.% HNO_3. Results for international standards PM-S and WS-E run as unknowns during analytical sessions. Concentrations of these standards are not significantly different from recommended values (Govindaraju et al. 1994). Precision was better than ±2% and ±5% for analyte concentrations of 50 and 5 ppm, respectively.

Samples for Sr and Nd isotope analysis (Supp. Table S2) were digested in the same way as for ICP-MS analysis, using ultra-clean reagents and analysed by thermal ionization mass spectrometry (TIMS) in a Finnigan Mat 262 spectrometer after chromatographic separation with ion exchange resins at CIC-UGR. Normalization values were $^{87}Sr/^{86}Sr = 0.1194$ and $^{146}Nd/^{144}Nd = 0.7219$. Blanks were 0.6 nanograms for Sr and 0.09 nanograms for Nd. The external precision (2σ), estimated by analysing 10 replicates of standard WS-E (Govindaraju et al. 1994), was better than 0.003% and 0.0015% for $^{87}Sr/^{86}Sr$ and $^{143}Nd/^{144}Nd$, respectively. The $^{87}Sr/^{86}Sr$ measured value in the laboratory for NBS 987 international standard was 0.710250 ± 0.0000044 for 89 cases. Measurements of La Jolla Nd international standard on this mass spectrometer yield a mean $^{143}Nd/^{144}Nd$ ratio of 0.511844 ± 0.0000065 for 49 cases.

5. Results

5.1.Petrography

5.1.1. Mabujina Amphibolite Complex

The amphibolites show nematoblastic texture and most of the samples have a near-peak metamorphic foliation (Figures 4a & 4d), although less deformed samples show faint or no foliation and still retain a subvolcanic texture (Figure 4b, c). Based on the mineral assemblages, the MAC metabasites classify as epidote-amphibolite and amphibolite, essentially composed of amphibole (~40– 80%) and plagioclase (~5–40%) in varying proportions and with, respectively, epidote and (locally) clinopyroxene as a stable peak phase. Minor biotite may be present, while titanite, apatite, magnetite, and lesser amount of ilmenite are accessory. Relicts of magmatic pyroxene in the least deformed samples are locally preserved variably replaced by amphibole ± metamorphic pyroxene (Figure 4a). Neoformed/recrystallized clinopyroxene exhibits polygonal textures indicating equilibrium with amphibole and plagioclase. The retrograde assemblages are characterized by actinolite-hornblende amphibole, epidote, albite, and chlorite, suggesting conditions at the epidote-amphibolite and greenschist facies.

Orthogneisses within the MAC are medium-grained phaneritic, generally inequigranular-sized granitoids variably deformed and metamorphosed (Figures. 4e–g). The mineral assemblage is composed of plagioclase, quartz, potassium feldspar, amphibole, biotite, and local garnet. Apatite and zircon are accessory minerals. In some samples, quartz shows strong undulose extinction denoting deformation while in other samples it is almost completely recrystallized, indicating recovery after intense deformation that may develop mylonitic fabric. Chlorite and epidote usually appear as retrograde minerals.

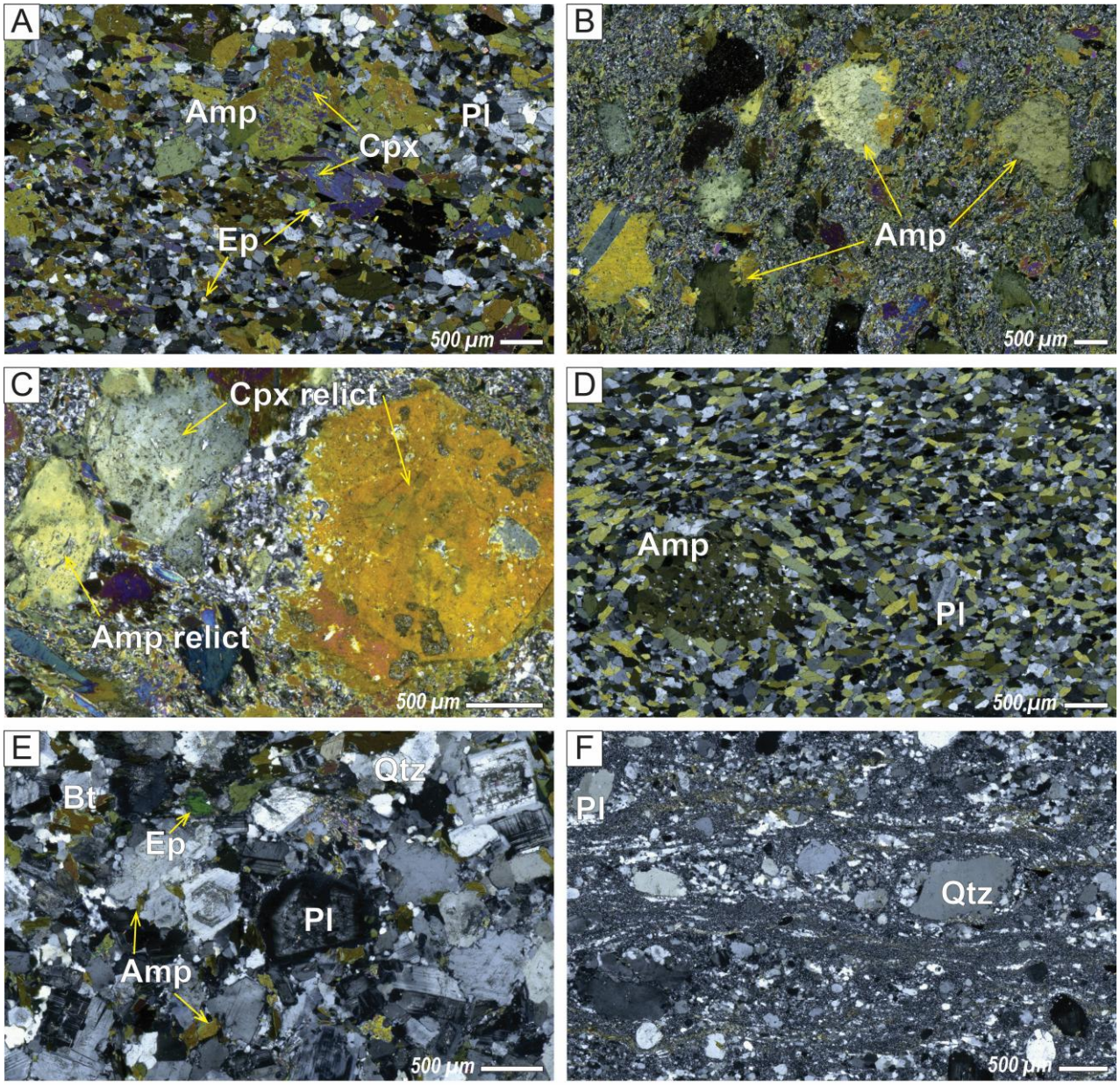

Figure 4a. *Photomicrographs of igneous and metamorphic rocks from the Mabujina Amphibolite Complex (a-g) and Los Pasos Formation (H-L) under cross-polarized light. (a) Sample LV50: foliated epidote-amphibolite shows relics of magmatic clinopyroxenes. (b) Sample 7LV9: non-foliated amphibolite with remaining porphyritic subvolcanic texture from basaltic protolith. (c) Sample 7LV9: metamorphic amphiboles replacing igneous phenocrysts of clinopyroxene and amphibole. (d) Sample LV52: foliated amphibolite consisting of amphibole and plagioclase. Note porphyroblastic amphibole with small plagioclase inclusion. (e) Sample 8LV20B: medium-grained undeformed tonalite from the MAC with oscillatory-zoned plagioclase crystals. (f) Sample LV43A: concordant felsic vein from the MAC shows mylonitic texture, ribbons of quartz and plagioclase with pressure shadows. White bar indicates 500 µm.*

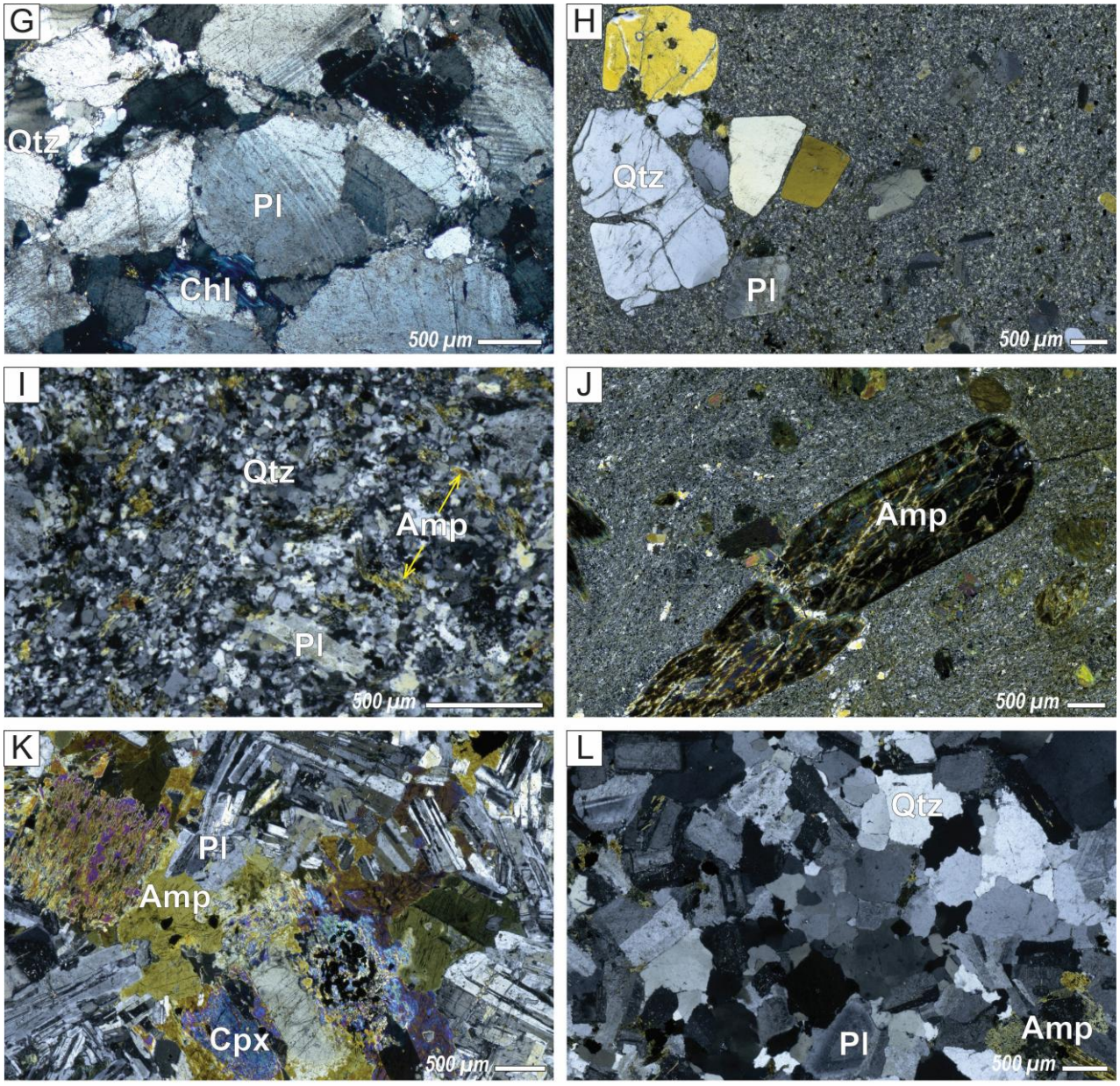

Figure 4b. continued *(g) Sample 8CF3: completely recrystallized quartz and deformed plagioclase with flame-shape twining in an orthogneiss from the MAC. (h) Sample CU158: fractured quartz phenocrysts in a porphyritic plagiorhyolite from Los Pasos Formation. (i) Sample CU213: finegrained plagiodacite shows allotriomorphic texture. (j) Sample CU214: porphyritic andesite with elongate one-centimetre-size amphibole phenocryst. (k) Sample CU142: gabbroic diorite from Los Pasos Formation shows clinopyroxenes partly replaced by late amphibole that filled in the space between plagioclases. (l) Sample CU160: medium-grained tonalite from Los Pasos Formation. Abbreviations: Amp: amphibole; Bt: biotite; Chl: chlorite; Cpx: clinopyroxene; Ep: epidote; Ms: muscovite; Pl: plagioclase; Qtz: quartz. White bar indicates 500 µm.*

5.1.2. Los Pasos formation

The Los Pasos Fm. is composed of abundant plagiorhyolite and less abundant plagiodacite, basaltic andesite, and gabbro-diorite (see below for geochemical classification of these rocks; Figs. 4h–l). In general, plagiorhyolites show holocrystalline porphyritic textures consisting of quartz and plagioclase phenocrysts with local ilmenite inclusions. The groundmass is largely composed of anhedral fine-grained quartz and plagioclase (Figure 4h). The plagiodacites show fine grained seriate panidiomorphic textures (Figure 4i) defined by elongated amphibole and plagioclase laths surrounded by anhedral quartz, and plagioclase, and minor amounts of ilmenite. Plagioclase grains are commonly sericitized. Andesite shows a porphyritic texture (Figure 4j) with phenocrysts dominated by elongated amphibole grains commonly rimmed by overprinting actinolite, and less abundant plagioclase phenocrysts with amphibole inclusions. Phenocrysts are surrounded by quartz aggregates and the groundmass is made up of fine-grained amphibole laths and anhedral plagioclase and ilmenite. Gabbro-diorite is characterized by an inequigranular hypidiomorphic texture (Figure 4k) and consists of plagioclase, clinopyroxene, and amphibole with minor amounts of ilmenite. Clinopyroxene grains are usually rimmed and partly replaced by amphibole. Amphiboles are anhedral and fill the interstitial space between elongated plagioclase laths. The tonalites that intruded into the Los Pasos Fm. show medium-grained hypidiomorphic textures (Figure 4l) and comprise plagioclase, quartz, and a minor amount of amphibole and ilmenite. Chlorite and epidote are present as secondary minerals in post-igneous alteration in all types of rock.

5.2.Whole-rock major and trace element geochemistry

5.2.1. Metamorphism and alteration

The studied rocks yield variable loss on ignition (LOI) values ranging between 0.2 and 5.2 wt.% (Supp. Table S1), pointing to hydration during and after metamorphism. The effects of this process on the geochemical composition of the studied samples are evaluated in binary diagrams with mobile trace elements vs. LOI values (Supp. Fig. S1A). Most of the samples from the Los Pasos Fm. have undergone extensive sea-floor metamorphic imprint as well as hydrothermal alteration (Supp. Fig. S1B) which have been linked to the formation of volcanogenic massive sulphide ore deposits (VMS; e.g., Torró et al. 2016). This is probably reflected in the positive correlation of LOI with the Rb of samples. Samples from the MAC yield poor positive correlations. In general, many major (e.g., Si, Na, K, Ca) and trace (e.g., Cs, Rb, Ba, Sr) elements are easily mobilized by late and/or post-magmatic fluids, thus their current concentrations may not be indicative of their original contents. In the

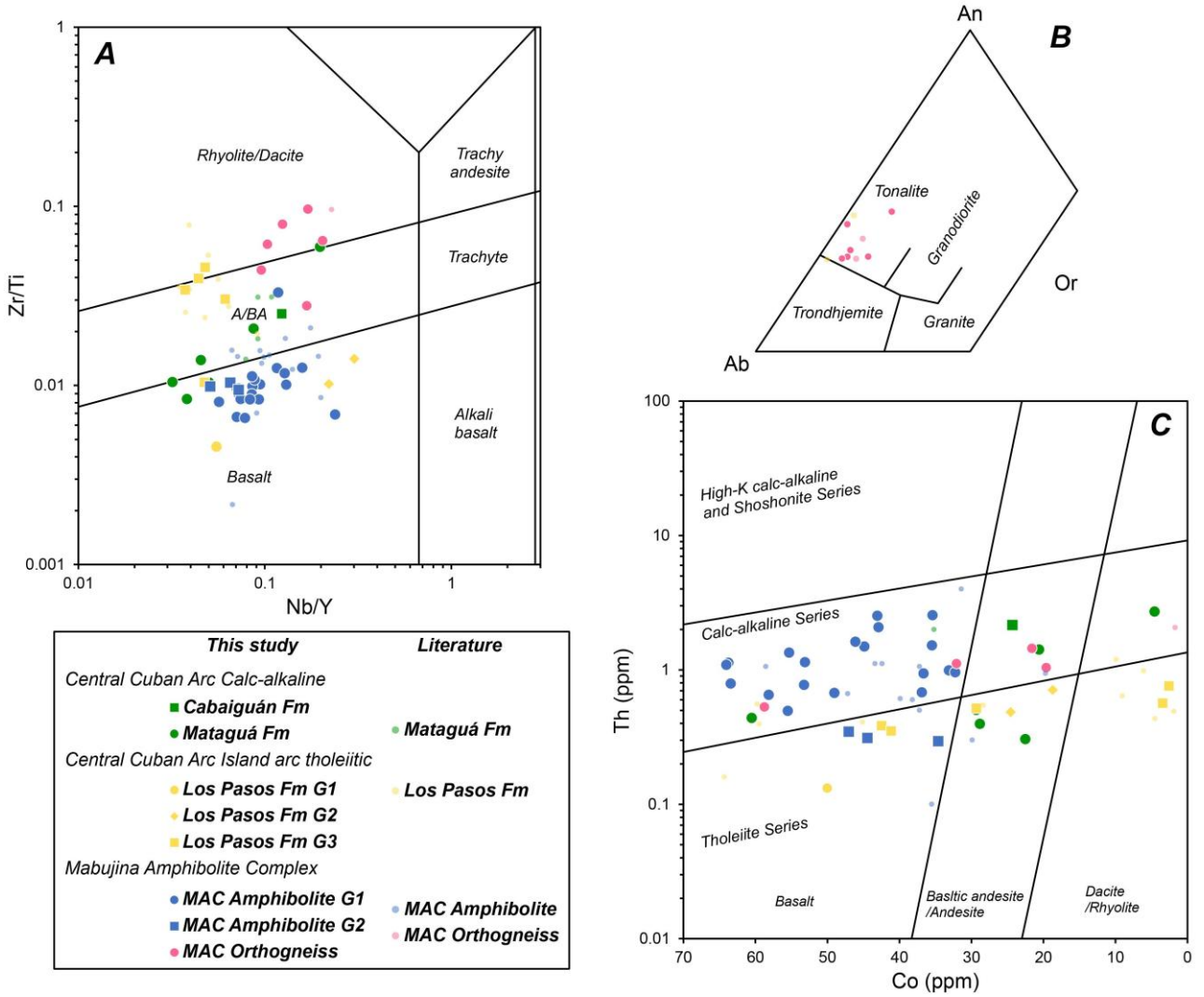

Figure 5. *Geochemical classification of studied mafic and felsic rocks from the MAC and Los Pasos, Mataguá and Cabaiguán formations. (a) Zr/Ti vs. Nb/Y (Pearce 1996 after Winchester and Floyd 1977). (b) CIPW normative mineral classification of orthogneiss from the MAC using Ab (albite), an (anorthite), and or (orthoclase) proportions (O`connor 1965). (c) Th/Co (Hastie et al. 2007) classification diagram. Additional geochemical data taken from the literature are from Blein et al. (2003); Rojas-Agramonte et al. (2016); Stanek et al. (2019) for the MAC amphibolite and orthogneiss, from Kerr et al. (1999) for basalts of the Mataguá Formation, and from Torró et al. (2016) and Rojas-Agramonte et al. (2016) for Los Pasos Formation.*

alteration diagram shown in Supp. Fig. S1C, most of the felsic rocks from the Los Pasos Fm. and MAC show alteration index values that may be related to albitization far from the mineralized centers. This diagram, however, does not take into account that some of the original rocks are rich in Na. On the other hand, the mafic rocks from these units show trends towards carbonation, even if carbonates

are not present in the analysed samples. Supp. Fig. S1B shows that most samples are not significantly altered in terms of major elements. However, due to the likely mobility of major and some trace elements, those considered immobile in post-magmatic conditions (e.g., high field strength elements, HFSE, Y, Zr, Hf, Ti, Nb; rare earth elements, REE, transition elements V, Cr, Ni, Sc; and Th; Pearce 2014) will be used for igneous rock classification and tectonic discrimination. All studied samples classify as subalkaline basalt, basaltic andesite/andesite, and rhyolite/dacite using the Zr/Ti vs. Nb/Y classification diagram (Figure 5a).

5.2.2. Los Pasos formation

Rocks of basaltic composition

The three analysed samples from the Los Pasos Fm. classified as basaltic in composition and can be separated into two groups based on their chondrite normalized (CN) REE patterns. Group 1 comprises only one sample (petrographically classified as gabbro, Figure 4k, geochemically classified as of basaltic composition, Figure 5a), characterized by relatively low TiO2 contents of 0.61 wt.%. The sample shows a slightly negative CN-REE pattern (La/Yb_{CN} = 1.79; La/Sm_{CN} = 1.21; Sm/Yb_{CN} = 1.48; Figure 6a) and a slight enrichment in Eu (Eu/Eu* = 1.22). It largely falls in the same range as the low-Ti tholeiites (LOTI) from the Los Pasos Fm. which present nearly flat patterns (La/Yb_{CN} = 0.83–1.00; La/Sm_{CN} = 0.79–1.00; Sm/Yb_{CN} = 0.94–1.17). They show relatively lower total REE contents compared to the normal island arc tholeiites (IAT; Díaz de Villalvilla et al. 2003; Rojas-Agramonte et al. 2016; Torró et al. 2016). The NMORB-normalized (NMN) extended trace elementsz pattern of the Group 1 sample reveals negative Nb and Zr anomalies, as in Los Pasos LOTI basalts. In contrast, it lacks any Ti anomaly and presents a weak enrichment in Th content (Figure 6b).

Even though Group 2 basalts show high silica contents of 62.47 and 62.54 wt.% (3.37 and 3.27 wt.% LOI respectively), they fall into the basalt field in Figure 5a, perhaps as a result of silicification. They are characterized by high MgO contents (5.01 and 7.43 wt.%) and high Mg# (73 and 75). In the CN-REE diagram, they show steep negative slopes (La/Yb_{CN} = 6.16, 9.22; La/Sm_{CN} = 2.09; Sm/Yb_{CN} = 2.94, 4.42, respectively; Figure 6c). These rocks show a systematic enrichment in Th and negative Nb, Zr, and Ti anomalies on the NMN extended trace element diagram (Figure 6d).

Plagiorhyolite/Dacite and andesite

Rocks of plagiorhyolitic/dacitic (4 samples) and andesite (1 sample) composition from the Los Pasos Fm. are classified as Group 3 in Figure 6. The least altered samples (LOI < 3 wt.%) have high alkali contents and high Na/K ratios (Na2O = 4.08–7.21 wt%; K2O = 0.06–0.90 wt%). Plagiorhyolitic/dacitic samples show marked negative Nb and Eu anomalies and positive Th anomalies in the NMN-extended trace elements diagrams, and some samples show negative Zr anomalies (Figure 6e, f). In addition, their CN-REE values show typical near-flat tholeiitic patterns (La/Yb_{CN} = 1.00–1.16; La/Sm_{CN} = 0.76–1.03; Sm/Yb_{CN} = 1.03–1.34) similar to previous studies (Kerr et al. 1999; Díaz de Villalvilla et al. 2003; Blein et al. 2003; Torró et al. 2016; Rojas-Agramonte et al. 2016), however with much depleted total REE contents. The andesite sample has a weakly negative slope on the CN-REE diagram (Figure 6e), while on the NMN-extended trace elements diagram (Figure 6f), it shows the typical positive Th anomaly and negative Nb, Zr, and Ti anomalies that are widely observed in other samples from the Los Pasos Fm.

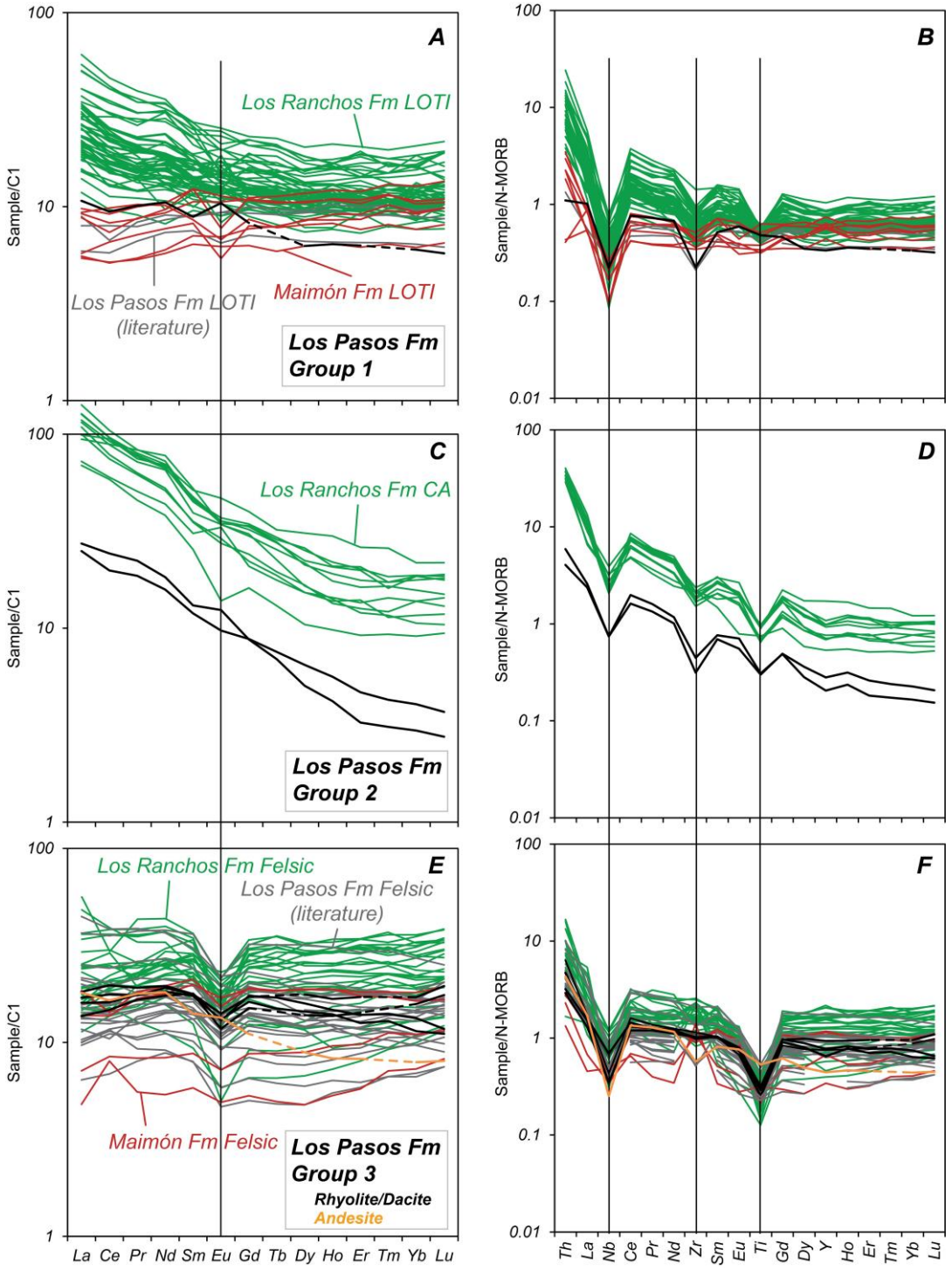

Figure 6. *Chondrite-normalized REE (a, c, e, g) and NMORB-normalized extended trace elements patterns (b, d, f, h) for studied samples from Los Pasos Formation. Chondrite (C1) values and N-MORB values from Sun and McDonough (1989). Geochemical data from Escuder-Viruete et al. (2006) and Torró et al. (2017) for Los Ranchos Formation; Torró et al. (2017) for Maimón Formation and Díaz de Villalvilla et al. (2003); Torró et al. (2016); Rojas-Agramonte et al. (2016) for Los Pasos Formation.*

5.2.3. Mataguá and Cabaiguán formations

Basalts and basaltic andesites

The 4 samples from Mataguá Fm. are classified as calc-alkaline basalts and basaltic andesites (Figures 5a & 5C). They are characterized by slight negative CN-REE patterns (La/Yb_{CN} = 1.64–2.62; La/Sm_{CN} = 1.15–1.46; Sm/Yb_{CN} = 1.43–1.80; Fig, 7A). In contrast, one basaltic sample from the Cabaiguán Fm. shows higher total REE concentration and a more fractionated REE pattern. A moderate negative Eu anomaly is observed in the Cabaiguán Fm. which is absent in basalts and basaltic andesites from the Mataguá Fm. In the NMN-extended trace elements diagram (Figure 7b), rocks from the Mataguá Fm. present typical subduction-related signatures with positive Th, and negative Nb, Zr, and Ti anomalies. The sample from the Cabaiguán Fm. presents higher total REE concentration and Th enrichment compared to rocks from the Mataguá Fm., accompanied by a slightly higher contribution of the subduction component (Th/Nb_{NMN} = 15.7 compared to 9.57–16.05 with an average of 13.08 in the Mataguá Fm.; Figure 7b) and weak negative Zr anomaly. The sample from the Cabaiguán Fm. encompasses the calc-alkaline composition of basalts from the Camujiro Fm (Camagüey region of central Cuba; Torró et al. 2020) and differs from the Mataguá Fm. rocks.

Rhyodacite and andesite

Two samples from the Mataguá Fm. are classified as rhyodacite and andesite (Figure 5a). Both samples show more fractionated CN-REE patterns than their mafic counterparts (La/Yb_{CN} = 5.41, 3.79; La/Sm_{CN} = 3.14, 2.28; Sm/Yb_{CN} = 1.72–1.66, respectively, Figure 7c). They also show stronger Th (Th/La_{NMN} = 3.02, 2.91) enrichment but a similar extent of the subduction component compared to the basalts and basaltic andesites. The andesite sample shows Nb, Zr, and Ti anomalies on the NMN-extended trace elements diagram, while the rhyodacite sample generally encompasses the composition of the andesite sample but lacks a Zr anomaly (Figure 7d).

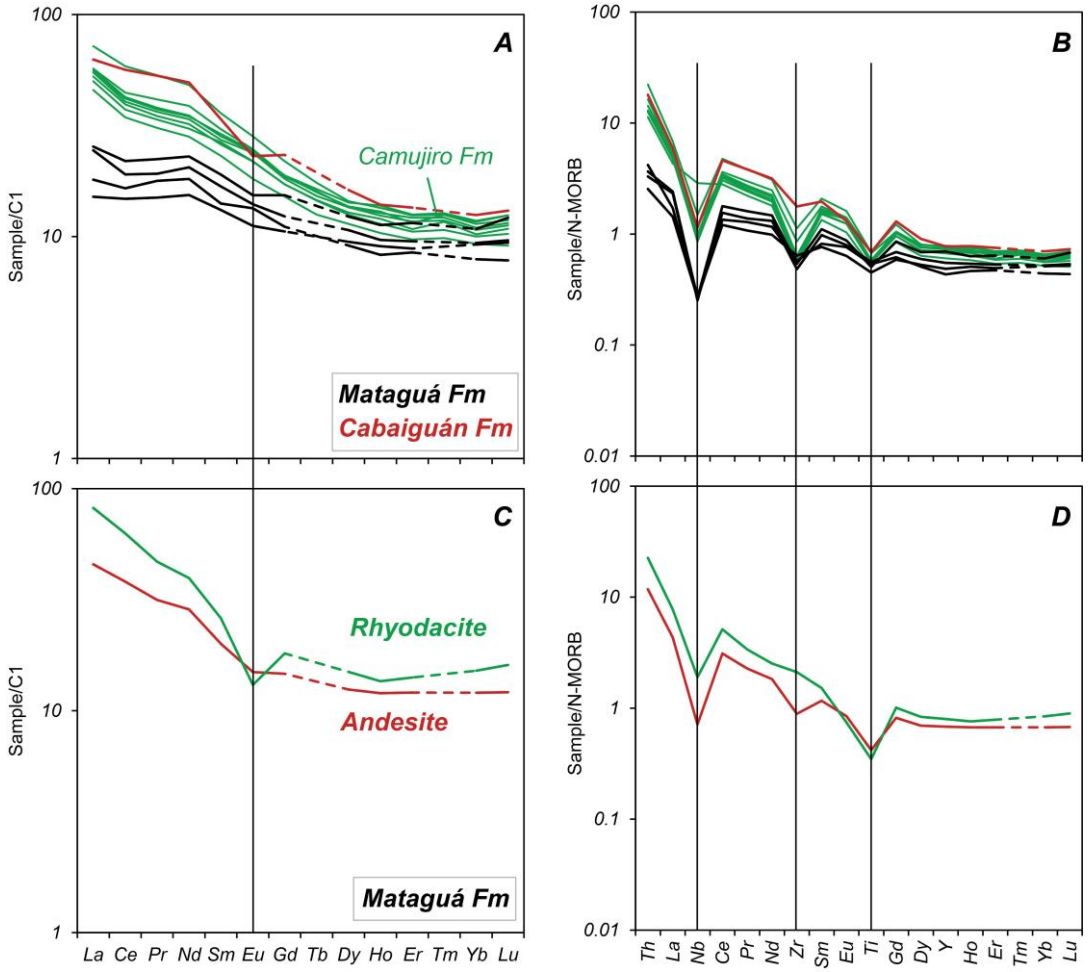

Figure 7. *Chondrite-normalized REE (a, c) and NMORB-normalized extended trace elements (b, d) patterns of the samples from the Mataguá and Cabaiguán Formations. Chondrite (C1) values and N-MORB values from Sun and McDonough (1989). Geochemical data of the Camujiro Formation are from Torró et al. (2020).*

5.2.4. Mabujina Amphibolite complex

Amphibolites

The amphibolites have basaltic and basaltic-andesite compositions (Figures 5a & 5c). These samples can be geochemically grouped into two main groups based on their normalized REE patterns:

Group 1 amphibolites (23 samples) comprise the majority of the basaltic samples of the MAC, which is characterized by fractionated CN-REE patterns (La/Yb_{CN} = 2.16–7.40; La/Sm_{CN} = 1.25–2.73; Sm/Yb_{CN} = 1.65–2.73; Figure 8a). NMN-extended trace elements patterns largely encompass the composition of the central Cuban Cretaceous Volcanic Arc rocks (Figure 8b, Mataguá, Cabaiguán,

and Camujiro Fms.) with calc-alkaline affinity (Figure 5c). Marked Nb, Zr, and Ti anomalies are observed together with a strong subduction component (average Th/Nb_{NMN} of 14.0; Figure 8b).

Group 2 amphibolites comprise three samples with basaltic composition. In the CN-REE diagram, this group shows a slight negative slope with low to moderate LREE depletion relative to MREE (La/Sm_{CN} = 0.54–0.89; Figure 8c). In contrast to Group 1 amphibolites, this group contains a lower total REE concentration (average total REE of 43.5 ppm compared to 59.5 ppm). The samples fall into the tholeiitic field in the Th-Co classification diagram (Figure 5b) due to lower Th contents. The NMN-extended trace elements pattern of this group of samples has similar Nb, Zr, and Ti anomalies as in Group 1, but they show lower subduction component (Th/Nb_{NMN} = 4.32–5.47; Figure 8d). On both normalized diagrams, Group 2 displays similar patterns to IAT rocks from the Los Pasos Fm (Figure 8C; Díaz de Villalvilla et al. 2003; Torró et al. 2016).

Orthogneisses

Orthogneisses (six samples) in the MAC are classified as tonalites using the CIPW normative minerals on the Ab-An-Or diagram of O`connor (1965) (Figure 5b). The SiO2 content varies between 60.6 to 70.3 wt.%. The tonalites in the MAC generally follow a calc-alkaline trend (Figure 5c) with CN-REE patterns similar to those of Group 1 MAC amphibolites (La/Yb_{CN} = 2.52–7.51; La/Sm_{CN} = 1.26–2.96; Sm/Yb_{CN} = 1.73–2.93; Figure 8e). On the NMN-extended trace elements diagram, strong negative Nb and Ti anomalies are observed together with variable degrees of the subduction component (Th/Nb_{NMN} = 2.99–15.00, average of 8.63). Tonalite shows variable Zr anomalies, with two samples showing moderate to strong negative Zr anomalies with Zr/Zr* of 0.40 and 0.74 respectively and one sample shows strong positive Zr anomaly with Zr/ Zr* of 3.25 (Figure 8f). This reflects significant zircon fractionation.

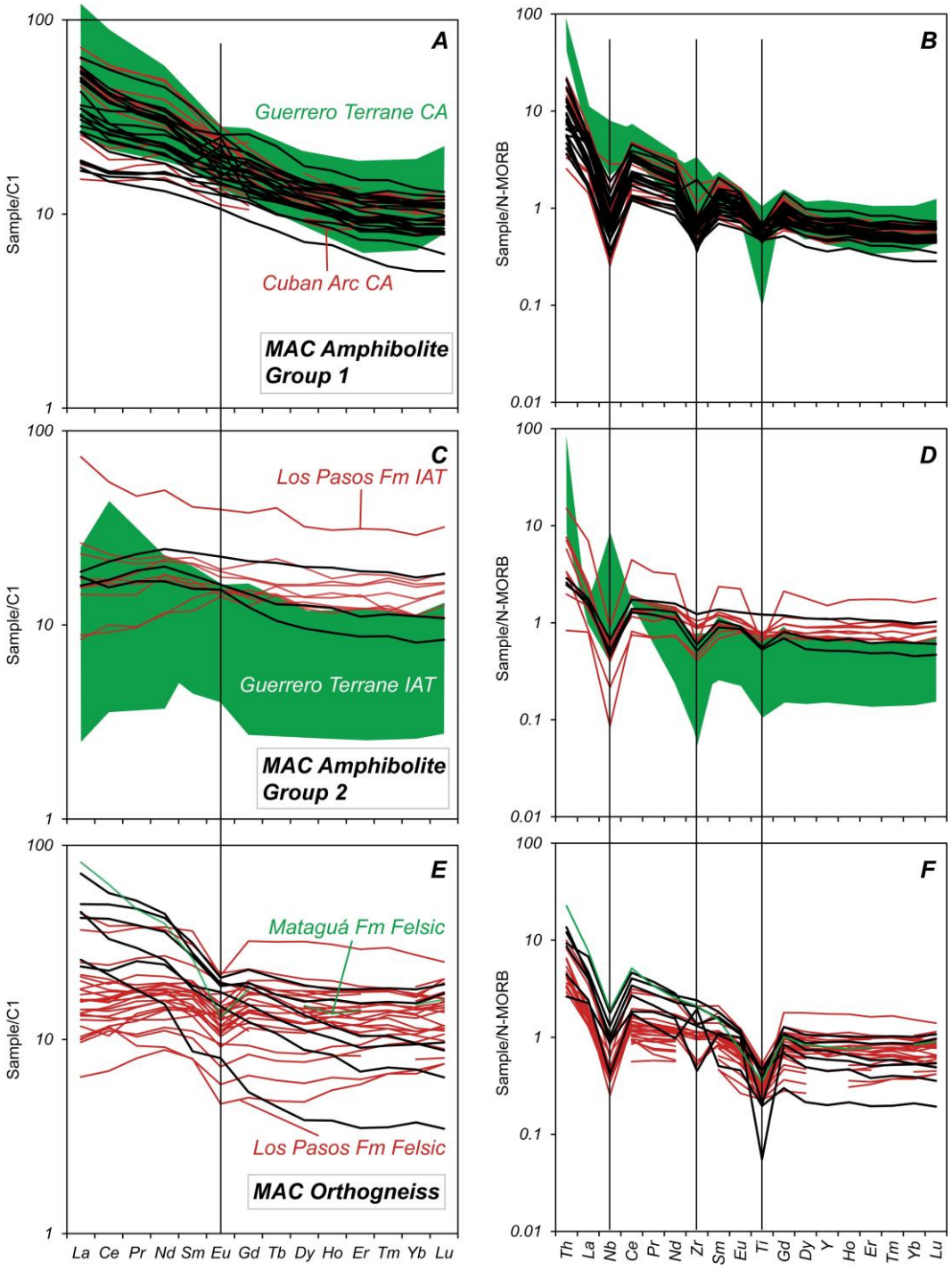

Figure 8. *Chondrite-normalized REE (a, c, e) and NMORB-normalized extended trace elements patterns (b, d, f) of the samples from the MAC. Chondrite (C1) values and NMORB values from Sun and McDonough (1989). Cuban arc calc-alkaline rocks refer to the Mataguá, Cabaiguán, and Camujiro Formations, geochemical data are from this study and Torró et al. (2020). Geochemical data of the Guerrero Terrane are from Mendoza and Suastegui (2000). Geochemical data of the Los Pasos Formation are from this study.*

5.3. Sr-Nd isotopic geochemistry

The initial Sr and Nd isotopic composition for 11 samples were calculated based on the assumption that the tholeiitic rocks developed prior to the calc-alkaline rocks in the MAC (Figure 9). The tholeiitic amphibolite sample was corrected to 135 Ma based on the age constraint of the oldest felsic intrusion within the MAC (oldest dated tonalitic gneiss intruded in basalt; Rojas-Agramonte et al. 2011). Group 1 amphibolites and orthogneisses from the MAC with calc-alkaline affinity were corrected to a younger age of 100 Ma since they are considered to have formed during later magmatism. The youngest protolith age of amphibolite with calc-alkaline affinity by Rojas-Agramonte et al. (2011) was dated as Late Cretaceous (ca. 93 Ma). The initial Sr ratios of the MAC amphibolites and orthogneiss show similar values, in the range of 0.70325 to 0.70406 and 0.70329 to 0.70396, respectively, and plot mostly within the field of the early intra-oceanic Caribbean arc (Rojas-Agramonte et al. 2016). Most of the samples from the MAC have initial Nd ratio between 0.51282 and 0.51299, except for one sample of orthogneiss that shows a lower value (0.51272), plot within the range of the IAT (Los Pasos Fm. from Cuba; Los Ranchos and Maimón Fms. from Hispaniola) and calc-alkaline (Camujiro Fm. from Cuba) lavas of the Caribbean arc (Figure 9). Furthermore, the variation in initial Nd ratios reflects that the protoliths of Group 1 MAC amphibolites and orthogneisses bear minor incorporation of subducted continental material, which is not appreciated in Group 2 MAC amphibolites.

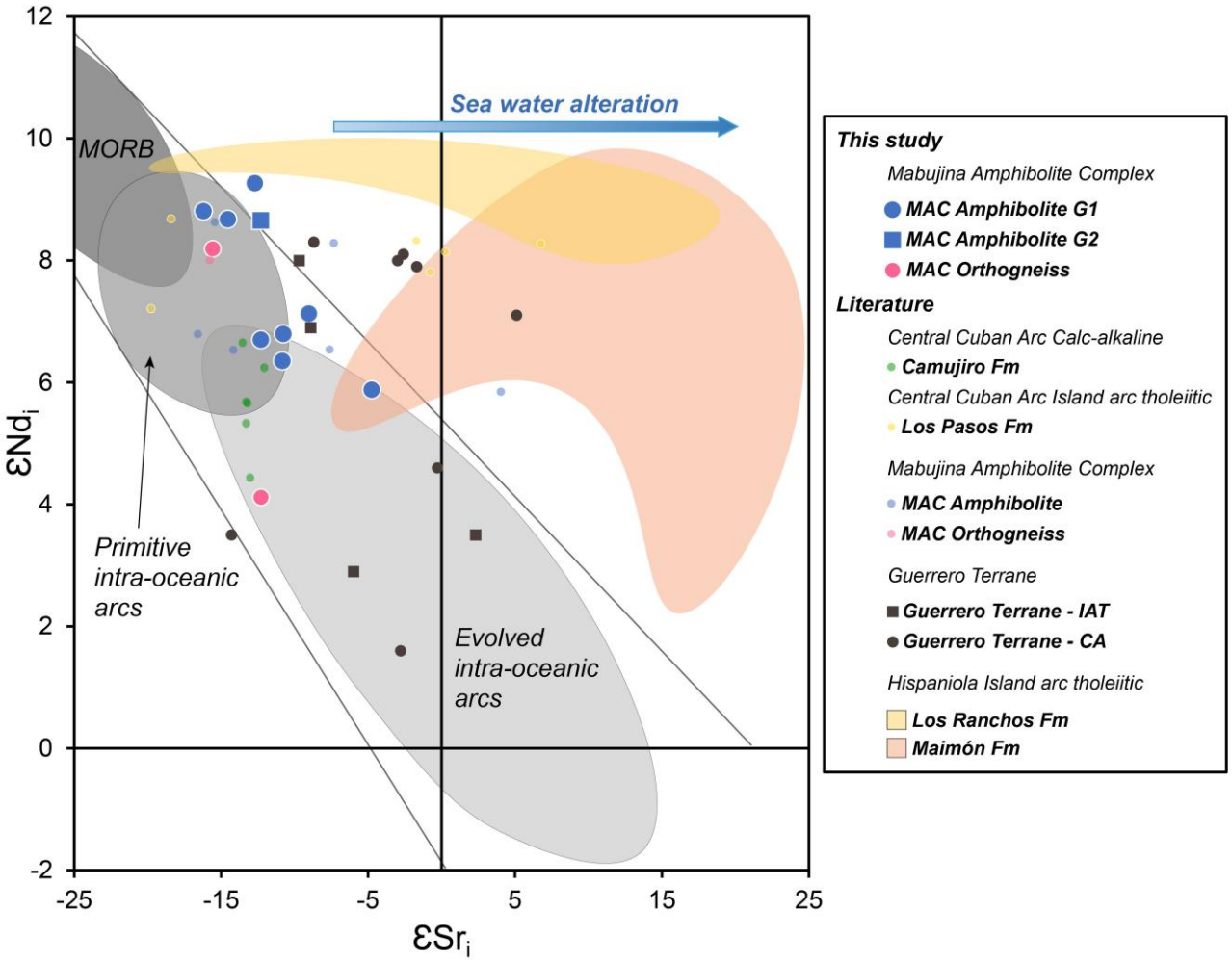

Figure 9. *Age-corrected Sr-Nd radiogenic isotope ratios of whole-rocks from amphibolite and orthogneisses of the MAC. Other geochemical data of the Los Pasos Formation and MAC amphibolite and orthogneiss are from Blein et al. (2003), Rojas-Agramonte et al. (2016) and Torró et al. (2016). Data of the Camujiro Formation are from Torró et al. (2020). Data of the Guerrero Terrane are from Mendoza and Suastegui (2000). ata of Los Ranchos and Maimón formations are from Escuder-Viruete et al. (2006) and Torró et al (2017, 2017). Fields of MORB, primitive and evolved intra-oceanic arcs are from Rojas-Agramonte et al. (2016).*

6. Discussion

6.1. Protolith of the Mabujina Amphibolite complex

In the 'subduction-initiation rule', Whattam and Stern (2011) proposed a model of diagnostic chemostratigraphic trends for subduction-initiation magmatism. These geochemical changes reflect

the shift from subduction-initiation to true-subduction regimes during the early evolution of island-arc systems. According to the model, during the initial stage, the spreading of the oceanic lithosphere above the nascent descending slab and the melting of the incipient mantle wedge produce NMORB-like forearc basalts (FAB; Reagan 2010). Fluids released from hydrated downgoing slab enable flux melting of extremely depleted mantle wedge to generate LOTI, IAT, and boninites. Finally, calc-alkaline basalts and basaltic andesites mark the establishment of a steady-state subduction regime (Ishizuka et al. 2014). This sequence is also reflected by progressive depletion in HFSE and the enrichment in Th and LILE.

The magmatic history and stratigraphy of the MAC are obscured because of the complexity of its internal structure due to the tectonic-metamorphic history of the complex (Somin and Millan 1981). Nevertheless, most mafic protoliths of amphibolites (Group 1 amphibolites) in the MAC record similar REE concentrations and CN-patterns as calc-alkaline igneous rocks described in the Late Cretaceous series of the Caribbean arc (Lidiak and Anderson 2015). The highly enriched LREE to HREE ratios (La/Yb_{CN} = 2.16–7.40, average 4.17; Figs. 8a, b) and Th of these rocks indicate their calc-alkaline affinity in contrast to the tholeiitic affinity presented by Group 2 amphibolites of the MAC which lack moderate to strong LREE-enrichment (La/Yb_{CN} = 1.07–2.19, average 1.53; Figs. 8c, d).

Felsic to intermediate magmatism in oceanic arcs and ophiolites may form through different processes (Rollinson 2009; Furnes and Dilek 2017; Marien et al. 2019). One of them includes the melting of a variety of mafic precursors like basaltic underplates, upwelling tectonic mélanges, and oceanic crust (Beard and Lofgren 1991; Atherton and Petford 1993; Koepke et al. 2007; Castro et al. 2010). Tonalitic orthogneisses of the MAC present moderate to strong LREE enrichment typical of calc-alkaline affinity and similar high initial Nd isotopic ratios to those of the amphibolite. This evidence supports that these felsic protoliths could have formed after the melting of a basaltic precursor similar to the mafic protolith of the MAC. This basaltic precursor does not crop out, however, for only limited hydrous partial melting of amphibolite (not granulite) occurs in the MAC. The felsic protoliths were likely produced as volcanic or subvolcanic rocks interbedded or intruded into the mafic protolith of the MAC in a developing oceanic arc setting without an overthicken crust. Studied samples lack a typical ‘adakitic’ signature that indicates high-pressure partial melts of the hydrated basaltic rocks in arc settings (Kay et al. 1990; Defant and Drummond 1990). However, a lower initial Nd isotopic ratio than the mafic counterpart was observed in one orthogneiss, which could be explained by further modification of the melt during crystallization and mixing in the lower

arc crust (Annen et al. 2006, 2015), for example, by simultaneous assimilation and fractional crystallization (AFC; DePaolo 1981) or mantle melting, assimilation of crustal rocks, storage, and homogenization (MASH; Hildreth and Moorbath 1988).

The age of the protolith is constrained by the zircons extracted from the orthogneisses that intruded into the mafic protolith of MAC. Therefore, the oldest mafic rocks of the MAC are older than 132.9 ± 1.4 Ma, while the youngest zircon age from an amphibolite sample provided an early Turonian age of ca. 93 Ma (Rojas-Agramonte et al. 2011; Niu et al. 2022). Thus, the protolith of MAC likely represents an arc sequence that was active during several tens of million years spanning from Early (Valanginian) to early Late Cretaceous (Early Turonian).

6.2. Provenance of the MAC and comparison to other island arc-terranes

The model suggesting that the MAC represents the metamorphosed root of the Cretaceous Volcanic Arc is based on the increasing metamorphic grade towards structurally lower units from the unmetamorphosed volcanic arc rocks of the Los Pasos Fm. through the greenschist facies Porvenir Fm. of the Mabujina Complex to the amphibolite facies of the MAC amphibolites and gneisses. Other studies, however, pointed to an exotic origin of allegedly Pacific provenance (i.e., the Guerrero Island arc terrane of central western Mexico), which would have been accreted to the base of the Cuban Cretaceous arc (Blein et al. 2003; Rojas-Agramonte et al. 2011). This argument is largely based on the assumption of an Early Cretaceous age of the protoliths of the MAC and the major geochemical differences between the MAC (tholeiitic to calc-alkaline) and Los Pasos Fm. and other early products of the Caribbean arc (tholeiitic). Due to the fact that the protoliths from the MAC exhibit tholeiitic to calc-alkaline affinity, below we compare the potentially correlated units (i.e., previously proposed central Cuban arc and Guerrero Terrane) with the MAC in light of the geochemical dataset of the Early Cretaceous tholeiitic island arc units and transitional to calc-alkaline arc rocks of the Caribbean arc (Hu et al. 2022), together with a consideration of geochronological constraints for the potential correlations.

In the Cretaceous Volcanic Arc of central Cuba, the Los Pasos Fm. is the earliest sequence of the volcanic suite of the Caribbean (Primitive island arc; Lidiak and Anderson 2015). The LOTI basalts from the Los Pasos Fm. largely resemble the composition of LOTI in the Maimón Fm. but show a more depleted nature than the LOTI from Los Ranchos Fm (Torró et al. 2016, 2017). The REE patterns of felsic rocks from Los Pasos Fm. are also similar to the felsic rocks from Los Ranchos and Maimón Fms. (Figures. 6e, f). Group 2 rocks from Los Pasos Fm. display similar patterns as andesites

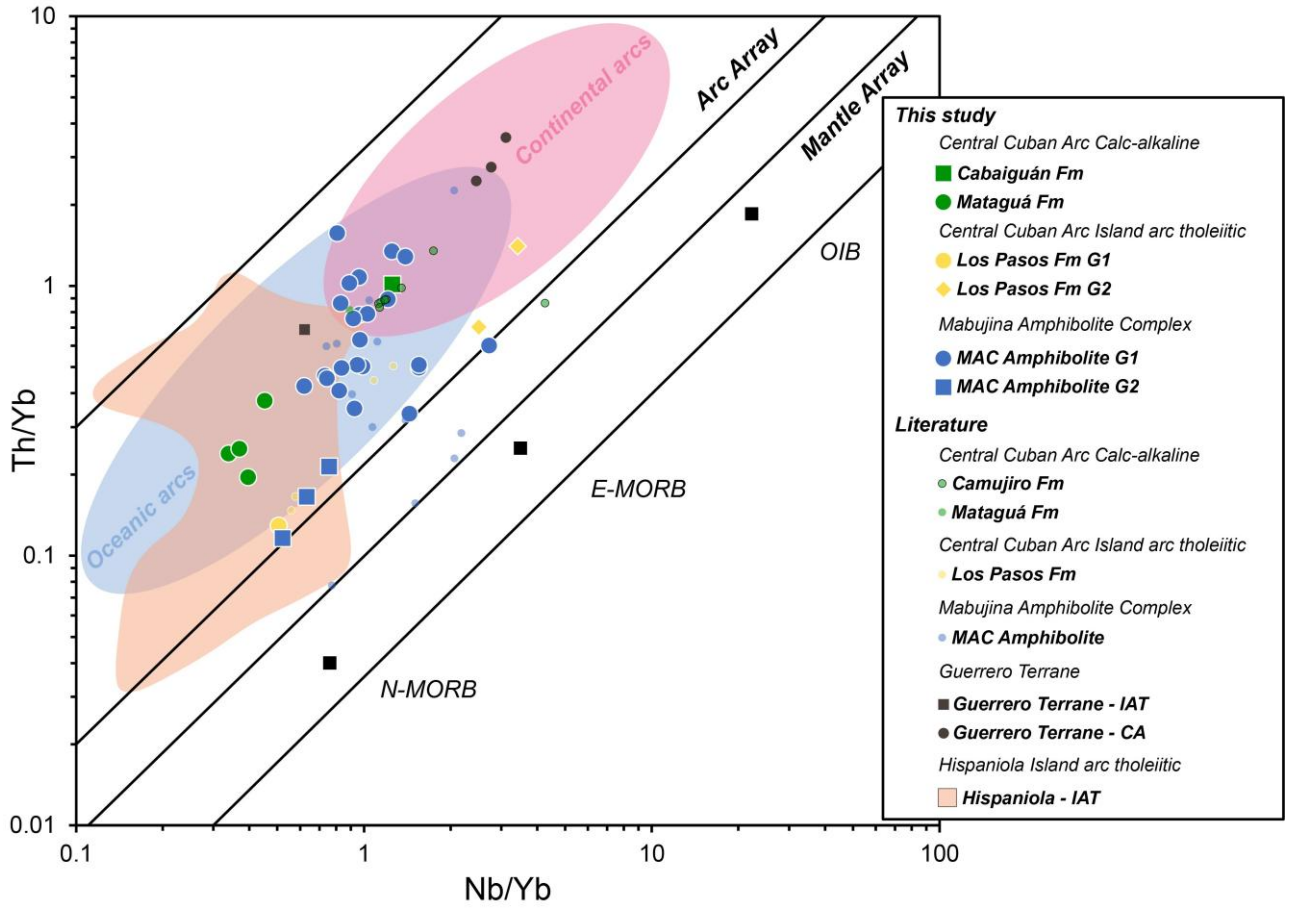

Figure 10. *Basaltic and basaltic andesitic samples plotted on the Th/Yb versus Nb/Yb of Pearce (2008). Literature data: Los Ranchos Formation from Escuder-Viruete et al. (2006) and Torró et al. (2017), Maimón Formation from Torró et al. (2017), Los Pasos Formation from Rojas-Agramonte et al. (2016) and Torró et al. (2016), MAC amphibolite from Blein et al. (2003), Rojas-Agramonte et al. (2016), and Stanek et al. (2019), Mataguá Formation from Kerr et al. (1999), Guerrero Terrane from Mendoza and Suastegui (2000).*

with calc-alkaline affinity from Los Ranchos Fm (Torró et al. 2017). on CN-REE and NMN-extended trace elements diagrams but with lower overall concentrations (Figures. 6c, d). Highly fractionated La/Yb_{CN} (up to 9.22 of Group 2 from Los Pasos Fm.) values are also observed in the ensuing Aptian to Albian Mataguá and Cabaiguán Fms., that mark the transition from tholeiitic to calc-alkaline magmatism in central Cuba and record the transition from the incipient to mature stages of the SW dipping subduction of the Proto-Caribbean lithosphere beneath the Caribbean Arc in the Early Cretaceous (Supp. Fig. S2; Pindell et al. 2012).

On the other hand, we compare below the tholeiitic and calc-alkaline volcanic arc sequences of the Guerrero Terrane given the potential provenance of the MAC protoliths from this terrane (Blein et al. 2003; Rojas-Agramonte et al. 2011). The Guerrero Terrane is a composite terrane formed in Mexico's western continental margin. It consists largely of middle Jurassic to Late Cretaceous intra-oceanic volcanic and volcanoclastic rocks (Freydier et al. 2000; Centeno-Garcia et al. 2011). The basement of the Guerrero Terrane consists of a Triassic turbidite deposit. Recent studies, however, have proposed that the Guerrero Terrane represents a slice of rifted and re-accreted active continental margin (Martini et al. 2014). Deformed plutons indicate that the Guerrero Terrane fully accreted to continental Mexico at around 100–95 Ma (Henry et al. 2003; Alsleben et al. 2008). Tholeiitic and calc-alkaline volcanic rocks from Guerrero Terrane are plotted on CN-REE and NMN extended trace elements diagrams for comparison (Figure 8).

Intra-oceanic arc systems are the oceanic endmember of arc-trench systems, with reduced influence of continental crust recycling (Stern 2010). The trace element budget of mafic rocks in oceanic arcs differs significantly from their counterpart in continental arcs. Volcanic rocks in oceanic arcs are generally poor in highly incompatible elements and enriched in HREE, resulting in low La/Yb, Th/Yb, and Nb/Yb ratios, whereas in continental arcs these ratios are higher because of the increased incorporation of recycled material and the thicker crust filtering out more mafic components near the base of the crust. On the Th/Yb vs. Nb/Yb diagram in Figure 10, most Group 1 amphibolites exhibit an offset from the mantle array to higher Th/Yb ratios relative to Nb/ Yb, reflecting a subduction component contribution. These rocks, however, largely overlap with rocks of calc-alkaline affinity from central Cuba, despite the fact that some samples from Mataguá display much lower Nb/Yb ratios indicating a more depleted mantle source. In contrast, calc-alkaline rocks from the Guerrero Terrane display higher Th/Yb and Nb/Yb ratios which extend into the field of continental arcs (Figure 10). Calc-alkaline rocks from Guerrero are characterized by significant enrichment in LREE, Th, and subduction components (average Th/Nb_{NMN} of 20.5). Thus, the plot on normalized diagrams of these calc-alkaline rocks differs from those of Group 1 amphibolites from the MAC. Group 2 amphibolites from the MAC, on the other hand, show a lower extent of subduction component similar to Groups 1and 2 from the Los Pasos Fm. (Figure 10). Regardless of the scarcity of data from the Guerrero Terrane, the tholeiitic samples from this terrane depart from its counterparts of the MAC and the Cuban arc formations with higher Th/Yb ratio reflecting a larger contribution of the subduction component. Tholeiitic rocks from the Guerrero Terrane show much lower total REE concentration

on both diagrams and stronger enrichment in Th contents than Group 2 MAC amphibolites (Figure 8).

Due to the sensibility of slab additions, Sr-Nd isotope systematics are commonly used in petrogenetic studies of volcanic arc rocks as tracers of the nature and source of magmas including the contribution of slab additions (DePaolo 1981; Cohen and O'Nions 1982). The high initial εNd values of Group 2 amphibolites and part of Group 1 amphibolites reflect a DMM source and show a similar range to those rocks from Los Pasos Fm. and IAT sequences of Los Ranchos and Maimón Fms. in Hispaniola (Figure 9). The low εSr(t) ratios and high positive εNd(t) of the tonalitic orthogneiss indicate derivation from a juvenile mafic source extracted from a DMM source, likely a non-exposed body similar in composition to the mafic protoliths of the MAC. The cluster of lower initial εNd values of Group 1 amphibolites also overlaps with the calc-alkaline Camujiro Fm. in the Camaguey region of central Cuba to the East of the studied area. The low initial εNd value of some tonalites from MAC was likely influenced by contamination from crustal material either inherited from compositional heterogeneity at crustal level or introduced in the subduction zone (Castro et al. 2010; Castro 2013). On the other hand, tholeiitic and calc-alkaline rocks from the Guerrero Terrane display lower initial εNd than the MAC, either reflecting a more evolved source or a higher extent of crustal contribution. Samples from Los Pasos Fm, Los Ranchos, and Maimón Fms and calc-alkaline rocks from the Guerrero Terrane show strong sea-water alteration extending towards higher initial εSr, while sea-water alteration only barely affected rocks of the Camujiro Fm. and the MAC (Figure 9).

In summary, the geochemistry of the protolith from the MAC largely resembles the contemporary Cretaceous volcanic rocks of the Caribbean arc in central Cuba (and Hispaniola). Despite the original stratigraphy of the MAC is undefined due to deformation and metamorphism, we conclude that the >135 – ca. 93 Ma protolith of the MAC has a strong calc-alkaline signature representing an intra-oceanic arc sequence from its tholeiitic infancy to a mature calc-alkaline stage. We hence conclude that its provenance is within the Caribbean plate, not requiring an exotic origin like the Guerrero terrane from Mexico.

6.3. Geodynamic implications for the Caribbean Arc

The geochemical similarity between the protolith of MAC and the Cretaceous sequences of the Caribbean arc in Cuba allows locating the >135 – ca. 93 Ma protolith of the MAC in the proximity of the Caribbean arc realm. However, the mechanism of the accretion of this section of the arc below the IAT rocks of Los Pasos Fm. and the corresponding palaeogeographic scenario remain uncertain.

An important constraint for understanding the evolution of the MAC and its relationship to the Cretaceous Volcanic Arc in central Cuba is the timing of the initiation of the intra-oceanic arc system. The oldest mafic protolith of the MAC is older than 133 Ma based on the zircon age of metamorphosed granitoids intruding the MAC (Rojas-Agramonte et al. 2011). The oldest arc unit in central Cuba (Los Pasos Fm.) is considered to be older than 125 Ma, perhaps as old as 135 Ma (García-Delgado 1998; Rojas-Agramonte et al. 2011; Iturralde-Vinent 2021), and the timing of the SW dipping subduction initiation below the Caribbean arc is constrained around 130 – 135 Ma (Escuder-Viruete et al. 2006; Rojas-Agramonte et al. 2011; Pindell et al. 2012; Lázaro et al. 2016; Hu et al. 2022; Niu et al. 2022). These relations imply that the protolith of the MAC probably formed only slightly earlier than the Cuban segment of the Caribbean arc if not contemporary, but within a relatively similar time frame. These age constraints hence support that the protolith of MAC represents a fragment of arc within the Caribbean arc.

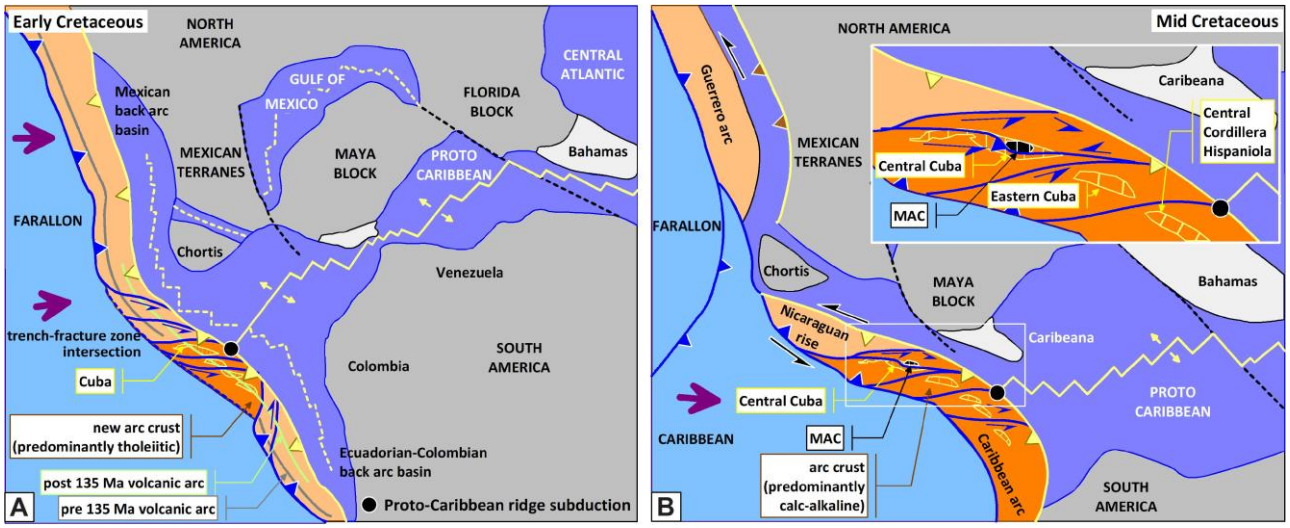

Figure 11. *a) and b) Early to Mid-Cretaceous geodynamic scenario for the development of the MAC following Pindell and Kennan (2009), Pindell et al. (2012), and Torró et al. (2016). The corresponding tholeiitic/calc-alkaline section of the Caribbean volcanic arc would have undergone metamorphism and deformation due to intra-arc collision triggered by strike-slip faulting and volcanic arc segmentation in a context of strong oblique subduction during the Cretaceous. b) Location of the Guerrero terrane in western Mexico related to Pacific (Farallon) subduction is indicated. Note that an exotic Guerrero origin of the MAC is not favoured in this geodynamic scenario. Inset in b) Inferred position of Central Cuba, Eastern Cuba and Hispaniola. Evidence for the subduction of the ridge during the Mid-Cretaceous have been documented in Hispaniola by Rojas-Agramonte et al. (2021) and Escuder-Viruete et al. (2007).*

Prior to the tectonic emplacement of MAC beneath the central Cuba section of the Caribbean arc, the proto-MAC consisted of mafic magmatic rocks that evolved from tholeiitic to calc-alkaline affinity with calc-alkaline tonalitic plutons, all developed during the Early Cretaceous to Late Cretaceous (ca. 93 Ma). This would locate the proto-MAC in close proximity to the central Cuban segment during the mid-Cretaceous time when sinistral strike-slip movements fragmented the Cretaceous arc due to oblique convergence (Figure 11b and references therein). The inferred position of the protolith of MAC relative to the central Cuban arc depends on the orientation and dip of the trans-compressive strike-slip fault system. Contemporary sinistral strike-slip movements are documented in other parts of the Caribbean arc, such as the arc-perpendicular shortening scenario and arc-parallel sinistral strike-slip shearing along the La Meseta shear zone in Hispaniola, which was active during <95–74 Ma (Escuder-Viruete et al. 2006). Torró et al. (2023) also proposed a Turonian-Coniacian transpressive event affecting the forearc in Hispaniola. Thus, a mid-Cretaceous transpression regime along the leading edge of the Caribbean plate would have facilitated the tectonic juxtaposition of crustal material along and across the strike of the subduction system (Rojas-Agramonte et al. 2016). An unconformity in the arc section located at the latest Turonian (ca. 90 Ma, Figure 2) would be consistent with this model. The nature of the intra-oceanic accretion/collision of the MAC protolith with the central Cuba section of the arc might be similar to other strongly deformed intra-oceanic arcs, such as the Cenozoic Philippine Arc (e.g., Hall 2002). However, the P-T-t path of the MAC would be needed to decipher the details of this accretion/collision event. After the emplacement of MAC beneath the central Cuban arc, the calc-alkaline plutonism associated to arc development (i.e., Manicaragua Batholith; starting at 89 Ma) intruded both, welding the newly accreted Mabujina Complex and the Cuban Cretaceous arc together.

7. Conclusion

The protolith of the Mabujina Amphibolite Complex (central Cuba) developed in an intra-oceanic arc setting during the Early Cretaceous to early Late Cretaceous (ca. 135–93 Ma) prior to its accretion/collision to the central Cuban arc at ca. 93 Ma. Immobile trace element concentrations reveal that the protoliths of the MAC are dominated by calc-alkaline mafic volcanic/subvolcanic and tonalitic rocks and less abundant island arc tholeiitic mafic rocks. These ages and geochemical characteristics of the MAC are explained by an arc sequence that evolved from incipient (tholeiitic) to mature (volumetric dominant calc-alkaline magmatism) subduction stages. Their high initial Nd

ratios reflect a DMM source and overlap with the Nd signature of the tholeiitic island arc and calc-alkaline rocks of the central Cuban arc. Due to the geochemical similarity between the protolith of the MAC and the Early Cretaceous series of the central Cuban section of the Caribbean arc, we propose that the magmatism represented in the MAC evolved within the leading edge of the Caribbean plate. An exotic origin, such as the Mexican Guerrero terrane, is not required to explain its volumetrically dominant calc-alkaline mafic protolith. In a geodynamic context of strong sinistral strike-slip tectonics that segmented the arc, the protolith of the MAC was tectonically emplaced underneath the central Cuban arc during the mid-Cretaceous time, prior to the emplacement of the calc-alkaline Manicaragua Batholith starting at 89 Ma. A detailed examination of the metamorphism of the MAC is still required to decipher the timing and nature of this accretion/collision event.

Acknowledgments

We greatly appreciate Joaquín A. Proenza and Lisard Torró for the constructive comments and suggestions that helped to improve the manuscript. Haoyu Hu acknowledges support by Federal State Funding at Kiel University. This research was funded by projects PID2019-105625RB-C21 and CGL2009- 12446 (Ministry of Science and Innovation, Spain). We thank Jose Carlos Pomo and Luis Bernal for field assistance.

Fund

The work was supported by the Christian-Albrechts-Universität zu Kiel [Federal State Funding]; Ministry of Education and Science, Spain Ministry of Science and Innovation, Spain [CGL2009-12446,CGL2006-08527/BTE].

Reference

Alsleben, H., Wetmore, P.H., Schmidt, K.L., Paterson, S.R., and Melis, E.A., 2008, Complex deformation during arc–continent collision: Quantifying finite strain in the accreted Alisitos arc, Peninsular Ranges batholith, Baja California: Journal of Structural Geology, v. 30, p. 220–236, doi:10.1016/j.jsg.2007.11.001.

Álvarez-Sánchez, H., 2022, Edades absolutas y paleontológicas del Complejo Anfibolítico de. Mabujina, Cuba. Revista Maya de Geociencias. Edición Agosto. Págs.57-65.

Álvarez-Sánchez, H., and Bernal-Rodríguez, L., 2015, Los mélanges Santa Clara y descanso del cinturón ofiolítico de Cuba central. Memorias, Trabajos y Resúmenes, VI Convención

Cubana de Ciencias de La Tierra (Geociencias' 2015), Sociedad Cubana de Geología, La Habana.

Álvarez-Sánchez, H., Millan Trujillo, G., Mainegra, V., Bernal-Rodríguez, L., and Ando, J., 1991, Significado geotectónico de las rocas eclogíticas de Cuba central. 13th Caribbean Geological Congress. Pinar Del Rio. Unpublished.

Annen, C., Blundy, J.D., Leuthold, J., and Sparks, R.S.J., 2015, Construction and evolution of igneous bodies: Towards an integrated perspective of crustal magmatism: Lithos, v. 230, p. 206–221, doi:10.1016/j.lithos.2015.05.008.

Annen, C., Blundy, J.D., and Sparks, R.S.J., 2006, The Genesis of Intermediate and Silicic Magmas in Deep Crustal Hot Zones: Journal of Petrology, v. 47, p. 505–539, doi:10.1093/petrology/egi084.

Atherton, M.P., and Petford, N., 1993, Generation of sodium-rich magmas from newly underplated basaltic crust: Nature, v. 362, p. 144–146, doi:10.1038/362144a0.

Beard, J.S., and Lofgren, G.E., 1991, Dehydration Melting and Water-Saturated Melting of Basaltic and Andesitic Greenstones and Amphibolites at 1, 3, and 6. 9 kb: Journal of Petrology, v. 32, p. 365–401, doi:10.1093/petrology/32.2.365.

Bibikova, E.V., Somin, M.L., Graceva, T.V., Makarov, V.A., Millan, G., and Chukoljukov, J.A., 1988, Pervye rezultaty U-Pb-datirovanija metamorficeskich porod Bolschoi Antillskoi dugi: vozrast kompleksa Mabuchina Kuby. Doklady AN SSSR, Ser. Geol., 302, 924–928.: Doklady AN SSSR, Ser. Geol., p. 924–928.

Blein, O., Guillot, S., Lapierre, H., de Lépinay, B.M., Lardeaux, J. -M., Trujillo, G.M., Campos, M., and Garcia, A., 2003, Geochemistry of the Mabujina Complex, Central Cuba: Implications on the Cuban Cretaceous Arc Rocks: The Journal of Geology, v. 111, p. 89–101, doi:10.1086/344666.

Boschman, L.M., van Hinsbergen, D.J.J., Torsvik, T.H., Spakman, W., and Pindell, J.L., 2014, Kinematic reconstruction of the Caribbean region since the Early Jurassic: Earth-Science Reviews, v. 138, p. 102–136, doi:10.1016/j.earscirev.2014.08.007.

Boyanov, I., Goranov, G., and Cabrera, R., 1975, Nuevos datos sobre Ia geología de los complejos de anfibolitas y granitoides en Ia parte sur de Las Villas: Serie Geológica del lnstituto de Geología y Paleontología (19): 1-14.

Butjosa, L., Cambeses, A., Proenza, J.A., Agostini, S., Iturralde-Vinent, M., Bernal-Rodríguez, L., and Garcia-Casco, A., 2023a, Relict abyssal mantle in a Caribbean forearc ophiolite (Villa

Clara, central Cuba): petrogenetic and geodynamic implications: International Geology Review, p. 1–32, doi:10.1080/00206814.2023.2179229.

Butjosa, L., Cambeses, A., Proenza, J.A., Blanco-Quintero, I.F., Agostini, S., Iturralde-Vinent, M.A., and Garcia-Casco, A., 2023b, Fluid flow in the subduction channel: Tremolite veins and associated blackwalls in antigoritite (Villa Clara serpentinite mélange, Cuba): Lithos, v. 436–437, p. 106973, doi:10.1016/j.lithos.2022.106973.

Castro, A., 2013, Tonalite–granodiorite suites as cotectic systems: A review of experimental studies with applications to granitoid petrogenesis: Earth-Science Reviews, v. 124, p. 68–95, doi:10.1016/j.earscirev.2013.05.006.

Castro, A., Gerya, T., Garcia-Casco, A., Fernandez, C., Diaz-Alvarado, J., Moreno-Ventas, I., and Low, I., 2010, Melting Relations of MORB-Sediment Melanges in Underplated Mantle Wedge Plumes; Implications for the Origin of Cordilleran-type Batholiths: Journal of Petrology, v. 51, p. 1267–1295, doi:10.1093/petrology/egq019.

Centeno-Garcia, E., Busby, C., Busby, M., and Gehrels, G., 2011, Evolution of the Guerrero composite terrane along the Mexican margin, from extensional fringing arc to contractional continental arc: Geological Society of America Bulletin, v. 123, p. 1776–1797, doi:10.1130/B30057.1.

Cohen, R.S., and O'Nions, R.K., 1982, Identification of recycled continental material in the mantle from Sr, Nd and Pb isotope investigations: Earth and Planetary Science Letters, v. 61, p. 73–84, doi:10.1016/0012-821X(82)90040-1.

Cruz-Gámez, E.M., Velasco-Tapia, F., Garcia-Casco, A., Despaigne Díaz, A.I., Lastra Rivero, J.F., and Cáceres Govea, D., 2016, Geoquímica del magmatismo mesozoico asociado al Margen Continental Pasivo en el occidente y centro de Cuba: Boletín de la Sociedad Geológica Mexicana, v. 68, p. 443–475, doi:10.18268/BSGM2016v68n3a5.

Defant, M.J., and Drummond, M.S., 1990, Derivation of some modern arc magmas by melting of young subducted lithosphere: Nature, v. 347, p. 662–665, doi:10.1038/347662a0.

DePaolo, D.J., 1981, Trace element and isotopic effects of combined wallrock assimilation and fractional crystallization: Earth and Planetary Science Letters, v. 53, p. 189–202, doi:10.1016/0012-821X(81)90153-9.

Despaigne-Díaz, A.I., Garcia-Casco, A., Caceres Govea, D., Jourdan, F., Wilde, S.A., and Millan Trujillo, G., 2016, Twenty-five million years of subduction-accretion-exhumation during the Late Cretaceous-Tertiary in the northwestern Caribbean: The Trinidad Dome, Escambray

Complex, Central Cuba: American Journal of Science, v. 316, p. 203–240, doi:10.2475/03.2016.01.

Despaigne-Díaz, A.I., Garcia-Casco, A., Cáceres Govea, D., Wilde, S.A., and Millán Trujillo, G., 2017, Structure and tectonic evolution of the southwestern Trinidad dome, Escambray complex, Central Cuba: Insights into deformation in an accretionary wedge: Tectonophysics, v. 717, p. 139–161, doi:10.1016/j.tecto.2017.07.024.

Díaz de Villalvila, L., 1997, Caracterización geológica de las formaciones volcánicas y volcano-sedimentarias en Cuba central, provincias Cienfuegos, Villa Clara, Sancti Spiritus. In: Estudios sobre Geología de Cuba (Eds. Furrazola Bermudez, G.F., Núñez Cambra, K.E.): Centro Nacional de Información Geológica, La Habana, Cuba, p. 259–270.

Díaz de Villalvilla, L. et al., 1994, Consideraciones geoquimicas acerca de los arcol volcanicos de Cuba [abs.]: in Secondo Congreso Cubano de Geologia y Mineria.

Díaz de Villalvilla, L., Milia-González, I., Santa Cruz Pacheco, M., and Aguirre, G., 2003, Formación Los Pasos: Geología, Geoquímica y su Comparación con el Caribe: Estudios Sobre los Arcos Volcánicos de Cuba, Centro Nacional de Información Geológica, Instituto de Geología y Paleontología de Cuba, Havana.

Dublan, L., and Alvarez, Sanchez., eds, 1986, Informe final del levantamiento geologico y evaluacion de minerales utiles, en escala 1:50.000, del polıgono CAME I, zona Centro. Centro Nacional Fondo Geolo´gico, MINBAS, La Habana (unpubl. report).

Ducea, M.N., Chapman, A.D., Bowman, E., and Balica, C., 2021, Arclogites and their role in continental evolution; part 2: Relationship to batholiths and volcanoes, density and foundering, remelting and long-term storage in the mantle: Earth-Science Reviews, v. 214, p. 103476, doi:10.1016/j.earscirev.2020.103476.

Ducloz, C., and Vuagnat, M., 1962, Apropose de l'age des serpentinites de Cuba. Arch. Sci. Phys. d'Histoire Nat., 15, pp. 309-332.

Escuder-Viruete, J., Díaz de Neira, A., Hernáiz Huerta, P.P., Monthel, J., Senz, J.G., Joubert, M., Lopera, E., Ullrich, T., Friedman, R., and Mortensen, J., 2006a, Magmatic relationships and ages of Caribbean Island arc tholeiites, boninites and related felsic rocks, Dominican Republic: Lithos, v. 90, p. 161–186, doi:10.1016/j.lithos.2006.02.001.

Escuder-Viruete, J., Contreras, F., Stein, G., Urien, P., Joubert, M., Ullrich, T., Mortensen, J., and Pérez-Estaún, A., 2006b, Transpression and strain partitioning in the Caribbean Island-arc: Fabric development, kinematics and Ar–Ar ages of syntectonic emplacement of the Loma

de Cabrera batholith, Dominican Republic: Journal of Structural Geology, v. 28, p. 1496–1519, doi:10.1016/j.jsg.2006.04.003.

Escuder-Viruete, J., Contreras, F., Stein, G., Urien, P., Joubert, M., Pérez-Estaún, A., Friedman, R., and Ullrich, T., 2007, Magmatic relationships and ages between adakites, magnesian andesites and Nb-enriched basalt-andesites from Hispaniola: record of a major change in the Caribbean island arc magma sources. Lithos, 99(3-4), 151-177.

Freydier, C., Lapierre, H., Ruiz, J., Tardy, M., Martinez-R, J., and Coulon, C., 2000, The Early Cretaceous Arperos basin: an oceanic domain dividing the Guerrero arc from nuclear Mexico evidenced by the geochemistry of the lavas and sediments: Journal of South American Earth Sciences, v. 13, p. 325–336, doi:10.1016/S0895-9811(00)00027-4.

Furnes, H., and Dilek, Y., 2017, Geochemical characterization and petrogenesis of intermediate to silicic rocks in ophiolites: A global synthesis: Earth-Science Reviews, v. 166, p. 1–37, doi:10.1016/j.earscirev.2017.01.001.

García-Delgado, D. E., 1998, Mapa geológico de Cuba central (provincias Cienfuegos, Villa Clara y Sancti Spiritus) Escala 1:100000: Instituto de Geología y Paleontología, La Habana.

Garcia-Casco, A., Iturralde-Vinent, M.A., and Pindell, J., 2008, Latest Cretaceous Collision/Accretion between the Caribbean Plate and Caribeana: Origin of Metamorphic Terranes in the Greater Antilles: International Geology Review, v. 50, p. 781–809, doi:10.2747/0020-6814.50.9.781.

Garcia-Casco, A., Torres-Roldán, R.L., Iturralde-Vinent, M.A., Millán, G., Cambra, K.N., Lázaro, C., and Vega, A.R., 2006, High pressure metamorphism of ophiolites in Cuba: Geologica Acta, p. 26.

Garcia-Casco, A., Torres-Roldan, R.L., Millan, G., Monie, P., and Schneider, J., 2002, Oscillatory zoning in eclogitic garnet and amphibole, Northern Serpentinite Melange, Cuba: a record of tectonic instability during subduction? Journal of Metamorphic Geology, v. 20, p. 581–598, doi:10.1046/j.1525-1314.2002.00390.x.

Govindaraju, K., Potts, P.J., Webb, P.C., and Watson, J.S., 1994, Report on Whin sill dolerite WS-S from England and Pitscurrie microgabbro PM-S from Scotland: assessment by one hundred and four international laboratories: Geostandards and Geoanalytical Research, v. 18, p. 211–300, doi:10.1111/j.1751-908X.1994.tb00520.x.

Grafe, F., Stanek, K.P., Baumann, A., Maresch, W.V., Hames, W.E., Grevel, C., and Millan, G., 2001, Rb–Sr and 40Ar/39Ar Mineral Ages of Granitoid Intrusives in the Mabujina Unit,

Central Cuba: Thermal Exhumation History of the Escambray Massif: The Journal of Geology, v. 109, p. 615–631, doi:10.1086/321966.

Hall, R., 2002, Cenozoic geological and plate tectonic evolution of SE Asia and the SW Pacific: computer-based reconstructions, model and animations: Journal of Asian Earth Sciences, v. 20, p. 353–431, doi:10.1016/S1367-9120(01)00069-4.

Hastie, A.R., Kerr, A.C., Pearce, J.A., and Mitchell, S.F., 2007, Classification of Altered Volcanic Island Arc Rocks using Immobile Trace Elements: Development of the Th–Co Discrimination Diagram: Journal of Petrology, v. 48, p. 2341–2357, doi:10.1093/petrology/egm062.

Hatten, C.W., Schooler, O.E., Giedt, N., and Meyerhoff, A.A., 1958, Geology of central Cuba, eastern Las Villas and western Camaguey provinces, Cuba. La Habana, Ministerio de Industrias archives, 250 pp. (unpublished report).

Henry, C.D., McDowell, F.W., and Silver, L.T., 2003, Geology and geochronology of granitic batholith complex, Sinaloa, México: Implications for Cordilleran magmatism and tectonics, in Tectonic evolution of northwestern Mexico and the Southwestern USA, Geological Society of America, doi:10.1130/0-8137-2374-4.237.

Hildreth, W., and Moorbath, S., 1988, Crustal contributions to arc magmatism in the Andes of Central Chile: Contributions to Mineralogy and Petrology, v. 98, p. 455–489, doi:10.1007/BF00372365.

van Hinsbergen, D.J.J., Iturralde-Vinent, M.A., van Geffen, P.W.G., Garcia-Casco, A., and van Benthem, S., 2009, Structure of the accretionary prism, and the evolution of the Paleogene northern Caribbean subduction zone in the region of Camagüey, Cuba: Journal of Structural Geology, v. 31, p. 1130–1144, doi:10.1016/j.jsg.2009.06.007.

Hu, H.Y., Stern, R.J., Rojas-Agramonte, Y., and Garcia-Casco, A., 2022, Review of Geochronologic and Geochemical Data of the Greater Antilles Volcanic Arc and Implications for the Evolution of Oceanic Arcs: Geochemistry, Geophysics, Geosystems, v. 23, doi:10.1029/2021GC010148.

Ishizuka, O., Tani, K., and Reagan, M.K., 2014, Izu-Bonin-Mariana Forearc Crust as a Modern Ophiolite Analogue: Elements, v. 10, p. 115–120, doi:10.2113/gselements.10.2.115.

Iturralde-Vinent, M.A., 2021, Compendio de geología de Cuba. Havana, Editorial CITMATEL (https://www.libreriavirtualcuba.com/geologia-de-cuba-compendio-2021).

Iturralde-Vinent, M.A., 1994, Cuban Geology: A New Plate-Tectonic Synthesis: Journal of Petroleum Geology, v. 17, p. 39–69, doi:10.1111/j.1747-5457.1994.tb00113.x.

Iturralde-Vinent, M.A., 2019, Geología de los Arcos Volcánicos del Cretácico in Geología de Cuba y del Caribe, Compendio (Third edition), CD-ROM. Editorial CITMATEL (2019) ISBN: 9-789592-572863.

Iturralde-Vinent, M.A., Garcia-Casco, A., Rojas-Agramonte, Y., Proenza, J.A., Murphy, J.B., and Stern, R.J., 2016, The geology of Cuba: A brief overview and synthesis: GSA Today, p. 4–10, doi:10.1130/GSATG296A.1.

Iturralde-Vinent, M.A., Millán, G., Korpás, L., Nagy, E., and Pajón, J., 1996, Geological interpretation of the Cuban K-Ar database, in Iturralde-Vinent, M.A. ed., Ofiolitas y Arcos Volcánicos de Cuba, Miami, International Geological Correlation Program (IGCP) Project 364, p. 48–69.

Iturralde-Vinent, M.A., Otero, C.D., Garcia-Casco, A., and van Hinsbergen, D.J.J., 2008, Paleogene Foredeep Basin Deposits of North-Central Cuba: A Record of Arc-Continent Collision between the Caribbean and North American Plates: International Geology Review, v. 50, p. 863–884, doi:10.2747/0020-6814.50.10.863.

Kantchev, I., Boyanov, I., Popov, N., Cabrera, R., Goranov, A., Lolkoev, N., Kanazirski, M., and Stancheva, M., 1978, Informe Geología de la provincia de Las Villas. Resultados de las investigaciones geológicas y levantamiento geológico a escala 1:250 000. Instituto de Geología, Academia de Ciencias de Bulgaria; Instituto de Geología y Paleontología (IGP), Academia de Ciencias de Cuba. Unpublished. Archivo del Instituto de Geología y Paleontología. La Habana.

Kay, S.M., Kay, R.W., Citron, G.P., and Perfit, M.R., 1990, Calc-alkaline plutonism in the intra-oceanic Aleutian arc, Alaska, in Geological Society of America Special Papers, Geological Society of America, v. 241, p. 233–256, doi:10.1130/SPE241-p233.

Kerr, A.C., Iturralde-Vinent, M.A., D. Saunders, A., and Tarney, J., 1999, New plate tectonic model of the Caribbean: Implications from a geochemical reconnaissance of Cuban Mesozoic volcanic rocks: Geological Society of America Bulletin, p. 19.

Koepke, J., Berndt, J., Feig, S.T., and Holtz, F., 2007, The formation of SiO2-rich melts within the deep oceanic crust by hydrous partial melting of gabbros: Contributions to Mineralogy and Petrology, v. 153, p. 67–84, doi:10.1007/s00410-006-0135-y.

Lázaro, C., Blanco-Quintero, I.F., Proenza, J.A., Rojas-Agramonte, Y., Neubauer, F., Núñez-Cambra, K., and Garcia-Casco, A., 2016, Petrogenesis and 40 Ar/ 39 Ar dating of proto-forearc crust in the Early Cretaceous Caribbean arc: The La Tinta mélange (eastern Cuba) and its easterly correlation in Hispaniola: International Geology Review, v. 58, p. 1020–1040, doi:10.1080/00206814.2015.1118647.

Lidiak, E.G., and Anderson, T.H., 2015, Evolution of the Caribbean plate and origin of the Gulf of Mexico in light of plate motions accommodated by strike-slip faulting, in Geological Society of America Special Papers, Geological Society of America, v. 513, p. 1–88, doi:10.1130/2015.2513(01).

Linares, E., Osadchiy, P.G., and et al., 1985, Mapa Geológico de la República de Cuba. Escala 1: 500,000. Ministerio de la Industria Básica. La Habana.

Marien, C.S., Hoffmann, J.E., Garbe-Schönberg, C.-D., and Münker, C., 2019, Petrogenesis of plagiogranites from the Troodos Ophiolite Complex, Cyprus: Contributions to Mineralogy and Petrology, v. 174, p. 35, doi:10.1007/s00410-019-1569-3.

Martini, M., Solari, L., and López-Martínez, M., 2014, Correlating the Arperos Basin from Guanajuato, central Mexico, to Santo Tomás, southern Mexico: Implications for the paleogeography and origin of the Guerrero terrane: Geosphere, v. 10, p. 1385–1401, doi:10.1130/GES01055.1.

Mendoza, O.T., and Suastegui, M.G., 2000, Geochemistry and isotopic composition of the Guerrero Terrane (western Mexico): implications for the tectono-magmatic evolution of southwestern North America during the Late Mesozoic: Journal of South American Earth Sciences, v. 13, p. 297–324, doi:10.1016/S0895-9811(00)00026-2.

Millán, G., 1997, Geologia del macizo metamórfico del Escambray, in Furrazola Bermudez, G. and Nuñez Cambra, K.E. eds., Estudios sobre Geología de Cuba, La Habana, Centro Nacional de Información Geológica, p. 271–288.

Millan, G., and Somin, M.L., 1985, Carateristicas del metamorphismo del complejo anfibolitico Mabujina, sur de Cuba central. Acad. Cie. Cuba Rep. Investig. Inst. Geol. Paleontol. 2:43–51.

Millán Trujillo, G., 1973, El metamorfismo del complejo vulcanógeno cretácico en los alrededores del Escambray y sus implicaciones. Actas, Instituto de Geología, Academia de Ciencias de Cuba, 3: 34-38.

Mossakovski, A., Nekrasov, G., and Sokolov, S., 1986, Los complejos metamórficos y el problema del fundamento de la estructura alpina de Cuba. Geotectonics 3; 5-24.

Niu, X., Yang, J., Llanes Castro, A.I., Feng, G., Li, Z., and Liu, F., 2022, Zircon ages, mineralogy, and geochemistry of ophiolitic mafic and island-arc rocks from central Cuba: Implications for Cretaceous tectonics in the Caribbean region: Lithos, v. 434–435, p. 106924, doi:10.1016/j.lithos.2022.106924.

O`Connor, J.T., 1965, A classification of quartz rich igneous rock based on feldspar ratios: US Geological Survey, 525B, B79-B84.

Pearce, J.A., 1996, A user's guide to basalt discrimination diagrams: Trace element geochemistry of volcanic rocks: applications for massive sulphide exploration. Geological Association of Canada, Short Course Notes, v. 12, p. 113.

Pearce, J.A., 2014, Immobile Element Fingerprinting of Ophiolites: Elements, v. 10, p. 101–108, doi:10.2113/gselements.10.2.101.

Pindell, J.L., and Kennan, L., 2009, Tectonic evolution of the Gulf of Mexico, Caribbean and northern South America in the mantle reference frame: an update: Geological Society, London, Special Publications, v. 328, p. 1–55, doi:10.1144/SP328.1.

Pindell, J., Kennan, L., Maresch, W.V., Stanek, K.-P., Draper, G., and Higgs, R., 2005, Plate-kinematics and crustal dynamics of circum-Caribbean arc-continent interactions: Tectonic controls on basin development in Proto-Caribbean margins, in Caribbean-South American plate interactions, Venezuela, Geological Society of America, doi:10.1130/0-8137-2394-9.7.

Pindell, J., Maresch, W.V., Martens, U., and Stanek, K., 2012, The Greater Antillean Arc: Early Cretaceous origin and proposed relationship to Central American subduction mélanges: implications for models of Caribbean evolution: International Geology Review, v. 54, p. 131–143, doi:10.1080/00206814.2010.510008.

Piñero Pérez, E., Quintana, M.A., and Marí Morales, T., 1997, Caracterización geológica de los depósitos vulcanógeno-sedimentarios de la región Ciego-Camagüey-Las Tunas. Estudios sobre Geología de Cuba. La Habana, Centro Nacional de Información Geológica, 345-356.

Reagan, M.K. et al., 2010, Fore-arc basalts and subduction initiation in the Izu-Bonin-Mariana system: Fore-arc basalts and subduction initiation: Geochemistry, Geophysics, Geosystems, v. 11, p. n/a-n/a, doi:10.1029/2009GC002871.

Rojas-Agramonte, Y. et al., 2011a, Timing and Evolution of Cretaceous Island Arc Magmatism in Central Cuba: Implications for the History of Arc Systems in the Northwestern Caribbean: The Journal of Geology, v. 119, p. 619–640, doi:10.1086/662033.

Rojas-Agramonte, Y., Garcia-Casco, A., Kemp, A., Kröner, A., Proenza, J.A., Lázaro, C., and Liu, D., 2016, Recycling and transport of continental material through the mantle wedge above subduction zones: A Caribbean example: Earth and Planetary Science Letters, v. 436, p. 93–107, doi:10.1016/j.epsl.2015.11.040.

Rojas-Agramonte, Y., Garcia-Casco, A., Kroner, A., Carrasquilla-Ortiz, S., Castro, A., Perez, M., Fonseca-Montero, A., Barth, M., and Liu, D., 2011b, Early Cretaceous arc formation and crustal inheritance in central Cuba: geochemistry and age of the Los Pasos Formation. In 19th Caribbean Geological Conference (Le Gosier, Guadeloupe, March 21-24). https://calamar. univ-ag.fr/cgc2011/images/stories/livret-cgc2011-red.pdf.

Rojas-Agramonte, Y., Hu, H. Y., Iturralde-Vinent, M., Lewis, J., de Lepinay, B, M., and Garcia-Casco, A., 2021, A Late Cretaceous Adakitic intrusion from Northern Haiti: additional evidence for slab melting and implications for migration of ridge-trench-trench triple junction during the Cretaceous in the Greater Antilles. International Geology Review, 1-10.

Rojas-Consuegra, R., Iturralde-Vinent, M., y Skelton, P.W.,1995. Stratigraphy, composition and age of Cuban rudist-bearing deposits. Revista Mexicana de Ciencias Geológicas, 12 (2): 272-291.

Rollinson, H., 2009, New models for the genesis of plagiogranites in the Oman ophiolite: Lithos, v. 112, p. 603–614, doi:10.1016/j.lithos.2009.06.006.

Schneider, J., Bosch, D., Monié, P., Guillot, S., Garcia-Casco, A., Lardeaux, J.M., Torres-Roldán, R.L., and Trujillo, G.M., 2004, Origin and evolution of the Escambray Massif (Central Cuba): an example of HP/LT rocks exhumed during intraoceanic subduction: Origin And Evolution of the Escambray Massif: Journal of Metamorphic Geology, v. 22, p. 227–247, doi:10.1111/j.1525-1314.2004.00510.x.

Somin, M.L., 1993, The Mabujina complex of Cuba: an example of metamorphic infrastructure of the ensimatic volcanic arc: Petrol. Miner. Tect. Tbilisi, Metsniereba., p. p.18-31.

Somin, M.L., and Millan, G., 1981, Geologija metamorficheskich kompleksov Kuby: Isdat. Nauka, Moskva, p. 219 p.

Somin, M.L., and Millan Trujillo, G., 1976, El complejo anfibolítico de Cuba surcentral y problemas de la posición tectónica de la serie eugeosinclinal de la isla. Bulletín MOIP, Geología, vol. 5, pp, 73-93 (In Russian).

Stanek, K.P., Maresch, W.V., Grafe, F., Grevel, C., and Baumann, A., 2006, Structure, tectonics and metamorphic development of the Sancti Spiritus Dome (eastern Escambray massif, Central Cuba): Geologica Acta, p. 20.

Stanek, K.P., Maresch, W.V., Scherer, E., Krebs, M., Berndt, J., Sergeev, S.S., Rodionov, N., Pfänder, J., and Hames, W.E., 2019, Born in the Pacific and raised in the Caribbean: construction of the Escambray nappe stack, central Cuba. A review: European Journal of Mineralogy, v. 31, p. 5–34, doi:10.1127/ejm/2019/0031-2795.

Stanik, E. et al., 1981, Informe del levantamiento geológico, geoquímico y trabajos geofísicos, realizados en la parte Sur de Cuba Central, en las Provincias Cienfuegos, Sancti Spiritus y Villa Clara. Centro Nacional del Fondo Geológico. La Habana. Cuba. 555 pags. (Inédito).

Stern, R.J., 2010, The anatomy and ontogeny of modern intra-oceanic arc systems: Geological Society, London, Special Publications, v. 338, p. 7–34, doi:10.1144/SP338.2.

Sukar, K., and Perez, M., 1997, Granitoides del arco volcánico de la región central de Cuba antigua provincia de Las Villas: v. In Furrazola Bermu´ dez, G. F., and Nu´ n˜ ez Cambra, K. E., eds. Estudios sobre geologı´a de Cuba. Havana, Instituto de Geologı´a y Paleontologı´a, Centro Nacional de Informacio´n Geolo´ gica, pp. 371–386.

Sun, S. -s., and McDonough, W.F., 1989, Chemical and isotopic systematics of oceanic basalts: implications for mantle composition and processes: Geological Society, London, Special Publications, v. 42, p. 313–345, doi:10.1144/GSL.SP.1989.042.01.19.

Torró, L. et al., 2016a, Mineralogy, geochemistry and sulfur isotope characterization of Cerro de Maimón (Dominican Republic), San Fernando and Antonio (Cuba) lower Cretaceous VMS deposits: Formation during subduction initiation of the proto-Caribbean lithosphere within a fore-arc: Ore Geology Reviews, v. 72, p. 794–817, doi:10.1016/j.oregeorev.2015.09.017.

Torró, L., Cambeses, A., Rojas-Agramonte, Y., Butjosa, L., Iturralde-Vinent, M., Lázaro, C., Piñero, E., Proenza, J.A., and Garcia-Casco, A., 2020, Cryptic alkaline magmatism in the oceanic Caribbean arc (Camagüey area, Cuba): Lithos, v. 376–377, p. 105736, doi:10.1016/j.lithos.2020.105736.

Torró, L., Garcia-Casco, A., Proenza, J.A., Blanco-Quintero, I.F., Gutiérrez-Alonso, G., and Lewis, J.F., 2016b, High-pressure greenschist to blueschist facies transition in the Maimón

Formation (Dominican Republic) suggests mid-Cretaceous subduction of the Early Cretaceous Caribbean arc: Lithos, v. 266–267, p. 309–331, doi:10.1016/j.lithos.2016.10.026.

Torró, L., Proenza, J.A., Camprubí, A., Nelson, C.E., Domínguez, H., Carrasco, C., Reynoso-Villafaña, R., and Melgarejo, J.C., 2017a, Towards a unified genetic model for the Au-Ag-Cu Pueblo Viejo district, central Dominican Republic: Ore Geology Reviews, v. 89, p. 463–494, doi:10.1016/j.oregeorev.2017.07.002.

Torró, L., Proenza, J.A., Farré-de-Pablo, J., Nelson, C., Román-Alpiste, M.J., and Garcia-Casco, A., 2023, Turonian-coniacian definition of the Caribbean plate: tectonic and metamorphic record in the Median Belt, Dominican Republic: International Geology Review, p. 1–16, doi:10.1080/00206814.2023.2165174.

Torró, L., Proenza, J.A., Marchesi, C., Garcia-Casco, A., and Lewis, J.F., 2017b, Petrogenesis of meta-volcanic rocks from the Maimón Formation (Dominican Republic): Geochemical record of the nascent Greater Antilles paleo-arc: Lithos, v. 278–281, p. 255–273, doi:10.1016/j.lithos.2017.01.031.

Whattam, S.A., and Stern, R.J., 2011, The ‘subduction initiation rule’: a key for linking ophiolites, intra-oceanic forearcs, and subduction initiation: Contributions to Mineralogy and Petrology, v. 162, p. 1031–1045, doi:10.1007/s00410-011-0638-z.

Wilson, F.H., Orris, G., and Gray, F., 2019, Preliminary geologic map of the Greater Antilles and the Virgin Islands: U.S. Geological Survey Open-File Report 2019–1036, pamphlet 50 p., 2 sheets, scales 1:2,500,000 and 1:300,000, https://doi.org/10.3133/ofr20191036.

Winchester, J.A., and Floyd, P.A., 1977, Geochemical discrimination of different magma series and their differentiation products using immobile elements: Chemical geology, v. 20, p. 325–343.

Formblatt Kumulative Dissertation Stand 14.02.2023

1. Publikation/*Publication*:

Vollständige bibliographische Referenz/*Complete bibliographic reference:*

Hu, H., Rojas-Agramonte, Y., Stern, R.J., Cambeses, A., Iturralde-Vinent, M.A., García-Delgado, D.E., Vermeesch, P., Liu, S., Wu, S. & Garcia-Casco, A. Prolonged evolution of an intra-oceanic island arc: The ~60 Myr record of Central Cuba

2. Erst- oder gleichberechtigte Autorenschaft/*First or equal authorship:* **Ja/*Yes*** ☑ **Nein/*No*** ☐

3. Veröffentlicht/*Published* ☐ **Zur Veröffentlichung akzeptiert/*Accepted*** ☐

Q1/Q2:* **Ja/*Yes*** ☑ **Nein/*No*** ☐

**SCImago Journal Rank (SJR) indicator*

Im Erscheinungsjahr oder im letzten verfügbaren Vorjahr/*In the year of publication or the last prior year available:* _____

Eingereicht/*Submitted* ☑ **Noch nicht eingereicht/*Not yet submitted*** ☐

4. Beteiligungen/*Contributions***

Contributor Role	**Doktorand/in/ *Doctoral student***	**Co-Autor/in 1/ *Co-author 1***	**Co-Autor/in 2/ *Co-author 2***
Name, first name	Haoyu Hu	Yamirka Rojas-agramonte	Robert J. Stern
Methodology	☑	☐	☐
Software	☐	☐	☐
Validation	☐	☐	☐
Formal analysis	☑	☑	☐
Investigation	☑	☑	☑
Resources	☐	☐	☐
Data Curation	☑	☐	☐
Writing-Original Draft	☑	☐	☐
Writing-Review&Editing	☑	☑	☑
Visualization	☑	☐	☐
Supervision	☐	☑	☐
Project administration	☐	☑	☐
Funding acquisition	☐	☑	☐

***Kategorien des CRediT (Contributor Roles Taxonomy, https://credit.niso.org/)*

Hiermit bestätige ich, dass alle obigen Angaben korrekt sind/*I confirm that all declarations made above are correct.*

Unterschrift/*Signature* _____ Doktorand/in/*Doctoral student*

_____ Co-Autor/in 1/*Co-author 1*

Robert Stern Digitally signed by Robert Stern Date: 2025.10.29 11:00:00 -07'00'

_____ Co-Autor/in 2/*Co-author 2*

Betreuungsperson/*Supervisor:*

Hiermit bestätige ich, dass alle obigen Angaben korrekt sind und dass die selbstständigen Arbeitsanteile des/der Doktoranden/in an der aufgeführten Publikation hinreichend und signifikant sind/*I confirm that all declarations made above are correct and that the doctoral student's independent contribution to this publication is significant and sufficient to be considered for the cumulative dissertation.*

Pro. Dr. Yamirka Rojas-agramonte
Name/*Name*

Unterschrift/*Signature*

30.10.2025
Datum/*Date*

Appendix 3

Prolonged evolution of an intra-oceanic island arc: The ~60 Myr record of Central Cuba

Authors

Haoyu Hu, Yamirka Rojas-Agramonte, Robert J. Stern, Aitor Cambeses, Manuel A. Iturralde-Vinent, Dora E. García-Delgado, Pieter Vermeesch, Shoujie Liu, Shitou Wu, Antonio Garcia-Casco

Abstract

The Cuban Arc preserves a ~60 Myr record of intra-oceanic island-arc construction, spanning Early Cretaceous tholeiitic (~135-125 Ma) to Late Cretaceous calc-alkaline magmatism (~90-75 Ma). Exceptional exposure of volcanic and intrusive igneous rocks across central Cuba enables integration of field relationships with geochemical signals, providing a rare natural laboratory for deciphering the temporal evolution and architecture of intra-oceanic arc formation. Zircon and apatite U-Pb geochronology combined with petrological, geochemical, and isotopic data documents an evolution from a nascent arc with melts derived from homogeneous depleted mantle to a hydrous magmatic plumbing system. Early low-K tholeiitic lavas display flat to slightly LREE-depleted REE patterns and limited enrichment in subduction-mobile elements, consistent with rapid ascent through thin crust and minimal crustal processing. Through the mid-Cretaceous, progressive mantle-wedge metasomatism by slab-derived fluids and melts enhanced LREE and Th enrichment and promoted magmatic differentiation. By the Cenomanian, calc-alkaline magmatism characterized by fractionated REE patterns, amphibole stabilization, and major plutonism with rising La/Yb and Sr/Y ratios indicating crustal thickening, marks the establishment of transcrustal plumbing systems capable of prolonged storage, recharge, and mixing. Isotopic proxies remain juvenile and homogeneous throughout the lifespan of the arc suggesting that temporal geochemical trends primarily reflect variations in slab input, magmatic differentiation, and crustal thickness, rather than changes in mantle source or involvement of continental crust. These results demonstrate how long-lived intra-oceanic arcs can progressively develop crustal architectures analogous to continental crust through secular tectono-magmatic processes.

INTRODUCTION

Intra-oceanic convergent margins (IOCMs) represent the oceanic end member of arc-trench systems where juvenile continental crust is generated by magmatic activity above subduction zones (Stern, 2010). They provide an ideal setting to study the generation and evolution of arc magmas, offering less complexity than found in continental arcs, where contamination by continental crust cannot be avoided. Because IOCM magmas are uncontaminated by continental crust, their igneous rocks more accurately record partial melting processes in the mantle wedge and fractional crystallization of basic magmas to create intermediate to acid derivatives. Comprising ~40% of present-day convergent plate margins, IOCMs include well-known examples such as the Izu-Bonin-Mariana, Tonga-Kermadec, Vanuatu, Solomon, New Britain, the western Aleutian arc, South Sandwich, and the Lesser Antilles (Leat & Larter, 2003). Changes in the chemistry of arc magmas have been linked to the temporal evolution of island arcs, with rapid magmatic changes accompanying subduction initiation when MORB-like forearc basalts and boninitic magmas are emplaced in a forearc environment (Whattam and Stern, 2011). This initial stage typically lasts 5-10 million years, after which magmatism migrates to a position approximately 100-150 kilometers above the subducting slab. Subsequent magmatic evolution progresses gradually, transitioning from depleted to increasingly enriched magmas over time, evolving from island arc tholeiite to calc-alkaline and, eventually, shoshonitic (alkaline) magmas (Stern, 2010; Straub et al., 2015).

Despite their significance, IOCMs are less studied than continental arcs because they mostly lie beneath sea level. Fossil IOCMs that have been uplifted, tilted and eroded provide opportunities to investigate IOCM crust, with notable examples including Kohistan (Jagoutz and Schmidt, 2012), Talkeetna (Greene et al., 2006), and the Famatinian arc (Ducea et al., 2015). This contribution examines another important example: the Cretaceous fossil IOCM of the Caribbean, which is accessibly exposed in central Cuba.

The Cuban segment of the Cretaceous Greater Antilles volcanic arc (part of the Great Arc of the Caribbean; Burke, 1988) was accreted to the North American Plate during its latest Cretaceous-mid Eocene. This happened through a series of collisions, first with the edge of the Maya Block and later the Bahamian borderland, which forms part of the North American continental margin (Iturralde-Vinent, et al., 2008; van Hinsbergen et al., 2009). Arc magmatism terminated in Cuba when that collision stopped subduction in latest Cretaceous time (ca. 70 Ma); this is when subduction/collision/accretion of passive margin sequences (now exposed in W, S and E Cuba and

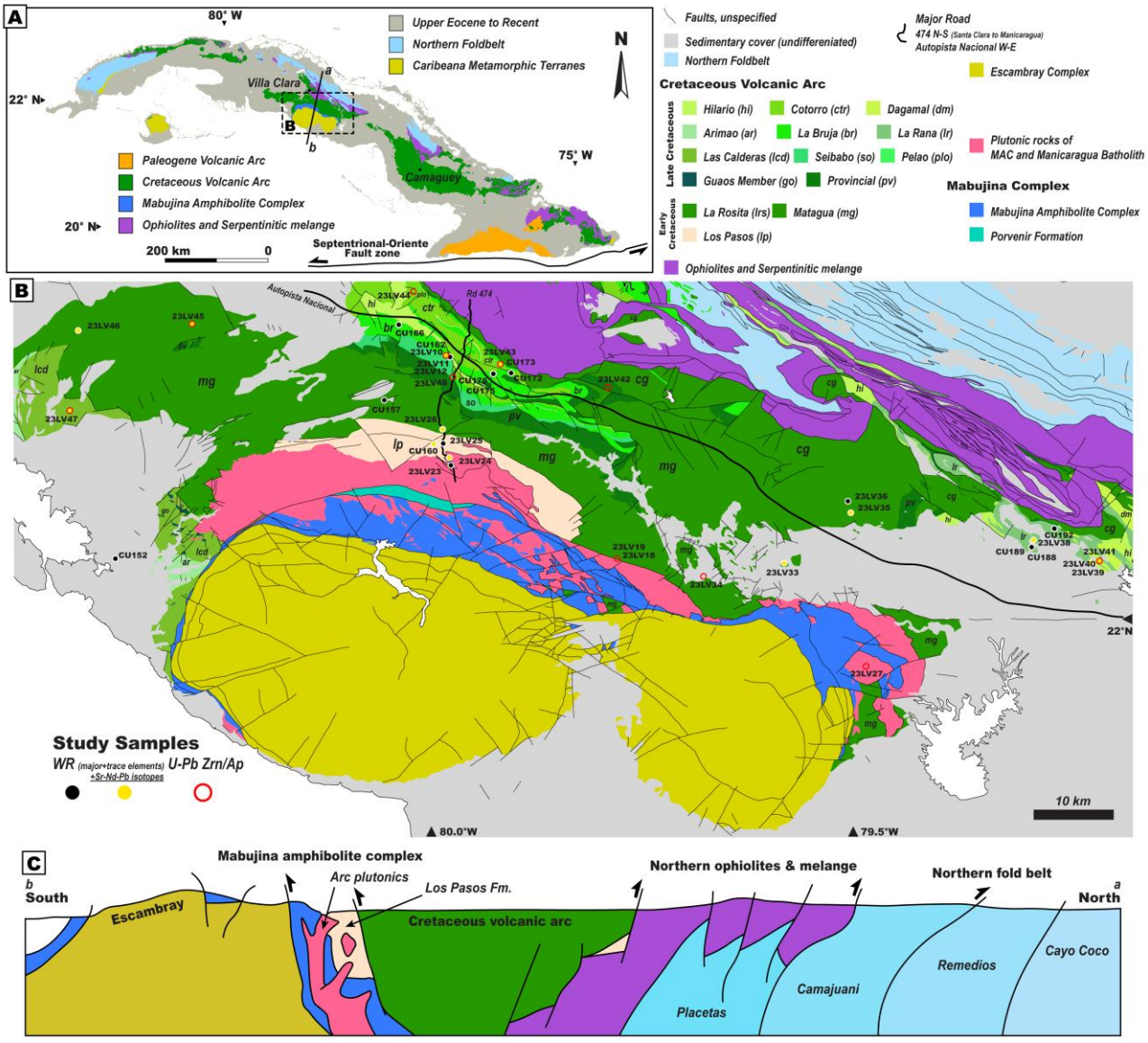

Figure 1. *(A) Simplified geological map of Cuba, modified after Wilson et al., (2019) and Hu et al. (2022). (B) Geological map of central Cuba showing sample locations, after García-Delgado (1998). (C) Cross-section of central Cuba (a-b in panel A), modified after Iturralde-Vinent (1998).*

Hispaniola) took place (Caribeana, Garcia-Casco et al., 2008) and arc-North American passive margin collision started (Iturralde-Vinent et al., 2008). Arc magmatism stopped in western and central Cuba, but resumed in eastern Cuba and to the east in Dominican Republic and Puerto Rico during the Paleocene-mid Eocene. Since the late Eocene, the polyphase Oriente Fault Zone, part of the North Caribbean Transform Fault System that marks the present-day North American-Caribbean plate boundary south of Cuba, separated Cuba from the rest of the Greater Antilles (Iturralde-Vinent, et al., 2016; Fig. 1). The Greater Antilles IOCM began to form during the Early Cretaceous (Fig. 2; as early

as ca. 133-135 Ma; Blanco-Quintero et al., 2011; Boschman et al., 2014; Braszus et al., 2021; Burke, 1988; Escuder-Viruete et al., 2014; Garcia-Casco et al., 2002; Jolly, 2001; Lázaro et al., 2009, 2016; Niu et al., 2022; Pindell and Kennan, 2009; Rojas-Agramonte et al., 2011; Rui et al., 2022, 2025) along the northern edge of the Caribbean plate. The Caribbean Plate formed as a consequence of two potentially related subduction events (Burke, 1998; Pindell & Kennan, 2009): one defining the eastern leading edge of the plate (~133-135 Ma) including the Greater Antilles Arc with westward-dipping subduction that involved the Proto-Caribbean plate, located between North and South American after the break-up of Pangea. Another defining the rear western edge (~100 Ma), where eastward-dipping subduction of the Pacific plate took place. The Cuban segment of the Greater Antilles Arc is well preserved and uplifted above sea level as a result of final "soft" collision with the North American plate (Garcia-Casco, et al., 2008; Iturralde-Vinent et al., 2016; van Hinsbergen et al., 2009). The Greater Antilles IOCM exposed in Cuba is a tilted and moderately to deeply eroded arc section extending more than 1000 km from west to east (Fig. 1). Over the past two decades, a wealth of geochemical and geochronological data on the Cuban magmatic arc has emerged as summarized in Hu et al. (2022).

The arc, as it outcrops in central Cuba, represents a nearly complete section that preserves a quasi-continuous record of magmatism since pre-middle Hauterivian time (~133-135 Ma; Rojas-Agramonte et al., 2011). Along the Greater Antilles, the stratigraphy of arc sections displays several nearly isochronous unconformities, where uplift, erosion and subsidence occurred, roughly dated to the Aptian, Santonian, late Campanian and Maastrichtian-Paleocene (Fig. 2; Iturralde-Vinent & Lidiak, 2006 and references therein). These discontinuities are probably associated with events that disrupted the normal steady-state subduction process, due to insertion of ridges as Caribeana terrain (Garcia-Casco et al., 2008) or segments of the westward extension of Atlantic Ocean ridge (Rojas-Agramonte et al., 2021). To decipher this tectonic conundrum, more detailed geochemical sampling, as well as a high-resolution seismic tomography, will be required to improve the temporal correlation between deep crustal and near surface events.

Previous geochemical studies have not provided an integrated comprehensive petrologic-geochemical-geochronologic model for the evolution of the arc from its infancy in the Early Cretaceous to its demise in the latest Cretaceous. This study presents new geochemical and isotopic data together with U-Pb zircon and apatite ages, and uses this information to develop such model. By integrating our results with data from the broader Caribbean region, we aim to offer a systematic

view of the regional magmatic evolution of the Greater Antilles IOCM and to contribute to a global understanding of IOCM magmatism.

GEOLOGICAL SETTING

The geodynamic evolution of the Caribbean realm began with the mid-Late Jurassic breakup of Pangea that formed the Proto-Caribbean ridge, the westward continuation of the Central Atlantic ridge. At the same time, an inter-American transform fault system likely developed between the Proto-Caribbean basin and the Farallon plate (Pindell et al., 2012). This system played an important role in the separation of North and South America. By ~135 Ma, subduction of Proto-Caribbean oceanic lithosphere began beneath the northern and eastern edge of the Farallon plate. On this allochthonous, Pacific (Farallon)-derived oceanic lithosphere the Greater Antilles Arc (GAA) developed during the Early Cretaceous from Cuba in the west to the Virgin Islands in the east (present-day coordinates). The subduction zone drove the east- and northward motion of the Caribbean plate into the inter-American gap, further facilitated by continued opening of the Central Atlantic since the Jurassic and of the South Atlantic since the Early Cretaceous (Burke, 1988; Eagles, 2007; Pindell et al., 2012; Pindell and Kennan, 2009).

Subduction along the Greater Antilles IOCM initiated with forearc seafloor spreading that generated ophiolitic sequences, such as the “northern ophiolites” and “eastern ophiolites” in Cuba (Butjosa et al., 2023; Domínguez-Carretero et al., 2025; Niu et al., 2022; Rui et al., 2022; Torró et al., 2017a; and references therein). GAA magmatism progressively shifted away from the trench, forming a volcanic-plutonic arc system as well as back-arc and intra-arc successions (Escuder-Viruete et al., 2014; Hastie et al., 2009; Lázaro et al., 2016; Lidiak and Anderson, 2015; Pindell and Kennan, 2009; Rojas-Agramonte et al., 2011, 2016). GAA magmatic compositions evolved from Early Cretaceous boninitic and island-arc tholeiitic signatures to more voluminous Late Cretaceous calc-alkaline magmas (Díaz de Villalvila, 1997; Donnely et al., 1990; Kerr et al., 1999; Lidiak and Anderson, 2015; Rojas-Agramonte et al., 2016; Torró et al., 2017a, b). Arc magmatism ceased by Late Campanian time but resumed in eastern Cuba and other parts of the Greater Antilles during the late Paleocene to middle Eocene (Iturralde-Vinent, 1996; Garcia-Casco et al., 2008; Rojas-Agramonte et al., 2006; Lidiak and Anderson, 2015). The late Campanian cessation has been attributed to collision of a rifted North American terrane, Caribeana, which is characterized by passive-margin sequences similar to those of the Maya Block and the Bahamas platform (Garcia-Casco et al., 2008; Iturralde-Vinent et al., 2016; and references therein). This collisional episode occurred between the latest Cretaceous

and middle Eocene (70-45 Ma; Iturralde-Vinent et al., 2008) and caused the Cuban section of Greater Antilles IOCM to override North American passive-margin sequences of the Bahamian Borderlands (Garcia-Casco et al., 2008; Iturralde-Vinent, 1996; Iturralde-Vinent et al., 2016; van Hinsbergen et al., 2009). Final collision and suturing between the Cuban segment of GAA and North America terminated with the accretion of the former to the latter, which favored a kinematic shift of the Caribbean plate to the south and formation of the Oriente transform fault south of Cuba and the Cayman spreading ridge, establishing a new plate boundary. This reorganization transferred the northwestern Caribbean plate, including Cuba, to the North American plate during the Paleogene (Iturralde-Vinent et al., 2016; Oliviera De Sá et al., 2024; and references therein).

The >1000 km of Cretaceous volcanic arc rocks in Cuba record three stages of volcano-sedimentary and plutonic activity with contrasting geochemical signatures, separated by unconformities (Díaz de Villalvila, 1997; Díaz de Villalvilla et al., 1994; Iturralde-Vinent, 1996; Iturralde-Vinent et al., 2016). Paleontological and geochronological data indicate an Early Cretaceous age for Cuba's ophiolites, interpreted as forming during subduction initiation (Butjosa et al., 2023; Domínguez-Carretero et al., 2025b; Niu et al., 2022; Proenza et al., 2018; Rui et al., 2022), marking the start of the Cuban IOCM magmatism.

In central Cuba, the Cretaceous arc is exceptionally well exposed, preserving a nearly complete arc section (Fig. 1 and 2). These exposures contain both volcanic and plutonic rocks which provide a unique opportunity to reconstruct this IOCM. In the Santa Clara region, a slightly deformed sequence of Cretaceous volcanic and plutonic arc rocks, exposed within a broad synform thrust along a north-south transect (Fig. 1), with the oldest and deepest units in the south in tectonic contact with the Mabujina Amphibolite Complex (metamorphic age ca. 92 Ma; protolith age 133-135 to >92 Ma; Rojas-Agramonte et al., 2011; Hu et al., 2024), and progressively younger rocks to the north trusted above the northern ophiolites (García-Delgado, 1998; Iturralde-Vinent, 1996, 2011). Island arc tholeiites (IAT) related to subduction initiation or early arc magmatism are mainly preserved in the Early Cretaceous Valanginn-Barremian Porvenir and Los Pasos formations (Dublan & Alvarez, 1986; Díaz de Villalvilla et al., 2003; Kerr et al., 1999; Rojas-Agramonte, et al., 2011; Torró et al., 2016). The Los Pasos Formation is overlain by the Aptian-Albian Mataguá Formation and by late Albian to mid Campanian arc-related volcanic and volcano-sedimentary successions with calc-alkaline signatures (Fig. 3 and 4; Díaz de Villalvila, 1997; Díaz de Villalvilla et al., 1994; Kerr et al., 1999). The calc-alkaline Manicaragua Batholith intruded the volcanic arc sequence and the Mabujina Amphibolite Complex between ca. 89 and 81 Ma (Rojas-Agramonte et al., 2011). It is composed

primarily of granodiorites and tonalites with subordinate quartz diorites containing mafic microgranular enclaves of dioritic composition (Bibikova et al., 1988; Blein et al., 2003; Somin, 1993; Somin and Millan, 1981; Sukar and Perez, 1997).

South of Santa Clara region of central Cuba, volcanic arc units rest structurally upon the Mabujina Complex, which comprises the Porvenir Formation and the Mabujina Amphibolite Complex (Millán-Trujillo, 1996). The Porvenir Fm. (Dublan & Alvarez, 1986), likely equivalent to the Los Pasos Fm., is a bimodal volcanic sequence metamorphosed under greenschist facies and tentatively dated as Berriasian?-Hauterivian? by regional correlation. The Mabujina Amphibolite Complex (MAC) consists of deformed, low- to intermediate-pressure amphibolites, including metaporphyritic, schistose/banded amphibolites, metagabbroic and metapyroxenitic (hornblendite) rocks, as well as intercalated tonalitic-trondhjemitic-granitic gneisses and veins, with local siliceous metasediments (Millan, 1996). Both units are arc-related with island-arc tholeiitic to calc-alkaline signatures (Kerr et al., 1999; Blein et al., 2003; Hu et al., 2024). U-Pb zircon ages from (meta-) tonalitic-trondhjemitic intrusions indicate that MAC developed during the Early-middle Cretaceous, with the oldest ages (~133 Ma) constraining the basaltic protoliths to at least Valanginian time (Rojas-Agramonte et al., 2011).

The Mabujina Amphibolite Complex tectonically overlies and encloses the high-pressure Escambray Complex, which forms a double-domal tectonic window (Trinidad and Sancti Spíritus) consisting mainly of Jurassic-Cretaceous passive margin metasediments with metabasite lenses and tectonically interleaved serpentinite-matrix mélanges with meta-ophiolitic blocks. The conditions of metamorphism are varied, ranging from low grade, intermediate-pressure (greenschist facies) and high-pressure (blueschist facies) to medium grade, high-pressure (eclogite facies) (Somin & Millán, 1972; Millán, 1997; Iturralde-Vinent, 1996; Despaigne-Díaz et al., 2016, 2017; Garcia-Casco et al., 2006, 2008; Schneider et al., 2004; Stanek et al., 2006, 2019). These metasedimentary units correlate with passive-margin successions in the Guaniguanico terrane of western Cuba and are interpreted as part of the Caribeana terrane, formed along the Maya block borderland (Garcia-Casco et al., 2008; Iturralde-Vinent, 2021).

The resulting orogenic belt in the Santa Clara region comprises thrust sheets derived from different lithospheric domains with distinct isotopic signatures, formed during and after the breakup of Pangea, including a coherent section of IOCM crust. These units encompass well-preserved passive margin

successions and allochthonous tectonic domains consisting of intra-oceanic volcanic arc sections and ophiolites (Kantchev et al 1978; Iturralde-Vinent et al, 2008).

Main formations

A detailed description of the stratigraphy of Central Cuba Arc is provided in Supplementary Material S1. Stratigraphy.

The Los Pasos Fm. (Díaz de Villalvilla et al., 1985; Pavlov, 1970) is the oldest exposed unit of the Central Cuba Arc, comprising bimodal volcanic rocks (rhyolite to basaltic andesite) with subordinate andesite, tuffs, breccias, and sedimentary intercalations. Effusive and subvolcanic facies dominate, with widespread hydrothermal alteration (epidote-actinolite, chlorite, sericite, quartz, carbonate, prehnite-pumpellyite) and common albitization of plagioclase (Díaz de Villalvilla, 1988; Díaz de Villalvilla et al., 1985; Dublan & Alvarez, 1986). The unit has low-Ti island-arc tholeiitic affinity with minor calc-alkaline affinity (Torró et al., 2016 and references therein). A ~125 Ma granodiorite intrusion corroborates that the Los Pasos Fm. is older than Barremian (Rojas-Agramonte et al., 2011).

The Mataguá Fm. (Brönnimann & Pardo, 1954; Zelepuguin et al., 1982) comprises porphyritic basalts, basaltic andesites, andesites, breccias, and tuffs, with rare acid lavas, and marks the transition from tholeiitic to calc-alkaline series. It is conformable with both the underlying Los Pasos Fm. and the overlying Cabaiguán Fm. (Hatten et al., 1958), which consists mainly of andesitic-dacitic tuffs, tuffites, sandstones, siltstones, and subordinate lavas, with diabase intrusions. The Provincial Fm. (Thiadens, 1937; Kantchev et al., 1978; Zelepuguin et al., 1985) is dominated by limestones (micritic, biogenic, biodetritic), marls, and calcareous conglomerates, lying concordantly above Mataguá and Cabaiguán Fms. These three units span the Aptian-Cenomanian.

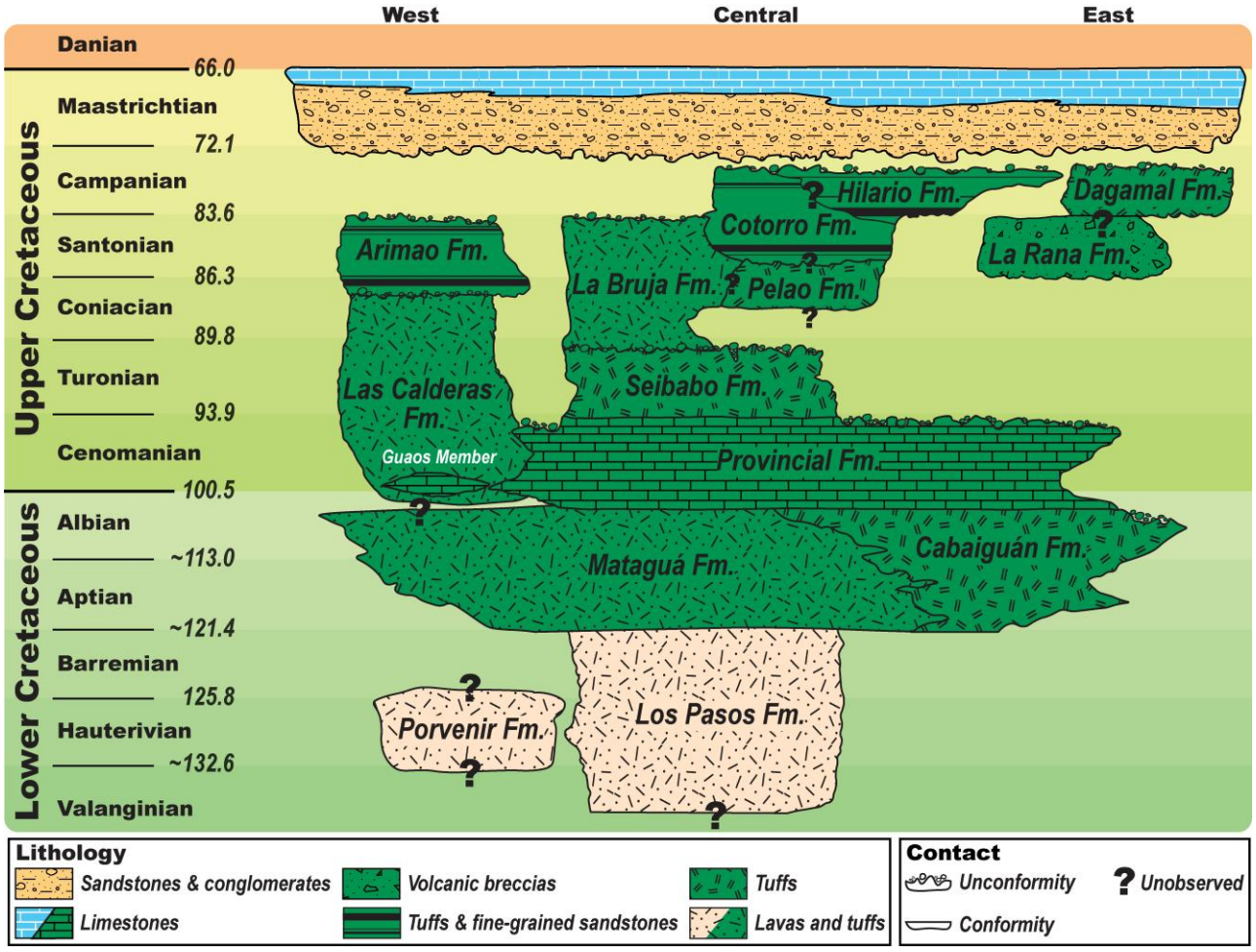

Figure 2. *Simplified stratigraphic framework of the central Cuban arc, modified after Iturralde-Vinent (2021). Lithostratigraphic units and contacts are compiled from the Geología de Cuba: Compendio (Iturralde-Vinent, 2021). Paleontologically constrained ages and field relationships from previous studies and mapping campaigns have been integrated with new observations from the 2023 fieldwork. The diagram emphasizes the main volcanic and volcaniclastic formations from which samples were collected. Further detailed mapping is required to refine unit boundaries and resolve remaining stratigraphic uncertainties.*

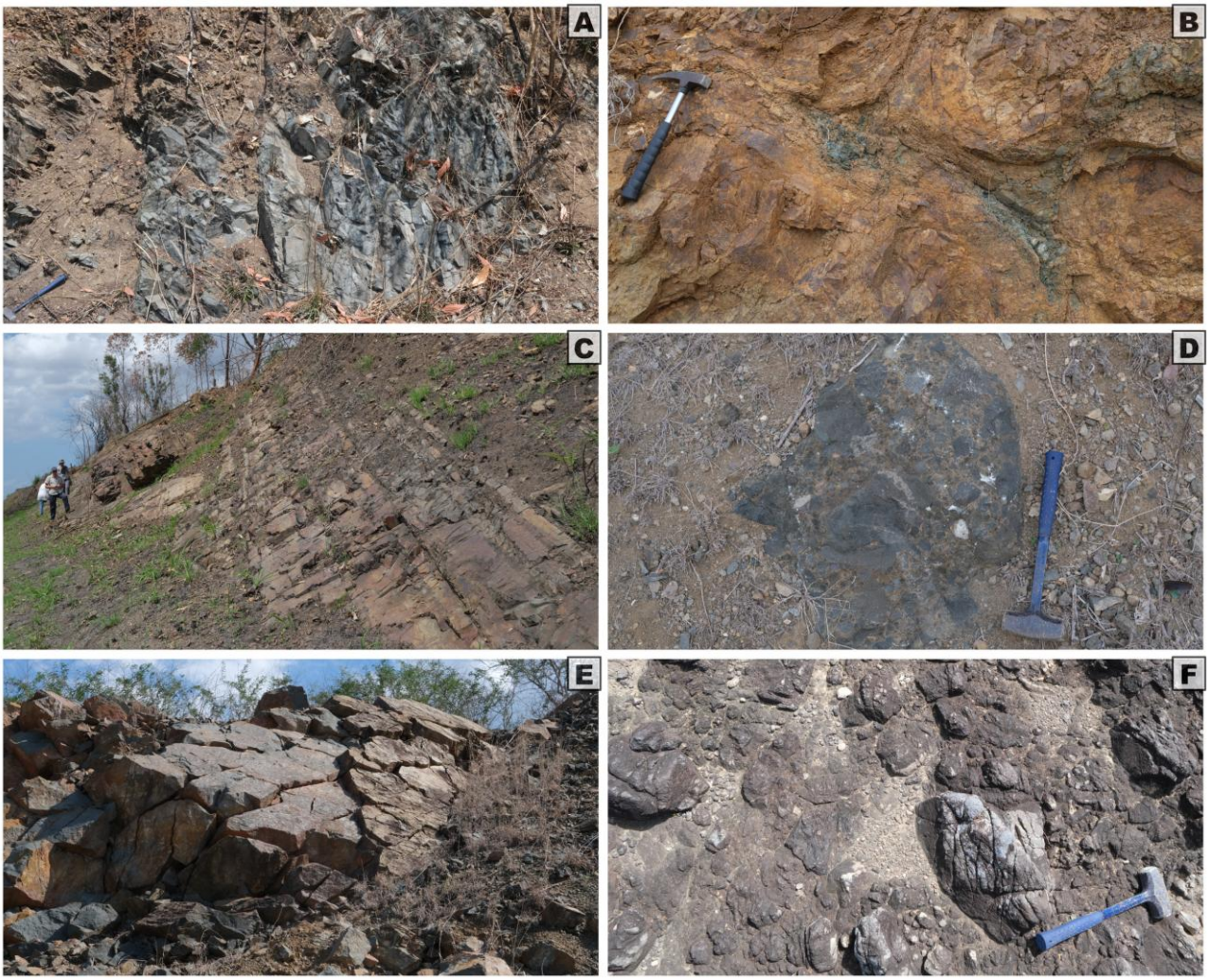

Figure 3. *Field photos of volcanic-sedimentary rocks from the Central Cuban Arc. (A) Massive plagiorhyolite of the Los Pasos Formation, early Cretaceous pre-Albian. (B) Strongly altered pillow lavas of the Cabaiguán Formation, early- to mid-Cretaceous Aliban-Cenomanian. (C) Well-stratified pyroclastic deposits composed of fine-grained tuff and lapilli tuff of the Seibabo Formation, late Cretaceous Cenomanian. (D) Peperite formed by intrusion of olivine basalt into unconsolidated sediment, La Bruja Formation, late Cretaceous Coniacian-Santonian. (E) Columnar jointing in a massive intermediate lava flow, Las Calderas Formation, mid- to late-Cretaceous Albian-Turonian. (F) Basaltic-andesitic volcanic breccia from the La Rana Formation, late Cretaceous Santonian.*

The overlying section record intermittent volcanism during the Late Cretaceous, marked by several unconformities associated with conglomerates and shallow carbonate platforms locally developed (Iturralde-Vinent, 1996; Iturralde-Vinent et al., 2008; Fig. 2). This succession embraces several lithostratigraphic units: The Turonian Seibabo Fm. (Brönnimann & Pardo, 1954, Kantchev et al., 1978) comprising alternating tuffs, marls, volcanogenic sandstones, and rare andesitic lavas. The Las Calderas Fm. (Dublan et al., 1986) containing diverse volcanic facies from basalts to dacites with strong hydrothermal alteration. The La Bruja Fm. (Brönnimann & Pardo, 1954; Kantchev et al., 1978) which consists mainly of andesite and dacite with breccias and tuffs (Coniacian-Santonian). The Coniacian-Santonian Arimao Fm. (Kantchev et al., 1978) comprises basaltic to dacitic lavas and tuffs interbedded with sediments. The Coniacian-Santonian Pelao Fm. (Kantchev et al., 1978; Díaz de Villalvilla, 1997) includes trachyandesitic welded tuffs. The Santonian-early Campanian Cotorro Fm. (Brönnimann & Pardo, 1954; Kantchev et al., 1978) is a volcaniclastic and polymictic flysch-like succession. The early Campanian Hilario Fm. (Brönnimann & Pardo, 1954; Kantchev et al., 1978) is dominated by zeolitized tuffs with interbedded marls and limestones. The Santonian La Rana Fm. (Hatten, 1958, Díaz de Villalvilla 1997) consists of calc-alkaline andesites, basaltic andesites, breccias, and tuffs (Santonian). The early Campanian Dagamal Fm. (Hatten et al., 1958) is dominated by andesitic-dacitic tuffs, often welded and lavas.

After a depositional and erosional hiatus, late Campanian-Maastrichtian clastic units and carbonate platforms deposited (e.g., Isabella Fm.) in syn-orogenic basins above the deformed volcanic arc series (Iturralde-Vinent, 1996; Iturralde-Vinent et al., 2008).

ANALYTICAL METHODS

Whole-rock major and trace elements were analysed by WD-XRF and ICP-MS at Kiel University (CAU) and the Centro de Instrumentación Científica of the University of Granada (CIC-UGR), respectively. Sr-Nd-Pb isotope ratios were measured by TIMS at the Complutense University of Madrid (UCM) and the GEOMAR Helmholtz Centre for Ocean Research Kiel (GEOMAR) using standard separation and double-spike procedures. Zircon U-Pb ages, trace elements, and Hf isotopes were obtained by SHRIMP and LA-MC-ICP-MS at the Chinese Academy of Geological Sciences (CAGS) and the Institute of Geology and Geophysics, Chinese Academy of Sciences (IGGCAS), and apatite U-Pb was analysed by LA-ICP-MS at IGGCAS and University College London (UCL). Mineral compositions were determined by EPMA at CAU. Full analytical methods and data quality information are provided in the Supplementary Material S2. Methodology.

RESULTS

Petrography

Here we present a summary of the studied samples; detailed field and petrographic descriptions of the samples are provided in the supplementary materials S3 Field Report and S4. Petrographic Descriptions.

The oldest volcanic arc sequence is represented by massive bimodal basic and acid volcanic rocks and outcrops of the Los Pasos Fm. Basaltic and basaltic-andesitic rocks, outcropping in the southern part of the Central Cuban Arc, were described by Díaz de Villalvilla et al. (2003) as having amygdaloidal aphyric to porphyritic textures, typical of subaqueous volcanic environments, and consist of plagioclase and clinopyroxene phenocrysts set in an intersertal to microlitic groundmass of plagioclase microlites. The acid rocks (plagio-rhyolites/dacites) generally display aphanitic to glomerophyric textures and contain plagioclase and quartz phenocrysts associated with Fe-Ti oxides, mostly magnetite. The felsitic groundmass locally shows secondary actinolite radiating from Fe-Ti oxides, and fiamme are occasionally present. Carbonatization is evidenced by calcite infilling and replacement of plagioclase phenocrysts accompanied by ubiquitous chloritization, suggesting that the rocks experienced lower greenschist facies metamorphism. Mafic dikes and granitic intrusions also occur. Mafic dikes are metadiabase; original clinopyroxene is commonly replaced by light green amphibole (actinolite) upon cooling and hydration, locally forming aggregates around magmatic relics. Some subvolcanic and gabbroic rocks contain brown magmatic amphibole overgrown by actinolite, a texture similar to that in the mafic dikes denoting hydration upon cooling. Tonalitic to trondhjemitic intrusions are composed mainly of quartz and plagioclase with variable amount of potassium feldspar and dark green amphibole. These rocks typically show minor deformation, recrystallization along grain boundaries, and cloudy altered plagioclase.

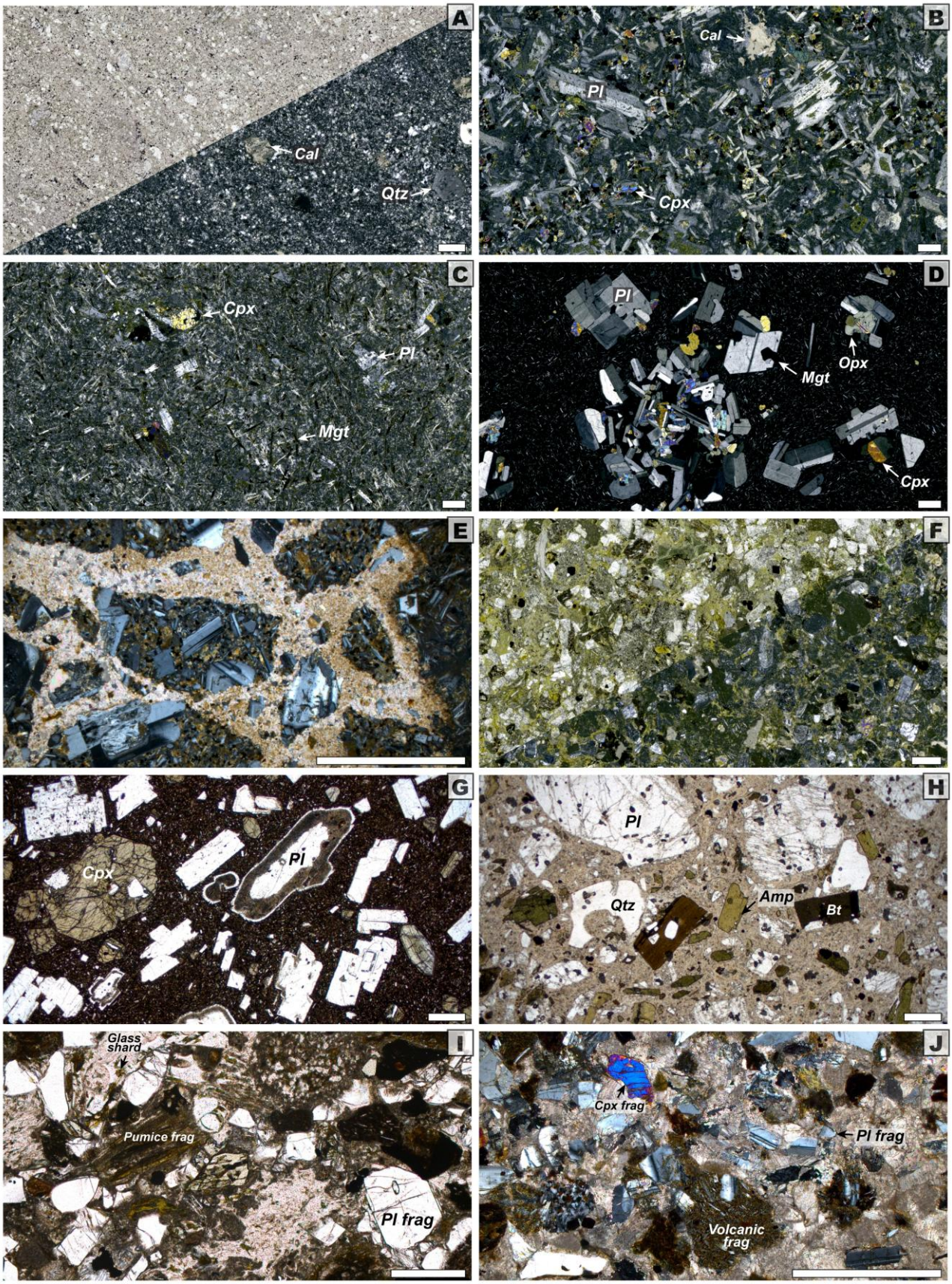
A
Cal
Qtz
B
Cal
Pl
Cpx
C
Cpx
Pl
Mgt
D
Pl
Mgt
Opx
Cpx
E
F
G
Cpx
Pl
H
Pl
Qtz
Amp
Bt
I
Glass shard
Pumice frag
Pl frag
J
Cpx frag
Pl frag
Volcanic frag

Figure 4. *Photomicrographs of volcanic-sedimentary rocks from the Central Cuban Arc. For A and F, plane-polarized (PPL) is shown on the left and cross-polarized light (XPL) on the right. (A) Sample 23LV25: Porphyritic plagiorhyolite show altered plagioclase phenocrysts replaced by calcite. (B) Sample 23LV33: Seriate basaltic andesite composed of tabular plagioclase laths and clinopyroxene and altered mesostasis, secondary chlorite and epidote are commonly observed. (C) Sample 23LV35: Glomerophyric andesitic pillow. Skeletal plagioclase and magnetite crystals display needle-shaped textures, locally exhibiting swallow-tail forms. (D) Sample CU176: Glomerophyric andesite with glomecrysts composed of clino- and orthpyroxenes, plagioclase and magnetite agglomerate embedded in a hyalopilitic matrix. (E) 23LV12: Peperite (autoclastic volcanic fragments) shows that the porphyritic basaltic lava shows jigsaw fit within fine-grained sedimentary matrix composed of carbonate and clay. A gradational transition from coarse volcanic clasts to finer sedimentary particles is evident. (F) Sample 23LV48B: A clast supported volcanic sandstone composed of lithic and crystal fragments. (G) Sample 23LV40A: Porphyritic basaltic andesite shows plagioclase and pyroxene phenocrysts with variety of complex textures of sieve and resorbed core and zonation. (H) Sample 23LV43: Dacitic welded crystal tuff display an apparent subvolcanic texture in the field, fragmented phenocrysts of amphibole, plagioclase are enveloped by recrystallized fine-grained ash exhibiting a rheomorphic structure. (I) Sample 23LV9B: A pyroclastic deposit of crystal and lithic fragments of varied source containing more than 20% recycled volcaniclastic material. (J) Sample 23LV9A: Calcareous volcanic sandstone with poorly sorted clasts including fragments of crystal and volcanic rocks of different rounding. Abbreviations: Amp: amphibole; Bt: biotite; Cpx: clinopyroxene; Mgt: magnetite; Pl: plagioclase; Qtz: quartz; frag: fragment. White bar indicates 500 µm.*

Subaqueous volcanic rocks are abundant in the overlying units, including the Mataguá and Cabaiguán Fms., which comprise basaltic hyaloclastites, basaltic-andesitic pillow lavas, evolved lava flows, and tuffs. Clinopyroxene and plagioclase phenocrysts are common, though zoning is generally absent. Textures range from vitrophyric to seriate and glomerophyric. Hydrothermal alteration is pervasive, with calcite filling interstices in the matrix. Sericitization and chloritization are also widespread across all lithologies. The Provincial Fm. is dominated by biomicritic limestone and calcareous volcanogenic sandstones containing abundant feldspar and volcanic lithic fragments. These volcanic fragments commonly display vitrophyric and porphyritic textures with wide compositional variation. The clasts are generally angular to subrounded and poorly sorted. Volcanic layers are locally interbedded with limestones.

In the northern part of the Central Cuban Arc, well-bedded volcaniclastic sediments dominate over lava flows. Lithologies and textures are diverse, but intermediate and acid volcanics are more abundant. Some mafic rocks are present, such as peperites from the La Bruja Fm., where olivine basalt intruded into unconsolidated calcareous sediments. Basaltic-andesitic breccias of the La Rana Fm. include minor mafic lithologies with phenocrysts of clinopyroxene, orthopyroxene, and olivine. Unzoned amphibole is present in intermediate and acid volcanic rocks. Disequilibrium textures are observed in pyroxene and plagioclase in La Rana Fm. basaltic andesites, while plagioclase in more evolved rocks commonly displays oscillatory and sector zoning. Biotite occurs in andesitic to dacitic welded crystal tuffs of the Pelao Fm. The volcaniclastic sequences are dominated by crystal and lithic fragments, with fewer sedimentary clasts. The lithic-crystal tuffs of the Hilario Fm. contain more than 20% recycled volcaniclastic material, including crystal fragments and rounded polygenetic volcanic clasts with varied textures and compositions. Matrices of volcaniclastic are dominantly calcareous. Overall, the lithological and textural variations indicate a temporal shift from quiet effusions of lava to increasingly explosive volcanic activity.

Whole rock geochemistry

Up to three stages of volcano-sedimentary rocks with contrasting geochemical signatures, separated by unconformities, are recognized in Cuba (e.g., Díaz de Villalvilla, 1997; Díaz de Villalvilla et al., 1994; Iturralde-Vinent, 1996, 2016; Torró et al., 2019). In this study, we assigned these units to three groups: Early Cretaceous tholeiitic, mid-Cretaceous transitional, and Late Cretaceous calc-alkaline sequences according to their whole rock geochemical features, as discussed below.

A total of 35 whole rock samples from Central Cuban Arc were analysed for geochemical composition. These include 4 samples from the Early Cretaceous Los Pasos Fm. tholeiitic sequence, 9 samples from the mid Cretaceous transitional sequence (Mataguá (6) and Cabaiguán Fms. (3)), and 22 samples from the Late Cretaceous calc-alkaline sequence: La Bruja (7), Las Calderas (4), La Rana (6), Pelao (2), Cotorro (1), Arimao (1), and Hilarios (1) Fms. The studied samples yield loss on ignition (LOI) values ranging mostly from 0.24 to 3.65 wt.%, reaching up to 8.24 wt.%, consistent with variable hydrothermal alteration (chloritization, sericitization, carbonatization, and silicification; see petrographic study and Supplementary Material S4. Petrographic Descriptions). To evaluate the extent of sub-solidus element mobility, major and trace elements were plotted against LOI and Th contents. Major elements show no correlation with LOI, indicating only minor element-mobility due to hydrothermal alteration or weathering (Fig. S1). Similarly, most trace elements (LILE, HFSE, REE,

Th) display no systematic relationship with LOI (not shown). Thorium, which is generally immobile during alteration and low-grade metamorphism of igneous rocks (Hastie et al., 2007), correlates well with La, Ba, Rb, Pb, and Nb (and weakly with K), implying limited post-magmatic element mobility in the analysed samples. However, K contents scatters particularly in transitional and calc-alkaline sequences. High-K samples commonly exhibit alteration textures and contain secondary K-rich mineral assemblages (e.g., sericite, K-feldspar, celadonite). This complicates using standard major element classification schemes such as TAS or K_2O vs. SiO_2 diagrams (Fig. 5A, B). Geochemical classification of the Central Cuban Arc samples is therefore based on immobile trace elements (Fig. 5C, D) and classifications based on major elements are offered for comparison, even if the two mostly agree.

Major and trace elements

Tholeiitic sequence (Los Pasos Fm.)

Studied samples from the Los Pasos Fm. include 2 rhyolites and 2 tonalites, as basaltic rocks were previously characterized (Díaz de Villalvilla et al., 2003; Torró et al., 2016); the more evolved lithologies are focused to obtain zircons for age determination, with tonalites analysed for comparison. Rhyolite samples contain 67 and 74 wt% SiO_2, are highly sodic (Na_2O around 5 wt%) and extremely K poor (K_2O = 0.05 wt%), yielding very high Na/K ratios and are classified as sub-alkaline rhyolites of tholeiitic affinity (Fig. 5). Available trace elements (Hu et al., 2022) are comparable to other acid volcanics from the Los Pasos Fm. (Díaz de Villalvilla et al., 2003; Hu et al., 2024; Rojas-Agramonte et al., 2016; Torró et al., 2016) with $[La/Sm]_{CN}$ = 0.7-1.45, $[Sm/Yb]_{CN}$ = 1.0-2.5 (most values <1.3), and Eu/Eu* = 0.63-0.99 (Fig. S2). Extended trace element patterns show pronounced Nb depletion ($[Nb/La]_{NMN}$ = 0.12-0.45). The tonalites (SiO_2 = 69-71 wt%; Na_2O = 3.6-4.3 wt%; K_2O = 0.15-0.22 wt%; Fig. 5) are classified using the Ab-An-Or normative diagram of O'Connor (1965). Their REE patterns are nearly flat, with $[La/Sm]_{CN}$ = 0.9-1.0, $[Sm/Yb]_{CN}$ = 1.2-1.3, and subtle Eu anomalies (Eu/Eu* = 0.92-0.96). Extended trace element patterns show pronounced Nb depletion ($[Nb/La]_{NMN}$ = 0.12-0.31), slight Th enrichment ($[Th/La]_{NMN}$ = 2.4-2.5), and very low Th contents (0.6-0.8 ppm).

Transitional sequence (Mataguá and Cabaiguán Fms.)

The studied samples from this sequence include basaltic (n = 2) and evolved volcanic rocks (n = 4; dacite to rhyolite) from Mataguá Fm., and three intermediate-acid volcanic rocks from the Cabaiguán

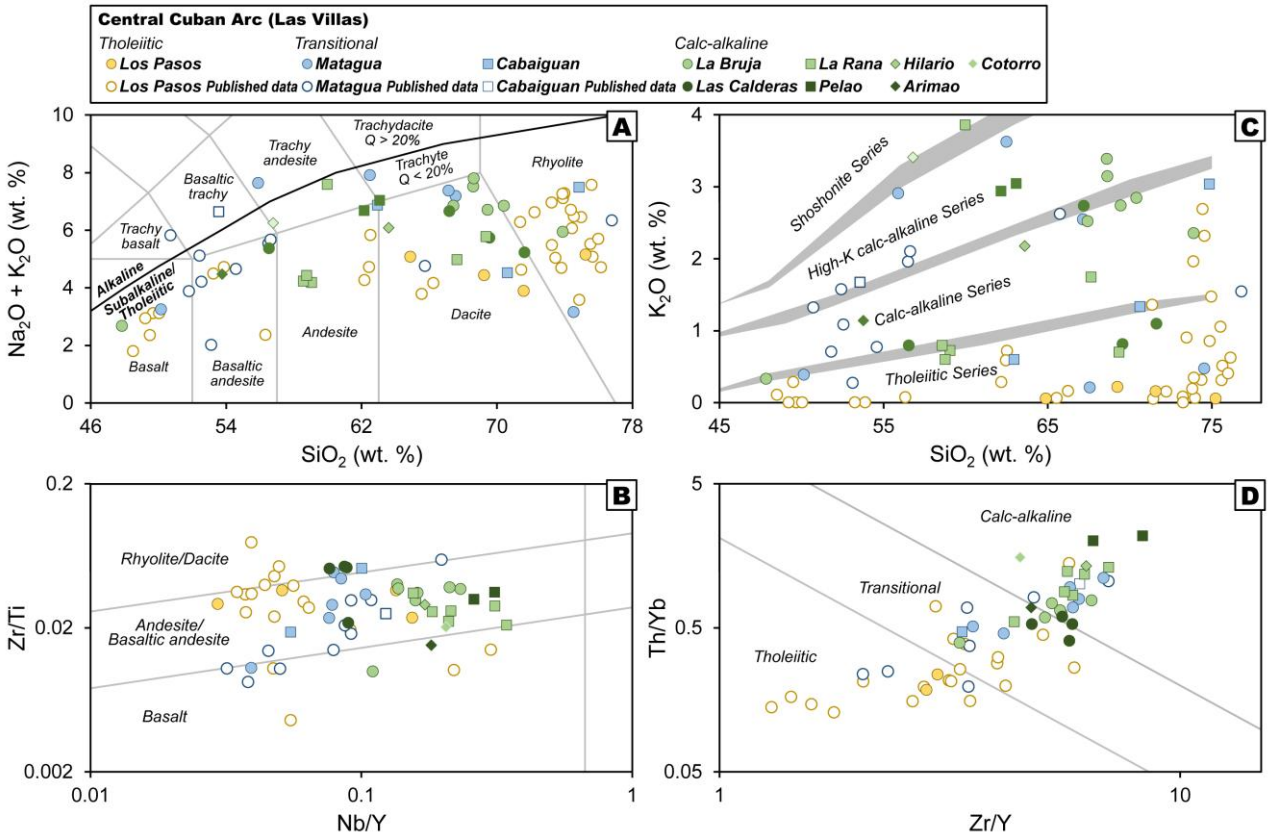

Figure 5. *Geochemical classification of studied rocks from the Central Cuban Arc. (A) Composition of the studied rocks in the TAS (after Le Bas et al., 1986). (B) SiO_2-K_2O (after Peccerillo and Taylor, 1976) classification diagrams. (C) Zr/Ti vs. Nb/Y (Pearce, 1996 after Winchester and Floyd, 1977). (D) Th/Yb vs. Zr/Y (after Ross and Bédard, 2009). Additional geochemical data for comparison are compiled from Kerr et al. (1999), Blein et al. (2003), Díaz de Villalvilla et al. (2003), Rojas-Agramonte et al. (2016), Torró et al. (2016), and Hu et al. (2024).*

Fm. (n = 3). In general, they show Nb depletion and greater Th enrichment ($[Th/La]_{NMN}$ = 2.1-3.6; Th contents from 0.92 to 4.09 ppm; Fig. S2) than the tholeiitic sequence, while high alkali content may reflect alteration. The mafic rocks (51-54 wt% SiO_2; K_2O = 0.4-2.8 wt%) are calc-alkaline basalt and basaltic andesite in Pearce (1996) and Hastie et al. (2007) classification diagrams, respectively. They are fractionated, with Mg# (Mg# = 100 × Mg / [Mg + Total Fe^{2+}]) values of 45-55. REE patterns show moderate LREE enrichment ($[La/Sm]_{CN}$ = 1.5-1.7), fractionation of MREE relative to HREE ($[Sm/Yb]_{CN}$ = 1.7-3.0), and modest Eu anomalies (Eu/Eu* = 0.8-1.2) (Fig. S2). Basalts and basaltic-andesites from previous studies (Hu et al., 2024; Kerr et al., 1999) show less fractionated REE patterns, with moderate LREE enrichment ($[La/Sm]_{CN}$ = 1.1-1.6), mild MREE-HREE fractionation ($[Sm/Yb]_{CN}$ = 1.4-2.5), and variable Th enrichment ($[Th/La]_{NMN}$ = 1.4-5.5) (Fig. S2), plotting within

the tholeiitic to transitional fields of Ross and Bédard (2009) (Fig. 5D). The acid volcanic rocks (64-71 wt% SiO_2; Na_2O = 2.6-6.9 wt%; K_2O = 0.2-3.7 wt%) range from dacite to rhyolite. They are classified as sub-alkaline dacite/rhyolite with calc-alkaline affinity. REE patterns are fractionated, with $[La/Sm]_{CN}$ = 1.7-2.0, $[Sm/Yb]_{CN}$ = 1.7-2.8, and negative Eu anomalies (Eu/Eu* = 0.7-0.9) (Fig. S2). The highest Th concentrations are observed in the evolved rocks of the transitional sequence between 1.2 and 4.1 ppm. The three Cabaiguán samples (SiO_2 = 61-76 wt%; Na_2O = 3.0-6.1 wt%; K_2O = 0.6-3.1 wt%) includes andesite and dacite. The analysed intermediate lava is classified as sub-alkaline andesite (Fig. 5), and shows moderate LREE-enrichment ($[La/Sm]_{CN}$ = 1.6) and strong Nb depletion ($[Nb/La]_{NMN}$ = 0.09) with ~1.8 ppm Th), lacking Eu anomaly (Fig. S2).

Calc-alkaline sequence (La Bruja, Las Calderas, La Rana, Pelao, Cotorro, Arimao, and Hilarios Fms)

Twenty two samples from the calc-alkaline sequence are volcanic and plutonic rocks comprising basalts (2), basaltic andesites-andesites (9), dacite-rhyolites (10), and one tonalite. They are consistently characterized by strong Nb depletion, moderately to strongly LREE- and MREE-enriched patterns ($[La/Sm]_{CN}$ = 1.4-3.5; $[Sm/Yb]_{CN}$ = 1.4-2.6), positive Th anomalies ($[Th/La]_{NMN}$ = 1.7-4.7), and Th concentrations between 0.6 and 4.1 ppm (Fig. S2). These features are comparable to calc-alkaline samples from the transitional sequence (Fig. 5), and plot in the calc-alkaline field of Hastie et al. (2007). Negative Eu anomalies are common in acid rocks, indicating plagioclase fractionation. Basalts are represented by one sample from the La Bruja Formation (47 wt% SiO_2, Th = 0.7 ppm, Mg# = 48) and one from the Arimao Formation (52 wt% SiO_2, Th = 1.1 ppm, Mg# = 44); both are sub-alkaline, moderately LREE-enriched ($[La/Sm]_{CN}$ = 1.4-2.1), and lack Eu anomalies (Fig. S2). Basaltic andesites-andesites show strong LREE enrichment ($[La/Sm]_{CN}$ = 1.7-3.5), Nb depletion, generally lack Eu anomalies, and Mg# ranging from 42 to 57. These dacite-rhyolite rocks are strongly LREE-enriched and display strongly negative Eu anomalies (Eu/Eu* = 0.6-0.9), especially in the Las Calderas Fm. Granitoid intruding the La Rana Fm. (68.8 wt% SiO_2, Th = 3.0 ppm) is trondhjemite using O'Connor's (1965) Ab-An-Or diagram; it shows LREE enrichment, Nb depletion, and a negative Eu anomaly (Eu/Eu* = 0.7) (Fig. S2).

Radiogenic isotope compositions

Figure 6 shows whole rock Nd, Sr and Pb radiogenic isotope compositions of the studied samples. Corrections for post-emplacement radiogenic growth are based on U-Pb zircon and apatite ages (see below) and biostratigraphic constraints discussed in the stratigraphy section. Tholeiitic samples yield

$^{143}Nd/^{144}Nd$ ratios between 0.512986 and 0.513052 (n = 4), and initial εNd between 7.0 and 8.3. Samples from the transitional series have very similar $^{143}Nd/^{144}Nd$ ratios between 0.512964 and 0.513063 (n = 8) and initial εNd between 7.2 and 8.7. Samples from the calc-alkaline series yield $^{143}Nd/^{144}Nd$ ratios between 0.512912 and 0.513081 (n = 12), and initial εNd between 6.1 and 9.2. Initial $^{87}Sr/^{86}Sr$ ratios decrease from tholeiitic ($^{87}Sr/^{86}Sr_t$ = 0.704399-0.704750) to transitional ($^{87}Sr/^{86}Sr_t$ = 0.703339-0.704379) to calc-alkaline ($^{87}Sr/^{86}Sr_t$ = 0.703154-0.703875) sequences.

The analysed tholeiitic (Los Pasos Fm.) sample has $^{206}Pb/^{204}Pb$ ratio of 18.617, $^{207}Pb/^{204}Pb$ of 15.556 and $^{208}Pb/^{204}Pb$ of 38.146. Seven samples from the transitional series (n = 7) have $^{206}Pb/^{204}Pb$ ratios of 18.544-20.072, $^{207}Pb/^{204}Pb$ of 15.551-15.626 and $^{208}Pb/^{204}Pb$ of 38.131-38.636. Calc-alkaline samples (n = 8) have $^{206}Pb/^{204}Pb$ ratio of 18.439-19.056, $^{207}Pb/^{204}Pb$ of 15.564-15.584 and $^{208}Pb/^{204}Pb$ of 38.105-38.578, all between DMM and EM2 reservoirs and plot broadly along the northern hemisphere reference line (NHRL).

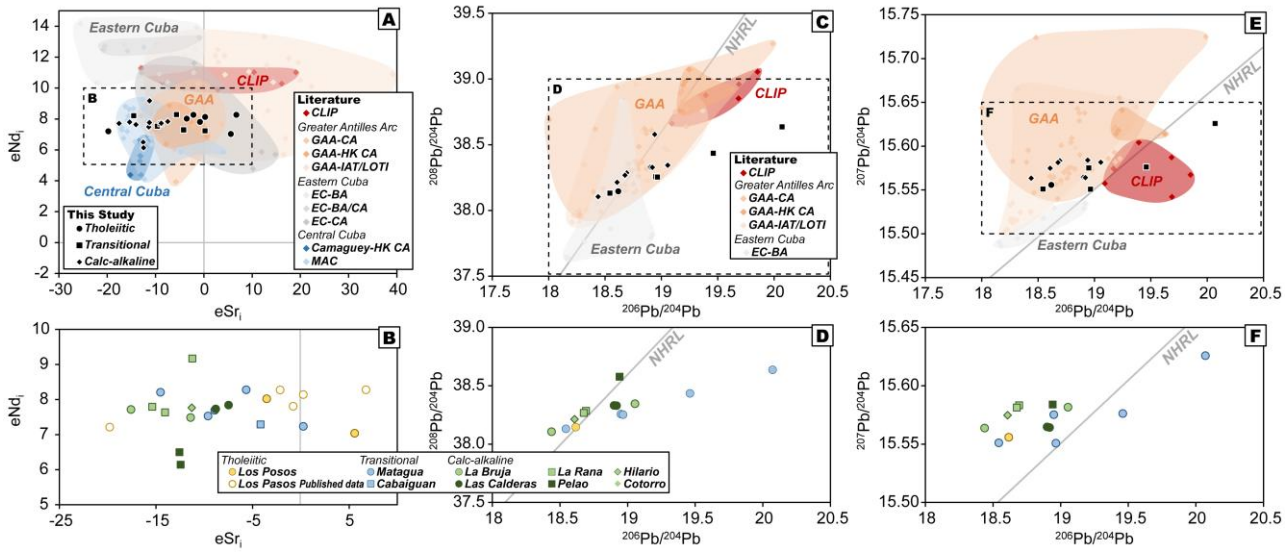

Figure 6. *(A) Age-corrected Sr-Nd radiogenic isotope ratios of whole-rocks from Central Cuban Arc. (B and C) Pb isotope system of $^{206}Pb/^{204}Pb$ vs. $^{208}Pb/^{204}Pb$ and $^{206}Pb/^{204}Pb$ vs. $^{207}Pb/^{204}Pb$. Colored field represent the compositional ranges of the Greater Antilles Arc, complied from Jolly et al. (1998; 2001; 2008); Frost et al. (1998); Hastie et al. (2008; 2009); Torró et al. (2017a; 2020); Marchesi et al. (2007); Hu et al. (2024); Blein et al. (2003); Rojas-Agramonte et al. (2016); Allibon et al. (2008); Schellekens (1998). Key: IAT = island arc tholeiites; LOTI = low-Ti IAT; CA = calc-alkaline; HK-CA = high-K calc-alkaline; BA = Back arc basalts; CLIP = Caribbean Large Igneous Province; MAC = Mabujina Amphibolite Complex.*

Mineral composition

Pyroxene

Clinopyroxene (Cpx) phenocrysts from the transitional sequence are characterized by low sodium contents (Na < 0.3 a.p.f.u.); low Ti (< 0.03 a.p.f.u.) and Cr (< 0.01 a.p.f.u., mostly below detection limits). In basaltic samples of this sequence, clinopyroxene phenocrysts belong to the diopside-augite solid solution (Fig. 7A1), though most are augite. They show variable Al_2O_3 (0.07-0.25 Al a.p.f.u.), Ca (0.70-0.88 a.p.f.u.), and elevated Mg# values ranging from 65 to 81. In andesite-dacite samples, clinopyroxenes are predominantly augite, with Mg# values between 61 and 76, variable Al_2O_3 (0.04-0.13 Al a.p.f.u.), and Ca (0.72-0.84 a.p.f.u.). Clinopyroxenes from the Mataguá Fm. display a positive correlation among Al_2O_3, TiO_2, Na_2O, and FeO*, and a negative correlation between these elements and MgO and SiO_2. In contrast, clinopyroxenes from the Cabaiguán Fm. show lower Na_2O and TiO_2 concentrations at a given Mg#.

Clinopyroxene phenocrysts from the calc-alkaline sequence are mostly augite, with occasional diopsidic cores, while pigeonite is in the groundmass associated with enstatite (Fig. 7A2). They show variable Al_2O_3 contents (0.04-0.38 Al a.p.f.u.), Ca (0.68-0.89 a.p.f.u.), and wide Mg# values (59-90), but consistently low alkali (Na < 0.06 wt%; K mostly below detection limit), Ti (< 0.05 a.p.f.u.), and Cr (< 0.04 a.p.f.u.) concentrations. In the La Bruja basalt, augite occurs as overgrowth rims and in the groundmass, whereas resorbed diopsidic cores contain higher Cr, Mg, and Ca and lower Ti (Mg# = 85; Ca = 0.89 a.p.f.u.) compared with the lower-Mg# augitic rims. The La Rana basaltic andesite contains augite phenocrysts (Al = 0.06-0.39, mostly <0.18 a.p.f.u.; Mg# = 63-87) that show positive correlations among Al_2O_3, TiO_2, Na_2O, and FeO*, and negative correlations with MgO and SiO_2. Texturally, clinopyroxenes and orthopyroxenes (Opx; enstatite, Mg# = 64-85) display diverse zoning styles (normal, reverse, and unzoned), with large variations in Al, Mn, Ti, and Cr both within and between crystals. The groundmass contains pigeonite with Ca (0.14-0.18 a.p.f.u.) and Mg# = 59-72; alkalis, Ti, and Cr contents are similar to augitic phenocrysts in the same samples. In La Bruja andesite, augite phenocrysts are compositionally restricted (Al_2O_3 = 1.26-1.73 wt%; Mg# = 68-69; Ca = 0.77-0.78 a.p.f.u.), with groundmass clinopyroxenes including augite (Mg# = 41-69; higher Al_2O_3 and Ti) and pigeonite (Mg# = 57-59; Ca = 0.20-0.23 a.p.f.u.); coexisting enstatite phenocrysts have Mg# = 63-65. Volcaniclastic samples from the La Bruja and Dagmal Fms. also contain augite phenocrysts (Mg# = 67-90; Ca = 0.74-0.89 a.p.f.u.; Al_2O_3 = 0.98-4.78 wt%) exhibit resorbed diopsidic core, comparable to those in volcanic counterparts (Fig. 7A3).

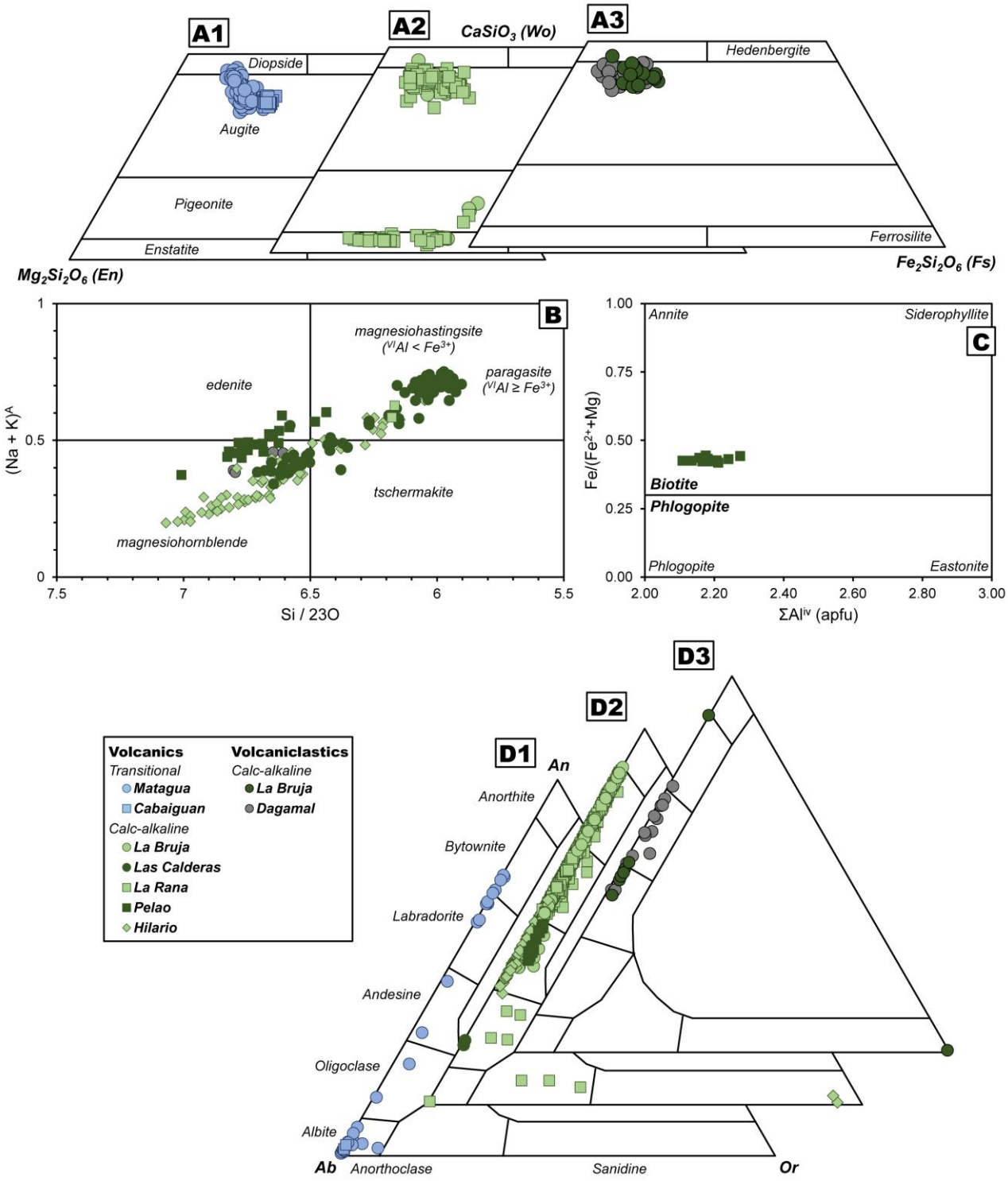

Figure 7. *(A) Ternary classification diagram for quadrilateral pyroxenes including analyses of clinopyroxene and orthopyroxene. (B) Amphibole classification diagram after Leake et al. (1997). (C) Biotite classification diagram after Rieder et al. (1998). (D) Composition of feldspars in terms of molar contents of anorthite (An), albite (Ab) and orthoclase (Or) components.*

Amphibole

Amphiboles (Amp) from the calc-alkaline sequence belong to the calcium subgroup and are classified as magnesio-hastingsite, magnesio-hornblende, tschermakite, edenite, and pargasite (Fig. 7B). They display wide compositional ranges, with Si = 5.90-7.07 a.p.f.u., Al_{tot} = 1.09-2.62 a.p.f.u., Mg = 2.66-3.61 a.p.f.u., and Fe_{tot} = 0.92-1.91 a.p.f.u. In position A, Na (0.16-0.67 a.p.f.u.) generally exceeds K (0.02-0.25 a.p.f.u.). In position B, Ca (1.53-1.93 a.p.f.u.) dominates over Na, Fe^{2+}, and Mn. In position C, Mg concentrations are systematically higher than the combined Fe^{2+}, Fe^{3+}, Al, and Ti contents. Mg and Fe^{2+} are inversely correlated with Ti, Fe^{3+}, and Al, reflecting exchange relationships within the actinolite-hornblende-pargasite system. In zoned crystals, the amphiboles display pargasitic-hastingsitic cores and hornblende rims.

In andesitic rocks, amphiboles from the Las Calderas Fm. classify as magnesio-hastingsite, magnesio-hornblende, edenite, pargasite, and tschermakite, with variable compositions (Si = 5.90-6.71; Al_{tot} = 1.47-2.62; Mg = 2.68-3.47; Fe_{tot} = 0.97-1.89). They commonly show thin overgrowth rims with lower Al and total alkali contents, lower Mg#, and higher Mn compared to crystal interiors, with Mg# ranging from 63 to 67, indicating decreasing crystallization temperatures. Amphiboles in the Pelao Fm. andesite are magnesio-hastingsite, magnesio-hornblende, and edenite (Si = 6.44-7.01; Al_{tot} = 1.09-1.78; Mg = 2.66-3.10; Fe_{tot} = 1.63-1.91), characterized by a narrower Mg# range of 58-65 and higher K and Mn contents. Core and rim from single grains yield similar composition. Amphiboles from the Hilario Fm. andesite classify as magnesio-hastingsite, magnesio-hornblende, and tschermakite (Si = 6.05-7.07; Al_{tot} = 1.12-2.34; Mg = 2.87-3.61; Fe_{tot} = 0.92-1.69), with Ca consistently dominant in position B (1.53-1.80). Amphiboles in the La Rana basaltic andesite occur as xenocrysts rimmed by Fe-Ti oxides and classify as magnesio-hastingsite. They are relatively uniform in composition (Si = 6.17-6.18; Al_{tot} = 2.17-2.21; Mg = 3.36-3.38; Fe_{tot} = 1.17-1.19), with position C dominated by Mg and lower Fe, Al, and Ti.

Amphiboles from volcaniclastic rock of the Dagamal Fm. are magnesio-hastingsite and magnesio-hornblende, with a narrower compositional range (Si = 6.34-6.80; Al_{tot} = 1.34-1.93; Mg = 3.01-3.14; Fe_{tot} = 1.44-1.66). Their chemistry is broadly similar to that of their volcanic counterparts, though more restricted in variation.

Biotite

Biotite (Bt) from the Pelao Fm. andesite is homogeneous (Fig. 7C). The octahedral (M) sites are mainly occupied by Mg, Fe, and Ti, with Mg# values of 55-58 and Ti contents of 0.24-0.30 a.p.f.u. The tetrahedral (T) site is systematically deficient in Si + Al (7.75-7.81), which would indicate that the T site must host Fe^{3+}, and exhibits Si/Al ratios of 2.4-2.7, consistent with equilibrium in alkaline magma (Fig. S3B). The interlayer site is nearly fully occupied (>1.82 a.p.f.u.), dominated by K (1.70-1.82) with minor Na (0.10-0.12).

Feldspar

Feldspar compositions in Central Cuban Arc lavas are variable, including abundant plagioclase (Pl; Ca-Na) ranging from bytownite to albite (An 89-1) and rare alkali feldspar (Na-K) (Fig. 7D1-D3). Phenocrysts and microlites of plagioclase commonly display complex zoning and resorption textures that record dynamic magmatic processes, whereas sodium- and potassium-rich feldspars are mostly secondary. The most calcic plagioclase occurs in mafic lithologies. In the Mataguá Fm. of the transitional sequence, plagioclase phenocrysts in basalts range from labradorite to bytownite (An 62-74), and inclusions within clinopyroxene are also labradorite. In dacitic samples from the Mataguá Fm., plagioclase phenocrysts are andesine (An 32-46). Albite and oligoclase are common replacements of calcic plagioclase and also occur as individual crystals and microlites in the groundmass. The calc-alkaline La Bruja basalt contains plagioclase in the matrix and as microlites, with compositions from labradorite to bytownite (An 67-90). Thin labradorite rims around more calcic cores show normal zoning, with decreases in An content of up to 11 mol%.

Basaltic andesites from the calc-alkaline La Rana Fm. show the most textural diversity. Phenocrysts display patchy and oscillatory zoning as well as sieve textures, with compositions spanning An 45-89. Patchy-zoned crystals contain irregularly corroded calcic cores (An 77-89) with glass and mineral inclusions, overgrown by more sodic plagioclase (An 51-60). The compositional transitions are abrupt, with decreases of 30-40 mol% An. Groundmass plagioclase forms two microlite generations: andesine-labradorite (An 38-62) and more sodic compositions including oligoclase (An 17-25), albite (An 5-6), and anorthoclase (An 5-6 Ab 63-75 Or 18-33). In the Hilario Fm., plagioclase phenocrysts range from andesine to labradorite (An 29-54) and are partly replaced by alkali feldspar. Andesites yield intermediate plagioclase compositions. In the La Bruja Fm., phenocrysts are andesine-labradorite (An 41-55) with oscillatory zoning, particularly in glomerocrysts, while microlites are more sodic (An 36-40). In the Pelao Fm., phenocrysts are andesine (An 38-46) and inclusions within

biotite and amphibole of similar composition (An 41-48). By contrast, the Las Calderas Fm. contains oligoclase (An 16-17), reflecting secondary alteration overprinting original magmatic compositions.

Volcaniclastic rocks from the La Bruja and Dagamal Fms. yield plagioclase compositions from andesine to bytownite (An 41-71), with rare examples up to An 89. In the La Bruja Fm., feldspars give a narrower range (An 41-48). Fragments from the Dagamal Fm. yield andesine-labradorite (An 42-63), with reverse zoning expressed as labradorite rims on andesine cores. Vitrophyric volcanic fragments contain labradorite-bytownite (An 53-71).

Geochronology and Zircon Hf isotopes

U-Pb igneous apatite and zircon ages

Zircon grains from five Central Cuban Arc igneous rock samples as well as apatite grains from eight samples were analysed for U-Pb ages using SHRIMP and LA-ICP-MS respectively. The zircon grains in each sample display similar textures and grain sizes and are well-formed prismatic crystals, indicating a single magmatic population with no evidence for inherited cores or xenocrystic contamination. U-Pb zircon ages resulted in five magma crystallization ages ranging from 125.1 ± 1.2 to 83.3 ± 0.9 Ma (Fig. 8A-E) from three formations, in agreement with existing geochronological and stratigraphic constraints.

On the other hand, LA-ICP-MS analysis of igneous apatites yielded ages ranging from 122+4/-5 Ma (CAS; MSWD = 1.6) and 129 ± 9 Ma (UCL; MSWD = 1.0) for the Mataguá Fm., to 76+5/-8 Ma (CAS; MSWD = 2.6) and 75 ± 12 Ma (UCL; MSWD = 0.8) for the Hilario Fm.

U-Pb detrital zircon ages

LA-ICP-MS U-Pb analysis of detrital zircons from intercalated sedimentary rocks of the Central Cuban Arc (173 analyses from 6 samples from 4 units) yielded U-Pb ages ranging from 122 to 62 Ma (Fig. 9). Zircons range from euhedral (prismatic to elongated) to broken grains; cathodoluminescence images (CL) show oscillatory and convolute zoning and signs of magmatic resorption. No systematic correlation exists between zircon shape and age.

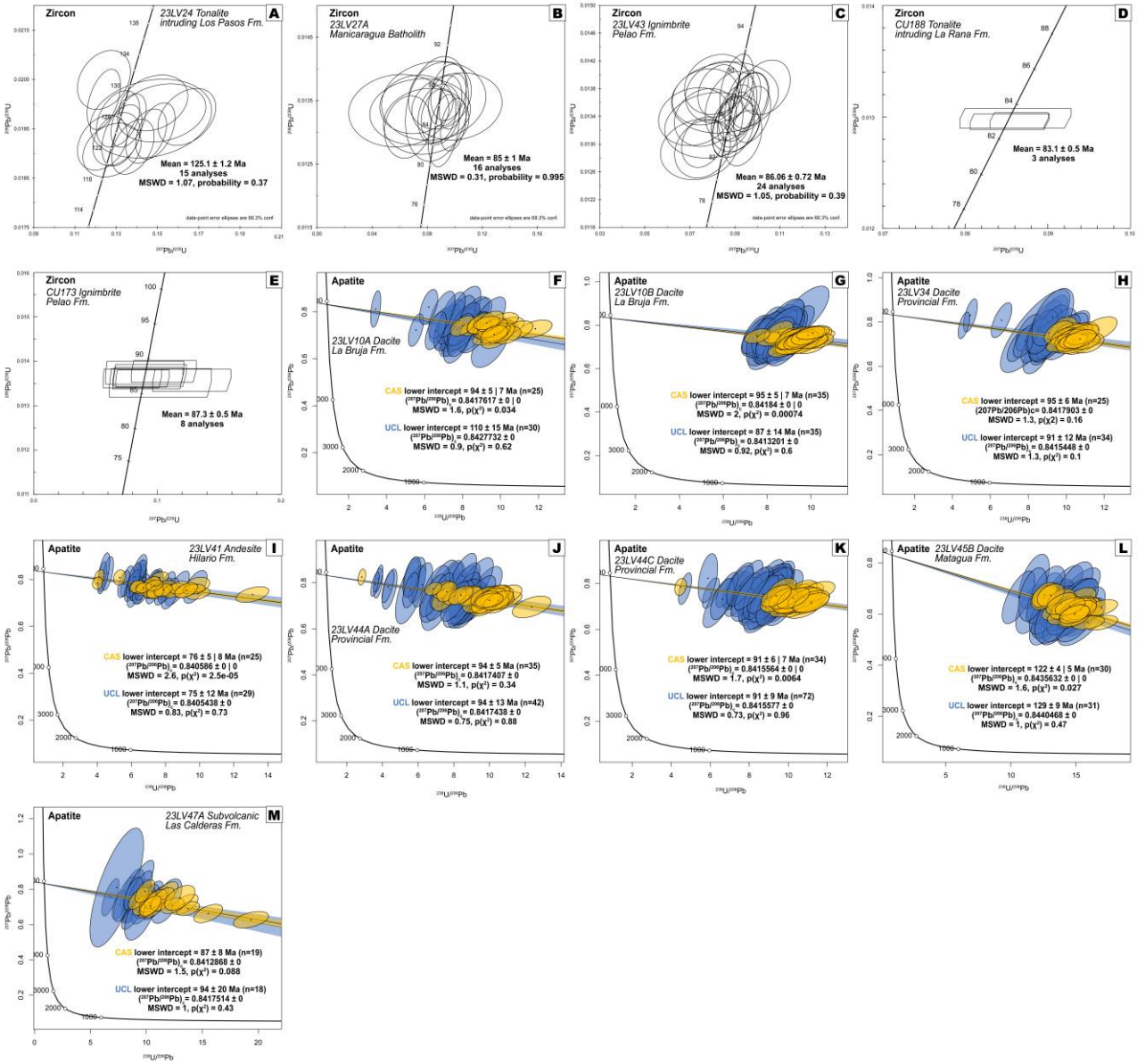

Figure 8. *Concordia (zircon) and Tera-Wasserburg (apatite) U-Pb diagrams obtained for the different accessory minerals analysed: (A-E) zircon and (F-M) apatite. CAS: China Academy of Science. UCL: University College, London.*

Hafnium isotope results

Early Cretaceous zircons from a tonalite intrusion yield variable εHf(t) values (+7.3 to +15.1), while late Cretaceous volcanic and plutonic rocks show εHf(t) values of +10.6 to +14.2 (Fig. 9A and B), typical of juvenile oceanic arc magmas. For detrital zircons, εHf(t) values are similarly juvenile (+8.7 to +17.7) and trace element signatures are magmatic arc-like (supplementary materials S5. Zircon CL Images and Trace Element).

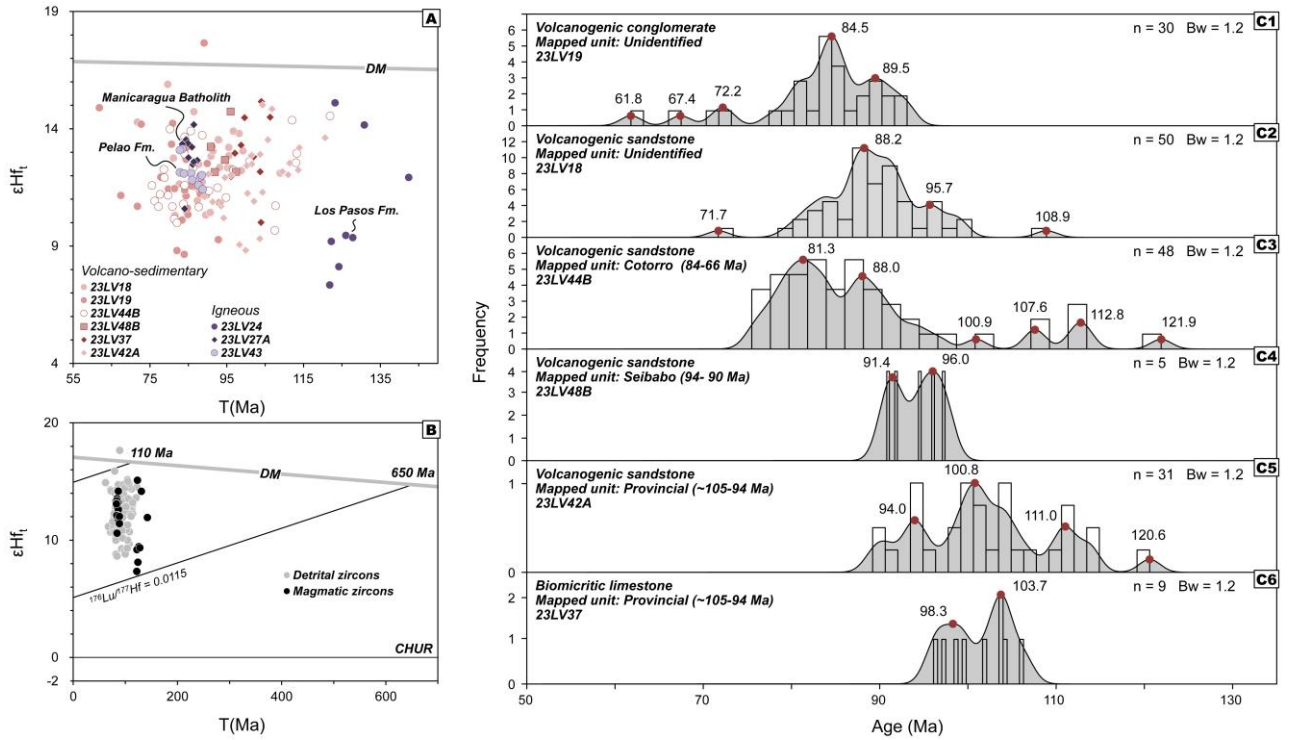

Figure 9. *(A and B) Plot of εHf (t) versus crystallization age of magmatic and detrital zircons from Central Cuban Arc and the intercepts between εHf (t) and the depleted mantle curve are based on a $^{176}Lu/^{177}Hf$ average crustal ratio of 0.0115. (C) Probability density plot showing U/Pb zircon ages of detrital zircon from volcano-sedimentary deposits of the Central Cuban Arc.*

DISCUSSION

Below we use our new data to discuss 5 topics concerning the evolution of the Central Cuban Arc: 1) age constraints of the arc; 2) intercalated sediment provenance inferred from detrital zircons; 3) Central Cuban Arc magmatic source components; 4) mineral records of the magmatic reservoirs; and 5) crustal growth of Central Cuban Arc.

Age constraint on the evolution of the Central Cuban Arc

Volcanic rocks from the Los Pasos Fm. have not been directly dated but inferred by their stratigraphic position as Early Cretaceous (Hauterivian?-Barremian; Iturralde-Vinent, 2011; Rojas-Agramonte et al.,2011). Unfoliated low-K trondhjemitic/tonalitic bodies intruding low-Ti IAT basalts of the Los Pasos Fm. provide concordant zircon U-Pb crystallization ages of 120 ± 0.4 and 125 ± 0.9 Ma (Barremian-Hauterivian transition; Rojas-Agramonte et al., 2016), constraining the minimum age of this formation. Similarly, the basaltic protoliths of the arc-related Mabujina Amphibolite Complex, tectonically below the Cretaceous Arc series in central Cuba, are older than 133 Ma (Rojas-

Agramonte et al., 2011), pointing to a Valanginian age of the oldest Central Cuban Arc lavas. On the other hand, the onset of subduction, related to the onset of the Early Cretaceous arc sequence, is constrained by supra-subduction ophiolitic rocks in central Cuba. Metadiabase dikes within central Cuban ophiolites, characterized by transitional N-MORB to IAT geochemistry (Butjosa et al., 2023), yielded a U-Pb zircon Valanginian age of 135.0 ± 1.7 Ma (Niu et al., 2022). All these data collectively constrain the timing of subduction initiation and the onset of arc magmatism to the Valanginian interval, at ca ~135 Ma, with further evolution until the Barremian-Hauterivian transition at ~125 Ma in Los Pasos Fm. Several paleontological data and abundant K-Ar dates of volcanic and plutonic rocks of the arc all along Cuba (Iturralde-Vinent, 1996, for review and references therein; see also Rojas-Agramonte et al., 2011, for review) and a U-Pb zircon age 83.6 ± 1.9 Ma, Niu et al., 2022) from a dacitic sample of the late arc sequence (Hilario Fm.) suggest quasi-continuous 60-65 Myrs arc magmatism, with minor interruptions until the late Campanian (70-75 Ma) collision/accretion of Caribeana (Garcia-Casco et al., 2008).

We employed SHRIMP zircon and LA-ICP-MS apatite U-Pb dating techniques to refine Central Cuban Arc magmatic evolution. Zircon U-Pb ages establish a coherent temporal framework for arc development. A tonalitic intrusion associated with early-stage low-Ti to normal IAT-type magmatism in the Los Pasos Fm. yielded an age of 125.1 ± 1.2 Ma, consistent with the earliest stages of arc magmatism (Rojas-Agramonte et al., 2016). Younger zircon ages of 86 Ma and 83 Ma were obtained from the Pelao Fm. (calc-alkaline ignimbrites) and the La Rana Fm. (tonalitic intrusion), respectively, marking the transition toward more evolved calc-alkaline magmatism. The Pelao Fm. zircon age (Coniacian) is slightly older than its stratigraphic constraint of Santonian to Campanian age (83.6-72.2 Ma). Zircons from a dacitic sample reported by Niu et al. (2022) yielded $^{206}Pb/^{238}U$ ages (^{204}Pb-corrected) between 90.6 ± 2.2 and 78.1 ± 2.8 Ma, with a weighted mean of 83.6 ± 1.9 Ma (n = 22, MSWD = 2.8). This locality corresponds to one of the Hilario Fm. outcrops examined in this study, although no zircons were recovered from our sampling here.

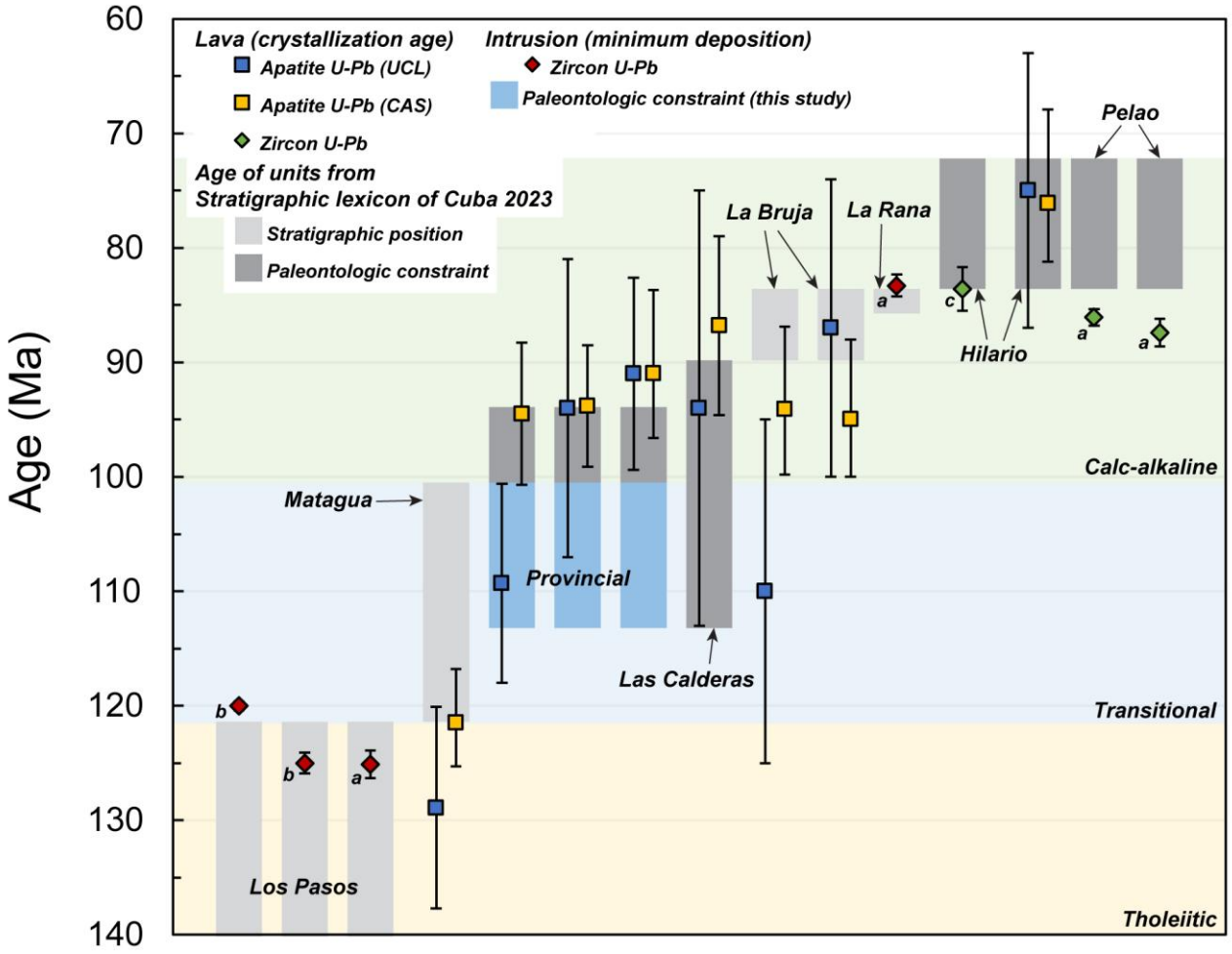

Figure 10. *Compilation of radiogenic ages of volcanic sequences from Central Cuban Arc includes U-Pb zircon and apatite age. Grey bar represents age range of the unit inferred by paleontological or stratigraphic constraints. Zircon data from this study labelled by (a); data from Rojas-Agramonte et al. (2016) are labeled (b); and data from Niu et al. (2022) are labeled (c). Stratigraphic and palentological data of the Central Cuban Arc units from Geología de Cuba: Compendio (Iturralde-Vinent, 2021).*

Because many Central Cuban Arc rocks contain low whole-rock Zr contents (<200 ppm), zircon occurrence is limited, making apatite a valuable complementary chronometer. Two sets of apatite U-Pb ages ranging from 129 to 75 Ma (obtained from the same samples measured across laboratories) define the temporal span of magmatism from early tholeiitic to voluminous calc-alkaline stages. The transitional sequence of the Mataguá Fm. yielded apatite ages of 122 +4/–5 Ma (CAS) and 129 ± 9 Ma (UCL), Barremian-Hauterivian, near the oldest limit of stratigraphic constraints. Intercalated volcanic deposits within the Provincial Fm. limestones produced ages consistent with paleontological

constraints but close to their younger limit (95-91Ma). Apatite from the Las Calderas Fm. yielded ages (87 ± 8 Ma from CAS and 94 ± 20 Ma from UCL) within the range defined by paleontological evidence, although with large uncertainties. In contrast, the La Bruja Fm. generally produced slightly older ages than expected from stratigraphy (110-87 Ma), but these remain compatible within analytical uncertainty.

Although apatite U-Pb dating is challenging due to the low U content of the mineral and the relatively young (Cretaceous) age of the rocks, the obtained apatite ages generally agree with both stratigraphic and paleontological constraints (Fig. 10). For instance, an andesite sample from the Hilario Fm. (23LV41) yielded an apatite age of 76.1 ± 5.1 Ma, slightly younger than the zircon results reported by Niu et al. (2022). The wide range of zircon ages from Niu et al. (2022) likely reflects incorporation of recycled zircon grains derived from earlier volcanic episodes, consistent with the presence of >20% rounded volcanic clasts that occur in the examined pyroclastic deposits from petrography study. Collectively, the zircon and apatite datasets indicate that calc-alkaline magmatism and plutonism were broadly coeval between ca. 89 and 81 Ma, consistent with geochronological evidence from the Manicaragua batholith (Rojas-Agramonte et al., 2011 and references therein). Zircon U-Pb data provide higher-precision constraints for interpreting magmatic timing, whereas apatite U-Pb ages, though less precise, extend the temporal record where zircon is absent, together refining the chronology of magmatic evolution in the Central Cuban Arc.

Detrital zircon provenance

Detrital zircon U-Pb ages from intercalated sediments in each of the studied units yielded weighted mean ages that broadly align with their paleontological constraints. The analysed Late Cretaceous volcanic-sedimentary sequences, namely the Provincial, Seibabo, and Cotorro Fms. yielded ages younger than 122 Ma, suggesting that the detrital sources were primarily eroded from contemporaneous or older (but exposed) island arc sequences. The similar range of positive εHf(t) values observed in both the studied detrital zircons and igneous zircons of the Central Cuban Arc, spanning from near-depleted mantle values +15.9 to +7.3 (Fig. 9), indicates isotopic heterogeneity in the source of the magmatic zircons. This heterogeneity likely reflects variable mixing between ancient crustal components (introduced in the source via subduction of continental-derived detrital material or by slab-derived fluids/melts) and juvenile mantle-derived material. Previous studies (Proenza et al., 2018; Rojas-Agramonte et al., 2016; Torró et al., 2018) documented inherited zircons ranging from Permian to Archean in age within the GAA from ophiolitic and early tholeiitic units in

Cuba and Dominican Republic. These grains are interpreted to reflect the recycling of subducted sediments with diverse provenance, potentially derived from nearby (during the Cretaceous) continental regions such as Mexico, the Maya Block and Colombia. Importantly, no significant assimilation of continental crustal material has been reported for the petrogenesis of Early Cretaceous tholeiitic and boninitic magmas within GAA (Lidiak and Anderson, 2015; Torró et al., 2018), consistent with our results. Our results both magmatic and detrital zircon ages and Hf isotopes are consistent with the Central Cuban Arc representing an intra-oceanic arc segment that formed at some distance from continental crust.

Central Cuban Arc Magmatic Source components

Geochemical and isotopic systematics record progressive arc maturation through the Cretaceous. Major element compositions show that Early Cretaceous low-K tholeiite volcanism lasted ~10 Ma, followed in the mid-Cretaceous by transitional magmas with progressively more evolved and enriched signatures for ~20 Ma, and culminating in Late Cretaceous calc-alkaline magmatism, which lasted for 30 Ma.

Most Central Cuban Arc samples have MORB-like Nb/Yb ratios, with systematic temporal shifts (Fig. 11): (i) tholeiitic sequences range between N-MORB and E-MORB (Nb/Yb = 0.29-3.42, with most cluster around 0.3-0.6) (ii) transitional sequences show generally more enriched values (Nb/Yb = 0.34-1.72), and (iii) calc-alkaline sequences display overall slightly elevated Nb/Yb ratios (most around 1.4-3.0). All groups plot above the mantle array with elevated Th/Yb ratios, especially in transitional and calc-alkaline sequences, indicating progressive metasomatism by slab-derived fluids or melts typical of intra-oceanic arcs (Pearce and Peate, 1995). REE patterns show flat MREE-HREE profiles, and LREE enrichment in the transitional and calc-alkaline lavas (Fig. 4 and S2), consistent with a subduction-related modification of a relatively homogeneous MORB mantle source. Trace element patterns, including enrichment in LILEs (Th, Cs, Rb, Ba, Sr) and depletion in HFSEs (negative Nb-Ta, Zr-Hf, and Ti anomalies; Fig. S2), show a typical subduction-related signature. To characterize the nature of mantle sources of the Central Cuban Arc sequences, we examined systematics of trace element that are sensitive to melting of both spinel and garnet peridotite sources. The absence of MREE/HREE fractionation in the basic rocks (SiO_2 < 55 wt.%; MgO > 3 wt.%) from all sequences is reflected in overall chondritic Dy_N/Yb_N ratios (0.99-1.30, average = 1.15). This indicates that mantle partial melting took place in the spinel peridotite stability field, constraining the depth of melting to less than 60 km (< 20 kbar).

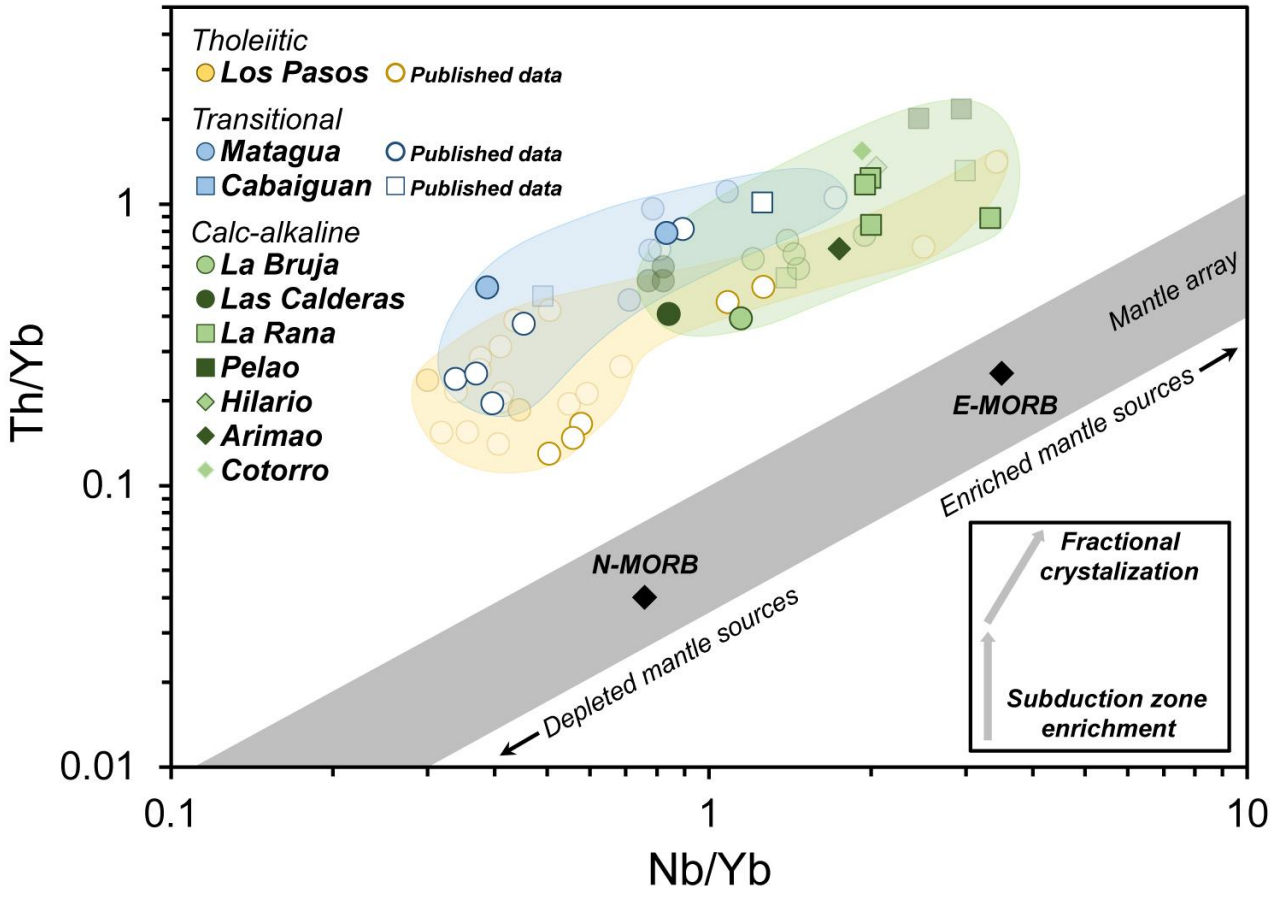

Figure 11. *Central Cuban Arc rocks plotted on the Th/Yb versus Nb/Yb of Pearce (2008). Basic rocks include basalts and basaltic andesite show in solid symbols and evolved rocks are in transparent color, field of each sequence is colored. Published data: Kerr et al. (1999); Blein et al. (2003); Díaz de Villalvilla et al. (2003); Rojas-Agramonte et al. (2016); Torró et al. (2016); Hu et al. (2024).*

Similar to trace element patterns, the Sr-Nd-Pb isotopic systematics show that most samples plot between the compositions of the depleted MORB mantle (DMM) and enriched mantle (EM) reservoirs and overlap with other GAA tholeiitic and calc-alkaline igneous suites. On the Sr-Nd isotopic diagram (Fig. 6), they mostly lie to the right of the mantle trend, as is common for global arc magmas (Hawkesworth et al., 1993). The Nd isotopic composition of Central Cuban Arc igneous rocks shows limited variability, clustering around εNd = +7 to +8 (Fig. 6A, B and S4) and, hence, with little evidence for continental sediment input, in agreement with the intra-oceanic nature of the arc. Relatively high radiogenic $^{87}Sr/^{86}Sr$ ratios decoupled from $^{143}Nd/^{144}Nd$ are commonly ascribed to subduction-related fluid input to the magmatic source and/or post-eruption seawater alteration. Considering the strong influence of secondary minerals, especially carbonates, alteration may contribute more significant than subduction-related input for radiogenic Sr ratios. This effect is

particularly evident in several samples from the Los Pasos Fm which overlap with other GAA IAT igneous suites. Indeed, elevated $^{87}Sr/^{86}Sr$ ratios in Early Cretaceous sequences likely reflect seawater-rock interaction during submarine eruption, consistent with field evidence (pillow lavas, autoclastic textures, supplementary materials S3 Field Report and S4 Petrographic Descriptions), while the younger sequences show minimal seawater alteration in line with a shift from predominantly submarine to subaerial volcanism. Hf isotopes in zircons likewise indicate an intra-oceanic arc source and suggest that the mantle feeding the Central Cuban Arc remained relatively homogeneous over ~60 Myr. Both magmatic and detrital zircons yield positive εHf(t) values ranging from +15.9 to +7.3 (Fig. 9), consistent with derivation from a dominantly juvenile depleted mantle source with only minor subducted sediment input. A heterogeneous mantle wedge remains a possible contributor to the isotopic signatures; however, the overall restricted range of εHf(t) values favors a source dominated by juvenile depleted mantle components. In arc magmatic systems, zircon often preserves variable and decoupled Hf isotope signatures compare to the relatively uniform whole-rock Nd isotopic compositions (Huang et al., 2019; Zhang et al., 2019). This occurs because zircon crystallizes early and incorporates most of the Hf budget of the melt, preserving isotopic heterogeneity inherited from distinct mantle and crustal components, whereas Nd resides in major silicate phases that equilibrate and homogenize within the melt. As a result, zircon εHf values can vary widely while whole-rock εNd remains relatively constant, recording a melt-averaged signal. The detrital zircons, derived from the arc itself, display similar εHf variability to the magmatic zircons, suggesting that sediment input did not vary substantially over time, consistent with the uniform Nd isotopic compositions. Late Cretaceous plutonic and volcanic zircons exhibit reduced εHf variability compared to Early Cretaceous magmatic zircons (Fig. 9A and B), implying more homogeneous melts and longer residence times that promoted isotopic equilibration prior to zircon crystallization. The transitional sequence represents an exception, showing unusually high $^{206}Pb/^{204}Pb$ at a given $^{208}Pb/^{204}Pb$ (Fig. 6; discussed below). Overall, the whole-rock Sr-Nd-Pb isotopic compositions of the Central Cuban Arc rocks match those of the rest of the GAA, and together with zircon Hf isotopes indicate a relatively homogeneous depleted mantle source variably modified by episodic, heterogeneous slab-derived sediment/fluid/melt inputs and by progressively more isotopically homogenized melt storage through time.

Sr-Nd-Pb isotope systematics further constrains subducted slab contributions. Binary mixing models (Fig. 12) between a depleted mantle (DM) source and Atlantic Cretaceous pelagic sediments (AKPS; DSDP 417 site; Jolly et al., 2006) and Atlantic Cretaceous sediments from DSDP 144 site (Carpentier

et al., 2008) indicate that only ~1% slab-derived fluids, enriched in fluid-mobile elements such as Sr and Pb, is sufficient to reproduce the observed isotopic signatures. A systematic increase in the sediment-derived fluid component, as reflected in Sr-Nd-Pb isotopic compositions (especially in Pb; Fig. 12 C and D), is evident from the tholeiitic (also when comparing to tholeiitic sequences from Hispaniola; e.g., Los Ranchos and Maimón Fms.) to the transitional and calc-alkaline sequences. Elevated $^{206}Pb/^{204}Pb$ ratios in the transitional sequences are best explained by involving sediments similar to the black shales recovered at DSDP Site 144 unit 3 (Carpentier et al., 2008). These shales, deposited in the Atlantic during mid-Cretaceous Oceanic Anoxic Events (OAE 2 and 3; ~96-84 Ma), are characterized by high U/Pb but normal Th/Pb ratios. However, subduction of such sediments cannot account for the enrichment observed in the Early Cretaceous or mid-Cretaceous transitional sequence. Instead, an older OAE event (e.g., Aptian-Albian OAE1a and b, ~120 and 112 Ma respectively; Alexandre et al., 2011; Herrle et al., 2004; Hofmann et al., 2001) within the Atlantic domain may be responsible. OAE1a and b has been reported in drill cores from both the western and eastern North Atlantic margins, including Blake Nose (ODP Site 1049) and the Mazagan Plateau (DSDP Site 545) (Browning & Watkins, 2008; Herrle et al., 2004). Moreover, DSDP Site 417, where AKPS has been proposed to have been subducted during the Cretaceous (Jolly et al., 2006), the older sedimentary sequences at this site were not included in AKPS analyses could contain OAE1b deposits (Jolly et al., 2006; Alexandre et al., 2011; Hofmann et al., 2001). Tholeiitic magmas could have been generated by high degrees of mantle melting in a relatively dry mantle wedge, with limited influx of slab-derived fluids (Grove and Baker, 1984). In contrast, calc-alkaline magmas are generally thought to require a hydrous mantle wedge (typically containing 2-6 wt.% H_2O), where slab-derived fluids and melts substantially enrich the source in volatiles and fluid-mobile elements, producing lower degrees of partial melting (Carlson et al., 2018; Grove et al., 2012; Kelemen et al., 2014; Schmidt and Jagoutz, 2017; Sisson and Grove, 1993). The low amount of sediment-derived fluid inferred from isotopic data contrasts with the larger fluid flux expected from the petrogenetic model. Figure 12 suggests that this mismatch may reflect additional input of non-radiogenic fluids released from altered oceanic crust (AOC) beneath the sediments, consistent with interpretations for other GAA tholeiitic and calc-alkaline suites (Escuder-Viruete et al., 2006; Torró et al., 2017a, 2020; Jolly et al., 2008; Marchesi et al., 2007).

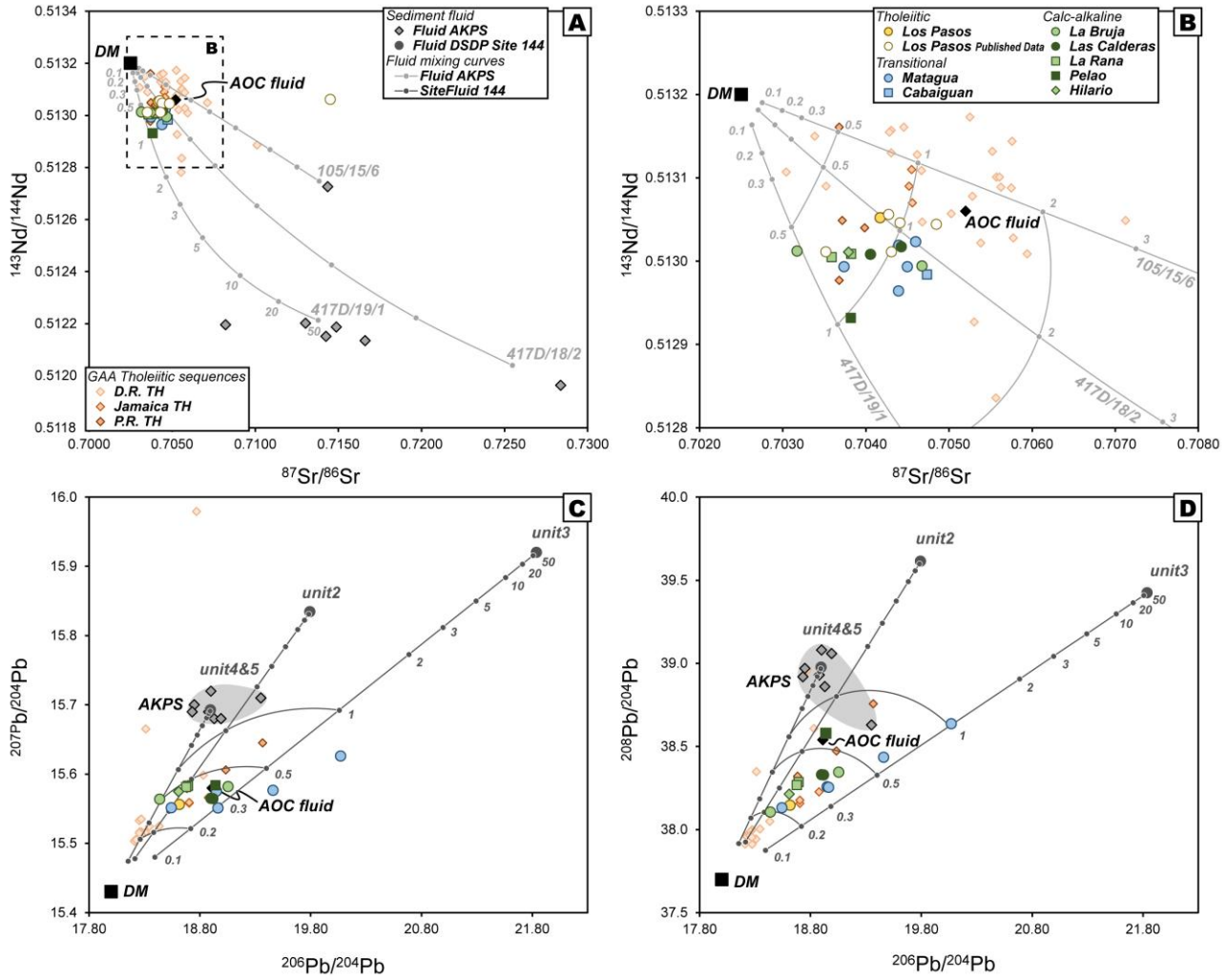

Figure 12. *Mixing curves of depleted mantle (DM) and fluids liberated from Atlantic Cretaceous pelagic sediments (Jolly et al., 2006) and sediments from DSDP site 144 unit 2-5 (Carpentier et al., 2008), shown in Sr-Nd-Pb isotope space.*

Mineral records of Central Cuban Arc magmatic reservoirs

Textures and chemical compositions of minerals in erupted lavas provide key records of magmatic evolution within complex crustal plumbing systems. The crystal cargoes preserve evidence of storage, recharge, mixing, and ascent conditions prior to eruption and therefore central to resolving magmatic evolution (e.g., Albert et al., 2022; Bachmann & Huber, 2016; Caracciolo et al., 2023; Humphreys et al., 2006; Jerram & Martin, 2008; Pelullo et al., 2022; Prieto-Torrell et al., 2025; Putirka, 2017). When integrated with temporal constrains, petrographic and geochemical observations from the Central Cuban Arc provide insight into the temporal evolution of magmatic processes within this intra-oceanic arc system.

Ferromagnesian phenocrysts in Early Cretaceous tholeiitic and mid-Cretaceous transitional volcanic sequences are dominated by clinopyroxene ± orthopyroxene, with rims that are weakly zoned or show normal zoning (decreasing Mg# towards rim). The assemblage and texture are consistent with tholeiitic differentiation favor under low pressure and dry conditions, in which plagioclase appears before FeTi-oxides in the liquid line of descent (Grove et al., 2003; Sisson & Grove, 1993; Zimmer et al., 2010). In contrast, Late Cretaceous calc-alkaline sequences record stronger crustal processing (fractionation and magma mixing), both in lavas and volcaniclastic deposits. The appearance of amphibole phenocrysts, coeval with granodiorite emplacement, reflecting H_2O-rich magma stored at greater depths within a thickened arc crust.

Phenocryst crystallization conditions

Equilibrium-based models and reconciliation among different methods for estimating crystallization pressure are essential for interpreting transcrustal magma storage conditions across a wide range of pressures (Hammer et al., 2016; Wieser et al., 2023a). Petrographic and mineral chemical data (e.g., sector-zoned mantles and resorbed cores) indicate that the volcanic units, especially the calc-alkaline sequences, contain disequilibrium mineral assemblages. The coexistence of crystals that are not in equilibrium complicates the estimation of magma storage conditions (Neave et al., 2019). Machine learning based thermobarometry approaches and traditional regression models can both be applied to sector-zoned mantles. For resorbed cores, traditional regression-based models calibrated using isothermal-isobaric experimental datasets or machine learning based models can still yield geologically realistic estimates of magmatic storage conditions (MacDonald et al., 2023). Accordingly, we estimated phenocryst crystallization conditions using multiple thermobarometers based on major-element compositions (detailed results and tables are available in supplementary material S6) and compared the results for consistency and geological validity. Comparing clinopyroxene-only, amphibole-only, and biotite-only thermobarometry reveals distinct crystallization pressures, from which depths are easily inferred. Amphibole phenocrysts occur only in late-stage calc-alkaline volcanic and volcaniclastic rocks, whereas biotite is observed in a single sample from the Pelao Fm. For clinopyroxene, temperatures range from approximately 950 to 1100 °C across all sequences (Ágreda-López et al., 2024; Higgins et al., 2022; Jorgenson et al., 2022; Petrelli et al., 2020; Wang et al., 2021). Pressure estimates from transitional lavas and early formed Late Cretaceous calc-alkaline rocks (e.g., Bruja Fm.) show no systematic differences in crystallization depth, with most values ~1.5-2.5 kbar (~5-8 km deep). In younger Late Cretaceous samples, clinopyroxene pressures increase to ~2-4 kbar ~6.5-13 km, consistent with crustal

thickening, yet still indicating upper- to mid-crustal crystallization conditions for the magma chambers where clinopyroxene formed. Amphibole phenocrysts, which are temporally associated with large-scale pluton emplacement, have mineral core pressures ranging from 6 to 8 kbar (~20-26 km depth) based on different calibrations, with rim pressures decreasing to around 2.5 kbar, suggesting amphibole crystallization during magma ascent and/or storage. In the crystal-rich Pelao Fm. ignimbrites, where biotite chemistry indicates from a more alkaline source (Fig. S3). Biotite compositions fall within the accepted calibration range of the thermobarometer (Li & Zhang, 2022) yields ~792-834 °C, 2.8-4.1 kbar, averaging ~3.4 kbar, whereas amphibole gives slightly higher temperatures estimates (~850 °; Ridolfi et al., 2010; Ridolfi 2021; Higgins et al., 2022). Pressure estimates of those amphiboles based on Ridolfi et al. (2010) and Ridolfi (2021) are lower, averaging ~1.7 kbar, compared to the 4.1 kbar calculated using the formulation of Higgins et al. (2022). Comparable P-T conditions are obtained from clinopyroxene and amphibole in coeval volcaniclastic rocks and lavas, suggesting a consistent record of magma storage conditions.

Late Cretaceous calc-alkaline units (e.g., basaltic andesite of the La Rana Fm.) show significant compositional variability in pyroxene and feldspar phenocrysts, which indicate mixing of genetically related crystals and antecrysts (Fig. S6). Even at the thin section scale, phenocrysts of Pl, Cpx, and Opx with contrasting textures occur side-by-side (Fig. 2G). The modal proportion of disequilibrium crystals varies among samples, and Pl lacks a common zoning sequence, implying a heterogeneous, multi-source crystal cargo assembled from grain to outcrop scale. Such heterogeneity cannot be explained by self-mixing within a single shallow crystal mush. Combining textural compositional and Cpx-Opx thermobarometry along with Cpx/Opx inclusions in Pl allows identifying crystal populations derived from deeper mafic mush zones. These crystals (Cpx-Opx-Pl phenocrysts) were entrained by ascending melts, transported rapidly to a shallower reservoir, experiencing decompression-driven resorption during ascent. A long residence time of the magma in shallow chambers allowed repeated recharge by crystal-rich magmas from depth, triggering magma mixing and chemical and textural diversity of the evolved magmas, as well as eventually triggering eruption (Boschetty et al., 2022; Coote and Shane, 2018; Mangler et al., 2022).

In a broader temporal context, Late Cretaceous amphibole in the volcanic rocks crystallized under higher pressure condition than clinopyroxene in the Early Cretaceous, reflecting a transition to hydrous, calc-alkaline magmatism associated with contemporaneous plutonism within long lived mid- to lower-crustal storage zones (Blatter et al., 2013; Krawczynski et al., 2012; Marxer et al., 2022; Ulmer et al., 2018). Mineral chemistry (esp. Mn and Ti abundances), together with predicted pressure

and temperature, supports a model of magma differentiation dominated by fractional crystallization accompanied by magmatic recharge and mixing. Prolonged residence at such depths promotes amphibole fractionation, which efficiently depletes magmatic MREE and HREE concentrations, driving calc-alkaline differentiation through the so-called “amphibole sponge” effect (Davidson et al., 2007; Smith, 2014). Late Cretaceous volcanism and associated plutonism were characterized by slower magma ascent, prolonged crustal residence, and enhanced differentiation, in contrast to the more primitive, rapidly emplaced magmas associated with the Early Cretaceous tholeiitic volcanism. These features are best explained by a vertically heterogeneous, transcrustal plumbing system containing crystal mush domains that were periodically recharged and remobilized by ascending magmas, accounting for the textures commonly observed in late-stage magmatic products. This is essentially a Magma Assimilation, Storage and Homogenization (MASH) zone (Annen et al., 2006; Hildreth & Moorbath, 1988).

Reviews (Wieser, et al., 2023a, b) highlight limitations of single-mineral thermobarometry (esp. clinopyroxene), particularly regarding the calibration of classical regression models (e.g., Putirka, 2008, 2017) and the lack of rigorous error propagation analysis. Further EPMA studies on amphibole and biotite crystals are necessary for a more accurate and complete discussion of these barometric constraints. Nevertheless, our single-mineral pressure estimates are broadly consistent with bulk-rock trace-element barometric proxies (Ce/Y in basic and La/Yb and Sr/Y in intermediate igneous rocks; Fig. S5), supporting progressive crustal thickening during the transition from tholeiitic to calc-alkaline arc magmatism.

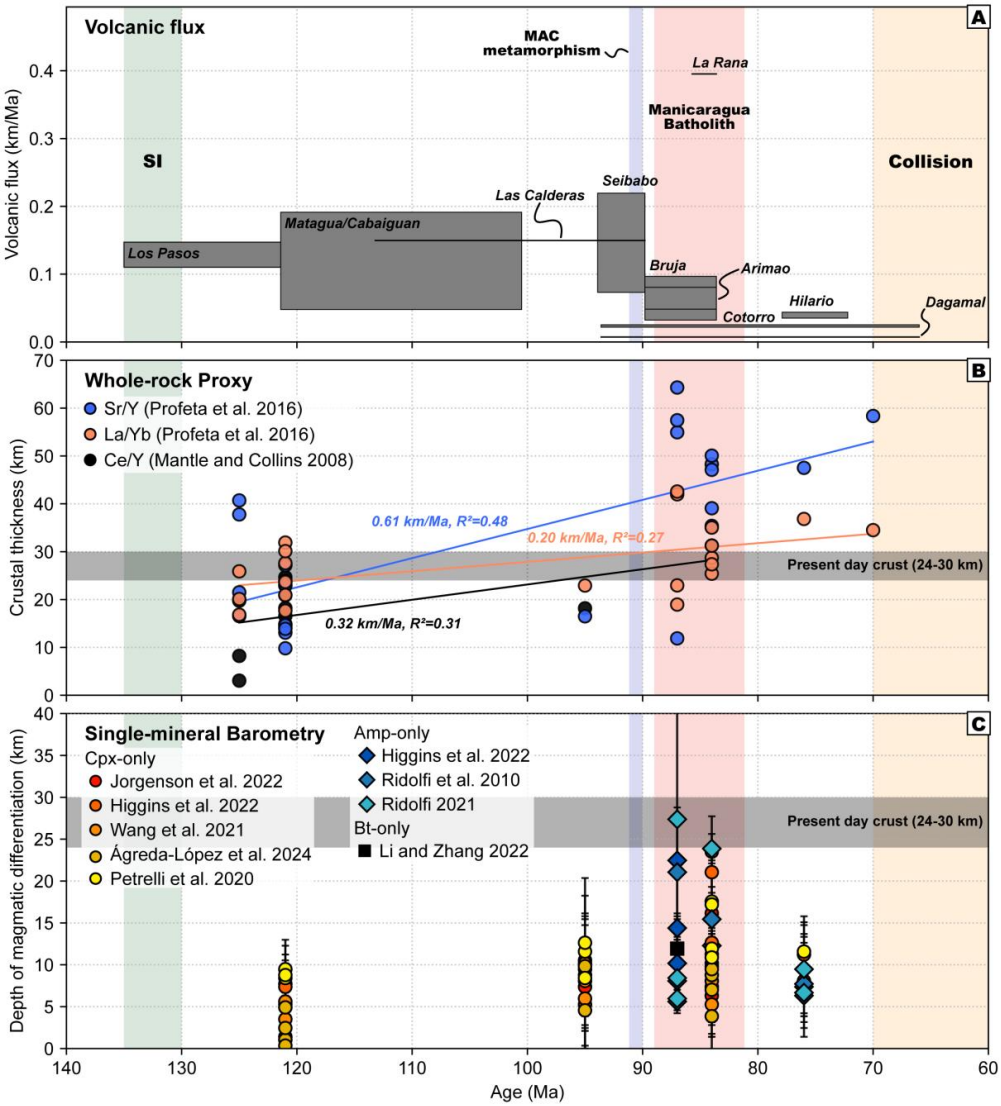

Figure 13. *Evolution of the Central Cuban arc illustrated by (A) volcanic flux calculated from the thickness and duration of each formation; thicknesses of lithostratigraphic units are compiled from the Geología de Cuba: Compendio (Iturralde-Vinent, 2021), with shaded bands showing low and high estimates, (B) whole-rock-derived crustal thickness with least-squares regression lines indicating linear rates of crustal growth (km/Ma) and corresponding R² values, using La/Yb and Sr/Y from intermediate rock after Profeta et al. (2016) and Ce/Y from basic rocks after Mantle & Collins (2008), and (C) single-mineral barometry-based crystallization depths converted to kilometers assuming a crustal density of 2900 kg/m³. Thermobarometry used: Clinopyroxene-only: Ágreda-López et al. (2024); Higgins et al. (2022); Jorgenson et al. (2022); Petrelli et al. (2020); Wang et al. (2021). Amphibole-only: Ridolfi et al. (2010); Ridolfi (2021); Higgins et al. (2022). Biotite-only: Li & Zhang (2022).*

Crustal growth of Central Cuban Arc

In this section, we discuss the processes governing crustal growth in the Central Cuban Arc, which are intrinsic to its magmatic and tectonic evolution. These processes record a secular transition from a primitive intra-oceanic arc to a mature, proto-continental crustal system. To evaluate this evolution, we integrate estimates of volcanic flux (based on the thickness and duration of each volcanic formations) with whole-rock geochemical proxies and mineral barometry. The estimated volcanic flux remained relatively constant between 135 and ~90 Ma at 0.1-0.2 km/Ma (Fig. 13A). Pressure-sensitive trace-element ratios (Ce/Y, La/Yb, Sr/Y) increase systematically through time, with weak but positive linear trends (Ce/Y: 0.32 km/Ma; La/Yb: 0.20 km/Ma; Sr/Y: 0.61 km/Ma; Fig. 13B). These trends imply enhanced crustal differentiation with overall crustal thickening from ~10-20 km in the Early Cretaceous to ~30 km by ~70 Ma. Mineral barometry corroborates this, indicating higher pressure crystallization condition (Fig. 13C).

A decline in volcanic flux during the main plutonic stage (<0.1 km/Ma) suggest that, if total magmatic flux remained constant, magma was largely emplaced within the mid- to lower crust, promoting plutonism over volcanism. An inversed correlation between magma flux and Moho depths observed in Quaternary volcanism of the Cascades Arc (Till et al., 2019), likely result in cooler thermal regimes and enhanced fractionation at depth. Island arc collision events promote tectonic overthickening (Niu et al., 2013), leading to reduced magmatic flux and generation of more hydrous magma that drive continental crust formation (Klein et al., 2023). These processes are consistent with transient deformation and metamorphism in the Mabujina Amphibolite Complex (~93-90 Ma, Rojas-Agramonte et al., 2011), interpreted as localized crustal stacking during oblique subduction (Hu et al., 2024). Notably, the onset of plutonism in the Las Villas region closely postdates metamorphism of the Mabujina Amphibolite Complex at ~90 Ma (Rojas-Agramonte et al., 2011), linking intra-arc deformation to the subsequent decline in volcanic flux. Intra-arc or arc-arc collision likely played a central role in producing the sudden change in petrologic and thermal structure of the arc crust.

The depth of crystallization of amphibole cores, calculated from crystallization pressures assuming a crustal density of 2900 kg/m^3, ranges from 21 to 28 km. These depths suggest that the Moho during the Cretaceous was comparable to present-day values of approximately 24-30 km beneath central Cuba (González et al., 2012; Moreno Toirán, 2003; Possee et al., 2021). A three-stage evolution of the crust is illustrated in Figures 14, showing a progression from tholeiitic to transitional and ultimately to calc-alkaline magmatism. This evolution was accompanied by progressive

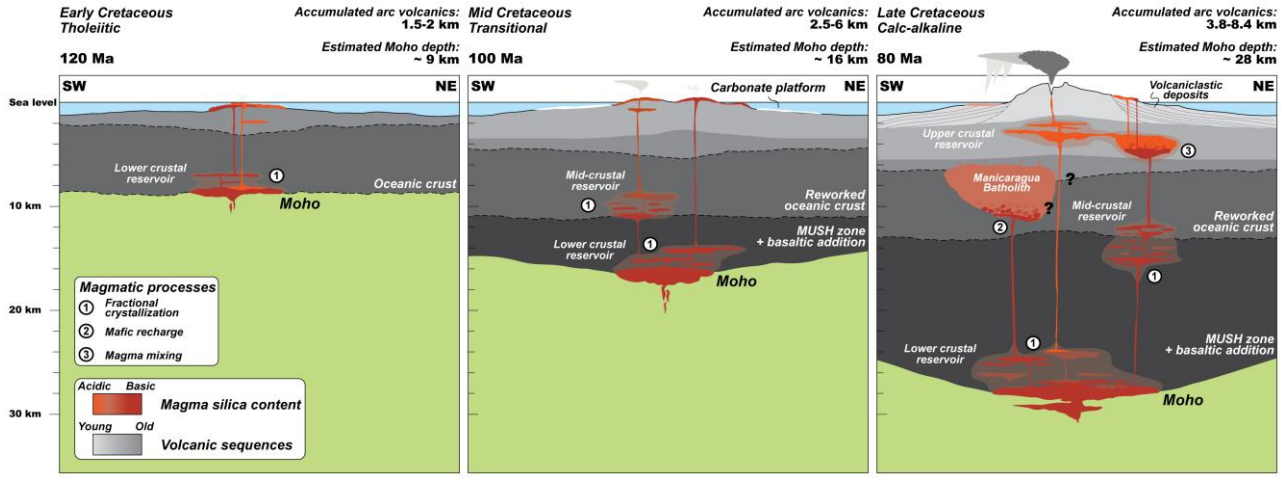

Figure 14. *Schematic cross-section of the arc crustal section illustrating three stages of progressive crustal thickning. In the early stage, a thin crust with limited magmatic differentiation produced tholeiitic to transitional magmas and led to formation of lower crustal cumulates. With continued thickening, a more hydrous and potentially cooler crustal structure favored differentiation toward calc-alkaline compositions, the development of multiple magma storage levels, magma mixing processes, and major plutonism. The thickness of volcanic sequences (upper crust) is based on Geología de Cuba: Compendio (Iturralde-Vinent, 2021) and interpreted Moho depth is constrined by single-mineral barometry from volcanic rocks of the Central Cuban Arc.*

accumulation of volcanic material, increasing from 1.5-2 km in the Early Cretaceous to approximately 8 km in the Late Cretaceous, together with thickening in the mid- and lower crust during this period. A decrease in eruptive flux between 100 and 80 Ma compared to 120-100 Ma coincided with major plutonism during the late calc-alkaline stage and likely reflects substantial crustal thickening in the mid- to lower crust during this period. By the Late Cretaceous, the Cuban arc crust likely attained a thickness of ~30 km, comparable to the modern crustal thickness. However, only the upper portion of this crustal column is now exposed. The pre-arc oceanic basement and the lower arc crust are not observed at the surface. These deeper levels are either preserved beneath the present arc or were displaced southwestward relative to the modern arc position during latest Cretaceous to middle Eocene thrusting, similar to the exposures documented in Puerto Rico (Lidiak et al., 2011).

CONCLUSION

The Central Cuban Arc preserves ~60 Myr of intra-oceanic arc evolution, from Early Cretaceous low-K tholeiitic magmatism (~135-125 Ma), through transitional (125-100 Ma) stages, to Late Cretaceous hydrous calc-alkaline systems (~95-75 Ma). Zircon and apatite U-Pb geochronology, integrated with petrology, geochemistry and isotopic data, records a shift from thin oceanic-arc crust to a ca. 30 km thick hydrous plumbing system. Early magmas derived from a relatively homogeneous depleted mantle with minimal slab input, display flat to slightly LREE-depleted REE patterns and weak enrichment in fluid-mobile elements. Through the mid-Cretaceous, increasing slab-derived metasomatism and crustal thickening are recorded by rising La/Yb and Ce/Y ratios, culminating in Cenomanian-Campanian calc-alkaline magmatism characterized by strong REE fractionation in the most silicic rocks, prolonged storage, recharge, and mixing, major plutonism, amphibole stabilization, and pervasive crystal recycling.

Despite pronounced geochemical and textural maturation, isotopic proxies indicate a persistently juvenile largely homogeneous mantle source with only limited episodic heterogenous sediment-derived contributions. The tholeiitic to calc-alkaline transition therefore chiefly reflects increasing slab-derived fluid input and crustal thickening, rather than a fundamental change in mantle source, a pattern echoed across the Greater Antilles Arc. Elevated initial Sr isotopic ratios in the earliest sequences are best explained by seawater alteration during submarine eruption, whereas younger units show minimal seawater influence, consistent with a shift to subaerial volcanism.

The exceptional exposures of volcanic and intrusive architectures of the Central Cuban Arc allows direct linkage among stratigraphy, mineral records, and geochemistry, providing a rare, time-resolved view of how juvenile oceanic arcs evolve into mature, proto-continental systems. These insights refine models of juvenile crust formation and the tectono-magmatic maturation of intra-oceanic arcs.

ACKNOWLEDGMENTS

Haoyu Hu gratefully thanks Romain Bousquet for his support during the field excursion and Peter Appel for assistance with the EPMA and XRF analyses. Haoyu Hu acknowledges financial support from the Federal State Funding at Kiel University. Special thanks are extended to the Cuban authorities and Kenya Nuñez Cambra from the Cuban Institute of Geology and Paleontology for organizing fieldwork permits, and to the laboratories of the Chinese Academy of Sciences (CAS) and the Beijing SHRIMP Center, Chinese Academy of Geological Sciences (CAGS), for analytical support. This is UTD Geosciences contribution #17xx.

REFERENCES CITED

Ágreda-López, M., Parodi, V., Musu, A., Jorgenson, C., Carfì, A., Mastrogiovanni, F., Caricchi, L., Perugini, D., & Petrelli, M. (2024). Enhancing machine learning thermobarometry for clinopyroxene-bearing magmas. Computers & Geosciences, 193, 105707. https://doi.org/10.1016/j.cageo.2024.105707

Albert, H., Trua, T., Fonseca, J., Marani, M. P., Gamberi, F., Spiess, R., & Marzoli, A. (2022). Time scales of open-system processes in a complex and heterogeneous mush-dominated plumbing system. Geology, 50(8), 869–873. https://doi.org/10.1130/G49934.1

Alexandre, J. T., Van Gilst, R. I., Rodríguez-López, J. P., & De Boer, P. L. (2011). The sedimentary expression of oceanic anoxic event 1b in the North Atlantic. Sedimentology, 58(5), 1217–1246. https://doi.org/10.1111/j.1365-3091.2010.01202.x

Allibon, J., Monjoie, P., Lapierre, H., Jaillard, E., Bussy, F., Bosch, D., & Senebier, F. (2008). The contribution of the young Cretaceous Caribbean Oceanic Plateau to the genesis of late Cretaceous arc magmatism in the Cordillera Occidental of Ecuador. Journal of South American Earth Sciences, 26(4), 355–368. https://doi.org/10.1016/j.jsames.2008.06.003

Annen, C., Blundy, J. D., & Sparks, R. S. J. (2006). The Genesis of Intermediate and Silicic Magmas in Deep Crustal Hot Zones. Journal of Petrology, 47(3), Article 3. https://doi.org/10.1093/petrology/egi084

Bachmann, O., & Huber, C. (2016). Silicic magma reservoirs in the Earth's crust. American Mineralogist, 101(11), 2377–2404. https://doi.org/10.2138/am-2016-5675

Blanco-Quintero, I. F., Rojas-Agramonte, Y., García-Casco, A., Kröner, A., Mertz, D. F., Lázaro, C., Blanco-Moreno, J., & Renne, P. R. (2011). Timing of subduction and exhumation in a subduction channel: Evidence from slab melts from La Corea Mélange (eastern Cuba). Lithos, 127(1–2), 86–100. https://doi.org/10.1016/j.lithos.2011.08.009

Blatter, D. L., Sisson, T. W., & Hankins, W. B. (2013). Crystallization of oxidized, moderately hydrous arc basalt at mid- to lower-crustal pressures: Implications for andesite genesis. Contributions to Mineralogy and Petrology, 166(3), 861–886. https://doi.org/10.1007/s00410-013-0920-3

Blein, O., Guillot, S., Lapierre, H., de Lépinay, B. M., Lardeaux, J. -M., Trujillo, G. M., Campos, M., & Garcia, A. (2003). Geochemistry of the Mabujina Complex, Central Cuba:

Implications on the Cuban Cretaceous Arc Rocks. The Journal of Geology, 111(1), Article 1. https://doi.org/10.1086/344666

Boschetty, F. O., Ferguson, D. J., Cortés, J. A., Morgado, E., Ebmeier, S. K., Morgan, D. J., Romero, J. E., & Silva Parejas, C. (2022). Insights Into Magma Storage Beneath a Frequently Erupting Arc Volcano (Villarrica, Chile) From Unsupervised Machine Learning Analysis of Mineral Compositions. Geochemistry, Geophysics, Geosystems, 23(4), e2022GC010333. https://doi.org/10.1029/2022GC010333

Boschman, L. M., van Hinsbergen, D. J. J., Torsvik, T. H., Spakman, W., & Pindell, J. L. (2014). Kinematic reconstruction of the Caribbean region since the Early Jurassic. Earth-Science Reviews, 138, 102–136. https://doi.org/10.1016/j.earscirev.2014.08.007

Braszus, B., Goes, S., Allen, R., Rietbrock, A., Collier, J., Harmon, N., Henstock, T., Hicks, S., Rychert, C. A., Maunder, B., Van Hunen, J., Bie, L., Blundy, J., Cooper, G., Davy, R., Kendall, J. M., Macpherson, C., Wilkinson, J., & Wilson, M. (2021). Subduction history of the Caribbean from upper-mantle seismic imaging and plate reconstruction. Nature Communications, 12(1), 4211. https://doi.org/10.1038/s41467-021-24413-0

Brönnimann, P., & Pardo, G. (1954). Annotations to the correlation chart and catalogue of formations (Las Villas province). Oficina Nacional de Recursos Minerales, MINBAS, La Habana (inédito).

Browning, E. L., & Watkins, D. K. (2008). Elevated primary productivity of calcareous nannoplankton associated with ocean anoxic event 1b during the Aptian/Albian transition (Early Cretaceous). Paleoceanography, 23(2), 2007PA001413. https://doi.org/10.1029/2007PA001413

Burke, K. (1988). Tectonic Evolution of the Caribbean. Annual Review of Earth and Planetary Sciences, 16(1), 201–230. https://doi.org/10.1146/annurev.ea.16.050188.001221

Butjosa, L., Cambeses, A., Proenza, J. A., Agostini, S., Iturralde-Vinent, M., Bernal-Rodríguez, L., & Garcia-Casco, A. (2023). Relict abyssal mantle in a Caribbean forearc ophiolite (Villa Clara, central Cuba): Petrogenetic and geodynamic implications. International Geology Review, 1–32. https://doi.org/10.1080/00206814.2023.2179229

Caracciolo, A., Bali, E., Halldórsson, S. A., Guðfinnsson, G. H., Kahl, M., Þórðardóttir, I., Pálmadóttir, G. L., & Silvestri, V. (2023). Magma plumbing architectures and timescales of magmatic processes during historical magmatism on the Reykjanes Peninsula, Iceland.

Earth and Planetary Science Letters, 621, 118378. https://doi.org/10.1016/j.epsl.2023.118378

Cárdenas-Párraga, J., García-Casco, A., Proenza, J. A., Harlow, G. E., Blanco-Quintero, I. F., Lázaro, C., Villanova-de-Benavent, C., & Núñez Cambra, K. (2017). Trace-element geochemistry of transform-fault serpentinite in high-pressure subduction mélanges (eastern Cuba): Implications for subduction initiation. International Geology Review, 59(16), 2041–2064. https://doi.org/10.1080/00206814.2017.1308843

Carlson, R. W., Grove, T. L., & Donnelly‐Nolan, J. M. (2018). Origin of Primitive Tholeiitic and Calc‐Alkaline Basalts at Newberry Volcano, Oregon. Geochemistry, Geophysics, Geosystems, 19(4), 1360–1377. https://doi.org/10.1029/2018GC007454

Carpentier, M., Chauvel, C., & Mattielli, N. (2008). Pb–Nd isotopic constraints on sedimentary input into the Lesser Antilles arc system. Earth and Planetary Science Letters, 272(1–2), 199–211. https://doi.org/10.1016/j.epsl.2008.04.036

Coote, A., & Shane, P. (2018). Open-system magmatic behaviour beneath monogenetic volcanoes revealed by the geochemistry, texture and thermobarometry of clinopyroxene, Kaikohe-Bay of Islands volcanic field (New Zealand). Journal of Volcanology and Geothermal Research, 368, 51–62. https://doi.org/10.1016/j.jvolgeores.2018.11.006

Cruz-Gámez, E. M., Velasco-Tapia, F., Garcia-Casco, A., Despaigne Díaz, A. I., Lastra Rivero, J. F., & Cáceres Govea, D. (2016). Geoquímica del magmatismo mesozoico asociado al Margen Continental Pasivo en el occidente y centro de Cuba. Boletín de La Sociedad Geológica Mexicana, 68(3), Article 3. https://doi.org/10.18268/BSGM2016v68n3a5

Davidson, J., Turner, S., Handley, H., Macpherson, C., & Dosseto, A. (2007). Amphibole “sponge” in arc crust? Geology, 35(9), 787. https://doi.org/10.1130/G23637A.1

Despaigne-Díaz, A. I., Garcia-Casco, A., Caceres Govea, D., Jourdan, F., Wilde, S. A., & Millan Trujillo, G. (2016). Twenty-five million years of subduction-accretion-exhumation during the Late Cretaceous-Tertiary in the northwestern Caribbean: The Trinidad Dome, Escambray Complex, Central Cuba. American Journal of Science, 316(3), Article 3. https://doi.org/10.2475/03.2016.01

Despaigne-Díaz, A. I., Garcia-Casco, A., Cáceres Govea, D., Wilde, S. A., & Millán Trujillo, G. (2017). Structure and tectonic evolution of the southwestern Trinidad dome, Escambray complex, Central Cuba: Insights into deformation in an accretionary wedge. Tectonophysics, 717, 139–161. https://doi.org/10.1016/j.tecto.2017.07.024

Díaz de Villalvila, L. (1997). Caracterización geológica de las formaciones volcánicas y volcano-sedimentarias en Cuba central, provincias Cienfuegos, Villa Clara, Sancti Spiritus. In: Estudios sobre Geología de Cuba (Eds. Furrazola Bermudez, G.F., Núñez Cambra, K.E.). Centro Nacional de Información Geológica, La Habana, Cuba, 259–270.

Díaz de Villalvilla, L. (1988). Caracterización geológica y petrológica de las asociaciones vulcanógenas del arco insular cretácico en Cuba central. Tesis de Doctorado en Ciencias Geológicas del Instituto de Geología y Pa l e o n t o l ogía. (Inédita).

Díaz de Villalvilla, L., Milia-González, I., Santa Cruz Pacheco, M., & Aguirre, G. (2003). Formación Los Pasos: Geología, Geoquímica y su Comparación con el Caribe. Estudios Sobre Los Arcos Volcánicos de Cuba, Centro Nacional de Información Geológica, Instituto de Geología y Paleontología de Cuba, Havana.

Díaz de Villalvilla, L., Perez, M., Sukar, K., Mari, T., Mendez, I., Rodreguez, R., Pinero, E., Quintana, M. E., Aguriie, G., Echeverria, B., & Milia, I. (1994). Consideraciones geoquimicas acerca de los arcol volcanicos de Cuba [abs.]. In Secondo Congreso Cubano de Geologia y Mineria, Libro de Programas y Resumenes: Santiago de Cuba, p. 173., Article Libro de Programas y Resumenes: Santiago de Cuba, p. 173.

Díaz de Villalvilla, L. & et al. (1985). Proposición para una división de la llamada Formación Tobas (provincias de Cienfuegos, Villa Clara y Sancti Spíritus).

Domínguez-Carretero, D., Proenza, J. A., Pujol-Solà, N., Gervilla, F., Villanova-de-Benavent, C., Colás, V., Núñez-Cambra, K., Piñero-Pérez, E., & Garcia-Casco, A. (2025). The gradual shift from forearc basalt-like to boninite-like magmatism during intra-oceanic subduction-initiation recorded by ophiolitic chromite deposits from Cuba. Mineralium Deposita. https://doi.org/10.1007/s00126-025-01355-x

Donnelly, T. W., Beets, D., Carr, M. J., Jackson, T., Klaver, G., Lewis, J., ... & Westercamp, D. (1991). History and tectonic setting of Caribbean magmatism.

Dublan, L., & Alvarez, Sanchez., eds. (1986). Informe final del levantamiento geologico y evaluacion de minerales utiles, en escala 1:50000, del polıgono CAME I, zona Centro. Centro Nacional Fondo Geolo´gico, MINBAS, La Habana (unpubl. Report).

Ducea, M. N., Saleeby, J. B., & Bergantz, G. (2015). The Architecture, Chemistry, and Evolution of Continental Magmatic Arcs. Annual Review of Earth and Planetary Sciences, 43(1), 299–331. https://doi.org/10.1146/annurev-earth-060614-105049

Eagles, G. (2007). New angles on South Atlantic opening. Geophysical Journal International, 168(1), 353–361. https://doi.org/10.1111/j.1365-246X.2006.03206.x

Escuder-Viruete, J., Castillo-Carrión, M., & Pérez-Estaún, A. (2014). Magmatic relationships between depleted mantle harzburgites, boninitic cumulate gabbros and subduction-related tholeiitic basalts in the Puerto Plata ophiolitic complex, Dominican Republic: Implications for the birth of the Caribbean island-arc. Lithos, 196–197, 261–280. https://doi.org/10.1016/j.lithos.2014.03.013

Frost, C. D., Schellekens, J. H., & Smith, A. L. (1998). Nd, Sr, and Pb isotopic characterization of Cretaceous and Paleogene volcanic and plutonic island arc rocks from Puerto Rico. In E. G. Lidiak & D. K. Larue, Tectonics and Geochemistry of the Northeastern Caribbean. Geological Society of America. https://doi.org/10.1130/0-8137-2322-1.123

García-Delgado, D. E., (1998). Mapa geológico de Cuba central (provincias Cienfuegos, Villa Clara y Sancti Spiritus) Escala 1:100000: Instituto de Geología y Paleontología, La Habana.

Garcia-Casco, A., Iturralde-Vinent, M. A., & Pindell, J. (2008). Latest Cretaceous Collision/Accretion between the Caribbean Plate and Caribeana: Origin of Metamorphic Terranes in the Greater Antilles. International Geology Review, 50(9), Article 9. https://doi.org/10.2747/0020-6814.50.9.781

Garcia-Casco, A., Torres-Roldán, R. L., Iturralde-Vinent, M. A., Millán, G., Cambra, K. N., Lázaro, C., & Vega, A. R. (2006). High pressure metamorphism of ophiolites in Cuba. Geologica Acta, 26.

Garcia-Casco, A., Torres-Roldan, R. L., Millan, G., Monie, P., & Schneider, J. (2002). Oscillatory zoning in eclogitic garnet and amphibole, Northern Serpentinite Melange, Cuba: A record of tectonic instability during subduction? Journal of Metamorphic Geology, 20(6), Article 6. https://doi.org/10.1046/j.1525-1314.2002.00390.x

González, O., Moreno, B., Romanelli, F., & Panza, G. F. (2012). Lithospheric structure below seismic stations in Cuba from the joint inversion of Rayleigh surface waves dispersion and receiver functions: Lithosphere below seismic stations in Cuba. Geophysical Journal International, 189(2), 1047–1059. https://doi.org/10.1111/j.1365-246X.2012.05410.x

Greene, A. R., Debari, S. M., Kelemen, P. B., Blusztajn, J., & Clift, P. D. (2006). A Detailed Geochemical Study of Island Arc Crust: The Talkeetna Arc Section, South–Central Alaska. Journal of Petrology, 47(6), Article 6. https://doi.org/10.1093/petrology/egl002

Grove, T. L., & Baker, M. B. (1984). Phase equilibrium controls on the tholeiitic versus calc-alkaline differentiation trends. Journal of Geophysical Research: Solid Earth, 89(B5), 3253–3274. https://doi.org/10.1029/JB089iB05p03253

Grove, T. L., Elkins-Tanton, L. T., Parman, S. W., Chatterjee, N., Muntener, O., & Gaetani, G. A. (2003). Fractional crystallization and mantle-melting controls on calc-alkaline differentiation trends. Contributions to Mineralogy and Petrology, 145(5), 515–533. https://doi.org/10.1007/s00410-003-0448-z

Grove, T. L., Till, C. B., & Krawczynski, M. J. (2012). The Role of H 2 O in Subduction Zone Magmatism. Annual Review of Earth and Planetary Sciences, 40(1), Article 1. https://doi.org/10.1146/annurev-earth-042711-105310

Hammer, J., Jacob, S., Welsch, B., Hellebrand, E., & Sinton, J. (2016). Clinopyroxene in postshield Haleakala ankaramite: 1. Efficacy of thermobarometry. Contributions to Mineralogy and Petrology, 171(1), 7. https://doi.org/10.1007/s00410-015-1212-x

Hastie, A. R., Kerr, A. C., Mitchell, S. F., & Millar, I. L. (2008). Geochemistry and petrogenesis of Cretaceous oceanic plateau lavas in eastern Jamaica. Lithos, 101(3–4), 323–343. https://doi.org/10.1016/j.lithos.2007.08.003

Hastie, A. R., Kerr, A. C., Mitchell, S. F., & Millar, I. L. (2009). Geochemistry and tectonomagmatic significance of Lower Cretaceous island arc lavas from the Devils Racecourse Formation, eastern Jamaica. Geological Society, London, Special Publications, 328(1), Article 1. https://doi.org/10.1144/SP328.14

Hastie, A. R., Kerr, A. C., Pearce, J. A., & Mitchell, S. F. (2007). Classification of Altered Volcanic Island Arc Rocks using Immobile Trace Elements: Development of the Th–Co Discrimination Diagram. Journal of Petrology, 48(12), Article 12. https://doi.org/10.1093/petrology/egm062

Hatten, C. W., Schooler, O. E., Giedt, N., & Meyerhoff, A. A. (1958). Geology of central Cuba, eastern Las Villas and western Camaguey provinces, Cuba. La Habana, Ministerio de Industrias archives, 250 pp. (Unpublished report).

Hawkesworth, C. J., Gallagher, K., Hergt, J. M., & McDermott, F. (1993). Mantle and Slab Contributions in ARC Magmas. Annual Review of Earth and Planetary Sciences, 21(1), 175–204. https://doi.org/10.1146/annurev.ea.21.050193.001135

Herrle, J. O., Kößler, P., Friedrich, O., Erlenkeuser, H., & Hemleben, C. (2004). High-resolution carbon isotope records of the Aptian to Lower Albian from SE France and the Mazagan

Plateau (DSDP Site 545): A stratigraphic tool for paleoceanographic and paleobiologic reconstruction. Earth and Planetary Science Letters, 218(1–2), 149–161. https://doi.org/10.1016/S0012-821X(03)00646-0

Higgins, O., Sheldrake, T., & Caricchi, L. (2022). Machine learning thermobarometry and chemometry using amphibole and clinopyroxene: A window into the roots of an arc volcano (Mount Liamuiga, Saint Kitts). Contributions to Mineralogy and Petrology, 177(1), Article 1. https://doi.org/10.1007/s00410-021-01874-6

Hildreth, W., & Moorbath, S. (1988). Crustal contributions to arc magmatism in the Andes of Central Chile. Contributions to Mineralogy and Petrology, 98(4), 455–489. https://doi.org/10.1007/BF00372365

Hofmann, P., Ricken, W., Schwark, L., & Leythaeuser, D. (2001). Geochemical signature and related climatic-oceanographic processes for early Albian black shales: Site 417D, North Atlantic Ocean. Cretaceous Research, 22(2), 243–257. https://doi.org/10.1006/cres.2001.0253

Hu, H., Rojas-Agramonte, Y., Carrasquilla, S., Lázaro, C., Iturralde-Vinent, M., & Garcia-Casco, A. (2024). Exotic vs local Caribbean origin for the arc-related Mabujina Amphibolite Complex (Cuba): Implications for segmentation of the Caribbean arc during the Cretaceous. International Geology Review, 66(1), Article 1. https://doi.org/10.1080/00206814.2023.2225080

Hu, H. Y., Stern, R. J., Rojas‐Agramonte, Y., & Garcia‐Casco, A. (2022). Review of Geochronologic and Geochemical Data of the Greater Antilles Volcanic Arc and Implications for the Evolution of Oceanic Arcs. Geochemistry, Geophysics, Geosystems, 23(4), Article 4. https://doi.org/10.1029/2021GC010148

Huang, H., Niu, Y., Teng, F.-Z., & Wang, S.-J. (2019). Discrepancy between bulk-rock and zircon Hf isotopes accompanying Nd-Hf isotope decoupling. Geochimica et Cosmochimica Acta, 259, 17–36. https://doi.org/10.1016/j.gca.2019.05.031

Humphreys, M. C. S., Blundy, J. D., & Sparks, R. S. J. (2006). Magma Evolution and Open-System Processes at Shiveluch Volcano: Insights from Phenocryst Zoning. Journal of Petrology, 47(12), Article 12. https://doi.org/10.1093/petrology/egl045

Iturralde-Vinent, M. Ed., (1996). Ofiolitas y arcos volcánicos de Cuba. First Contribution IGCP Project 364, University of Miami Press, 265 pp.

Iturralde-Vinent, M. (1998). Sinopsis de la Constitución Geológica de Cuba. Acta Geológica Hispánica, 33, Article 33.

Iturralde-Vinent, M. (2021). Compendio de geología de Cuba y del Caribe. DVD. Havana, CITMATEL.

Iturralde-Vinent, M., & Lidiak, E.G., (2006). Caribbean tectonic, magmatic, metamorphic and stratigraphic events: Implication for plate tectonics: Geologica Acta, v. 4, p. 1–5, doi: 10.1344/105.000000355.

Iturralde-Vinent, M., Garcia-Casco, A., Rojas-Agramonte, Y., Proenza, J. A., Murphy, J. B., & Stern, R. J. (2016). The geology of Cuba: A brief overview and synthesis. GSA Today, 4–10. https://doi.org/10.1130/GSATG296A.1

Iturralde-Vinent, M., Otero, C. D., García-Casco, A., & Van Hinsbergen, D. J. J. (2008). Paleogene Foredeep Basin Deposits of North-Central Cuba: A Record of Arc-Continent Collision between the Caribbean and North American Plates. International Geology Review, 50(10), 863–884. https://doi.org/10.2747/0020-6814.50.10.863

Jagoutz, O., & Schmidt, M. W. (2012). The formation and bulk composition of modern juvenile continental crust: The Kohistan arc. Chemical Geology, 298–299, 79–96. https://doi.org/10.1016/j.chemgeo.2011.10.022

Jerram, D. A., & Martin, V. M. (2008). Understanding crystal populations and their significance through the magma plumbing system. Geological Society, London, Special Publications, 304(1), 133–148. https://doi.org/10.1144/SP304.7

Jolly, W. T. (2001). Secular Geochemistry of Central Puerto Rican Island Arc Lavas: Constraints on Mesozoic Tectonism in the Eastern Greater Antilles. Journal of Petrology, 42(12), 2197–2214. https://doi.org/10.1093/petrology/42.12.2197

Jolly, W. T., Lidiak, E. G., & Dickin, A. (2006). Cretaceous to Mid-Eocene pelagic sediment budget in Puerto Rico and the Virgin Islands (northeast A. Geologica Acta, 17. https://doi.org/10.1344/105.000000357

Jolly, W. T., Lidiak, E. G., Dickin, A. P., & Wu, T.-W. (1998). Geochemical diversity of Mesozoic island arc tectonic blocks in eastern Puerto Rico. In E. G. Lidiak & D. K. Larue, Tectonics and Geochemistry of the Northeastern Caribbean. Geological Society of America. https://doi.org/10.1130/0-8137-2322-1.67

Jorgenson, C., Higgins, O., Petrelli, M., Bégué, F., & Caricchi, L. (2022). A Machine Learning-Based Approach to Clinopyroxene Thermobarometry: Model Optimization and Distribution

for Use in Earth Sciences. Journal of Geophysical Research: Solid Earth, 127(4), e2021JB022904. https://doi.org/10.1029/2021JB022904

Kantchev, I., Boyanov, I., Goranov, A., Iolkichev, N., Cabrera, R., Kanazirski, M., Popov, N., & Stancheva, M. (1978). Geología de la provincia de Las Villas. Resultados de las investigaciones geológicas y levantamiento geológico a escala 1:250000, realizado durante el período 1969—1975. Brigada Cubano-Búlgara. Instituto de Geología y Paleontología, ACC, La Habana (inédito).

Kelemen, P. B., Hanghøj, K., & Greene, A. R. (2014). One View of the Geochemistry of Subduction-Related Magmatic Arcs, with an Emphasis on Primitive Andesite and Lower Crust. In Treatise on Geochemistry (pp. 749–806). Elsevier. https://doi.org/10.1016/B978-0-08-095975-7.00323-5

Kerr, A. C., Iturralde-Vinent, M. A., D. Saunders, A., & Tarney, J. (1999). New plate tectonic model of the Caribbean: Implications from a geochemical reconnaissance of Cuban Mesozoic volcanic rocks. Geological Society of America Bulletin, 19.

Klein, B. Z., Jagoutz, O., Schmidt, M. W., & Kueter, N. (2023). A global assessment of the controls on the fractionation of arc magmas. Geochemistry, Geophysics, Geosystems, 24(5), e2023GC010888.

Krawczynski, M. J., Grove, T. L., & Behrens, H. (2012). Amphibole stability in primitive arc magmas: Effects of temperature, H2O content, and oxygen fugacity. Contributions to Mineralogy and Petrology, 164(2), 317–339. https://doi.org/10.1007/s00410-012-0740-x

Lázaro, C., Blanco-Quintero, I. F., Proenza, J. A., Rojas-Agramonte, Y., Neubauer, F., Núñez-Cambra, K., & Garcia-Casco, A. (2016). Petrogenesis and 40Ar/39Ar dating of proto-forearc crust in the Early Cretaceous Caribbean arc: The La Tinta mélange (eastern Cuba) and its easterly correlation in Hispaniola. International Geology Review, 58(8), 1020–1040. https://doi.org/10.1080/00206814.2015.1118647

Lázaro, C., García-Casco, A., Rojas Agramonte, Y., Kröner, A., Neubauer, F., & Iturralde-Vinent, M. (2009). Fifty-five-million-year history of oceanic subduction and exhumation at the northern edge of the Caribbean plate (Sierra del Convento mélange, Cuba). Journal of Metamorphic Geology, 27(1), 19–40. https://doi.org/10.1111/j.1525-1314.2008.00800.x

Le Bas, M. J. L., Maitre, R. W. L., Streckeisen, A., Zanettin, B., & IUGS Subcommission on the Systematics of Igneous Rocks. (1986). A Chemical Classification of Volcanic Rocks Based

on the Total Alkali-Silica Diagram. Journal of Petrology, 27(3), 745–750. https://doi.org/10.1093/petrology/27.3.745

Leake, B. E., Woolley, A. R., Arps, C. E. S., Birch, W. D., Gilbert, M. C., Grice, J. D., Hawthorne, F. C., Kato, A., Kisch, H. J., Krivovichev, V. G., Linthout, K., Laird, J., Mandarino, J., Maresch, W. V., Nickel, E. H., Rock, N. M. S., Schumacher, J. C., Smith, D. C., Stephenson, N. C. N., … Youzhi, G. (1997). Nomenclature of Amphiboles; Report of the Subcommittee on Amphiboles of the International Mineralogical Association Commission on New Minerals and Mineral Names. Mineralogical Magazine, 61(405), 295–310. https://doi.org/10.1180/minmag.1997.061.405.13

Leat, P. T., & Larter, R. D. (2003). Intra-oceanic subduction systems: Introduction. Geological Society, London, Special Publications, 219(1), Article 1. https://doi.org/10.1144/GSL.SP.2003.219.01.01

Li, X., & Zhang, C. (2022). Machine Learning Thermobarometry for Biotite‐Bearing Magmas. Journal of Geophysical Research: Solid Earth, 127(9), Article 9. https://doi.org/10.1029/2022JB024137

Lidiak, E. G., & Anderson, T. H. (2015). Evolution of the Caribbean plate and origin of the Gulf of Mexico in light of plate motions accommodated by strike-slip faulting. In Geological Society of America Special Papers (Vol. 513, pp. 1–88). Geological Society of America. https://doi.org/10.1130/2015.2513(01)

Lidiak, E. G., Jolly, W. T., & Dickin, A. P. (2011). Pre-arc basement complex and overlying early island arc strata, Southwestern Puerto Rico: Overview, geologic evolution, and revised data bases. Geologica Acta, 273–287.

MacDonald, A., Ubide, T., Mollo, S., Pontesilli, A., & Masotta, M. (2023). The Influence of Undercooling and Sector Zoning on Clinopyroxene–Melt Equilibrium and Thermobarometry. Journal of Petrology, 64(10), egad074. https://doi.org/10.1093/petrology/egad074

Mangler, M. F., Petrone, C. M., & Prytulak, J. (2022). Magma recharge patterns control eruption styles and magnitudes at Popocatépetl volcano (Mexico). Geology, 50(3), 366–370. https://doi.org/10.1130/G49365.1

Mantle, G. W., & Collins, W. J. (2008). Quantifying crustal thickness variations in evolving orogens: Correlation between arc basalt composition and Moho depth. Geology, 36(1), 87. https://doi.org/10.1130/G24095A.1

Marchesi, C., Garrido, C. J., Bosch, D., Proenza, J. A., Gervilla, F., Monie, P., & Rodriguez-Vega, A. (2007). Geochemistry of Cretaceous Magmatism in Eastern Cuba: Recycling of North American Continental Sediments and Implications for Subduction Polarity in the Greater Antilles Paleo-arc. Journal of Petrology, 48(9), Article 9. https://doi.org/10.1093/petrology/egm040

Marxer, F., Ulmer, P., & Müntener, O. (2022). Polybaric fractional crystallisation of arc magmas: An experimental study simulating trans-crustal magmatic systems. Contributions to Mineralogy and Petrology, 177(1), Article 1. https://doi.org/10.1007/s00410-021-01856-8

Millan, G. (1996). Geología del Complejo Mabujina. In: Ofiolitas y Arcos Volcánicos de Cuba (Ed. Iturralde-Vinent, M.A.). IGCP Project 364, Special Contribution 1, 3–35.

Millán, G. (1997). Geologia del macizo metamórfico del Escambray, in Furrazola Bermudez, G. and Nuñez Cambra, K.E. eds., Estudios sobre Geología de Cuba, La Habana, Centro Nacional de Información Geológica, p. 271–288.

Moreno Toiran, B. (2003). The crustal structure of Cuba derived from Receiver Function Analysis. Journal of Seismology, 7(3), 359–375. https://doi.org/10.1023/A:1024566803893

Neave, D. A., Bali, E., Guðfinnsson, G. H., Halldórsson, S. A., Kahl, M., Schmidt, A.-S., & Holtz, F. (2019). Clinopyroxene–Liquid Equilibria and Geothermobarometry in Natural and Experimental Tholeiites: The 2014–2015 Holuhraun Eruption, Iceland. Journal of Petrology, 60(8), 1653–1680. https://doi.org/10.1093/petrology/egz042

Niu, X., Yang, J., Llanes Castro, A. I., Feng, G., Li, Z., & Liu, F. (2022). Zircon ages, mineralogy, and geochemistry of ophiolitic mafic and island-arc rocks from central Cuba: Implications for Cretaceous tectonics in the Caribbean region. Lithos, 434–435, 106924. https://doi.org/10.1016/j.lithos.2022.106924

O`Connor, J. T. (1965). A classification of quartz rich igneous rock based on feldspar ratios. US Geological Survey, 525B, B79-B84.

Oliviera De Sá, A., Leroy, S., d'Acremont, E., Lafuerza, S., Granja-Bruña, J. -L., Moreno, B., Cabiativa Pico, V., & Letouzey, J. (2024). The Protracted Evolution of a Plate Boundary: Eastern Cuba Block and Old Bahamas Channel. Geochemistry, Geophysics, Geosystems, 25(5), e2023GC011230. https://doi.org/10.1029/2023GC011230

Pavlov, I. (1970). Informe sobre los trabajos de búsqueda-levantamiento a escala 1:50,000, realizados en 1969-70 en el área comprendida entre las ciudades de Cumanayagua y Fomento (Provincia de las Villas). 289 págs.

Pearce, J. A. (1996). A user's guide to basalt discrimination diagrams. Trace Element Geochemistry of Volcanic Rocks: Applications for Massive Sulphide Exploration. Geological Association of Canada, Short Course Notes, 12(79), Article 79.

Pearce, J. A. (2008). Geochemical fingerprinting of oceanic basalts with applications to ophiolite classification and the search for Archean oceanic crust. Lithos, 100(1–4), Article 1–4. https://doi.org/10.1016/j.lithos.2007.06.016

Pearce, J. A., & Peate, D. W. (1995). Tectonic Implications of the Composition of Volcanic ARC Magmas. Annual Review of Earth and Planetary Sciences, 23(1), 251–285. https://doi.org/10.1146/annurev.ea.23.050195.001343

Peccerillo, A., & Taylor, S. R. (1976). Geochemistry of eocene calc-alkaline volcanic rocks from the Kastamonu area, Northern Turkey. Contributions to Mineralogy and Petrology, 58(1), 63–81. https://doi.org/10.1007/BF00384745

Pelullo, C., Chakraborty, S., Cambeses, A., Dohmen, R., Arienzo, I., D'Antonio, M., Pappalardo, L., & Petrosino, P. (2022). Insights into the temporal evolution of magma plumbing systems from compositional zoning in clinopyroxene crystals from the Agnano-Monte Spina Plinian eruption (Campi Flegrei, Italy). Geochimica et Cosmochimica Acta, 328, 185–206. https://doi.org/10.1016/j.gca.2022.04.007

Petrelli, M., Caricchi, L., & Perugini, D. (2020). Machine Learning Thermo-Barometry: Application to Clinopyroxene-Bearing Magmas. Journal of Geophysical Research: Solid Earth, 125(9), e2020JB020130. https://doi.org/10.1029/2020JB020130

Pindell, J. L., & Kennan, L. (2009). Tectonic evolution of the Gulf of Mexico, Caribbean and northern South America in the mantle reference frame: An update. Geological Society, London, Special Publications, 328(1), Article 1. https://doi.org/10.1144/SP328.1

Pindell, J., Maresch, W. V., Martens, U., & Stanek, K. (2012). The Greater Antillean Arc: Early Cretaceous origin and proposed relationship to Central American subduction mélanges: implications for models of Caribbean evolution. International Geology Review, 54(2), 131–143. https://doi.org/10.1080/00206814.2010.510008

Possee, D., Rychert, C., Harmon, N., & Keir, D. (2021). Seismic Discontinuities Across the North American Caribbean Plate Boundary From S-to-P Receiver Functions. Geochemistry, Geophysics, Geosystems, 22(7), e2021GC009723. https://doi.org/10.1029/2021GC009723

Prieto-Torrell, C., Albert, H., Aulinas, M., González-Esvertit, E., Arienzo, I., Gisbert, G., Troll, V. R., Fernandez-Turiel, J.-L., Rodriguez-Gonzalez, A., & Perez-Torrado, F.-J. (2025). Mush

system heterogeneities control magma composition and eruptive style on the Ocean Island of El Hierro, Canary Islands. Contributions to Mineralogy and Petrology, 180(5). https://doi.org/10.1007/s00410-025-02216-6

Proenza, J. A., Díaz-Martínez, R., Iriondo, A., Marchesi, C., Melgarejo Draper, J. C., Gervilla, F., & ... & Blanco-Moreno, J. A. (2006). Primitive Cretaceous island-arc volcanic rocks in eastern Cuba: The Téneme Formation. Geologica Acta, 4(1-2)(0103–121).

Proenza, J. A., González-Jiménez, J. M., Garcia-Casco, A., Belousova, E., Griffin, W. L., Talavera, C., Rojas-Agramonte, Y., Aiglsperger, T., Navarro-Ciurana, D., Pujol-Solà, N., Gervilla, F., O'Reilly, S. Y., & Jacob, D. E. (2018). Cold plumes trigger contamination of oceanic mantle wedges with continental crust-derived sediments: Evidence from chromitite zircon grains of eastern Cuban ophiolites. Geoscience Frontiers, 9(6), 1921–1936. https://doi.org/10.1016/j.gsf.2017.12.005

Profeta, L., Ducea, M. N., Chapman, J. B., Paterson, S. R., Gonzales, S. M. H., Kirsch, M., Petrescu, L., & DeCelles, P. G. (2016). Quantifying crustal thickness over time in magmatic arcs. Scientific Reports, 5(1), Article 1. https://doi.org/10.1038/srep17786

Putirka, K. (2017). Geothermometry and Geobarometry. In P. Bobrowsky & B. Marker (Eds.), Encyclopedia of Engineering Geology (pp. 1–19). Springer International Publishing. https://doi.org/10.1007/978-3-319-39193-9_322-1

Putirka, K. D. (2008). Thermometers and Barometers for Volcanic Systems. Reviews in Mineralogy and Geochemistry, 69(1), 61–120. https://doi.org/10.2138/rmg.2008.69.3

Ridolfi, F. (2021). Amp-TB2: An Updated Model for Calcic Amphibole Thermobarometry. Minerals, 11(3), 324. https://doi.org/10.3390/min11030324

Ridolfi, F., Renzulli, A., & Puerini, M. (2010). Stability and chemical equilibrium of amphibole in calc-alkaline magmas: An overview, new thermobarometric formulations and application to subduction-related volcanoes. Contributions to Mineralogy and Petrology, 160(1), Article 1. https://doi.org/10.1007/s00410-009-0465-7

Rieder, M., Cavazzini, G., D'yakonov, Y. S., Frank-Kamenetskii, V. A., Gottardi, G., Guggenheim, S., Koval', P. W., Müller, G., Neiva, A. M. R., Radoslovich, E. W., Robert, J.-L., Sassi, F. P., Takeda, H., Weiss, Z., & Wones, D. R. (1998). Nomenclature of the Micas. Clays and Clay Minerals, 46(5), 586–595. https://doi.org/10.1346/CCMN.1998.0460513

Rojas-Agramonte, Y., Garcia-Casco, A., Kemp, A., Kröner, A., Proenza, J. A., Lázaro, C., & Liu, D. (2016). Recycling and transport of continental material through the mantle wedge above

subduction zones: A Caribbean example. Earth and Planetary Science Letters, 436, 93–107. https://doi.org/10.1016/j.epsl.2015.11.040

Rojas-Agramonte, Y., Kröner, A., Garcia-Casco, A., Somin, M., Iturralde-Vinent, M., Mattinson, J. M., Millán Trujillo, G., Sukar, K., Pérez Rodríguez, M., Carrasquilla, S., Wingate, M. T. D., & Liu, D. Y. (2011). Timing and Evolution of Cretaceous Island Arc Magmatism in Central Cuba: Implications for the History of Arc Systems in the Northwestern Caribbean. The Journal of Geology, 119(6), 619–640. https://doi.org/10.1086/662033

Rojas-Agramonte, Y., Neubauer, F., Bojar, A. V., Hejl, E., Handler, R., & García-Delgado, D. E. (2006). Geology, age and tectonic evolution of the Sierra Maestra Mountains, southeastern Cuba. Geologica Acta, 28.

Rojas-Agramonte, Y., Hu, H. Y., Iturralde-Vinent, M., Lewis, J., de Lepinay, B, M., & García-Casco, A. (2024). A Late Cretaceous Adakitic intrusion from Northern Haiti: Additional evidence for slab melting and implications for migration of ridge-trench-trench triple junction during the Cretaceous in the Greater Antilles. International Geology Review, 66(1), 228-237.

Ross, P.-S., & Bédard, J. H. (2009). Magmatic affinity of modern and ancient subalkaline volcanic rocks determined from trace-element discriminant diagrams. 46, 17.

Rui, H.-C., Duan, W.-Y., Yang, J.-S., Maresch, W. V., Schertl, H.-P., Cai, P.-J., Llanes-Castro, A. I., & He, H.-P. (2025). Ultrahigh-pressure to high-pressure eclogite in Cuban ophiolitic mélange reveals proto-Caribbean spreading ridge subduction. Geological Society of America Bulletin, 137(3–4), 1006–1020. https://doi.org/10.1130/B37647.1

Rui, H.-C., Yang, J.-S., Zheng, J.-P., Llanes Castro, A. I., Liu, F., Wu, Y., Wu, W.-W., Valdes Mariño, Y., & Masoud, A. E. (2022). Early Cretaceous subduction initiation of the proto-Caribbean plate: Geochronological and geochemical evidence from gabbros of the Moa-Baracoa ophiolitic massif, Eastern Cuba. Lithos, 418–419, 106674. https://doi.org/10.1016/j.lithos.2022.106674

Schellekens, J. H. (1998). Geochemical evolution and tectonic history of Puerto Rico. In E. G. Lidiak & D. K. Larue, Tectonics and Geochemistry of the Northeastern Caribbean. Geological Society of America. https://doi.org/10.1130/0-8137-2322-1.35

Schmidt, M. W., & Jagoutz, O. (2017). The global systematics of primitive arc melts. Geochemistry, Geophysics, Geosystems, 18(8), Article 8. https://doi.org/10.1002/2016GC006699

Schneider, J., Bosch, D., Monié, P., Guillot, S., Garcia-Casco, A., Lardeaux, J. M., Torres-Roldán, R. L., & Trujillo, G. M. (2004). Origin and evolution of the Escambray Massif (Central Cuba): An example of HP/LT rocks exhumed during intraoceanic subduction: ORIGIN AND EVOLUTION OF THE ESCAMBRAY MASSIF. Journal of Metamorphic Geology, 22(3), Article 3. https://doi.org/10.1111/j.1525-1314.2004.00510.x

Sisson, T. W., & Grove, T. L. (1993). Experimental investigations of the role of H2O in calc-alkaline differentiation and subduction zone magmatism. Contributions to Mineralogy and Petrology, 113(2), 143–166. https://doi.org/10.1007/BF00283225

Smith, D. J. (2014). Clinopyroxene precursors to amphibole sponge in arc crust. Nature Communications, 5(1), 4329. https://doi.org/10.1038/ncomms5329

Stanek, K. P., Maresch, W. V., Grafe, F., Grevel, C., & Baumann, A. (2006). Structure, tectonics and metamorphic development of the Sancti Spiritus Dome (eastern Escambray massif, Central Cuba). Geologica Acta, 20.

Stanek, K. P., Maresch, W. V., Scherer, E., Krebs, M., Berndt, J., Sergeev, S. S., Rodionov, N., Pfänder, J., & Hames, W. E. (2019). Born in the Pacific and raised in the Caribbean: Construction of the Escambray nappe stack, central Cuba. A review. European Journal of Mineralogy, 31(1), Article 1. https://doi.org/10.1127/ejm/2019/0031-2795

Stern, R. J. (2010). The anatomy and ontogeny of modern intra-oceanic arc systems. Geological Society, London, Special Publications, 338(1), Article 1. https://doi.org/10.1144/SP338.2

Straub, S. M., Woodhead, J. D., & Arculus, R. J. (2015). Temporal Evolution of the Mariana Arc: Mantle Wedge and Subducted Slab Controls Revealed with a Tephra Perspective. Journal of Petrology, 56(2), Article 2. https://doi.org/10.1093/petrology/egv005

Thiadens, 1937. Geología de la parte sur de la Provincia de Santa Clara, Cuba. Geographische en Geologische Mededeelingen, Physiographisch-Geologische Reeks, 2 (12): 1-69, Utrecht, Holanda, Instituut der Rijksuniversiteit

Torró, L., Cambeses, A., Rojas-Agramonte, Y., Butjosa, L., Iturralde-Vinent, M., Lázaro, C., Piñero, E., Proenza, J. A., & Garcia-Casco, A. (2020). Cryptic alkaline magmatism in the oceanic Caribbean arc (Camagüey area, Cuba). Lithos, 376–377, 105736. https://doi.org/10.1016/j.lithos.2020.105736

Torró, L., Proenza, J. A., Marchesi, C., Garcia-Casco, A., & Lewis, J. F. (2017a). Petrogenesis of meta-volcanic rocks from the Maimón Formation (Dominican Republic): Geochemical

record of the nascent Greater Antilles paleo-arc. Lithos, 278–281, 255–273. https://doi.org/10.1016/j.lithos.2017.01.031

Torró, L., Proenza, J. A., Camprubí, A., Nelson, C. E., Domínguez, H., Carrasco, C., Reynoso-Villafaña, R., & Melgarejo, J. C. (2017b). Towards a unified genetic model for the Au-Ag-Cu Pueblo Viejo district, central Dominican Republic. Ore Geology Reviews, 89, 463–494. https://doi.org/10.1016/j.oregeorev.2017.07.002

Torró, L., Proenza, J. A., Melgarejo, J. C., Alfonso, P., Farré de Pablo, J., Colomer, J. M., Garcia-Casco, A., Gubern, A., Gallardo, E., Cazañas, X., Chávez, C., Del Carpio, R., León, P., Nelson, C. E., & Lewis, J. F. (2016). Mineralogy, geochemistry and sulfur isotope characterization of Cerro de Maimón (Dominican Republic), San Fernando and Antonio (Cuba) lower Cretaceous VMS deposits: Formation during subduction initiation of the proto-Caribbean lithosphere within a fore-arc. Ore Geology Reviews, 72, 794–817. https://doi.org/10.1016/j.oregeorev.2015.09.017

Torró, L., Proenza, J. A., Rojas-Agramonte, Y., Garcia-Casco, A., Yang, J.-H., & Yang, Y.-H. (2018). Recycling in the subduction factory: Archaean to Permian zircons in the oceanic Cretaceous Caribbean island-arc (Hispaniola). Gondwana Research, 54, 23–37. https://doi.org/10.1016/j.gr.2017.09.010

Ulmer, P., Kaegi, R., & Müntener, O. (2018). Experimentally Derived Intermediate to Silica-rich Arc Magmas by Fractional and Equilibrium Crystallization at 1·0 GPa: An Evaluation of Phase Relationships, Compositions, Liquid Lines of Descent and Oxygen Fugacity. Journal of Petrology, 59(1), 11–58. https://doi.org/10.1093/petrology/egy017

van Hinsbergen, D. J. J., Iturralde-Vinent, M. A., van Geffen, P. W. G., Garcia-Casco, A., & van Benthem, S. (2009). Structure of the accretionary prism, and the evolution of the Paleogene northern Caribbean subduction zone in the region of Camagüey, Cuba. Journal of Structural Geology, 31(10), Article 10. https://doi.org/10.1016/j.jsg.2009.06.007

Wang, X., Hou, T., Wang, M., Zhang, C., Zhang, Z., Pan, R., Marxer, F., & Zhang, H. (2021). A new clinopyroxene thermobarometer for mafic to intermediate magmatic systems. European Journal of Mineralogy, 33(5), 621–637. https://doi.org/10.5194/ejm-33-621-2021

Whattam, S. A., & Stern, R. J. (2011). The ‘subduction initiation rule’: A key for linking ophiolites, intra-oceanic forearcs, and subduction initiation. Contributions to Mineralogy and Petrology, 162(5), Article 5. https://doi.org/10.1007/s00410-011-0638-z

Wieser, P. E., Kent, A. J. R., & Till, C. B. (2023a). Barometers Behaving Badly II: A Critical Evaluation of Cpx-Only and Cpx-Liq Thermobarometry in Variably-Hydrous Arc Magmas. Journal of Petrology, 64(8), Article 8. https://doi.org/10.1093/petrology/egad050

Wieser, P. E., Kent, A. J. R., Till, C. B., Donovan, J., Neave, D. A., Blatter, D. L., & Krawczynski, M. J. (2023b). Barometers Behaving Badly I: Assessing the Influence of Analytical and Experimental Uncertainty on Clinopyroxene Thermobarometry Calculations at Crustal Conditions. Journal of Petrology, 64(2), egac126. https://doi.org/10.1093/petrology/egac126

Wilson, F. H., Orris, G., & Gray, F. (2019). Preliminary geologic map of the Greater Antilles and the Virgin Islands: U.S. Geological Survey Open-File Report 2019–1036, pamphlet 50 p., 2 sheets, scales 1:2,500,000 and 1:300,000, https://doi.org/10.3133/ofr20191036.

Zelepuguin, V. N., Díaz de Villalvilla, L., Fonseca, E., Dilla, M., Domínguez, E., & Torres, M. (1985). Petrología de las rocas vulcanógenas y vulcanógeno-sedimentarias de Cuba. Oficina Nacional de Recursos Minerales, Ministerio de la Industria Básica, La Habana (inédito).

Zelepuguin, V. N., Fonseca, E., & Díaz de Villalvilla, L. (1982). Asociaciones vulcanógenas de la provincia de Pinar del Río. Serie Geológica, Centro Investigaciones Geológicas, Ministerio de la Industria Básica, La Habana, 6:42—74.

Zhang, C., Santosh, M., Luo, Q., Jiang, S., Liu, L., & Liu, D. (2019). Impact of residual zircon on Nd-Hf isotope decoupling during sediment recycling in subduction zone. Geoscience Frontiers, 10(1), 241–251. https://doi.org/10.1016/j.gsf.2018.03.015

Zimmer, M. M., Plank, T., Hauri, E. H., Yogodzinski, G. M., Stelling, P., Larsen, J., ... & Nye, C. J. (2010). The role of water in generating the calc-alkaline trend: new volatile data for Aleutian magmas and a new tholeiitic index. Journal of Petrology, 51(12), 2411-2444.

Supplementary Materials

Appendix: Data Repository

All supplementary materials associated with this dissertation are permanently archived on heiBOX, provided through the account of Prof. Dr. Yamirka Rojas-Agramonte. The repository contains all datasets, figures, and additional resources referenced in the main text.

Repository name: HH PhD Supplementary Materials

Permanent heiBOX URL:

https://heibox.uni-heidelberg.de/d/cf7f6e562c6e46ebae6f/

QR code:

Acknowledgements

I hardly know where to begin to comprehend this amazing journey of my doctoral study. First and foremost, I would like to deeply appreciate my supervisor, Yamirka Rojas-Agramonte. I feel incredibly fortunate to have met her and to have started this PhD journey. From Kiel to Spain, to Cuba, and finally to Heidelberg, she was always there (sometime not there but out in the field) with such supportive and inspiring energy that carried me through many places and all the ups and downs along the way. I am also truly grateful to Bob, who has supported me since my Master's and made it possible for me to meet Yami and begin this adventure. And to Antonio, from Spain to Cuba, thank you for mentoring me with such patience and for guiding me into the fascinating world of Caribbean geology.

I would also like to thank all my colleagues and co-authors who contributed to shaping this research project, from Kiel, Heidelberg, Spain, Cuba and during my stay in China. I will always remember their effort and support for this research project: Romain, Peter, Andreas, Dora, Kenya, Manuel, Pieter, Chen, and Shoujie, thank you all.

My deepest gratitude goes to my dear girlfriend Lu and my family for always being there for me (even when not physically here). To Arne, for all the goofy talks in the kitchen. To Anna, for introducing me to bouldering. To Clayton, being countless times dinner buddy. Congrats to Nuria and Pol, and a warm "Hi" to little Laia :). To Sarah, such a great local guide in Granada. To my not often seen flatmate Estefany. And to my lunch assembly here in Heidelberg: Carlos, Eduardo, Alessia, Enrico, and sometime Petar and Rezvaneh. To all the friends and people, I haven't named but who have been there with me and helped me through this incredible journey, thank you sincerely.

And finally, to Jadie, the last friend I met before handing in this thesis, thank you too.

Heidelberg, 31 October 2025

00:31 a.m.

Yours,

Haoyu